GENETIC AND FUNCTIONAL CHARACTERISATION OF CATECHOLAMINERGIC POLYMORPHIC VENTRICULAR TACHYCARDIA

A thesis submitted to The University of Manchester for the degree of Doctor of Philosophy in the Faculty of Biology, Medicine and Health

2020

DAMILOLA B. OLUBANDO

SCHOOL OF MEDICAL SCIENCES

Division of Cardiovascular Science

Contents

Final Word count: 61572

Figures

Tables

Abbreviations

ADP - Adenosine diphosphate

AF - Atrial fibrillation

AM - Acetoxymethyl

ANOVA - Analysis of variance

AP - Action potential

ATP- Adenosine triphosphate

AVN – Atrioventricular node

bp - Base pairs

Ca^{2+} - Calcium ion

CaMKII - Calcium-calmodulin-dependent protein kinase II

cAMP - Cyclic adenosine monophosphate

cDMEM - Complete Dulbecco's modified eagle's medium, supplemented with 10 % FCS and 2 % PSG

CICR - Calcium-induced calcium release

CPVT - Catecholaminergic polymorphic ventricular tachycardia

CASQ2 – Calsequestrin2

DAD - Delayed afterdepolarization

DMEM - Dulbecco's modified eagle medium

DMSO - Dimethyl sulfoxide

eGFP - Enhanced green fluorescent protein

ER - Endoplasmic reticulum

ExAC - Exome aggregation consortium

FBS - Foetal bovine serum

FKPB12.6 - FKBP protein (12.6 kDa) also referred to as calstabin2

gnomAD - The Genome Aggregation Database

GOF – Gain of function

HEK293 - Human embryonic kidney cells 293

hRyR2 - Human cardiac ryanodine receptor

IP3Rs - Inositol 1,4,5-trisphosphate receptors

kb - Kilobases

KRH - Krebs Ringer Heinslet buffer

K^+ - Potassium ion

LB - Luria-Bertani

MCGM - Manchester Centre for Genomic Medicine

Mg^{2+} - Magnesium ion

MIM - Mendelian Inheritance in Man

Na^+ - Sodium ion

NGS – Next generation sequencing

NW Genomic Laboratory Hub – North West Genomic Laboratory Hub

PBS - Phosphate buffered saline

PCR - Polymerase chain reaction

PKA - Cyclic AMP-dependant kinase

PSG - Penicillin-Streptomycin-Glutamine

ROI - Region of interest

RYR - Ryanodine receptor

RYR2 – cardiac ryanodine receptor

SALVO - Synchrony-Amplitude-Length-Variability of Oscillation software

SAN – Sinoatrial node

SERCa2a - Cardiac sarcoplasmic reticulum calcium-ATPase

SNP – Single nucleotide polymorphism

SNS – Sympathetic nervous system

SOF – Suppression of function

SOICR - Store overload-induced calcium release

SR - Sarcoplasmic reticulum

T-tubule – Transverse tubule

TAE - Tris base, acetic acid, EDTA

TBE -Tris, Borate, EDTA

TRDN - Triadin

w/v - Weight by volume

WT – Wild type

Abstract

Catecholaminergic polymorphic ventricular tachycardia (CPVT) is a rare, genetically heterogeneous arrhythmogenic disorder characterised by ventricular tachycardia and syncope triggered by physical or emotional stress. Heterozygous missense variants in *RYR2* are the most common cause. Here, I undertook analysis to classify the pathogenicity and mechanism of action of *RYR2* variants.

RYR2 variants were collated with phenotypic data where available. Each variant was assessed based on minor allele frequencies, in silico prediction tools and appraisal of functional studies and classified according to the 2015 American College of Medical Genomics guidelines. Of the 326 identified *RYR2* missense variants, 55 (16.9%), previously disease-associated variants were re-classified as benign. Application of the gnomAD database allowed reclassification of 11 variants more than the smaller ExAC database, indicating the utility of larger control datasets in variant classification.

In contrast to the gain of function *RYR2* variants that cause CPVT, rare *RYR2* loss of function variants can also result in ventricular arrhythmias. We used splice prediction tools and an ex vivo splicing assay to investigate whether *RYR2* missense variants result in altered splicing. Ten *RYR2* variants were consistently predicted to disrupt splicing, however none altered splicing in the splicing assay.

The RyR2 Phe4905Leu variant was identified in an 18-year-old male who died during sleep. We performed cascade screening on the proband's family and functionally analysed full length RyR2 channels mutagenized with the Phe4905Leu variant in HEK 293 cells. Calcium release events in HEK 293 cells expressing eGFP tagged RyR2 Phe4905Leu had a significantly greater duration ($P < 0.005$), rise rate ($P < 0.005$), and fall rate ($P < 0.005$), but a lower amplitude ($P < 0.05$) compared to cells expressing WT RyR2. Furthermore, Phe4905Leu RyR2 was found to be less sensitive to caffeine compared to WT RyR2.

In summary, the reclassification of *RYR2* variants as benign is important as family members previously tested to carry these variants may not be at increased risk and those

without these variants may have been falsely reassured and remain at risk of arrhythmia or sudden cardiac death. *RYR2* missense variants are unlikely to alter splicing. Lastly, functional characterisation of a novel *RYR2* variant reported in a family with an unusual phenotype, has generated data to support classification of this variant as pathogenic and facilitate diagnostic cascade screening within the family.

Declaration

No portion of the work referred to in this thesis has been submitted in support of an application for another degree or qualification of this or any other university or other institute of learning.

Copyright statement

iv. Further information on the conditions under which disclosure, publication and commercialisation of this thesis, the Copyright and any Intellectual Property and/or Reproductions described in it may take place is available in the University IP Policy (seehttp://documents.manchester.ac.uk/DocuInfo.aspx?DocID=24420), in any relevant Thesis restriction declarations deposited in the University Library, The University Library's regulations (seehttp://www.library.manchester.ac.uk/about/regulations/) and in The University's policy on Presentation of Theses.

Acknowledgements

I would like to thank my supervisor; Prof. William Newman for accepting me into his group, designing my research project and providing me with feedback and support on experiments and manuscripts. I would like to thank Dr. Luigi Venetucci for helping in experimental design and providing feedback on manuscripts. I would like to thank Dr. Raymond O'Keefe and Dr. Huw Thomas for teaching me the techniques needed to carry out the minigene assays. I would like to thank Prof. Christopher George and Dr. Lowri Thomas for teaching me the techniques used in the functional characterisation of RyR2 variants and providing me with hRYR2 cDNA.

In addition to my supervisory team I would like to thank all the members of the Newman and O'Keefe labs for their support and feedback. I would also like to thank all the clinicians that provided *RYR2* variant data.

I am grateful to the British Heart Foundation for funding my Ph.D. and making this research possible.

I would like to thank my family for their continued support and encouragement.

Lastly, I would like to thank God for making this possible.

Rationale for Journal Format

The work compiled to form this thesis is presented in the journal format with each separate section of the thesis being suitably structured for publication as an individual paper in a peer reviewed journal. Chapter 3 has been published in Journal of Human Genetics and chapter 4 has been accepted for publication in Cardiogenetics. Chapter 5 has been presented in a format suitable for publication in a peer reviewed journal but has not been submitted for publication.

The work in this thesis aims to aid the diagnosis and management of CPVT by classifying as many *RYR2* variants as possible as either pathogenic or benign. Initially 326 *RYR2* variants were reclassified by application of the American College of Medical Genetics guidelines on variant classification, using computational tools, a minor allele frequency threshold and existing functional data. To further aid *RYR2* variant classification and understanding of the disease mechanism the means by which *RYR2* missense variants, the most prevalent known genetic cause of CPVT, elicit a pathogenic effect was investigated. Lastly, we explored whether the heterogeneity in CPVT phenotypes can be attributed to variations in the properties of mutant RyR2 channels, by establishing the significant differences in the calcium handling properties of variants in HEK cells. The different experimental techniques and methods used to achieve each of the aims in this thesis, from the collation and classification of hundreds of *RYR2* variants to the more detailed study of single *RYR2* variants meant that each chapter formed a discrete story. Thus, the presentation of this thesis in the journal format provides a clearer and more linear trajectory for each chapter than would be achieved using the traditional format.

Chapter 3 details the classification of 326 CPVT associated *RYR2* variants using a range of computational tools and statistical approaches to establish a frequency threshold for a pathogenic *RYR2* variant. The variants were reclassified using control datasets of different sizes and in doing so demonstrated the usefulness of larger control datasets. The analysis resulted in the reclassification of 55 *RYR2* variants previously reported to be CPVT associated as benign and 26 variants as pathogenic or likely pathogenic. The phenotypic heterogeneity of CPVT was introduced in this chapter, and *RYR2* variants associated with

sleep related sudden death were more likely to occur in the C-terminus of the protein. Furthermore, CPVT related *RYR2* variants clustered in regions outside of the pre-established hotspots for pathogenic variants.

In Chapter 4 an alternative mechanism by which *RYR2* missense variants may cause CPVT was explored and to some extent this validated functional studies on mutagenized full length RyR2. Computational tools were applied to predict the likelihood of *RYR2* missense variants altering splicing. Those variants consistently predicted to alter splicing were studied using a minigene assay as *RYR2* expression is limited to the heart and brain and tissue samples were unavailable. None of the variants predicted to affect splicing had an effect on splicing in the minigene assay, suggesting *RYR2* missense variants are unlikely to disrupt transcript splicing.

In chapter 5 the functional properties of an *RYR2* variant associated with an unusual phenotype in HEK 293 cells were studied. Full length eGFP tagged *RYR2* cDNA was mutagenized and transfected into HEK 293 cells and calcium imaging was used to study the calcium handling properties of the cells. With the data generated this novel *RYR2* variant was reclassified as pathogenic and the unique functional properties of the variant, which was found to present both the gain of function properties typically associated with *RYR2* variants in CPVT and less common suppression of function properties, were highlighted.

Each chapter of this thesis is united to the underlying theme of CPVT associated *RYR2* variant classification. However, the phenotypic and mechanistic heterogeneity of CPVT required questions to be addressed that would lead to the use of different experimental approaches, as a result the most appropriate format to present this thesis was the journal format.

Author Contributions

The work presented in this thesis was undertaken with the contributions of several collaborators. The contributions of my collaborators and myself for each experimental chapter of this thesis have been listed below.

Chapter 3. Classification and correlation of RYR2 missense variants in individuals with catecholaminergic polymorphic ventricular tachycardia reveals phenotypic relationships

Damilola Olubando, Claire Hopton, James Eden, Richard Caswell, N. Lowri Thomas, Stephen A. Roberts, Deborah Morris-Rosendahl, Luigi Venetucci, William G. Newman

I collated CPVT associated *RYR2* variants with assistance from Claire Hopton, James Eden, N. Lowri Thomas and Deborah Morris-Rosendahl. I investigated the association of *RYR2* variant location and phenotype. I determined the minor allele frequency threshold for a pathogenic dominant CPVT associated *RYR2* variant under the guidance of Stephen A Roberts. I defined the regions where CPVT associated *RYR2* variants clustered under the guidance of Stephen A Roberts. I calculated the conservation score for each amino acid position where an *RYR2* variant occurred under the guidance of Richard Caswell. I wrote the manuscript under the guidance of William G. Newman and Luigi Venetucci. All authors reviewed the manuscript and gave comments.

Chapter 4. Assessment of disease-associated missense variants in RYR2 on transcript splicing

Damilola Olubando, Huw Thomas, Minoru Horie, Raymond T. O'Keefe, Luigi Venetucci, William G. Newman

I performed the computational analysis on CPVT associated RYR2 missense variants. I performed the minigene assays under the guidance of Huw Thomas and Raymond T. O'Keefe. Minoru Horie identified and provided clinical information on *RYR2* variants. I

wrote the manuscript under the guidance of William G. Newman and Luigi Venetucci. All authors reviewed the manuscript and gave comments.

Chapter 5. Characterisation of a novel RYR2 missense variant in a family with a history of sudden death

Damilola Olubando, N. Lowri Thomas, Christopher George, Luigi Venetucci, William G. Newman

I functionally characterised the *RYR2* variant under the guidance of N. Lowri Thomas. Christopher George provided the eGFP tagged human *RYR2* cDNA that was used for mutagenesis. Luigi Venetucci provided clinical information on the patients with the *RYR2* variant. I wrote the manuscript under the guidance of N. Lowri Thomas, Christopher George, William G. Newman and Luigi Venetucci. All authors reviewed the manuscript and gave comments.

Chapter 1: Introduction

1.1 Calcium Signalling

In order to respond to ever changing environments, cells require means of communicating; they do this using messengers whose concentration at particular times and locations represent specific states and/or a need for action (Clapham, 2007). The versatility of calcium ions (Ca^{2+}) has enabled cells to use them as messengers for a wide range of processes, from fertilization to cell proliferation (Berridge et al., 2000). At rest cells have a Ca^{2+} concentration of 100 µM and are activated when Ca^{2+} concentrations rise to approximately 1000 µM.

However, this simple rise in Ca^{2+} concentration is able to specifically regulate a number of independent processes (Berridge et al., 2000). The ability for different pathways to interact contributes to this versatility, but the versatility of Ca^{2+} as a messenger is mainly achieved through the numerous components of what is known as the Ca^{2+} signalling toolkit, the components of the Ca^{2+} signalling toolkit can be assembled in various ways to form different combinations and ultimately to produce Ca^{2+} signals unique in their spatial and temporal profiles (Berridge et al., 2000).

1.1.2 The calcium signalling toolkit

The members of the Ca^{2+} signalling toolkit can be grouped according to their role in the signalling process. The first group is Ca^{2+} mobilising signals like inositol-1,4,5-trisphosphate (Ins(1,4,5)P3), these components are generated in response to a stimuli that acts on cell surface receptors like receptor tyrosine kinases and G-protein linked receptors (Berridge et al., 2000). Secondly, ON mechanisms including intracellular Ca^{2+} channels like the Ins(1,4,5)P3 receptor (InsP3R) and ryanodine receptor (RYR), which are activated by Ca^{2+} mobilising signals, release Ca^{2+} into the cytoplasm from intracellular stores (Berridge et al., 2000). Thirdly, the increase in Ca^{2+} concentration in the cytoplasm acts as a messenger signal, mediating several Ca^{2+} sensitive processes; these processes vary from one cell type to another due to factors such as buffer capacity. For instance neurons contain high concentrations of parvalbumin and calbindin that act as buffers by binding to and thus reducing the concentration of free Ca^{2+}, restricting the location of Ca^{2+} signals in neurons to the synapses triggering the release of neurotransmitters (Berridge et al., 2000). Lastly, OFF mechanisms consist of the pumps and exchangers that

remove Ca^{2+} from the cytoplasm and restore the resting concentration (Berridge et al., 2000).

1.2 Role of calcium signalling in the heart

1.2.1 Structure and function of cardiac muscle

Cardiac muscle consists of cardiomyocytes, elongated single nuclei cells that are typically 50-100 µm long and 10-20 µm wide (Severs, 2000). The cytoplasmic constituents of the cardiomyocyte are separated from extracellular material by the surrounding plasma membrane known as the sarcolemma. The sarcolemma protrudes into the cytoplasm at numerous points at 1.8 µm intervals; these invaginations are 150 to 300 nm wide and referred to as transverse (T)-tubules (Eisner et al., 2017). T-tubules contain a number of ion channels and pumps, like L-type calcium channels and sodium-calcium exchangers that facilitate the movement of ions between the cytoplasm and extracellular fluid. Large regions of the sarcoplasmic reticulum that extend along T-tubules are called terminal cisternae, at these points L-type calcium channels and RyR channels are in close proximity with each other (approximately 15 nm apart), allowing the formation of the cardiac dyad which is important for calcium signalling in cardiomyocytes (Severs, 2000).

1.2.2 Excitation contraction coupling

In order for the heart to effectively eject blood, sufficient pressure must develop within the ventricle through the shortening of cardiomyocytes (Eisner et al., 2017). Cardiomyocytes contain tube like structures called myofibrils that contain repeating contractile units known as sarcomeres. Sarcomeres are made of titin filaments and elongated proteins that arrange to form myofilaments (Gautel and Djinović-Carugo, 2016). Myofilaments composed of actin and regulatory proteins tropomyosin and troponin are called thin filaments whereas those composed of myosin are called thick filaments (Gautel and Djinović-Carugo, 2016). At rest and in the presence of ATP myosin heads are activated by the breakdown of ATP and are bound to troponin and tropomyosin, the latter occupies a position that inhibits the binding of actin. At increased Ca^{2+} concentrations, Ca^{2+} binds to troponin inducing a shift in the configuration of the myofilament complex, displacing tropomyosin from the inhibitory position. This enables the formation of a cross-bridge between the activated myosin head and actin, and

generates tension between these elements (Gautel and Djinović-Carugo, 2016). The activated myosin heads shift to a lower energy position causing the actin containing thin filaments to slide along the thick filaments, shortening the myofilament complex. The release of ADP and Pi allows the binding of ATP to the myosin heads, resulting in the release of actin from the myosin cross-bridge. Myosin bound ATP is broken down by myosin ATPase activating the myosin heads and this process is repeated (Gautel and Djinović-Carugo, 2016). The cross-bridge cycle continues so far as Ca^{2+} concentrations are sufficiently high for Ca^{2+} to remain bound to troponin C exposing the actin active sites and ATP is present. Each cross-bridge cycle only shifts actin a short distance, thus one muscle twitch may require thousands of cycles. Once cytoplasmic Ca^{2+} levels are lowered through the action of pumps like the sodium-calcium exchanger Ca^{2+} no longer binds troponin C and thus the actin active site cannot interact with the myosin cross-bridge, compaction of the myofilament complex ceases and cardiomyocytes return to a relaxed state (Gautel and Djinović-Carugo, 2016).

1.2.3 The cardiac action potential

The electrical events that govern cardiac contraction are referred to as action potentials (AP). Cellular patch clamp studies have led to a detailed understanding of many of these events, which can be divided in to four distinct phases (Oudit and Backx, 2018). There are slight variations between APs in different cardiac cells, which include cells of the sinoatrial node (SAN), atrial muscle, atrioventricular node (AVN), Purkinje fibres, and ventricular muscle (Feher, 2012). In health, action potentials are initiated in a small cluster of specialised cells protected by connective tissue that lies between the superior vena cava and the inferior vena cava, called the SAN (Boyett et al., 2000). In P cells at the centre of the SAN, the funny current, a diastolic current generated by the flow of Na^+ and K^+ ions through hyperpolarization-activated, cyclic-nucleotide gated (HCN) channels depolarizes the membrane towards the threshold potential of -40 mV to -55 mV, this is known as phase 4 or diastolic depolarisation (Chandler Natalie et al., 2009, DiFrancesco and Noble, 2012, Feher, 2012). Diastolic depolarisation triggers the activation of fast Na^+ currents and L-type calcium channels resulting in rapid membrane depolarisation. This is also promoted by some of the extracellular Ca^{2+} entering the cell activating the cardiac ryanodine receptor (RYR2) and triggering Ca^{2+} release from the sarcoplasmic reticulum

(SR). This phase is known as phase 0 or the upstroke, during this phase the membrane potential reaches +40 mV (Dobrzynski et al., 2013). Phase 1 (early rapid repolarization) follows phase 0, in this phase the almost immediate inactivation of the fast Na^+ currents and the activation of outward K^+ currents causes rapid but moderate repolarization. The fast Na^+ currents remain inactivated until the resting potential is restored (Feher, 2012). During Phase 2 (the plateau phase), the general membrane conductance of ions is reduced. This is followed by phase 3, in which L-type Ca^{2+} currents are inactivated, the sarcoplasmic reticulum calcium ATPase (SERCa2a) pumps Ca^{2+} back in to the SR and outward K^+ currents are amplified, resulting in the repolarization of the cell to the resting potential (approximately -85 mV) (Feher, 2012, Dobrzynski et al., 2013). The cell remains at rest until the membrane potential reaches -40 mV once again due to diastolic depolarisation and another AP is triggered (Figure 1.1) (Feher, 2012).

1.2.4 Propagation of the cardiac action potential

Each cardiomyocyte is electrically coupled to surrounding cells through gap junctions, allowing electrical impulses to spread from the SAN across the atria and to the ventricles via the AVN, which is the only element electrically connecting the atria and ventricles (Prinzen et al., 2017).The exact mechanism by which electrical impulses generated in the SAN travel across the atria to the AVN is unknown; however the involvement of defined electrical roads has been suggested (Prinzen et al., 2017). What is known is the bilateral electrophysiological nature of the atrioventricular conduction axis. There are two pathways in which APs can travel through to reach the AVN, the travel of APs through the nodal extension is known as the slow pathway, whereas the travel of APs through a bridge composed of transitional cells is known as the fast pathway (Dobrzynski et al., 2013). Upon arrival at the AVN APs are propagated through the fibrous sheath responsible for the electrical separation of the atria and ventricles, However the transmission of APs through the AVN is slowed down due to the reduced expression of large or intermediate conductance connexions like Cx40 and Cx43 (Dobrzynski et al., 2013). At the base of the AVN a connection is formed with the bundle of His, which is composed of cells similar to those of the AVN and acts as the electrical junction between the atria and ventricles. The bundle of His splits as it extends into the ventricles forming the left and right bundle branches, each of which are covered in a sheath of connective

tissue, electrically isolating them from the surrounding myocardium, preventing the activation of ventricular cardiomyocytes before the AP arrives at the base of the heart (Sánchez-Quintana and Yen Ho, 2003). The left and right bundle branches form the foundation for vast networks of smaller branches that extend radially to cover the wall of the myocardium and parts of the septum, these extensions are known as the Purkinje system. Purkinje fibres transmit APs rapidly at a rate of 2.3 m/s, these action potentials are transferred from unsheathed regions of Purkinje fibres to the ventricular myocardium through bridges of transitional cells (Desplantez et al., 2007, Tranum-Jensen et al., 1991).

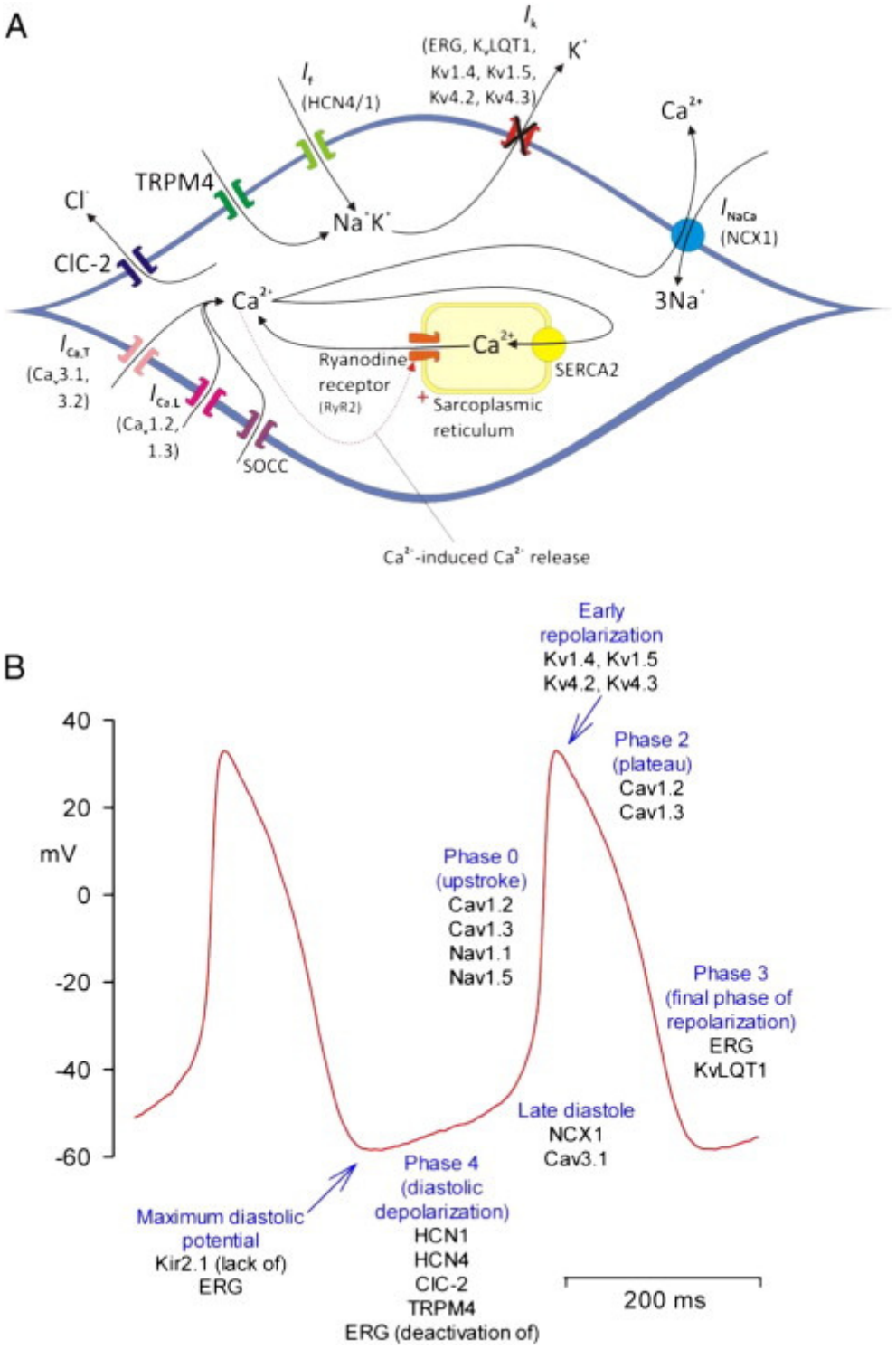

Figure 1.1. The pacemaking mechanisms of the SAN. (A) the numerous ion channels, currents and Ca^{2+}-handling proteins that form the membrane and contribute to the Ca^{2+} clocks involved in pacemaking. (B) The various phases of the cardiac action potential and the channels and currents responsible for them. Copied from Dobrzynski et al. (2013).

1.3 The β-adrenergic pathway

The sympathetic nervous system (SNS) induced "fight or flight" response is initiated in response to stress (both physical and emotional) and is mediated by the β-adrenergic signalling pathway. Under stress conditions neural fibres of the SNS in the heart release catecholamines like epinephrine (adrenaline) to maintain homeostasis (Cole and Sood, 2012). Catecholamines mediate their effect through β -adrenergic receptors, catecholaminergic stimulation of β-adrenergic receptors activates the Gαs guanine nucleotide-binding protein which in turn promotes the synthesis of cyclic AMP (cAMP) by adenylyl cyclase (Cole and Sood, 2012). The resulting transient increase in cAMP has an array of downstream effects that collectively lead to an increase in cardiac contractility (positive inotropic effect), the rate of cardiac relaxation (positive lusitropic effect), and heart rate (positive chronotropic effect) (Xiao, 2001).

One means by which cAMP exerts its cardiac effect is through the activation of protein kinase A (PKA), PKA phosphorylates and consequently activates several proteins that contribute to excitation contraction coupling and energy metabolism (Xiao, 2001). For example, PKA phosphorylation of L-type calcium channels increases the channels open state probability, resulting in more Ca^{2+} entering the cell during phase 0 of the action potential, increasing Ca^{2+} induced Ca^{2+} release and thus the force of cardiac contraction. This effect is enhanced by PKA phosphorylation of phospholamban, which relieves its inhibitory effect on SERCA2a and expedites the restoration of SR Ca^{2+} stores, providing more Ca^{2+} for the following contraction. Other regulatory proteins phosphorylated by PKA include troponin, titin, RyR2 and glycogen phosphorylase kinase (Xiao, 2001).

1.4 Abnormal action potential initiation and propagation can cause arrhythmias

Abnormal AP initiation and/or propagation can cause sudden death in young and seemingly healthy individuals free from structural cardiac or other anatomical disorders. The cause of death in these individuals was puzzling for some time, until the first detailed reports of long QT syndrome (LQTS). A report from Jervell and Lange-Nielsen in the late 1950s on a large family in which three of six siblings experienced sudden death under the age of 9 years provided clues of the genetic nature of these conditions. A delay in

ventricular repolarization observed as an elongated Q-T interval that was amplified following exercise was detected in three of the siblings through electrocardiographic studies. They summarised their findings stating 'The disorder may be in some cases a possible cause of inexplicable death in children' (Jervell and Lange-Nielsen, 1957). The discovery of the first genes found to cause LQTS was made some time after by Mark Keating's group (Wang et al., 1995, Curran et al., 1995). The discovery of the underlying causes of LQTS prompted the identification of other genes involved in the generation or transmission of APs that are associated with arrhythmogenic conditions. For instance, Priori et al. (2001) found pathogenic variants in *RYR2* in affected individuals in four families with catecholaminergic ventricular tachycardia (CPVT) but not in 400 unaffected relatives, providing the first evidence that *RYR2* missense variants cause CPVT (Priori Silvia et al., 2001).

1.5 The cardiac ryanodine receptor

1.5.1 RYR2 structure

The 2 MDa RyR2 homotetramer is the largest known ion channel. The 4967 amino acids of RyR2 form an umbrella shaped like structure (Figure 1.2), with the N-terminal accounting for the majority of the channels mass and forming the cytoplasmic cap that facilitates the binding and regulatory action of numerous molecules and enzymes (Van Petegem, 2012). The C-terminal of the RyR2 channel forms the relatively small stalk domain that consists of a number of transmembrane helices that extend through the SR membrane into the SR lumen (Van Petegem, 2012, Leenhardt et al., 2012, Bers, 2004). Similar to the potassium channel the more central helices make-up the pore forming region and the narrowest parts of the pore confer ion selectivity (Bers, 2004, Van Petegem, 2012). The stalk and the cytoplasmic cap are connected by four heavy columns (Samsó et al., 2005b). The large globular structures and solvent filled cavities that form the 3 domains (A, B and C) of the large 28 × 28 nm cytoplasmic cap provide 80 % of the channels mass (Bers, 2004). Figure 1.2 illustrates the arrangement of a number of these regions and structures. Despite the predominance of the RyR2 cytoplasmic cap studies have demonstrated it is not essential for channel function and is only required to regulate channel activity (Liu et al., 2015). In one such study Liu et al. (2015) generated mutant RyR2 channels each missing a specific region of the cytoplasmic cap, they found all

mutant channels, including those in which the entire cytoplasmic cap had been deleted to be functional and responsive to agonist-activation, indicating the C-terminal is the minimal requirement for RyR2 channel gating (Liu et al., 2015).

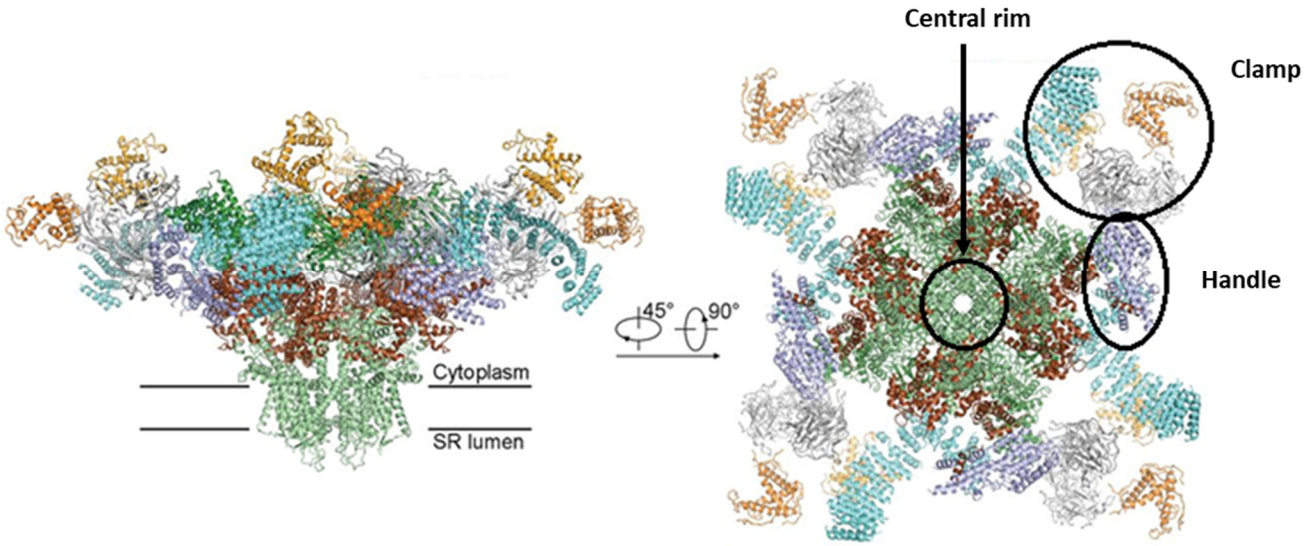

Figure 1.2. Cryo-EM structure of RyR2 from porcine heart in a closed state. Black rings highlight central, clamp and handle domains. Adapted from Peng et al. (2016).

Cryo-electron microscopy structures highlight the extensive similarities between RyR2 and its paralogue RyR1, which is the isoform that is mainly expressed in skeletal muscle. However, more detailed x-crystallography studies show how the interactions between the N-terminal domains in the two isoforms differ (Kimlicka et al., 2013). In RyR2 the network of ionic pairs that maintain and stabilize the connections between N-terminal domains A, B and C in RyR1 are substituted for a chloride ion that connects the domains by shielding the repulsive forces of adjacent arginine residues and electrostatically bonding with specific residues of domains B and C (Arg420, Arg298, and Arg276) (Kimlicka et al., 2013, Karshikoff and Ladenstein, 2001). The removal of the stabilizing chloride ion from RyR2 expectedly destabilizes the cytoplasmic cap; however the binding of chloride to this region is reversible, presenting the possibility of chloride binding to this site playing a regulatory role (Kimlicka et al., 2013). In this case RyR2 would need to possess an affinity

for chloride ions at mM concentrations. In addition to the possible regulation of RyR2 through the chloride mediated destabilization of the N-terminal cap, chloride ions may also regulate channel function through other means. Studies demonstrating chloride ions activate both RyR2 and RyR1, the latter of which lacks an N-terminal chloride binding site, suggest RyRs may contain multiple binding sites for chloride ions (Liu et al., 1998, Fruen et al., 1996).

1.5.2 Coupling of RYR2 channels

RyR2 channels do not operate independently, in cardiomyocytes clusters of around 100 RyR2 channels form at regions where the sarcolemmal membrane and the SR meet. RyR2 clusters align with each other and interact weakly with L-type calcium channels to form structures known as junctions (Bers, 2004). Within junctions neighbouring RyR2 channels are connected to each other, through physical interactions formed at their clamp domains, which are located at the corners of the cytoplasmic cap. Each channel interacts with 4 surrounding channels (Bers, 2004, Samsó et al., 2005b). RyR2 channels are activated by increased concentrations of cytoplasmic Ca^{2+} resulting from Ca^{2+} influx through L-type calcium channels. Upon activation the RyR2 clamp domain as well other domains go through conformational changes that result in the transition from a closed state to an open state and the release of Ca^{2+} from the SR as Ca^{2+} sparks (Bers, 2004). These transitions occur simultaneously in physically coupled channels in the presence of FKBP12.6 and coupled channels have been shown to exhibit higher conductance, indicating the channel coupling may also regulate RyR2 channel function. This is evidenced by the functional relationship of coupled RyR2 channels remaining intact for currents other than Ca^{2+} currents, excluding the possibility of functional coupling being the result Ca^{2+} induced Ca^{2+} release in which channel activation occurs due to the action of Ca^{2+} released from nearby channels (Marx Steven et al., 2001).

1.5.3 RYR2 channel gating

The exact mechanism by which RyR2 channels transition between open and closed states remains unclear. A gating mechanism constituting the inner helices and branches moving outwards to produce a kink while the outer regions of the cytoplasmic cap transition towards the stalk was proposed (Samsó et al., 2009). A similar mechanism of activation

has been established for Mthk (a calcium gated potassium channel) which is structurally similar to RyRs in many ways. Despite this it has been suggested that the inner helices are also kinked in the closed conformation so kinking does not contribute to channel activation (Ludtke et al., 2005). The different theories may be a result of the fact that the mechanism by which RyR2 activation occurs may vary depending on the trigger that activates the channel and other contributors like anion binding. Caffeine, aminophylline, theophylline and ATP have been shown to activate RyR2 through a mechanism that involves marked conformational changes in the clamp domain whereas such changes are not observed in cytosolic Ca^{2+} RyR2 activation (Tian et al., 2013). Like the clamp domain the conformational changes that occur in the inner helices during activation may vary. Furthermore, the RYR2 structure reported to show the closed channel with a kink in the clamp domain may actually represent RyR2 in an intermediate semi-closed state (Ludtke et al., 2005).

1.5.4 RyR2 regulation

1.5.4.1 RyR2 regulation by Ca^{2+}

Many proteins and physiological ligands regulate the activity of RyR2 mainly through interactions with its cytoplasmic cap (Table 1.1); however, RyR2 is also regulated by luminal Ca^{2+}. The contribution of luminal Ca^{2+} to RyR2 regulation was proposed as early as 1975 and since then further work has supported this (Fabiato and Fabiato, 1975, Gaburjakova et al., 2013). The means by which luminal Ca^{2+} regulates RyR2 activity is yet to be established, but several potential mechanisms have been suggested. In the “true luminal” model increased luminal Ca^{2+} concentrations promote the binding of Ca^{2+} directly to sites or regulatory proteins on the surface of RyR2 (Figure 1.3). Another proposed mechanism is the “feed through” model in which luminal Ca^{2+} feeds through the channel pore and binds to the surrounding regions of the cytoplasmic cap (Figure 1.3). Evidence in support of the “feed through” mechanism remains limited; contrastingly in favour of the “true luminal” model studies have demonstrated the indirect binding of Ca^{2+} to RyR2 through luminally bound proteins like calsequestrin 2 (CASQ2), a glycoprotein that binds Ca2+ (Gaburjakova et al., 2013). CASQ2 is made up of three domains each containing thioredoxin folds. The hydrophobic centres of CASQ2 domains are made up of aromatic residues and the electronegative outer regions are composed of mainly acidic

residues. Joining the three domains are hydrophobic loops and cations in the inter domain space stabilize the proteins structure, facilitating increased Ca^{2+} binding (Faggioni and Knollmann, 2012).

Elevated concentrations of cytosolic Ca^{2+} have also been shown to activate RyR2 in single channel studies, in which RyR2 channels were isolated from heart tissue from both healthy and failing hearts. In both cases increasing cytosolic Ca^{2+} concentrations increased the number of channel opening events significantly (Holmberg and Williams, 1989, Walweel et al., 2014).

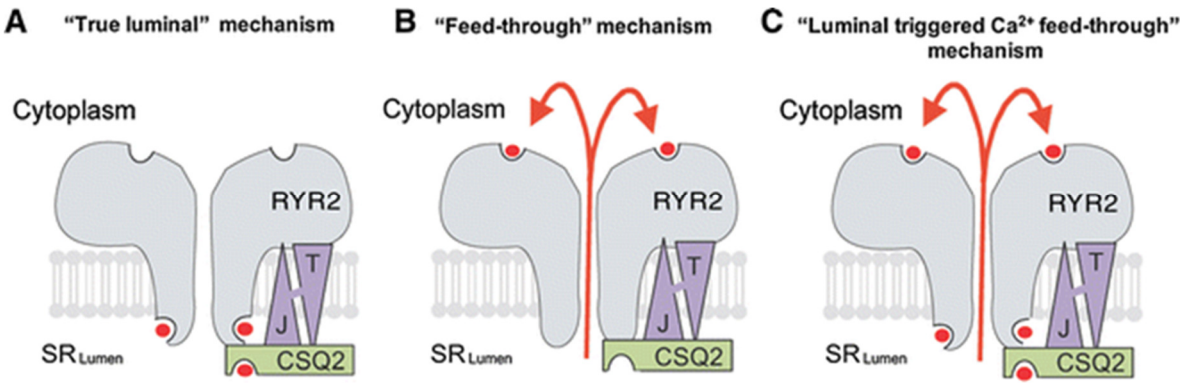

Figure 1.3. The various mechanisms of RyR2 regulation by luminal Ca^{2+} that have been proposed. (A) In the "true luminal" model increased luminal Ca2+ concentrations promote the binding of Ca2+ directly to sites or regulatory proteins on the surface of RyR2. (B) In the "feed through" model luminal Ca2+ feeds through the channel pore and binds to the surrounding regions of the cytoplasmic cap. (C) The "luminal triggered Ca^{2+} feed-through" model is a combination of the "true luminal" and "feed-through" models. Copied from Gaburjakova et al. (2013).

1.5.4.2 RyR2 regulation by ATP and Mg^{2+}

RyR2 is also regulated by ATP and Mg^{2+}, the former is an activator and the latter is a potent inhibitor (Fill and Copello, 2002). In most cells ATP and Mg^{2+} are present at concentrations of approximately 5 mM and 1 mM, respectively, thus the majority of cytosolic ATP is bound to Mg^{2+} and only a small proportion is in the free form that binds to and increases RyR2 open probability. The inhibitory effect of Mg^{2+} on RyR2 is likely to be the result of competition with Ca^{2+} for the Ca^{2+} activation site on RyR2, reducing RyR2 Ca^{2+} sensitivity (Fill and Copello, 2002).

1.5.4.3 RyR2 regulatory proteins

There are multiple means by which CASQ2 and numerous other proteins may regulate RyR2 activity (Table 1.1). As previously mentioned luminal Ca^{2+} has been shown to regulate RyR2 activity and this remains true even in the absence of CASQ2 (Sitsapesan and Williams, 1994, Györke and Györke, 1998, Gaburjakova and Gaburjakova, 2006). As CASQ2 is able to bind Ca^{2+} with a low affinity due the acidic residues at its surface it is possible that CASQ2 indirectly regulates RyR2 activity by modulating the concentration of free Ca^{2+} in the SR lumen (Liu et al., 2009). As well as the regulatory role CASQ2 plays by influencing luminal free Ca^{2+} concentrations the Ca^{2+} binding protein also influences RyR2 activity by binding to the RyR2 complex. CASQ2 may bind directly to RyR2 or it may bind to the associated proteins triadin and junctin that extend through the SR membrane into the lumen to form a complex with RyR2 and CASQ2 (Bers, 2004, Zhang et al., 1997). At increased luminal Ca^{2+} concentrations (approximately 300 μM) CASQ2 undergoes a conformational change to a more structured and condensed state, in which the polymerization of individual monomers through their C-terminal domains is more favourable (Gaburjakova et al., 2013). Although, CASQ2 may bind to the RyR2 complex as polymers and/or monomers it has been shown the binding of CASQ2 to the complex supresses RyR2 activity and its dissociation increases it (Gaburjakova et al., 2013, Qin et al., 2009). The lack of evidence supporting direct interactions between RyR2 and CASQ2 and the fact *in vitro* studies have demonstrated the activating effects of triadin and junctin on RyR2, presents the possibility CASQ2 monomers bind to the complex through triadin and junction inhibiting triadin-RyR2 and/or junction-RyR2 activating interactions (Gaburjakova et al., 2013). In skeletal muscle CASQ2 exerts this inhibitory effect through

direct interactions with junctin (Wei et al., 2009). The inhibitory effects of CASQ2 monomers may be relieved by increased Ca^{2+} concentrations, as polymerization may cause the dissociation of CASQ2 from the RyR2 complex. Györke et al. (2004) provided evidence of this, they reported triadin and junctin on the luminal side of RyR2 have an activating effect, whereas the further addition of CASQ2 has the opposite effect (Györke et al., 2004).

Collectively, the inhibitory action of CASQ2 and the dissociation of Ca^{2+} from its luminal binding site on RyR2 at lower luminal Ca^{2+} concentrations are likely to contribute to the positive feedback mechanism that regulates Ca^{2+} induced Ca^{2+} release from RyR2 channels. In support of this a reduction in luminal Ca^{2+} concentration below a threshold level results in the termination of Ca^{2+} sparks (Zima et al., 2008).

Table 1.1. Interaction sites and functions of RyR2 associated proteins which may be causally related to CPVT.

Protein	Molecular weight (KDa)	Interaction site	Function
RyR2	565,000	RyR2 channels interact with each other through their clamp regions which are located within the cytoplasmic cap (Samsó et al., 2005a).	RyR2 channels that interact physically through their clamp regions display coupled gating (Bers, 2004).
FKBP12.6	12,600	FKBP12.6 has been reported to interact with multiple sites on RyR2, both in the C-terminal and N-terminal of the protein. This may explain the influence FKBP12.6 has on both channel conductance and the coupling of neighbouring channels. (Zissimopoulos and Lai, 2005). One study suggests FKBP12.6 has a greater binding affinity for the N-terminal as comparative binding assays revealed unlike C-terminal fragments N-terminal fragments were unable to displace FKBP12.6 (Zissimopoulos and Lai, 2005, Marx et al., 2001).	The binding of FKBP12.6 to RyR2 channels is believed to have a stabilizing effect on coupled channels, and thus promote RyR2 channels being in a high conductance state (Marx et al., 2001). Some variants in RyR2 that cause CPVT have been shown to disrupt RyR2- FKBP12.6 interactions (Aizawa et al., 2005). Despite this there are yet to be reports of CPVT associated FKBP12.6 variants.
Calmodulin	16,800	Calmodulin interacts with both RyR1 and RyR2 in a similar manner. It binds to a conserved region of the handle domain in the N-terminus of RyRs (Yamaguchi et al., 2003). The binding affinity of calmodulin for RyR2 suggests an amount of the protein remains constantly bound to RyR2 (Sigalas et al., 2009).	The overall effect calmodulin has on RyR2 function remains unclear. At physiologically relevant Ca^{2+} concentrations the minority of calmodulin molecules have an inhibitory effect on RyR2 but the majority of calmodulin molecules have an activating effect (Sigalas et al., 2009). The differing effects of calmodulin on RyR2 may be due to calmodulin interacting differently with different RyR2 conformers. Another possibility is the existence of multiple calmodulin populations with different effects on RyR2. A study by Burger *et al*. (1984) showed the number of calcium molecules that bind to each calmodulin varies. Calmodulin is associated with CPVT, heterozygous calmodulin variants have been identified in

			CPVT patients (Gomez-Hurtado et al., 2016).
CaMKII	68,000	Immunoprecipitation experiments show CaMKII binds to RyR2; however, the sites at which they interact is yet to be established. What is known is CaMKII phosphorylates Ser2815 and Ser2809 on RyR2 and interacts with the RyR2 cytoplasmic cap (Wehrens et al., 2004). RyR2 Ser2815 phosphorylation has been reported to promote FKBP12.6 dissociation from the RyR2 complex (Wehrens et al., 2004).	CaMKII phosphorylates RyR2 which increases RyR2 channel sensitivity to activation by calcium and thus increases channel open probability (Wehrens et al., 2004). However, studies show that FKBP12.6-RYR2 binding is undisrupted in the presence of CaMKII this could be an indication CaMKII does not phosphorylate RyR2 Ser2809 (Wehrens et al., 2004).
PKA	96,000	PKA interactions with RyR2 are mediated through mAKAP (muscle-selective A-kinase anchoring protein). PKA binds to mAKAP which through its regulatory domain forms leucine zipper interactions with a region ranging from RyR2 residues 3003-3039 in the cytosolic cap (Bers, 2004).	PKA phosphorylation of RyR2 at Ser2809 is believed to promote the dissociation of FKBP12.6 and have an activating effect on RyR2. However, some have argued against the dissociation of FKBP12.6 from RyR2 (Marx et al., 2000, Bers, 2004).
PP1	35,000	PP1 does not bind to RyR2 directly but binds to spinophilin which interacts with RyR2 residues 554-588 to form leucine zipper interactions (Bers, 2004).	PP1 has an inhibitory effect of RyR2 activity by dephosphorylating the channel (Chiang et al., 2014).
PP2A	35,000	PP2A interacts with RyR2 in a similar manner to PP1. PP2A binds to PR130 which forms leucine zipper interactions with RyR2 residues 1603–1631 (Bers, 2004).	Similar to PP1 PP2A dephosphorylates RyR2 and thus has an inhibitory effect on RyR2 channel activity (Bers, 2004).
Sorcin	22,000	Sorcin interacts with RyR2 at a site that has not been determined.	At elevated calcium concentrations sorcin binds to RyR2 inhibiting the channel. Sorcin also exerts its inhibitory effect on RyR2 by inhibiting CaMKII (Anthony et al., 2007, Bers, 2004).
Cav1.2	100,000	Cav1.2 is believed to interact with RyR2 through its II-III loop (Bers, 2004).	At rest Cav1.2 may interact with RyR2 to exert an inhibitory effect (Bers, 2004).
Homer	41,000	Homer has been proposed to interact with RyR2 through its N-terminal domain. Homer has been shown to interact with the N-terminal domain of	Different homer proteins interact with RyR2 to exert various effects on channel activity. Homer 1b activates RyR2 by relieving some of the autoinhibitory effects

		IP3Rs (inositol 1,4,5-trisphosphate receptors) which have many regions that display high sequence homology with RyR2 (Bosanac et al., 2005). Homer proteins may also bridge interactions between Cav1.2 and RyR2 (Pouliquin et al., 2009).	introduced by RyR2s C-terminal tail. On the other hand, homer 1c has an inhibitory effect on RyR2 activity (Pouliquin et al., 2006, Westhoff et al., 2003).
CASQ2	45,000	CASQ2 binds to the RyR2 complex through the RyR2 C-terminal bound proteins triadin and junction (Leenhardt et al., 2012).	CASQ2 is a calcium binding protein and may regulate RYR2 activity by regulating the levels of luminal calcium. CASQ2 may also exert an inhibitory effect on RyR2 by disrupting activating interactions between RyR2, triadin and junction (Gaburjakova et al., 2013). Homozygous CASQ2 variants have been found to cause CPVT, heterozygous changes in CASQ2 can also cause CPVT however this is rarer (Gray et al., 2016, Song et al., 2007a).
Triadin	35,000	Triadin binds to RyR2 through the channels C-terminal domain (Leenhardt et al., 2012).	Triadin has been shown to have an activating effect on RyR2 in both animal and single channel studies (Gaburjakova et al., 2013). Homozygous and heterozygous variants in triadin have been associated with CPVT (Rooryck et al., 2015, Walsh et al., 2016, Roux-Buisson et al., 2012).
Junctin	26,000	Junctin binds to RyR2 through the channels C-terminal domain (Leenhardt et al., 2012).	Junctin has been shown to have an activating effect on RyR2 in both animal and single channel studies (Gaburjakova et al., 2013).
HRC	170,000	HRC (histidine-rich Ca^{2+}-binding protein) interacts with RyR2 indirectly through triadin but may also form direct interactions with the channel (Lee et al., 2001).	HRC variants have been shown to promote the spontaneous release of calcium from the SR. The exact mechanism HRC regulates RyR2 is unclear but it may alter luminal calcium concentrations (Zhang et al., 2014).

1.6 Catecholaminergic polymorphic ventricular tachycardia

Catecholaminergic polymorphic ventricular tachycardia (CPVT, MIM 604772) is a rare genetic arrhythmogenic condition affecting approximately one in 10,000 individuals. CPVT is characterised by unexpected episodes of ventricular dysrhythmia triggered by physical exercise or emotional stress in individuals with structurally intact hearts (Liu et al., 2008). Commonly, ventricular tachycardias in CPVT patients are bidirectional with the QRS axis rotating 180° from one beat to the next, contrastingly, up to 35 % of CPVT patients present polymorphic ventricular tachycardia. In many cases ventricular tachycardia progresses to ventricular fibrillation and results in sudden cardiac death, which may be the first clinical manifestation (Liu et al., 2008, Priori et al., 2002, Napolitano et al., 2014). A family history of sudden cardiac death and arrhythmias is common in CPVT patients, however, the phenotypic characteristics of the condition can vary widely between members of the same family (Napolitano et al., 2014).

1.6.1 Genetic etiology of CPVT

The detailed description and study of CPVT in two large Finnish families with a history of sudden death contributed largely to our current understanding of the genetic basis of the condition. *KVLQT1* and *SCN5A*, two genes commonly associated with arrhythmias were initially suspected to cause CPVT but this theory was eliminated by the condition being linked to a locus on chromosome 1q42–43. *TWIK-1*, a potassium channel and established contributor to phase IV of the cardiac action potential that was known to be in this region was considered the most probable candidate, but no CPVT patients were found to carry pathogenic variants in this gene (Swan et al., 1999). An early description of CPVT by Leenhardt et al. (1995) highlighted striking similarities with digitalis toxicity and this caused Priori et al. (2001) to investigate the association between CPVT and altered Ca^{2+} handling (Leenhardt et al., 1995, Priori Silvia et al., 2001). Subsequently, they identified heterozygous missense *RYR2* variants in four probands affected by CPVT that were absent in 400 asymptomatic relatives (Priori et al., 2001). A separate study by Laitinen et al. (2001) produced similar results establishing heterozygous missense variants in *RYR2* cause CPVT (Laitinen Päivi et al., 2001).

Differently to variants in *CASQ2*, which are relatively rare, *RYR2* variants associated with CPVT are typically heterozygous changes (heterozygous variants have also been reported in *CALM1* and *TRDN* in CPVT patients) (Napolitano et al., 2014, Nyegaard et al., 2012, Devalla et al., 2016, Broendberg et al., 2017) (Table 1.2). CPVT cases can be divided into 2 classes based on the inheritance pattern of the condition; CPVT1 refers to CPVT inherited in an autosomal dominant manner, whereas CPVT2 refers to the rare cases of CPVT inherited in an autosomal recessive pattern. Approximately 50% of CPVT cases are caused by variants in *RYR2* the vast majority of which are missense changes and heterozygous (Napolitano et al., 2014). CPVT associated *RYR2* variants have been found to cluster in 4 mutation hotspot regions within *RYR2* (George et al., 2007). As many as 83 % of CPVT associated *RYR2* variants have been reported to occur within the mutation hotspots, however this varies between studies (Medeiros-Domingo et al., 2009, Tester et al., 2006).

Table 1.2. Proportion of pathogenic CPVT variants in associated genes. Adapted from Napolitano et al., (2004).

Gene	**Proportion of CPVT Attributed to Pathogenic Variants in This Gene**
TECRL	<1%
CALM1	<1%
CASQ2	2%-5%
RYR2	50%-55%
TRDN	1%-2%
Unknown	35%-45%

1.6.2 Effects of CPVT causing variants

1.6.2.1 Altered domain interactions

CPVT associated RyR2 variants can alter channel function and cause disease through a number of proposed and experimentally supported mechanisms, one of which is the disruption of interactions between and within domains (Kimlicka et al., 2013). For instance, in the N-terminus of the protein variants in the anion binding site, like Arg420Gln prevent the binding of chloride ions, this causes a shift in N-terminus domains A and B of 1.4 Å relative to domain C. The rearrangement of the domains abolishes stabilising interactions between them and the resulting energy barriers for channel activation that they introduce. Thus, these variants destabilize the entire cytoplasmic cap and increase the activity of RyR2 channels, as they are able to transition from a closed state to an open state without the expense of energy through the binding of ligands (Kimlicka et al., 2013). Other RyR2 mutations in the N-terminal and central domains are believed to alter channel function through similar mechanisms, but in these instances stabilising interactions between these two separate domains are disrupted. Disruption of these interactions between the N-terminal and central domain is referred to as unzipping as they are believed to prevent the formation of the zipped complex that stabilises the channels closed state, sensitising RyR2 channels to Ca^{2+} induced activation (Figure 1.4) (Yamamoto and Ikemoto, 2002, Yang et al., 2006).

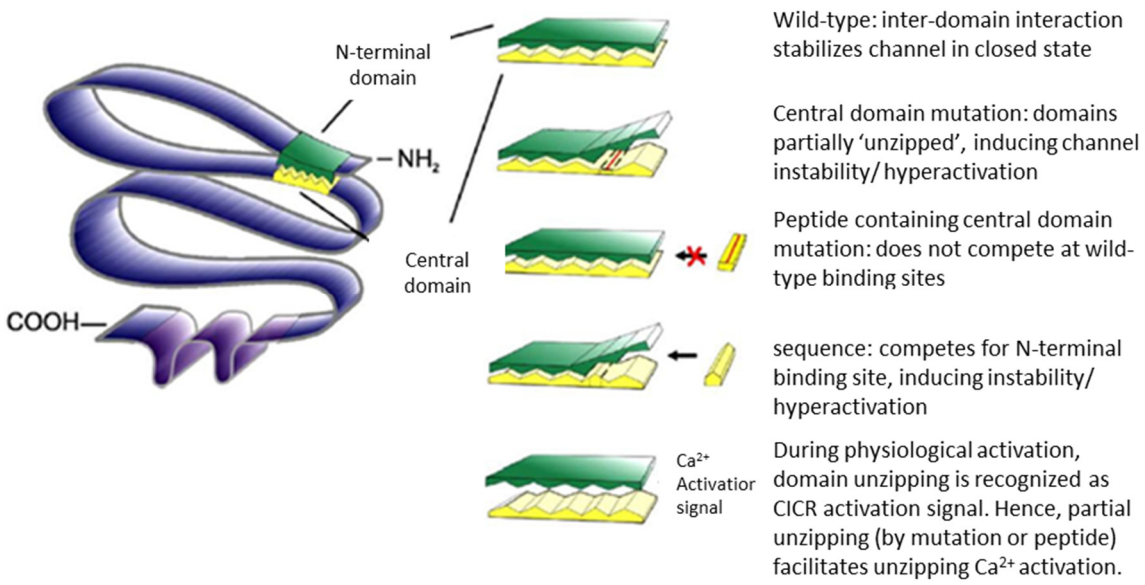

Figure 1.4. The proposed interaction between the N-terminal and central domains (left). The postulated domain Unzipping is caused either by the Arg2474Ser mutation or a competitive interaction with DPc10 (right). Adapted from Yang et al. (2006).

1.6.2.2 Altered interactions with regulatory proteins

The binding of FKBP12.6 is believed to stabilize physically coupled RyR2 channels (Marx et al., 2001). Mutations in the FKBP12.6 binding site like Ser2246Leu, Arg2474Ser, and Arg4497Cys are believed to cause CPVT by promoting the release of FKBP12.6 from the RyR2 complex, destabilizing the channel resulting in a Ca^{2+} leak from the SR. Adrenergic stimulation also contributes to the release of FKBP12.6 from the complex through PKA phosphorylation (Liu and Priori, 2007). Abnormal interactions with regulatory proteins can also be the result of variants in the regulatory proteins rather than RyR2. Variants in CASQ2 have been reported to abolish CASQ2 inhibition of RyR2 channels and activate them. However, non-inhibitory CASQ2 mutants are still able to bind to RyR2 as the addition of WT CASQ2 after the addition of CASQ2 mutants to RyR2 channels did not restore CASQ2 mediated RyR2 inhibition (Terentyev et al., 2006).

1.6.2.3 Altered calcium sensitivity

Numerous CPVT associated RyR2 variants have been shown to be more sensitive to activation by cytosolic Ca^{2+}, resulting in a continuous SR Ca^{2+} leak (Xiao et al., 2016).

Single channel studies by the Chen group demonstrated many mutations that alter cytosolic Ca^{2+} sensitivity are located in the central domain (amino acid range 3778-4201), indicating the central domain plays a crucial role in mediating Ca^{2+} sensitivity (Xiao et al., 2016). In support of this RyR1 does not contain a mutation hotspot in this region, it has been argued this is could be due to the different mechanisms of excitation-contraction coupling between the different RYR paralogues (Wu et al., 2006, Xiao et al., 2016). Differently to RyR2 which is activated by an increase in cytosolic Ca^{2+} through Ca^{2+} induced Ca^{2+} release, RyR1 is activated indirectly by membrane depolarization through the voltage sensor cav1.1 (Van Petegem, 2015, Bers, 2002). Thus, variants altering cytosolic Ca^{2+} sensitivity may have a lesser effect on RyR1 function.

The alteration of RyR2 Ca^{2+} sensitivity is not limited to cytosolic Ca^{2+} in CPVT. Jiang et al. (2005) demonstrated HEK cells expressing CPVT associated variants in the N-terminal, central and C-terminal domains of RyR2 all have a decreased threshold for activation by luminal Ca^{2+}. Mutant channels displayed more spontaneous Ca^{2+} release events at lower Ca^{2+} concentrations. The increased activity of RyR2 channels due to a reduction in the critical threshold for SR Ca^{2+} release is referred to as 'store overload induced Ca^{2+} release', a term first introduced by Jiang et al. (Jiang et al., 2005).

1.6.3 Splice Variants

Splicing is the process in which introns are removed and exons are joined together in pre-mRNA producing mRNA which is transported out of the nucleus and is used to synthesis proteins. Splicing involves two successive transesterification reactions at conserved sequences within exons and the intermediate intron. The process is initiated with the 2' OH group of the adenosine in the branch site, located in the intron, carrying out a nucleophilic attack on the 5' splice site. As a result of this reaction the 5' splice site is cleaved exposing an OH group and the 5' end of the intron becomes ligated to the branch site adenosine. Next, the 3' splice site is attacked by the 3'OH of the 5' exon generated in the previous reaction, removing the intron and ligating the two exons (Will and Lührmann, 2011). This process is facilitated by the spliceosome, a large ribonucleoprotein that is formed in close proximity to splice sites. It requires the recognition of the 5' splice site, branch site, polypyrimidine tract (PPT) and AG of the 3' splice site by components of

the spliceosome. The recognition of a splice site by the spliceosome is dependent on a number of factors (Will and Lührmann, 2011). In addition to factors such as splice site strength and the size of the exon and neighbouring introns, which determine the basal level of exon recognition , exons contain features which either enhance or supress the recognition of splicing sites, these sequences are known as exonic splicing enhancers (ESEs) and exonic splicing silencers (ESSs), respectively (Kornblihtt et al., 2013). Missense variants may affect splicing by disrupting exonic regulatory elements, existing splice sites or by introducing new splice sites. An example of this is the point mutation within exon 11 of the LMNA gene that produces an ectopic splice site, shortening the protein generated by introducing a premature stop codon, and causing Hutchinson-Gilford progeria (Eriksson et al., 2003).

Either of the mechanisms for disrupting splicing described above can cause a frameshift and introduce a premature termination codon which can lead to nonsense-mediated decay of the mRNA, alternatively a truncated version of the protein may be produced. Truncated RyR2 proteins without the autoinhibitory effect of the C-terminal tail may have similar effects as CPVT causing gain of function *RYR2* variants and the nonsense mediated decay of *RYR2* mRNA may have similar effects to CPVT associated loss of function variants through haploinsufficiency (Pouliquin et al., 2006). Interestingly many of the variants that make up the 15% of single nucleotide variants that have a causative role in disease by affecting splicing are exonic and not near splice junctions (Krawczak et al., 1992). Although, only intronic spliceogenic *RYR2* variants, such as *RYR2* c.6167-2A>G, have been reported in CPVT it is possible a proportion of the more prevalent exonic *RYR2* variants also alter splicing (Lieve et al., 2019). These variants may have gone undetected due to splice variants other than those at the U2 canonical splice site being more likely to go undetected, as splice variants at other positions where consensus sequences are less defined are less likely to be identified using existing algorithms (Shaikh et al., 2018).

1.6.4 Molecular mechanisms of *RYR2* associated CPVT

CPVT causing RyR2 variants can increase RyR2 activity through a range of mechanisms, enabling the spontaneous release of Ca^{2+} from the SR. The spontaneous release of Ca^{2+} from the SR has been the subject of extensive studies and reported for numerous different RyR2 variants (Watanabe and Knollmann, 2011). β-adrenergic stimulation worsens the SR Ca^{2+} leak, as previously described in section 1.3 the rise in cAMP activates PKA, RyR2 is then activated by PKA phosphorylation (Wehrens et al., 2003). Furthermore, CAMKII is also activated by β-adrenergic stimulation as a result of increased NO, CAMKII further phosphorylates RyR2 (Curran et al., 2014). The spontaneous release of Ca^{2+} from the SR results in local increases in Ca^{2+} concentration, which are observed as Ca^{2+} sparks. Ca^{2+} propagates through the cell in a wave like manner, possibly as a result of Ca^{2+} induced Ca^{2+} release, in which Ca^{2+} released from one channel activates adjacent channels (Figure 1.5) (Venetucci et al., 2007). Mechmann and Plott (1986) carried out single channel recordings of guinea pig atrial myocytes, showing the depolarizing inward current that follows an increase in intracellular Ca^{2+} as a result of SR Ca^{2+} release is generated by the action of the Na-Ca exchanger (Mechmann and Pott, 1986). They found on approaching the Ca^{2+} and Na^{+} transmembrane gradients the depolarizing current weakened. If the magnitude of the delayed after depolarization (DAD) resulting from the action of the Na-Ca exchanger is sufficient the threshold membrane potential for an AP will be reached and ectopic beats may be generated (Figure 1.5) (Mechmann and Pott, 1986). Optical mapping experiments of mouse hearts with the Arg4496Cys RyR2 variant showed arrhythmogenic APs originate from the His–Purkinje networks of the right and left ventricles in CPVT, explaining the bidirectionalty of the ventricular tachycardia observed in CPVT patients. Bidirectional ventricular tachycardia was changed to monodirectional ventricular tachycardia through right bundle branch blockage (Cerrone et al., 2007). Whether arrhythmogenic action potentials originate from the His–Purkinje network for all *RYR2* variants or just those that alter Ca^{2+} sensitivity is yet to be established but the bidirectional nature of the ventricular tachycardia in many CPVT cases could be interpreted as evidence of this.

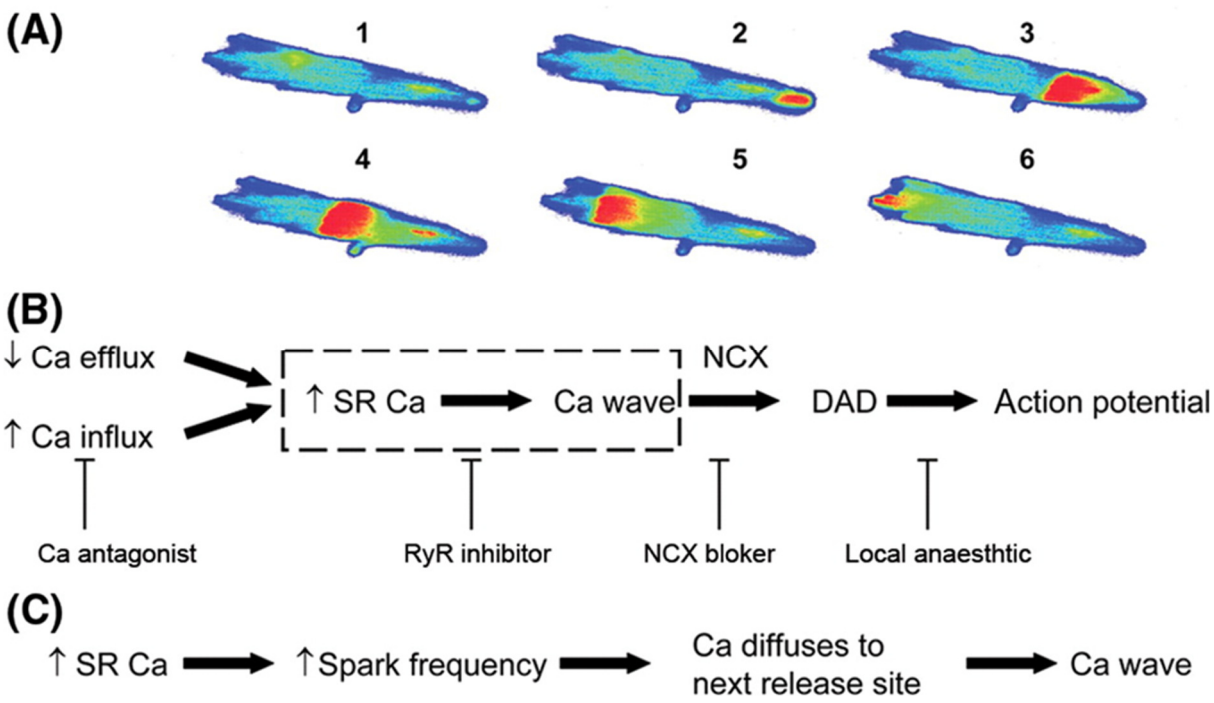

Figure 1.5. Flow diagram presenting the steps involved in the initiation of calcium waves. (A) Images generated by confocal microscopy of calcium waves in ventricular myocytes from rats. (B) An outline of the events that generate calcium waves. Increases in influx or decreases in the efflux of calcium from the SR results in an increase in the SR Ca^{2+} content, this leads to the generation of calcium waves, delayed after depolarisations and potentially action potentials. The points at which therapeutic agents may disrupt this process are shown below the flow diagram. (C) a more descriptive outline of the events in section B. Copied from Venetucci et al. (2007).

1.6.5 Heterogeneity of CPVT mechanisms

The cause of arrhythmias in CPVT by a continuous SR leak due to overactive RyR2 channels, worsened by adrenergic stimulation has been studied extensively and many findings support this mechanism; however, it is unlikely that all CPVT related genetic variants cause arrhythmias in this way. In addition to findings that some gain of function CPVT associated *RYR2* variants do not appear to be sensitive to adrenergic stimulation there is a growing body of evidence that *RYR2* suppression of function variants also cause CPVT and sudden cardiac death (Roston et al., 2017). A single explanation of the mechanism by which CPVT variants cause arrhythmias is not sufficient, and further alternative disease mechanisms may be relevant. In support of this RyR2-Ala4860Gly, one of the earlier studied CPVT mutations, was found to reduce RYR2 sensitivity to luminal Ca^{2+} resulting in a build-up of Ca^{2+} in the SR and subsequently prolonged SR Ca^{2+} release and early afterdepolarizations (Roston et al., 2017). What appears to be a common feature of suppression of function *RYR2* variants is there lack of sensitivity to adrenergic stimulation, in fact *in vivo* studies have reported *RYR2* suppression of function variants to protect against adrenergically triggered arrhythmias (Roston et al., 2017). What then triggers arrhythmias in patients with these mutations remains unclear. To further complicate matters the Arg420Gln-*RYR2* variant has been reported to display both gain of function and suppression of function effects depending on the levels of cytosolic Ca^{2+} (Domingo et al., 2015). Patients with such variants may be susceptible to arrhythmias by multiple triggers.

1.6.6 CPVT diagnosis

Early detection of CPVT is crucial as untreated CPVT has a greater risk of mortality (Napolitano et al., 2014, Tester et al., 2012). The exercise ECG or exercise stress test is commonly used in the diagnosis of CPVT as under physical stress arrhythmias can often be provoked in CPVT patients. However, not all CPVT patients present arrhythmias by exercise stress testing and some patients require multiple tests before producing symptoms (Roston et al., 2017). Furthermore, the clinical features of CPVT may overlap with those of other arrhythmogenic conditions like ATS1 (Andersen Tawil syndrome, MIM 170390) and ankyrin B–mediated LQT4 (MIM 600919), both of which can cause bidirectional ventricular tachycardia (Tester et al., 2006). Tester et al. (2006) were only

able to distinguish the ECG traces of three women with ATS1 from that of a CPVT patient by a slightly abnormal U-wave (U-waves were enlarged and biphasic in ATS1 patients) at rest. CPVT has been reported to be more arrhythmogenic and fatal than ATS1, so the correct identification of CPVT is important, justifying the use of other diagnostic tools like genetic testing, which presents its own challenges (Tester et al., 2006).

Genetic testing for CPVT is complicated by the large size of *RYR2*, which makes screening the whole gene using conventional methods like Sanger sequencing time consuming and costly (Napolitano et al., 2014). As a result many labs previously screened only the 3 or 4 hotspot regions where CPVT associated variants are believed to cluster in *RYR2* (George et al., 2007). In a study by Medeiros-Domingo et al. (2009) on CPVT patients with no known relation to each other *RYR2* was sequenced and in 83 % of the 155 patients *RYR2* variants were located in the hotspot regions (Medeiros-Domingo et al., 2009). More recently next generation sequencing (NGS) has become more widely accessible and all coding exons of *RYR2* can be screened rapidly and relatively cheaply. This has led to an increase in the number of novel *RYR2* variants being reported in individuals with cardiac dysrhythmia or associated symptoms of palpitations, syncope or sudden unexplained death. However, not all of these *RYR2* variants play a causative role in CPVT and distinguishing benign variants from pathogenic variants is crucial for NGS data to aid CPVT diagnosis (Jabbari et al., 2013). Jabbari et al. (2013) found the prevalence of potentially pathogenic CPVT associated variants to be 1 in every 150, a sizable difference from the expected 1 in 10,000 people, indicating a large proportion of variants proposed to be associated with CPVT are unrelated or contribute minimally to the disease phenotype. Concomitant with this has been the increase in *RYR2* variants identified in apparently healthy individuals collated through international resources including Exome Aggregation Consortium (http://exac.broadinstitute.org) and Genome Aggregation Database (gnomAD) (https://gnomad.broadinstitute.org). With functional data available for below 15 % of *RYR2* variants and NGS producing large amounts of DNA sequence data, the use of computational tools may be the most practical means of classifying pathogenic and benign *RYR2* variants and identifying patients with a high risk of experiencing cardiac events (Medeiros-Domingo et al., 2009).

1.6.7 CPVT Treatment

CPVT is commonly treated with non-selective as opposed to selective beta-blockers. This is because non-selective beta-blockers like propranolol have been reported to be more effective at reducing the arrhythmic window and severity of arrhythmias (Leren Ida et al., 2015). This may be due to their action on other ion channels, as Na/Ca exchanger upregulation and cAMP promoted activation of L-type calcium channels may also contribute to β-adrenergically triggered arrhythmias (Dorian, 2005). Similar to the local anaesthetic flecainide, propranolol was reported to suppress inward sodium currents (van der Werf and Lieve, 2016). Flecainide is used to treat CPVT in combination with β-blockers but has also been shown to be effective as a monotherapy in *in vitro* and *in vivo* studies (Steinfurt et al., 2015). The means by which flecainide prevents the onset of arrhythmias remains unclear, the direct inhibition of RyR2 by flecainide has been proposed but this has been contested (Watanabe and Knollmann, 2011, Bannister Mark et al., 2015). In both single channel and cell studies Bannister et al. (2015) found that even at concentrations exceeding those of therapeutic relevance flecainide failed to reduce the open probability of RyR2 channels (the maximum flecainide concentration tested was 50 µmol/L) (Bannister Mark et al., 2015). These findings may indicate inward sodium currents contribute to a larger extent than expected to adrenergically triggered arrhythmias in CPVT patients.

In many individuals with CPVT, treatment with non-selective beta-blockers is sufficient to suppress arrhythmias, but for as many as 30% of CPVT cases non-selective beta-blockers are ineffective and of these patients 19% experience sudden cardiac death (Liu et al., 2008). With CPVT being attributable to a plethora of mutations that are likely to cause arrhythmias through different mechanisms the nonuniformity in drug responsiveness presented by CPVT patients comes as no surprise. Some CPVT related genetic variants like those that affect channel regulation by CASQ2 can cause an increase in the levels of RyR2, however other mutations like RyR2 Arg4496Cys, which is believed to alter Ca^{2+} sensitivity do not (Fernández-Velasco et al., 2009, Song et al., 2007b). Thus, patients with mutations that disrupt CASQ2 regulation may be less responsive to drugs like carvedilol and possibly flecainide that directly inhibit RyR2 (Watanabe and Knollmann, 2011, van der Werf and Lieve, 2016). Furthermore, for patients with arrhythmias that are not adrenergically

triggered like many of those with *RYR2* suppression of function variants, both beta-blockers and RyR2 inhibitors may not be the most suitable treatments.

1.7 Research project aims and hypotheses

Hypotheses:

1. Bioinformatics and statistical tools can be used to determine the pathogenicity of *RYR2* variants.
2. *RYR2* missense variants may cause a CPVT like phenotype through different mechanisms.

Project Aims;

The general aim of this study is to improve the diagnosis, understanding and management of *RYR2* associated CPVT by providing an effective means of distinguishing pathogenic *RYR2* variants, exploring potential disease mechanisms and functionally characterising pathogenic variants.

1. Classification of CPVT associated *RYR2* variants

Heterozygous Variants in *RYR2* proposed to cause CPVT represent a much higher prevalence of 1 in every 150 individuals compared to the expected disease prevalence of 1 in 10,000 people. This suggests that many of the variants reported to cause CPVT may in fact be unrelated to the disease phenotype or be subtle contributors (Jabbari et al., 2013). Arbitrary cut off values for minor allele frequencies of 1 and 0.1% for dominant variants in control/healthy population datasets are often used when filtering out variants which occur too frequently and are thus less likely to be disease causing. However, this method may lead to the use of cut off threshold frequencies which are too lenient as it fails to take into account differences in disease prevalence as well as other factors. To address this Whiffin et al. (2017) developed a statistical framework to evaluate whether variants occur at frequencies low enough to cause penetrant Mendelian disease (Whiffin et al., 2017). Their method takes into account various disease specific factors such as penetrance and prevalence. They were able to justify the use of cut-off frequencies much lower than the commonly used 0.1% for several dominant disease phenotypes, allowing

the exclusion of a further two thirds of variants previously considered to be potentially pathogenic and cause hypertrophic cardiomyopathy (HCM) (Whiffin et al., 2017). Although the basis of the equation presented by Whiffin et al. (2017) was centred on the classification of genetic variants in *MYBPC3* proposed to cause HCM, they demonstrated the applicability of the method to various other inherited cardiac conditions such as CPVT, Marfan's syndrome and classic Ehlers-Danlos syndrome, but did not provide evidence to support these assertions (Whiffin et al., 2017).

In this study *RYR2* variants reported to be associated with CPVT or an associated phenotype in the literature, clinical variant databases and the North West Genomic Laboratory Hub, will be collated. The reported CPVT associated *RYR2* variants will be reclassified as described by Whiffin et al. (2017), using a cut-off-frequency for variant pathogenicity in large control populations including the gnomAD database (gnomAD contains exome data from 141,456 individuals) and the guidelines set by the ACMG (American College of Medical Genetics) (Whiffin et al., 2017, Richards et al., 2015).

2. Consideration that missense variants in *RYR2* result in loss of function rather than activation

As many as 10% of disease-associated single nucleotide variants in the Human Gene Mutation Database (HGMD) result in splice alterations (Krawczak et al., 2007). Recent studies have shown that some individuals with ventricular arrhythmias with similarity to CPVT can be attributed to loss of function variants in *RYR2* (Roston et al., 2017). Therefore, spliceogenic variants resulting in loss of function may manifest as CPVT. Indeed, a canonical splice site RYR2 variant c.6167-2A>G was recently identified in an individual with CPVT (Lieve et al., 2019). In the present study I proposed that some CPVT associated *RYR2* missense variants cause a loss of function by altering splicing, resulting in frameshifts and haploinsufficiency. I will investigate this using computational splice prediction tools and an *ex vivo* splicing assay.

3. Functional characterisation of a CPVT associated *RYR2* variant

The exact mechanisms by which *RYR2* variants cause arrhythmias and sudden death is not clear in all cases. Initially CPVT was a condition reported to be strictly associated with

adrenergic stimulation during stress or exercise, however reports of CPVT patients experiencing cardiac episodes in the absence of these triggers and with negative exercise stress tests is challenging this paradigm. Paech et al. (2014) identified the *RYR2* variant p.Lys4594Arg in a family that presented normal exercise stress tests but had a history of sudden death and arrhythmias; they stated "patients with *RYR2* variants but no induced ventricular arrhythmias during exercise stress testing are rather classified as idiopathic ventricular fibrillation, assuming a different arrhythmogenic mechanism" (Paech et al., 2014). It's possible that the arrhythmogenic mechanism in some RYR2 related arrhythmias differs from those of typical CPVT. To address this, I will introduce a variant into full length hRYR2 cDNA and study the effects of the variant on calcium handling in HEK 293 cells. The variant to be characterised will be from a patient that experiences cardiac episodes in the absence of triggers typically associated with CPVT such as stress and physical exercise.

Chapter 2: Materials and methods

2.1 Compilation of CPVT associated RYR2 variants

A comprehensive search for *RYR2* variants identified in individuals undergoing genetic testing for CPVT or an associated arrhythmia was performed. A total of 326 different *RYR2* variants was obtained from the North West Genomic Laboratory Hub, UK (a service that has been undertaking clinical diagnostic testing of *RYR2* for >10 years), the literature and clinical variant databases, including ClinVar and the Human Gene Mutation Database (HGMD). The literature search was performed on PubMed and Google Scholar using the search terms 'CPVT', 'RYR2 variant' and 'RYR2 mutation'. Both ClinVar and HGMD are freely accessible archives of the reports of genetic variants and their associated phenotypes. All sources of variant information were limited by the lack of detailed clinical information for most variants, which reduced the surety of CPVT diagnoses. This study could have been limited to those variants identified in patients with a confident CPVT diagnosis, but that would remove the potential of a significant proportion of *RYR2* variants being reclassified and aiding CPVT diagnosis. Allele frequencies of *RYR2* variants were obtained from the gnomAD and ExAC databases as comparators. The gnomAD and ExAC databases were accessed online from https://gnomad.broadinstitute.org and http://exac.broadinstitute.org, respectively. Variants obtained from gnomAD and ExAC were assumed have been detected in individuals without an arrhythmogenic phenotype. gnomAD was used because it was the largest control dataset available, which is useful when studying rare genetic diseases like CPVT and ExAC was used as comparator due its relatively smaller size and its popular use in studies before the release of gnomAD. gnomAD has age data for approximately 97,000 of the individuals tested and over a quarter of the data comes from individuals below the age of 50, thus there is the possibility some data is from patients with cardiac conditions that are yet to show symptoms. However, limiting the control dataset to only those individuals above the age of 50 will limit the power of the variant classification method used.

2.2 Phenotype-Genotype analysis

All *RYR2* variants both in control and CPVT populations were mapped to the domains, structural motifs and regions in which they are located in the RyR2 protein (using the

universal protein resource (UniProt) accession number Q92736) with Mutation Mapper from the cBio Cancer Genomics Portal (https://www.cbioportal.org/mutation_mapper). The mapping of variants to their location within the protein was performed in order to identify relationships between specific phenotypes and the location of their associated variants. As the crystal structure for RyR2 is limited to a portion of the N-terminal region some of the structural and functional information on domains is based on cryo-EM data from the RyR1 channel, and thus may not be completely accurate. For the purpose of our analysis *RYR2* regions that were not associated with any known functional or structural domains were individually labelled as 'no domain' followed by a number ranging from 1 to 9 corresponding to their protein location. The proportion of missense variants in each region/domain of *RYR2* in control and CPVT populations were compared using the Fisher's exact test using GraphPad prism. As comparisons were made not only between controls and the total CPVT population but also between subgroups of the CPVT population (like patients that experienced sudden death or sleep related sudden death), and the likelihood of erroneous inferences occurring are increased when making multiple comparisons, a more stringent p-value < 0.005 was considered significant.

2.3 Conservation analysis

The extent to which an amino acid or nucleic acid is conserved is largely influenced by its structural or functional importance. As a result of this a number of conservation tools (listed in section 2.4.5) were used in the reclassification of *RYR2* variants. Most conservation tools used were reported in a similar study by Denham et al. (2019) and were used to create some uniformity in the variant classification process. Separate to the conservation tools used by Denham et al (2019) Consurf (http://consurf.tau.ac.il/) was used to measure conservation of amino acid positions of variants in controls and CPVT patients. Consurf was used because it uses the Bayesian method as well as the maximum likelihood method for estimating conservation, resulting in more accurate conservation scores, as the Bayesian method is less dependent on the training data. The Consurf scores of the amino acid positions of control, CPVT and sudden death cases were compared using the Mann-Whitney test using GraphPad prism, p-value <0.005 was considered significant.

2.4 ACMG classification of *RYR2* variants

Recently the American College of Medical Genetics and Genomics and the Association for Molecular Pathology (ACMG-AMP) proposed guidelines to standardise the classification of genetic variants and overcome some of the challenges of sequence interpretation, like inconsistencies in the evidence required for a specific classification (Richards et al., 2015). The group responsible for producing the guidelines consisted of both clinicians and laboratory directors, they outlined a series of criteria based on commonly used variant evidence (like functional evidence and segregation data) to categorise variants into five groups (benign, likely benign, variant of uncertain significance, likely pathogenic and pathogenic). In this study *RYR2* variants were classified based on the 2015 ACMG-AMP guidelines (Richards et al., 2015). As reported by Denham et al. (2018) 12 of the 27 criteria listed in the ACMG-AMP guidelines were excluded from this study as they were considered non-applicable (Table 2.1). The application of these guidelines has been previously reported, with the exception of minor modifications (Table 2.2 and 2.3) (Denham et al., 2018).

Table 2.1. Removed ACMG classification rules. Adapted from Denham et al., (2019).

Rule	Reason for exclusion
PVS1 - Null RYR2 variant (nonsense, frameshift, canonical ±1 or 2 splice sites, initiation codon, single or multiexon deletion)	This study focused on the classification of *RYR2* missense variants.
PM3 - For recessive disorders, detected in trans with a pathogenic variant	This criterion applies to conditions with recessive inheritance and has therefore been removed.
PM6 - Assumed de novo, but without confirmation of paternity and maternity	This criterion was excluded as segregation data was unavailable for a significant proportion of variants and CPVT is characterised by incomplete penetrance.
PP2 - Missense variant in a gene that has a low rate of benign missense variation and in which missense variants are a common mechanism of disease.	The ACMG-AMP guidelines have included this as a criterion for genes with very little benign variation. While missense variants in RYR2 are well recognized as a cause of CPVT, the gene has a high background variation rate. Therefore, PP2 was not applicable for analysis of pathogenicity.
PP4 - Patient's phenotype or family history is highly specific for a disease with a single genetic etiology	This criterion has been removed based on the locus heterogeneity for CPVT.
PP5 - Reputable source recently reports variant as pathogenic, but the evidence is not available to the laboratory to perform an independent evaluation	This criterion was removed as no such reports exist at the time of the literature search
BS2 - Observed in a healthy adult individual for a recessive (homozygous), dominant (heterozygous), or X-linked (hemizygous) disorder, with full penetrance expected at an early age	This criterion has been removed based on the fact that CPVT is associated with incomplete penetrance and adult onset of disease
BP1 - Missense variant in a gene for which primarily truncating variants are known to cause disease	This criterion has been removed as missense variants are a recognized cause of CPVT
BP2 - Observed in trans with a pathogenic variant for a fully penetrant dominant gene/disorder or observed in cis with a pathogenic variant in any inheritance pattern	This criterion was removed as only *RYR2* variants were the inclusion criteria for the systematic analysis.
BP3 - In-frame deletions/insertions in a repetitive region without a known function	This criterion does not apply as only missense variants were analysed.
BP4 - Variant found in a case with an alternative molecular basis for disease	This criterion did not apply as there is no alternative pathophysiological basis for CPVT with a stronger evidence base than *RYR2*.
BP6 - Reputable source recently reports variant as pathogenic/benign, but the evidence is not available to the laboratory to perform an independent evaluation	This criterion was not deemed relevant to this study
BP7 - A synonymous (silent) variant for which splicing prediction algorithms predict no impact to the splice consensus sequence nor the creation of a new splice site AND the nucleotide is not highly conserved.	This criterion was removed as non-coding *RYR2* variants were excluded from the final analysis.

Table 2.2 Criteria for classifying variants. Adapted from Denham et al., (2019)

Criteria for classifying pathogenic variants			
	Strength of evidence	Original ACMG classification	Modified criteria for scoring variants
[P1] Null variant	Strong	PS1	Same amino acid change as a previously established pathogenic variant (with different nucleotide change)
[P2] De novo variant	Strong	PS2	De novo variant (both maternity and paternity confirmed) in a patient with CPVT and no family history
[P3] Functional implications of variant	Strong	PS3	Animal, calcium imaging, cellular electrophysiology and single channel studies analysis showing either a significant reduction or gain of channel function
[P4] Frequently reported unique variant	Strong	PS4	"Ultra-rare" variant (absent in gnomAD) reported in >5 unrelated individuals with CPVT. "Rare" (allele count below 4 in gnomAD) reported in >10 unrelated individuals with CPVT. Prevalence of the variant in affected individuals is significantly increased compared with the prevalence in controls
[P5] Critical location of variant	Moderate	PM1	Located in a well-established functional domain (transmembrane or pore-forming domain) of the ion channel. Does not apply if meeting [P1] null variant
[P6] Unique variant	Moderate	PM2	"Ultra-rare" (absent in gnomAD)
	Moderate	PM3	For recessive disorders, detected in *trans* with a pathogenic variant
[P7] Location of variant	Moderate	PM5	Novel missense change at an amino acid residue where a different missense change

associated with pathogenicity			determined to be pathogenic has been seen before
	Moderate	PM6	Assumed de novo, but without confirmation of paternity and maternity
[P8] Segregation of CPVT and variant	Supporting	PP1	Cosegregation with CPVT and/or complex phenotypes in multiple affected family members
	Supporting	PP2	Missense variant in a gene that has a low rate of benign missense variation and in which missense variants are a common mechanism of disease
[P9] Predicted implications of variant	Supporting	PP3	Agreement between ≥6 bioinformatic prediction tools that the variant is pathogenic
	Supporting	PP4	Patient's phenotype or family history is highly specific for a disease with a single genetic etiology
	Supporting	PP5	Reputable source recently reports variant as pathogenic, but the evidence is not available to the laboratory to perform an independent evaluation
Criteria for classifying benign variants			
[B1] Very high frequency in control population	Stand alone	BA1	Variants occurring more frequently than the maximum tolerated allele count in gnomAD
[B2] Higher frequency in control population	Strong	BS1	"Common" (present in ≥5 individuals in global gnomAD cohort)
	Strong	BS2	Observed in a healthy adult individual for a recessive (homozygous), dominant

			(heterozygous), or X-linked (hemizygous) disorder, with full penetrance expected at an early age
[B3] No functional implication of variant	Strong	BS3	Well-established in vitro functional studies show no effect on RyR2 channel function
[B4] Absence of segregation	Strong	BS4	Absence of segregation of variant evidenced by presence of one or more family members who are genotype-negative phenotype-positive for CPVT
	Supporting	BP1	Missense variant in a gene for which primarily truncating variants are known to cause disease
	Supporting	BP2	Observed in *trans* with a pathogenic variant for a fully penetrant dominant gene/disorder or observed in *cis* with a pathogenic variant in any inheritance pattern
	Supporting	BP3	In-frame deletions/insertions in a repetitive region without a known function
[B5] Predicted implications of the variant	Supporting	BP4	Agreement between ≤2 bioinformatic prediction tools that the variant is pathogenic
	Supporting	BP5	Variant found in a case with an alternate molecular basis for disease
	Supporting	BP6	Reputable source recently reports variant as benign, but the evidence is not available to the laboratory to perform an independent evaluation

	Supporting	BP7	A synonymous (silent) variant for which splicing prediction algorithms predict no impact to the splice consensus sequence nor the creation of a new splice site AND the nucleotide is not highly conserved

Table 2.3 ACMG guidelines for classifying DNA sequence variants.

Variant classifications	Rules		
Pathogenic	1 very strong	and one of:	(a) ≥1 strong (b) ≥2 moderate (c) 1 moderate and 1 supporting (d) 2 supporting
	≥2 strong		
	1 strong	and one of:	(a) ≥3 moderate (b) 2 moderate and 2 supporting
Likely pathogenic	1 very strong	and	1 moderate
	1 strong	and	(a) 1-2 moderate (b) 2 supporting
	≥3 moderate		
	2 moderate	and	2 supporting
Likely Benign	1 strong	and	1 supporting
Benign	1 stand alone		
	≥2 strong		
Variant of unknown significance	(a) Any above criteria not met		

(b) contradictory combination of pathogenic and benign criteria

2.4.1 Criteria for segregation

Pathogenic variants are likely to segregate with the disease phenotype within a family and not be present in unaffected relatives. The criteria for a variant to qualify for variant segregation (PP1) one or more of the following conditions were met: (1) the variant was present in two or more members of the same family with a CPVT like phenotype (arrhythmias, syncope, bradycardia or sudden death). The occurrence of affected individuals in whom the putative variant did not segregate was considered strong evidence for a benign classification (BS4).

2.4.2 Criteria for functional studies

Functional studies including animal models, calcium imaging, cellular electrophysiology and single channel analysis showing either a significant reduction or gain of function were considered strong evidence for pathogenicity (PS3). Conflicting functional data on variants was not considered as evidence. Functional studies that report no change in channel function were considered evidence for a benign classification (BS3).

Animal studies and studies on recombinant RYR2 were both included in this study as both have their advantages, animal studies report data on RyR2 channels composed of combinations of WT and mutant monomers which are more representative of channels in vivo, whereas although studies on recombinant RYR2 investigate channels consisting of only mutant monomers they are studying human RyR2 which may differ structurally and functionally from RyR2 in animal models.

2.4.3 Criteria for variant frequency

Variants that were absent from gnomAD were considered ultra-rare (PM2) and variants with an allele count of below 4 were considered rare as this was the frequency threshold for pathogenicity calculated using the statistical framework developed by Whiffin et al. (2017).

The frequency at which variants occurs in population databases such as gnomAD and EXAC provides some indication to variant pathogenicity. It is widely accepted that in order for a variant to cause a Mendelian disease, among other criteria, it must be absent from or occur at a sufficiently low frequency in population databases. Arbitrary cut of values of 1 and 0.1% are often used when filtering out variants thought to occur too frequently and are thus less likely to be disease causing. However, this method may lead to the use of cut off frequencies which are too lenient as it fails to take into account differences in disease prevalence which in some cases reflects the severity of the condition. To address this Whiffin et al. (2017) developed a statistical framework used to evaluate whether variants occur at frequencies low enough to cause penetrant Mendelian disease. To summarize, the statistical framework involves two stages the first of which is the determination of the maximum credible population allele frequency for a variant in *RYR2* that causes CPVT. This was calculated taking in to account the genetic nature of the condition. As CPVT is a dominant condition the maximum credible population allele frequency was defined using the approach outlined in Tables 2.4 and 2.5. Where the maximum allelic contribution is determined by the heterogeneity of the condition, it represents the maximum proportion of CPVT patients where the disease phenotype may be attributed to a single allele, for CPVT *RYR2* c.1258C>T (which results in amino acid change RyR2 Arg420Trp) is the most prevalent causative allele change, occurring in 10/487 cases and absent from control databases (ExAC and gnomAD). The highest disease prevalence estimate reported for CPVT in the literature was used. The maximum allelic contribution was calculated based on data available in the literature, Human Gene Mutation Database, ClinVar and from the genetic diagnostic laboratory at St. Mary's Hospital. Once the maximum credible population allele frequency was calculated this was multiplied by the number of samples in the control database to obtain the mean expected events in the population database.As the true population allele frequency of variants are unknown and estimates are based on population samples which are limited in size, a binomial distribution of the mean expected events in the population database was generated for our sample of CPVT cases (observed allele number) and the upper bound of the 95% confidence interval (the maximum tolerated allele count) was used as the cut off frequency. Variants that occurred more frequently than the maximum tolerated allele count in ExAC or gnomAD were considered common and this was strong evidence for a benign classification (BS1).

This method of identifying benign variants may be effective for variants that occur commonly in control databases like gnomAD, however, it is ineffective at identifying rare benign variants which have been shown to be common in control datasets. For instance, 1600 of the 1975 (81%) *RYR2* missense variants reported in gnomAD have a minor allele count below four. For such variants other criteria like functional studies or computational data will play a more important role in variant classification.

Table 2.4 Calculation of the maximum tolerated allele count for a CPVT RYR2 variant using gnomAD.

number of cases with Arg420Trp mutation/ total number of CPVT cases with RYR2 mutations	10/440	
binomial confidence interval	0.023 (0.012 - 0.041)	
upper bound of the maximum allelic contribution	0.041	
prevalence per individual	0.0001	
number of chromosomes	2	
allelic prevalence	0.00005	prevalence/chromosomes
penetrance (Napolitano et al., 2013)	0.6	
Number of samples in population database (gnomAD)	251496	
Maximum Credible population allele frequency	3.44167E-06	allelic prevalence*max allele contribution/penetrance
mean expected events in population database	0.866	no of samples*max credible allele frequency
Max tolerated allele count	3	upper 95% CI of expected events

Table 2.4. Outline of the statistical framework used to identify variants that occur too frequently in the gnomAD database to be pathogenic (Whiffin et al., 2017). The maximum credible population allele frequency for a missense variant in RYR2 that causes CPVT was calculated based on CPVT being a dominant condition with a penetrance of approximately 60% (Napolitano et al., 2013). A binomial distribution of the maximum credible allele frequency was generated for our sample of CPVT cases (observed allele number) and the upper bound of the 95% confidence interval (the maximum tolerated allele count) was used as the cut off frequency. Variants that occurred more frequently than the maximum tolerated allele count in gnomAD were considered common and this was strong evidence for a benign classification (BS1).

Table 2.5 Calculation of the maximum tolerated allele count for a CPVT RYR2 variant using ExAC.

number of cases with Arg420Trp mutation/ total number of CPVT cases with RYR2 mutations	10/440	
binomial confidence interval	0.023 (0.012 - 0.041)	
upper bound of the maximum allelic contribution	0.041	
prevalence per individual	0.0001	
number of chromosomes	2	
allelic prevalence	0.00005	prevalence/chromosomes
penetrance (Napolitano et al., 2013)	0.6	
Number of samples in population database (gnomAD)	121412	
Maximum Credible population allele frequency	3.44167E-06	allelic prevalence*max allele contribution/penetrance
mean expected events in population database	0.418	no of samples*max credible allele frequency
Max tolerated allele count	2	upper 95% CI of expected events

Table 2.5. Outline of the statistical framework used to identify variants that occur too frequently in the ExAC database to be pathogenic (Whiffin et al., 2017). The maximum credible population allele frequency for a missense variant in RYR2 that causes CPVT was calculated based on CPVT being a dominant condition with a penetrance of approximately 60% (Napolitano et al., 2013). A binomial distribution of the maximum credible allele frequency was generated for our sample of CPVT cases (observed allele number) and the upper bound of the 95% confidence interval (the maximum tolerated allele count) was used as the cut off frequency. Variants that occurred more frequently than the maximum tolerated allele count in ExAC were considered common and this was strong evidence for a benign classification (BS1).

2.4.4 Criteria for variant enrichment in CPVT cases

Enrichment analysis involves the identification of associations between variants and phenotypes that occur too frequently to be attributed to chance. Ultra-rare and rare variants were considered for variant enrichment analysis. The presence of an ultra-rare or rare variant in at least five or ten CPVT cases, respectively, was considered as strong evidence (PS4). This analysis was performed with the assumption that CPVT is caused by single genetic variants as there is no evidence to date of oligomeric cases of CPVT, however, with the cause of CPVT being unknown in approximately 50 % cases this is a possibility that cannot be excluded.

2.4.5 Criteria for computational evidence

Most computational prediction tools are based on measures of evolutionary sequence conservation and/or structural properties, databases of known homologous sequences and structures are used for analysis. As previously reported by Denham *et al.* (2019), five protein-level in silico prediction tools: SIFT, PolyPhen, Mutation Taster, Mutation assessor, FATHMM and three conservation tools GERP++, PhyloP conservation and SiPhy were used for our computational analysis (to remain consistent with previous studies GERP++, PhyloP, and SiPhy scores of 4.4, 1.6, and 12.17, respectively were set as thresholds for conservation) (Table 2.6). A prediction of pathogenicity by six or more *in silico* tools was interpreted as supporting evidence for pathogenicity, whereas a prediction of pathogenicity by less than 2 tools was interpreted as evidence in support of a benign classification. Computational tools were accessed through Ensembl's Variant Effect Predictor (https://www.ensembl.org/Tools/VEP). Using a threshold of six computational tools being in agreement is likely to reduce the number of false positives. However, this does not take into account some tools may be more effective at predicting the pathogenicity of particular variants, for instance PolyPhen may be better suited for predicting the pathogenicity of variants that cause structural changes as it considers structural information compared to tools like SIFT which do not, increasing the likelihood of false negatives.

Table 2.6 Algorithm by which the various tools predict pathogenicity and/or conservation

Pathogenicity/ conservation tool	Tool prediction algorithm
SIFT	SIFT measures the probability of an amino acid substitution affecting functional properties of the protein, the method considers sequence homology and the difference in the physico-chemical properties of the alternate amino acids.
PolyPhen	PolyPhen measures the probability of an amino acid substitution affecting structural and functional properties of a protein. PolyPhen uses sequence homology and structural information from databases like the Protein Data Bank (PDB).
Mutation Taster	Mutation taster uses a number of integrated tools like ClinVar, ExAC and phyloP to identify benign polymorphisms. The conservation of the amino acid positions altered by the SNPs that are not filtered out is measured using phyloP. Mutation taster also considers the loss of functional domains, shortening of the protein and effects on splicing.
Mutation assessor	Mutation Assessor predicts the effect an amino acid change will have on the functional properties of a protein. Mutation Assessor measures the evolutionary conservation of the amino acid position where the change occurs using protein homologs.
FATHMM	FATHMM creates multiple sequence alignments with homologous sequences and uses this to create a hidden markov model (HMM) in which conservation is measured through the match states in the model (a match state represents the probability of an amino acid occurring at a position, this is based on the make-up of the column within the sequence alignment). Also, the conservation of positions within HMMs manually constructed by aligning conserved protein domains is measured, this allows the consideration of important structural and evolutionary constraints that may be overlooked using when using automatically generated multiple sequence alignments of homologous sequences.
GERP++ (Genomic Evolutionary Rate Profiling)	GERP creates multiple sequence alignments with homologous sequences and identifies constrained sequences by comparing the level of variation at an amino acid position to the level expected in the absence of functional constraint.

PhyloP conservation	Unlike hidden markov models PhyloP measures conservation within each column of a multiple sequence alignment independent of neighbouring columns. PhyloP can measure both evolutionary conservation and acceleration and generates p-values for these measurements.
SiPhy	SiPhy uses a HMM to identify constrained and non-constrained sequences. Analysis of multiple sequence alignments of homologous sequences identifies unlikely substitution patterns and evolutionary conservation/acceleration.

2.4.6 Criteria for critical functional domain

The location of a missense variant in the transmembrane 4-6 region or ion-trans domain of the protein was considered as moderate evidence for a pathogenic classification, as the functional significance of these regions have been established (Liu et al., 2015). Other RyR2 domains were not considered critical functional domains as RyR2 channels with entire N-terminal domain removed have been shown to be functional (Liu et al., 2015).

2.5 Splicing predictions

As investigating all *RYR2* variants using an in vitro minigene assay would be impractical computational tools were used to select those variants most likely to alter splicing. To remain consistent with a previous study by Thery et al. (2011) in which 5 out of 12 exonic variants predicted to alter splicing using computational tools were found to alter splicing using a minigene assay, the effect variants are likely to have on splicing was predicted computationally using Alamut version 2.0 (Interactive Biosoftware, Rouen, France). Alamut incorporates five splicing prediction tools that use a variety of algorithms (Table 2.7). Those variants in which a 100% change was seen in the confidence score for the presence or absence of a splice feature in the WT compared to the variant were chosen to be studied in the *ex vivo mini* gene assay. Using this method decrease the chances of obtaining false positives, however, as some tools may be more effective at predicting the effects of particular splice variants than others such methods increase the likelihood of obtaining false negatives. Furthermore, other tools could have been used in combination

with the tools used in this study that are better able to predict the effects variants have on exonic splicing enhancers and suppressors (Cartegni et al., 2003).

Table 2.7 Algorithm by which the various tools predict splicing effects.

Splicing tool	Splice prediction algorithm
NNSplice http://www.fruitfly.org/seq_tools/splice.html	NNSplice uses a neural network that identifies motifs with consensus sequences. It also takes into account commonly occurring neighbouring sequences (Jian et al., 2014).
SpliceSiteFinder-like https://www.interactive-biosoftware.com/doc/alamut-visual/2.6/splicing.html	SpliceSiteFinder-like uses position weight matrices developed from a database of human exon/intron boundaries for both donor and acceptor sites.
MaxEntScan http://genes.mit.edu/burgelab/maxent/Xmaxentscan_scoreseq.html	The maximum entropy principle is used to model sequence motifs. The short sequence motifs involved RNA splicing are modelled with a maximum energy distribution (Yeo and Burge, 2004).
Human Splicing Finder http://www.umd.be/HSF/	Human splicing finder uses position weight matrices supplemented with position-based logic. Each nucleotide is assigned a weight, the assigned weight is dependent on the frequency of the nucleotide and the comparative importance of its location within the sequence motif (Desmet et al., 2009).
GeneSplicer http://ccb.jhu.edu/software/genesplicer/	GeneSplicer uses a combination of a second order Markov model and the maximal dependence decomposition decision tree method. Markov models predict a base by studying the surrounding bases. In this case a region consisting of the 16 and 29 bases is scored for donor sites and acceptor sites, respectively. The MDD aligns a set of sequences of varying sizes and creates a model that incorporates the most vital dependencies from one position to another (Pertea et al., 2001).

2.6 Primer design

The Primer3 software (http://bioinfo.ut.ee/primer3-0.4.0/) was used to design all primers. Primers were designed using the default settings. Only those primers without SNPs were used, the absence of SNPs was confirmed using SNPCheck (https://secure.ngrl.org.uk/SNPCheck/snpcheck.htm). Primers were purchased from Sigma-Aldrich, (Sigma-Aldrich, St. Louis, MO, USA) in water at a concentration of 100 µM.

2.7 DNA and RNA quantification

DNA and RNA samples were quantified using a NanoDrop 8000 spectrophotometer (ThermoFisher Scientific Inc, Waltham, MA, USA).

2.8 Agarose gel electrophoresis

The size of PCR products was determined by running 25 µL of PCR product on a 1% (w/v) agarose gel (1 g of agarose in 100 mL of Tris/Borate/EDTA (TBE) buffer) with a 1 Kb Plus DNA Ladder (Invitrogen, Carlsbad, CA, USA). To allow the visualization of DNA 8 µL of Safe View (NBS Biologicals, Huntingdon, UK) was added to agarose gels. PCR products were run in a gel tank filled with TBE buffer for 45 minutes at 70 V before gels were viewed under a UV light.

2.9 HEK293 cell maintenance and subculture

The immortalised HEK 293 cell line was used for both minigene assays and calcium imaging experiments. This cell line was chosen because HEK 293 cells are adherent cells and do not express RYRs or any of its luminal accessory proteins, thus calcium release events are attributable to the action of recombinant RyR2. Furthermore, the transfection efficiency in HEK 293 cells is high and the calls efficiently translate proteins. A potential disadvantage of using HEK cells is both the splicing process and calcium handling may vary between HEK cells and cardiomyocytes.

HEK 293 cells obtained from the European Collection of Authenticated Cell Cultures (ECACC) were cultured with cDMEM (complete DMEM, Dulbecco's modified eagle's medium, with 10 % (v/v) fetal calf serum and 2 % (w/v) Penicillin-Streptomycin-Glutamine) (Thermo Fisher Scientific Inc, Waltham, MA, USA). The cells were cultured at

37 °C at 5 % CO_2 in T75 cm^2 culture flasks in a ThermoScientific HeraCELL 240i CO_2 incubator.

HEK cells were routinely passaged every 2-3 days to avoid cultures becoming over confluent. Cells were washed twice with 7.5 mL of phosphate buffered saline (PBS, Gibco, Waltham, MA, USA) before being trypsinized for 1 minute with 0.25 % Trypsin EDTA (Gibco, Waltham, MA, USA). The action of trypsin was neutralised after one minute with the addition of 9 mL of cDMEM. Cells were mixed by gentle pipetting and transferred into a 15 mL tube in preparation for centrifugation.

Cells were counted using a haemocytometer. Once the number of cells suspended in media was determined the cells were pelleted by centrifugation at 1000x g for 5 minutes using an Allegra 6R centrifuge, Beckman. Cells were resuspended in the necessary volume of cDMEM to achieve the desired concentration and transferred to fresh plates.

2.10 Amplification of *RYR2* fragments for Gibson assembly

The 3.8 kb pSpliceExpress minigene splicing reporter vector gifted from Stefan Stamm (Addgene plasmid # 32485; http://n2t.net/addgene:32485 ; RRID:Addgene_32485) was used for the minigene assays. The pSpliceExpress vector contains sites that allow the insertion of DNA fragments with ends that overlap with the ends of the plasmid. The inserted DNA sequence is positioned between two rat insulin exons which during the splicing process are spliced together with the inserted exon. The pSpliceExpress minigene was used over minigenes generated by conventional cloning due to the faster speed splicing reporter constructs can be generated and the ability to clone any DNA fragment as the use of restriction enzymes is not necessary.

The 3.8 kb pSpliceExpress minigene splicing reporter vector was amplified by PCR with Phusion High-Fidelity DNA Polymerase (Thermo Fisher Scientific Inc, Waltham, MA, USA) and restriction digested with either NheI/BamHI (Thermo Fisher Scientific Inc, Waltham, MA, USA) to produce sticky ends. Two halves of an *RYR2* DNA sequence containing an exon of interest as well as ~100 bp of the flanking 5' and 3' intronic sequences were amplified separately by PCR from genomic DNA using Phusion High-Fidelity DNA Polymerase. This was done using two primer pairs that were designed to generate two fragments that overlap with each other at one end and the vector fragment at the other

ends, by approximately 20 bp and 10 bp, respectively. Overlapping primer sequences were modified where needed in such a way to produce CPVT associated *RYR2* variants. ~100 bp of the flanking 5' and 3' intronic sequences were included as in most reported cases regulatory elements are in close proximity to regulated exons. One study showed that the intronic sequences flanking alternatively spliced exons were conserved suggesting some regulatory function, however, the level of conservation decreased in regions further away from the regulated exon. The average length of the conserved intronic sequences was approximately 100 bp both downstream and upstream from the regulated exon (Sorek and Ast, 2003). There are cases where regulatory elements are up to 1 kb away from the regulated exon and with the method used in this study effects on regulatory elements over ~100bp from the exon studied would not be detected (Gallegos and Rose, 2019).

The generation of the two overlapping fragments by PCR was performed with the following reaction constituents: 10 µL GC Buffer, 1 µL dNTPs, 2.5 µL forward primer at 10 mM, 2.5 µL reverse primer at 10 mM, 0.5 µL Phusion Polymerase, 32.5 µL water, 1 µL Genomic DNA. The PCR program used is detailed below (Table 2.8).

Table 2.8 PCR conditions

Stage	Temp °C	Time
1	98	30 sec
2 (35 cycles)	98	10 sec
	54-60	30 sec
	72	40 sec
3	72	10 min
	4	Hold

2.11 Purification of PCR products

After being amplified by PCR the two overlapping fragments and pSpliceExpress minigene splicing reporter vector were purified before being ligated together using the Gibson method. The purification of PCR products removes components of the PCR reaction like dNTPs, primers and enzymes, which I found reduced the efficiency of the Gibson assembly reaction. The purification of PCR samples was performed using a QIAquick PCR

purification kit (Qiagen, Hilden, Germany) according the manufacturer's instructions and DNA was eluted in 30 µL of elution buffer.

2.12 Gibson assembly

The overlapping *RYR2* DNA fragments and the PspliceExpress vector fragment for the minigene assays were ligated together using the Gibson Assembly cloning kit (New England Biolabs, Ipswich, MA, USA) according to the manufacturer's protocol (Figure 2.1). The Gibson assembly method involves the use of a 5' exonuclease to generate sticky ends or overhangs on a DNA fragment that compliments the sticky ends of the fragment in which it will be joined to. The gaps created by the exonuclease are filled by a polymerase enzyme and a DNA ligase seals the nicks between the two fragments. The Gibson method was chosen because multiple DNA fragments can be joined simultaneously in a single reaction without the need for compatible restriction sites, allowing both the incorporation of the variant of interest into the DNA sequence being studied and the insertion of the DNA fragments into the pSpliceExpress vector.

Briefly, to perform DNA ligation using the Gibson method 50 ng of vector DNA was mixed with 250 ng of fragment 1 DNA and 250 ng of fragment 2 DNA. The DNA was then added to 10 µL of 2X Gibson Assembly Master Mix and the resulting mixture was made up to 20 µL with deionized water. The sample was incubated at 50 °C for 30 minutes. The resulting circularized DNA was transformed into *E. coli* cells.

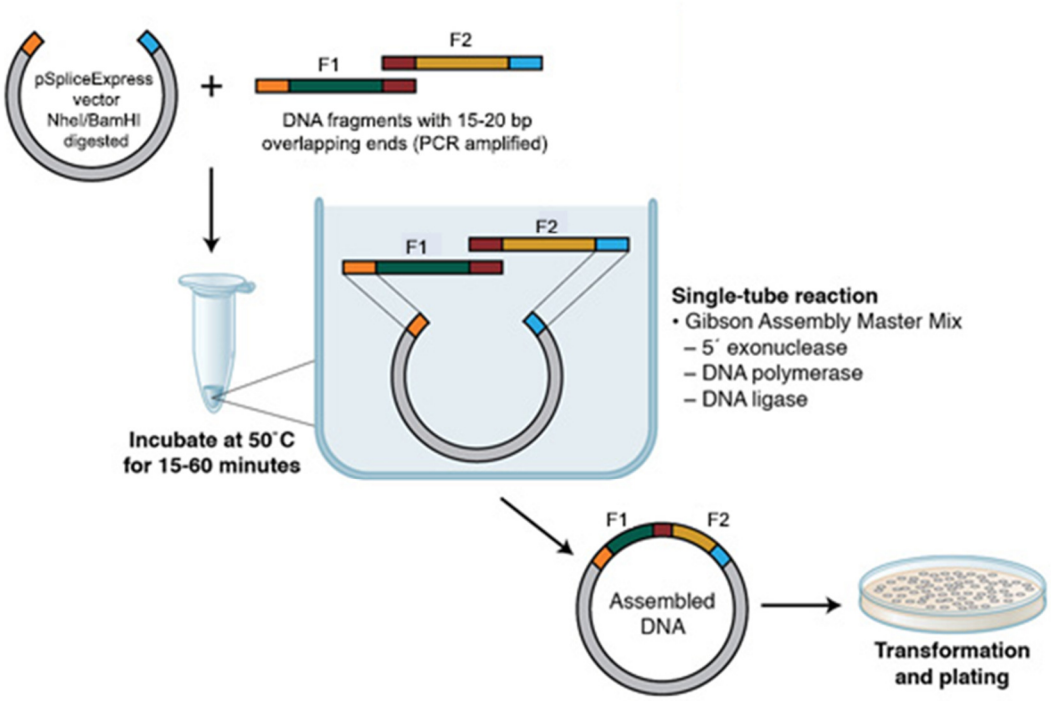

Figure 2.1. Diagrammatic outline of plasmid DNA assembly using Gibson method. Adapted from https://international.neb.com/applications/cloning-and-synthetic-biology/dna-assembly-and-cloning/gibson-assembly

2.13 Bacterial transformation and culture

In order to propagate plasmid DNA it was transformed into highly competent bacterial cells, XL-10 (XL10-gold, Agilent Technologies, Santa Clara, CA, USA). XL-10 cells were used because they grow faster and produce larger colonies and although more susceptible to spontaneous intraplasmid recombinations than Stbl2 cells, which were used for the propagation of full length RYR2, this did not affect the propagation of the pSpliceExpress vector. XL-10 cells (50 µL) were thawed on ice and approximately 1 ng of plasmid DNA was added to the cells before gently mixing them. The plasmid DNA-cell mixture was then incubated on ice for 30 minutes before being heat shocked in a 42 ˚C water bath for 30 seconds. The cells were then incubated on ice for 2 minutes. NZY broth (500 µL) kept at room temperature was added to the cells before and they were incubated at 37 ˚C for an hour before 200 µL of the cell suspension was taken and spread on an LB (Luria-Bertani media: 10 g/L Tryptone, 5 g/L Yeast Extract, 5 g/L NaCl (Sigma-Aldrich, St. Louis, MO,

USA)) agar plate containing carbenicillin (100 mg/mL). The plates were incubated over night at 37 ˚C and were observed for colonies the next morning. Single colonies were picked and suspended in 6 mL of LB broth supplemented with ampicillin, the cells were incubated overnight at 37 ˚C while being shaken at 225 rpm.

2.14 Small-scale Purification of Plasmid DNA from bacterial cells

The small-scale isolation of DNA from bacterial cells was performed using the QIAprep Spin Miniprep Kit (Qiagen), a kit that is designed for the purification and isolation of up to 20 µg of plasmid DNA. Small scale DNA purification was performed either to restriction digest the isolated DNA to ensure full length *RYR2* had been propagated without spontaneous recombination occurring, or for the minigene assays to transfect HEK 293 cells as this quantity of plasmid DNA was sufficient to study the effects of variants on splicing. The procedure was carried out following the manufacturer's instructions. Bacterial cell pellets were resuspended in 250 µL of buffer P1 containing RNase A and EDTA. The EDTA in buffer P1 prevents DNases from damaging the plasmid DNA to be purified by chelating divalent cations, it also weakens the cell membrane. RNase degrades cellular RNA released once the cells are lysed. The cells were then lysed using the alkaline lysis method by adding 250 µL of solution P2 (containing NaOH and SDS) and mixed by inverting them repeatedly. The solution was then neutralised with 350 µL of solution P3 before being centrifuged at 14,000 rpm for 10 minutes at 4 ˚C in the QIAprep Spin Column. DNA is selectively adsorbed onto the silica-gel membrane in the spin column at the high salt concentrations produced by the neutralization buffer. The flow through was discarded and the column was washed by adding 500 µL of high salt concentration PB buffer and centrifuging for 1 minute. The column was washed further by adding 750 µL of high salt concentration PE buffer and centrifuging for 1 minute at 14,000 rpm. After both washes the flow-through was discarded. The columns were then centrifuged for 2 minutes to remove any remaining buffer. The column was then placed in a collection tube before adding 30 µL of ddH_2O and centrifuging for 1 minute at 14,000 rpm to elute the DNA. The QIAprep Spin Miniprep Kit was used because it alleviates the need to perform time consuming phenol–chloroform extraction and alcohol precipitation steps.

2.15 Sanger sequencing

The insertion of the correct fragments into the pSpliceExpress minigene splicing reporter vector and introduction of the correct single nucleotide change was confirmed by Sanger sequencing using “minigene RT PCR-for” and “minigene RT PCR-rev” primers. Sanger sequencing was performed externally by Eurofins (Eurofins, GSC, LUX). Sequencing traces were analysed using SNAPgene.

2.16 Lipofectamine transfection

Plasmid DNA (0.2 µg) was transfected into HEK 293 cells for the minigene assays, where the splicing machinery of the cell was utilized to produce mRNA. HEK 293 cells were transfected at confluence of 40-60% grown in Dulbecco’s modified Eagle’s medium high-glucose, DMEM (Thermo Fisher Scientific Inc, Waltham, MA, USA), supplemented with 10 % foetal bovine serum (Thermo Fisher Scientific Inc, Waltham, MA, USA) in tissue-culture treated 6-well plates at 37 °C and with 5 % CO_2. Transfections were performed using Lipofectamine 2000 (Thermo Fisher Scientific Inc, Waltham, MA, USA) according to the manufacturer’s protocol. Lipofectamine contains lipid molecules that form liposomes that take up DNA molecules, the positively charged surface of the liposomes enables them to fuse with the negatively charged plasma membrane allowing the entrapped DNA molecules to cross the membrane into the cytoplasm where they can be replicated or expressed. Lipofectamine was used because of its superior transfection efficiency, partly due to lipofectamine/DNA complexes evading metabolic degradation by the random Brownian motion of the complexes within the cytoplasm (Cardarelli et al. 2016). The Brownian motion does not utilize microtubules in the active transport of lipid/DNA complexes unlike the movement of numerous other lipid based DNA complexes, the microtubule dependent active transport of lipid/DNA complexes may increase the transport of lipid/DNA complexes to lysosomes (Wang and Macdonald, 2004).

To transfect HEK 293 cells with plasmid DNA 2.5 µL of lipofectamine was mixed with 250 µL of Otpi-MEM (reduced serum medium (Life Technologies, Carlsbad, CA, USA)). 200 ng of plasmid DNA was mixed with 250 µL of Opti-MEM. The two mixtures were added together and allowed to sit for 25 minutes before being gently added to the cells. RNA

was extracted from HEK 293 cells after a 48-hour incubation period in at 37 °C with 5 % CO_2, using phenol/chloroform precipitation using Trizol.

2.17 RNA extraction and purification

RNA was extracted from HEK 293 cells transfected with the pSpliceExpress vector containing the exons of interest and flanking intronic sequences to study the effects the variants had on splicing. RNA was extracted using Trizol. Trizol reagent contains guanidinium isothiocyanate a potent protein denaturant that prevents the degradation of RNA by inactivating RNases. Trizol reagent also contains a monophasic solution of phenol that allows RNA to be separated into the aqueous phase of the solution when mixed with chloroform. Trizol reagent was used to isolate RNA because of its speed and reliability, other methods like the spin column method can suffer from low yields due to the membrane becoming clogged or contamination with DNA or proteins.

To extract RNA HEK 293 cells were washed twice each time with 7.5 ml of PBS. 1 ml Tri Reagent (Sigma-Aldrich, St. Louis, MO, USA) was added to the cells and the resulting cell suspension was passed through a pipette multiple times to homogenize the lysate before transferring it to a 1.5 mL tube. The cell homogenate was allowed to stand for 5 minutes at room temperature. 200 µL of chloroform was added to the cells and they were shaken vigorously for 15 seconds, and then allowed to stand for 15 minutes at room temperature. The resulting mixture was centrifuged for 15 minutes at 4 °C at 12000 rpm. 500 µL of the upper aqueous phase produced was transferred to a 1.5 mL tube and 500 µL isopropanol was added to the tube, the mixture was mixed by inverting the tube several times and allowed to stand for 5 minutes. The mixture was then centrifuged at 12000 rpm for 10 minutes. The supernatant was removed and discarded, and the resulting RNA pellet was washed with 500 µL of 75 % (v/v) ethanol. The RNA pellet was reformed by centrifugation. RNA was allowed to air dry for 10 minutes before being resuspended in water 21.5 µL of RNase-free water.

2.18 DNase treatment

As all RNA samples contain trace amounts of contaminants such as DNA which can affect the purity and reliability of the RT-PCR products DNase treatment was carried out with the Invitrogen DNA free kit using the manufacturer's instructions (Invitrogen, Carlsbad,

CA, USA). The DNA-free kit was used as it contains DNase I for the total degradation of contaminating DNA and also a DNase removal agent that quickly removes DNases from RNA samples without the need for heat inactivation of DNases that can damage RNA.

The DNase treatment of RNA samples was performed as follows: 2 µL of 10x DNase and 1 µL of rDNase I was added to 2 µg of total RNA before incubating the mixture at 37 °C for 1 hour. 2 µL of DNase inactivating beads were added to the RNA, which was then mixed every 30 seconds for 2 minutes. The mixture was centrifuged at 12000 rpm for 2 minutes and 20 µL of the RNA containing supernatant was removed. RNA was quantified as previously described in section 2.7 and diluted to 500 ng/µL with RNase-free water.

2.19 Reverse transcription

Superscript Reverse Transcriptase II (Thermo Fisher Scientific Inc, Waltham, MA, USA) was used to synthesise cDNA from the RNA extracted from HEK cells transfected with the pSpliceExpress vector containing exons of interest according to the manufacturers protocol. Superscript Reverse Transcriptase II is a genetically engineered Moloney Murine Leukemia Virus Reverse Transcriptase with lower RNase H activity and greater thermal stability in comparison to the WT. These qualities make Superscript Reverse Transcriptase II ideal for reverse transcribing RNAs of various lengths and with strong secondary structures as the higher temperatures denature strong secondary structures that may cause the reverse transcriptase to stall.

Reverse transcription with Superscript Reverse Transcriptase II was performed as follows: 2 µL of total RNA at 500 ng/mL was added to 1 µL of random hexamers (500 µg/mL), 1 µL dNTP (10 mM) and 9 µl water. The mixture was heated at 65 °C and then placed on ice before the addition of 4 µl of 5X first strand buffer and 2 µl of 0.1 M DTT. The sample was then heated for 2 minutes at 42 °C. 1 µL of Superscript II reverse transcriptase was added to the sample which was incubated at 42 °C for 50 minutes and then at 72 °C for 15 minutes. The cDNA produced was amplified using Phusion High-Fidelity DNA Polymerase (Thermo Fisher Scientific Inc, Waltham, MA, USA) as previously described using “minigene RT PCR-for” and “minigene RT PCR-rev” primers. The resulting PCR products were electrophoresed on an agarose gel (1 %), to establish the sequence of the spliced

products the purified DNA was sequenced by direct Sanger sequencing performed by Eurofins Genomics.

2.20 Purification of DNA from agarose gels

DNA was purified from agarose gels using a QIAquick Gel Extraction Kit (Qiagen, Hilden, Germany) according to the manufacturer's protocol. The QIAquick Gel Extraction Kit uses spin columns with silica-membranes that bind DNA at high salt concentrations. This method was used because its faster and allows the extraction of DNA in smaller volumes of water, so the DNA concentration is higher compared to electroelution methods.

2.21 Full-length human *RYR2*-eGFP

To study the effects of the RYR2-Phe4905Leu variant the cDNA sequence encoding full-length human *RYR2* with an N-terminus enhanced green fluorescent protein (eGFP) tag in the mammalian expression vector PCDNA3 (pcDNA3-eGFP-hRyR2) was obtained from Dr Christopher George (George et al., 2003). The use of a single sequence of *RYR2* cDNA does not take into account SNPs that may be present the patients DNA and affect the impact of the variant on RyR2 activity. The eGFP tag that was used to assess the efficiency of *RYR2* transfection was used because it has been shown not to affect RyR2 channel function (Thomas et al., 2004).

2.22 Production of *RYR2* cassettes

Due to the large size of the full length *RYR2* cDNA which increases its susceptibility to damage and spontaneous recombination, restriction enzymes were used to produce smaller *RYR2* fragments (cassettes) that were easier to mutagenize. Furthermore, the selected method for mutagenesis of *RYR2* cDNA was site directed mutagenesis which is limited to the alteration of DNA sequences of up to approximately 8 kb in length, the full length *RYR2* cDNA plasmid is over 21 kb and thus cannot be mutagenised using this method. Restriction enzymes are enzymes that cleave DNA at specific recognition sites by cleaving the sugar phosphate backbone on each strand of the double helix, for this study restriction enzymes were purchased from (Qiagen, Hilden, Germany). Restriction digests were performed according to the manufacturer's instructions with 1 µg of DNA, 1-10 U of High Fidelity endonuclease and 1x endonuclease buffer made up to 20 µL with distilled

water. Reactions were carried out in a 37 °C water bath for 30 minutes and the resulting DNA fragments were run on an agarose gel and extracted.

The introduction of the Phe4905Leu (c.14713T>C) variant was performed using NheI/XhoI *RYR2* fragment (5320 bp) subcloned into pSL118ONX (Amersham Biosciences, UK). pcDNA3-eGFPhRyR2 was digested with the restriction enzymes NheI/XhoI as previously described. The resulting DNA fragments were gel electrophoresed and then extracted and purified. The purified NheI/XhoI *RYR2* fragment and the pSL118ONX vector were ligated together using the Roche Rapid DNA ligation kit (Roche, Basel, Switzerland) using the manufacturer's protocol. 50 ng of DNA containing NheI/XhoI *RYR2* fragment DNA mixed with vector DNA at a ratio of 3 moles to 1 was added to T4 DNA ligase at a concentration of 5 U/µL and ligase buffer. The reaction mixture was incubated for 16 hours at 4 °C. The resulting intermediate plasmid containing the *RYR2* c-terminal cassette was transformed into XL-10 competent cells, propagated and purified as previously described.

2.23 Site directed mutagenesis

Site directed mutagenesis was performed on the intermediate vector containing the *RYR2* C-terminal cassette using the Quick Change XL kit (Agilent Technologies, Santa Clara, CA, USA), introducing the *RYR2* c.14713T>C change which results in the replacement of Phe with Leu at the amino acid position in the inserted fragment corresponding to position 4905 in the full length RyR2 sequence (Figure 2.2). The contents of the site directed mutagenesis reaction are listed in table 2.9 and the thermocycling parameters used are listed in table 2.10.

Site directed mutagenesis involves a PCR reaction using two complementary oligonucleotide primers that bind to the DNA fragment introduced into the intermediate vector and contain a complementary mismatch that corresponds to the single nucleotide change to be inserted in the DNA fragment. The PCR reaction amplifies the DNA vector containing the inserted fragment and variant of interest. The main disadvantage of using site directed mutagenesis is the generation of products with additional unwanted mutations due to the error prone nature of particular DNA polymerases, this was overcome by using Phusion High Fidelity DNA Polymerase which has a high level of accuracy. After the site-directed mutagenesis reaction was complete 1 µL of the DpnI

enzyme was incubated with the reaction product for 90 minutes at 37 °C. DpnI is a restriction endonuclease that specifically digests methylated DNA, and so it digested the plasmid template DNA used in the SDM reaction, which is methylated as it was purified from E. coli, but DpnI did not digest the newly formed and mutated plasmid DNA produced during the site-directed mutagenesis reaction. The resulting plasmid DNA with the mutated RYR2 fragment insert was then transformed into XL-10 competent cells for propagation and isolated as previously described in section 2.14. The correct mutagenesis of the inserted fragment was confirmed by Sanger sequencing.

Oligonucleotides used for SDM:

Forward primer: CACAGTGCCACATGGCCTTGAAACCCACACTTTACAGG

Reverse primer: CCTGTAAAGTGTGGGTTTCAAGGCCATGTGGCACTGTG

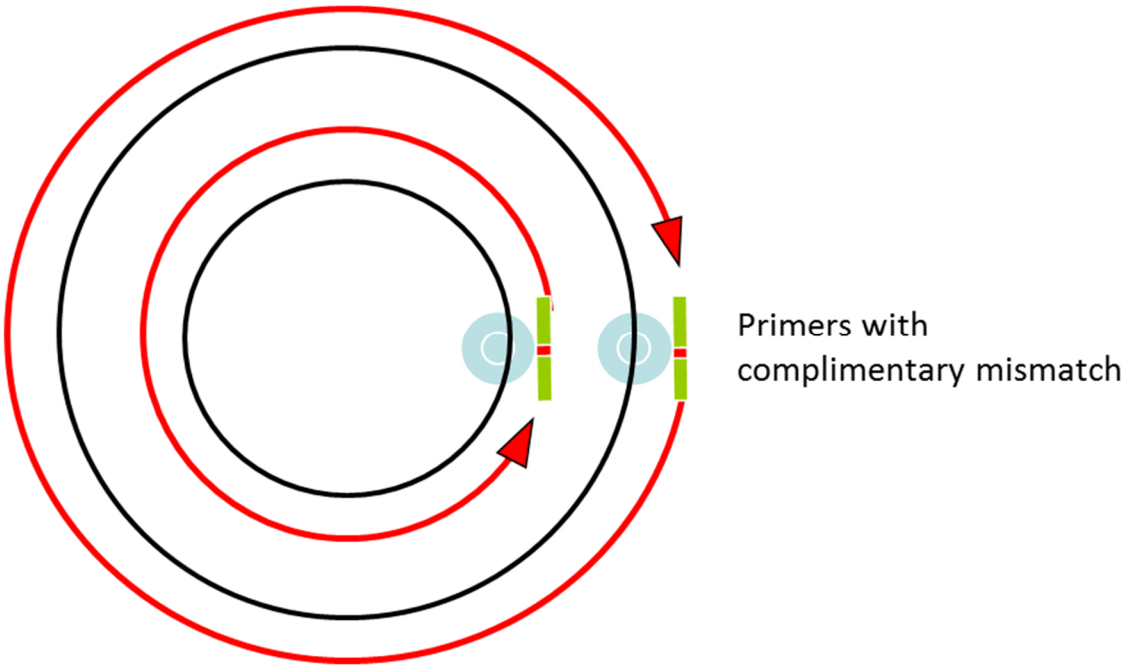

Figure 2.2. The variant was introduced into the *RYR2* fragment in the intermediate vector. This was done using a PCR reaction using two complementary oligonucleotide primers (green rectangles) and the intermediate vector containing the *RYR2* fragment as a template (black circles). The primers each contain a complementary mis-match (red squares) (i.e. the base that needs to be changed), and are designed so that this mis-matched base is at the centre of the long primers, ensuring significant H-bonding on either side. After thermal cycling, the product DNA (red circle) is treated with the endonuclease DpnI, which is specific for methylated DNA i.e. the parental DNA which was propagated in *E. coli*. The mutated plasmid is then transformed into bacteria, where the amplified ssDNA is converted into duplex form *in vivo*.

Table 2.9 Reaction constituents for site directed mutagenesis with QuikChange XL kit

10× reaction buffer	5 µL
dsDNA template	10 ng
oligonucleotide primer (forward)	125 ng
oligonucleotide primer (reverse)	125 ng
dNTP mix	1 µL
QuikSolution	3 µL
Deionized distilled water	to a final volume of 50 µL

Table 2.10 Thermocycling parameters for the QuikChange XL method

Segment	Cycles	Temperature (°C)	Time
1	1	95	1 minutes
2	18	95	50 seconds
		60	50 seconds
		68	1 minutes/ kb plasmid DNA
3	1	68	7 minutes

The *RYR2* fragment now containing the *RYR2* c.14713T>C variant was cut out of the PSL1180NX intermediate plasmid using the restriction enzymes Xho1 and Fse1 (Thermo Fisher Scientific Inc, Waltham, MA, USA), and full length pcDNA3-eGFP-hRyR2 was cut with the same enzymes. The products of these reactions were run on an agarose gel. The band corresponding to full length pcDNA3-eGFP-hRyR2 without the C-terminal fragment, and the band corresponding to the C-terminal fragment containing the *RYR2* c.14713T>C variant were cut out of the gel using a scalpel and purified using the QIAEX II kit (Qiagen, Hilden, Germany) as previously described in section 2.20. The products of the purification were run on a gel again to ensure they remained unchanged. A ligation reaction was then carried out using the Roche Rapid DNA ligation kit (Roche, Basel, Switzerland), with digested full length pcDNA3-eGFP-hRyR2 without the C-terminal fragment and the *RYR2* c.14713T>C containing C-terminal fragment being ligating together, creating Phe4905Leu-pcDNA3-eGFP-hRyR2. The introduction of the correct nucleotide change was confirmed by direct Sanger sequencing.

2.24 Propagation of full length *RYR2* cDNA

In order to propagate the Phe4905Leu and WT pcDNA3-eGFP-hRyR2 plasmids (21.22 kb), to have sufficient quantity of DNA for calcium imaging experiments, they were transformed into highly competent bacterial cells, MAX Efficiency® Stbl2™ chemically competent cells (Invitrogen, Carlsbad, CA, USA). These cells were used due to their relatively efficient ability to propagate large and unstable plasmid DNA (like pcDNA3-eGFP-hRyR2) that is prone to spontaneous recombination. Stbl2 cells (50 µL) were thawed on ice and approximately 1 ng of the pcDNA3-eGFP-hRyR2 plasmid was added to the cells before gently mixing them. The pcDNA3-eGFPhRyR2- Stbl2 cell mixture was then incubated on ice for 30 minutes before being heat shocked in a 42 ˚C water bath for 30 seconds. The cells were then incubated on ice for 2 minutes. 500 µL of NZY broth (NZY:

magnesium chloride 0.94 mg/L, sodium chloride 5 mg/L, citric acid anhydrous 0.19 mg/L, Peptone 140 9.8 mg/L, Yeast Extract 5 mg/L) kept at room temperature was added to the cells and they were incubated at 37 ˚C for 1 hour while being shaken at 225 rpm. 200 µL of the cell suspension was taken and spread on an LB agar plate containing ampicillin (100 mg/mL). The plates were incubated overnight (~ 20 hours) at 30 ˚C and were observed for colonies the next morning. Single colonies were picked and suspended in 6 mL of LB broth supplemented with ampicillin, the cells were incubated for 16 hours at 30 ˚C while being shaken at 225 rpm. 3 mL of the culture was used for the small scale isolation of plasmid DNA (as described in section 2.13) and the second half of the culture was diluted with LB broth supplemented with ampicillin and incubated for a further 4 hours at 30 ˚C while being shaken at 225 rpm in preparation for the growth of large scale bacterial cultures.

2.25 Restriction mapping

To verify the plasmid DNA obtained after propagation is pcDNA3-eGFP-hRyR2 rather than a product of intra-plasmid recombination restriction digests were performed with the following restriction enzymes: EcoR1, HindIII, BamHI and BglII (Thermo Fisher Scientific Inc, Waltham, MA, USA) as previously described. The products of the restriction digest were run on an agarose gel. Those cultures with restriction patterns corresponding to those of pcDNA3-eGFP-hRyR2 were used to begin large scale bacterial cultures in which the plasmid could be propagated further (Figure 2.3). The expected restriction digest patterns for pcDNA3-eGFP-hRyR2 were obtained using the NEB cutter tool (Table 2.11) (http://tools.neb.com/NEBcutter2/).

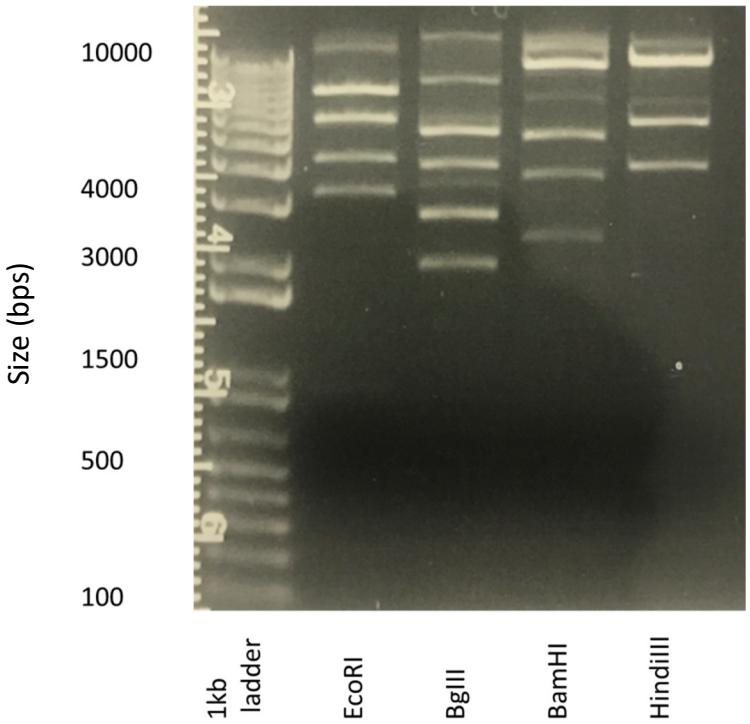

Figure 2.3. pcDNA3-eGFP-hRyR2 fragments produced by restriction digestion with various restriction enzymes (EcoRI, BglII, BamHI and HindiIII) run on a 1 % (w/v) agarose gel with a 1 kb DNA ladder.

Table 2.11 Sizes of RYR2 fragments produced by various restriction enzymes

Restriction enzyme	Recognition sequence	Fragment sizes produced (bp)
EcoRI	G/AATTC	7683 5741 3952 3015 838
BglII	A/GATCT	5182 3805 ~23600 ~1900 649
BamHI	G/GATCC	10664 4971 3461 2199 34
HindIII	A/AGCTT	11759 5700 3700

2.26 Large scale propagation of plasmid DNA

The small-scale bacterial cultures containing the pcDNA3-eGFP-hRyR2 plasmid were identified by purifying the DNA using QIAprep Spin Miniprep Kit (Qiagen) and restriction mapping, only these cultures were used for the large scale propagation of plasmid DNA. 400 µL of small scale bacterial culture was added to 400 mL of LB media supplemented with ampicillin, the bacterial cells were then allowed to propagate at 30 °C while being shaken at 225 rpm for ~16 hours. The media was then removed from the cell suspension by centrifugation at 6000 xg for 15 minutes at 4 °C (Avanti J-25, Beckman) and the resulting bacterial cell pellet was kept for large scale DNA purification. The lower incubation temperature of 30 °C was used due to the instability of the pcDNA3-eGFP-hRyR2 plasmid, at this temperature the plasmid is less prone to spontaneous recombination.

2.27 Large scale purification of plasmid DNA

The large scale purification of pcDNA3-eGFP-hRyR2 plasmid DNA from bacterial cells was performed using a HiSpeed Plasmid Maxi Kit (Qiagen, Hilden, Germany) following the

manufacturer's protocol, similar to the QIAprep Spin Miniprep Kit the HiSpeed Plasmid Maxi Kit (Qiagen, Hilden, Germany) uses the alkaline lysis method, however this kit is capable of purifying up to 750 µg of plasmid DNA. To purify pcDNA3-eGFP-hRyR2 plasmid DNA bacterial cells were resuspended in 10 mL of buffer P1 supplemented with RNase A and LyseBlue reagent. Cells were lysed with the addition of 10 mL of buffer P2 (lysis buffer), vigorous mixing and incubation at room temperature for 5 minutes. The completion of cell lysis was indicated by the solution turning blue. Buffer P2 was neutralised with the addition of 10 mL of chilled buffer P3 and gentle mixing so not to damage the DNA. The cell lysate was then poured into a QIAfilter Cartridge and incubated at room temperature for 10 minutes, meanwhile 10 mL of buffer QBT was added to a HiSpeed Maxi Tip for the purposes of equilibration. The cap was removed from the QIAfilter Cartridge outlet nozzle and the plunger was gently inserted into the top of the QIAfilter Maxi Cartridge and pushed downwards to filter the cell lysate into the equilibrated HiSpeed Maxi Tip. The cleared cell lysate was allowed to enter the HiSpeed Maxi Tip resin by gravity flow. The HiSpeed Maxi Tip was washed twice with 30 mL Buffer QC to remove proteins and RNA before DNA was eluted with 15 mL of buffer QF, which has a high salt content. DNA was precipitated by adding 10.5 mL of isopropanol to the eluted DNA and incubating the mixture at room temperature for 5 minutes. The eluate/ isopropanol mixture was filtered through a QIAprecipitator Maxi Module using a syringe. The QIAprecipitator Maxi Module bound DNA was washed with 2 mL of 70 % (v/v) ethanol and then air dried by gently pushing air through the QIAprecipitator Maxi Module with the syringe ~3 times. An unused 5 mL syringe was then used to pass 1 mL of dH_2O through the QIAprecipitator Maxi Module eluting the plasmid DNA. The successful purification of pcDNA3-eGFP-hRyR2 was confirmed by restriction mapping and the presence of the RYR2-Phe4905Leu variant was confirmed by Sanger sequencing.

2.28 Effectene transfection of HEK 293 cells

In order to study the effects of variants on calcium handling the pcDNA3-eGFP-hRyR2 plasmid either containing the Phe4905Leu variant or without it was transfected into HEK 293 cells using an effectene transfection kit (Qiagen, Hilden, Germany). The DNA is condensed by the kits enhancer reagent before being immersed in cationic lipids by the effectene reagent allowing the DNA to be transferred into the cells. This method was

chosen due to its reproducibility and relatively lower cell toxicity. Alternative methods such as calcium phosphate transfection result in higher rates of cell death, which is unsuitable for the imaging of live cells.

HEK 293 cells were seeded in a 200 µL menisci of cDMEM at a density of approximately $1x10^5$ per plate onto 10 mm glass coverslips coated in poly-D-lysine to increase cell adherence (Mattek Corporation). The cells were incubated at 37 °C at 5 % CO_2 for 4 hours before being flooded with cDMEM and incubated for a further 20 hours. For the transfection of 7-8 coverslips 0.8 µg of eGFP-hRyR2 DNA was made up to 100 µL with Buffer EC (a buffer that promotes DNA condensation) before 6.4 µL of enhancer was added. The mixture was then vortexed for 10 seconds and incubated at room temperature for 5 minutes. Effectene (0.8 µg or 20 µL) was added to the reaction before vortexing the solution for 10 seconds and incubating the solution at room temperature for 10 minutes, allowing time for the formation of effectene-DNA complexes. 600 µL of cDMEM was added the solution before mixing by pipetting. The medium was removed from the cells and replaced with 200 µL meniscus of cDMEM. 100 µL of the effectene-DNA containing solution was added dropwise to each coverslip and the cells were incubated for 24 hours. The cells were then flooded with cDMEM and incubated for another 24 hours before calcium imaging.

2.29 Cell loading with Fluo-3

Despite the study of RyR2 channels in artificial lipid bilayers being the method in which more detailed information on how variants cause channel dysfunction can be obtained, as single channels can be studied, this method may be limited by some changes in channel properties being caused by the experimental environment rather than the variant of interest. Contrastingly, calcium imaging experiments investigate the properties of RyR2 channels in living cells and thus results obtained using this method may be more representative of RyR2 activity in vivo. Calcium imaging involves the use of dyes that exhibit increased fluorescence upon binding to free calcium. The calcium bound dye is excited by a high-powered laser and fluoresces at specific wavelengths that are detected, but only light emitted from the focal plane is detected as light from other regions is blocked by the pinhole located in front of the detector, as a result images produced are of a higher resolution compared to those from wide-field microscopes. Due to the

fluorescence of the dye being dependant on binding to free calcium changes in fluorescence intensity reflect the release of calcium from the ER through RyR2. A factor other than the variant being studied that can influence the activity of RyR2 is the ER load as RyR2 is regulated by luminal calcium, and the ER load is partly dependant on the activity of SERCA which pumps calcium back into the ER. As a result of this the ER load of HEK cells expressing both WT and mutant RyR2 channels was measured.

Calcium imaging experiments were performed using HEK 293 cells, due to the absence of accessory proteins and lack of expression of *RYR2* in this cell line, which may influence the results obtained as native channels may contribute to the fluorescence signal. Furthermore, HEK 293 cells are widely used for the study of recombinant RyR2 channels and although lacking the proteins that regulate RyR2 function HEK 293 cells have been shown to generate functional data for RyR2 channels similar to that produced from studies in cardiomyocytes (Li and Chen, 2001). The fluorescent dye Fluo-3 was selected to enable the visualisation of Ca^{2+} release events with confocal microscopy. Despite its higher susceptibility to photobleaching Fluo-3 was chosen due its relatively larger dynamic range, lower tendency to compartmentalise and suitable Ca^{2+} binding affinity (Thomas et al. 2000).

Cells were loaded with an acetoxymethyl (AM) conjugated form of Fluo-3, enabling it to penetrate the cell membrane before degradation. A 3 mM stock solution of Fluo-3 AM was made by suspending Fluo-3 AM (50 µg, AAT Bioquest) in 15 µL of a 20 % (w/v) DMSO-pluronic acid mixture. This was diluted with mDMEM (minimal DMEM, Dulbecco's modified eagle's medium with no supplements) to 10 µM. cDMEM was removed from the transfected HEK cells grown on coverslips and replaced with a 200 µL meniscus of Fluo-3 AM in mDMEM. The loaded cells were incubated at 37 °C at 5 % CO_2 for 45 minutes before de-esterification by flooding with mDMEM and further incubation for 10 minutes.

2.30 Calcium imaging

The calcium dependent fluorescence in fields of view containing HEK cells transfected with WT *RYR2* (N = 27) or Phe4905Leu *RYR2* (N = 27) was observed using confocal microscopy with a Leica SP5 scanning confocal microscope at x20 magnification and with an Argon laser. mDMEM was removed from the cells and replaced with a 200 µL meniscus

of Krebs-Ringer-Hepes (KRH: 9 g/L glucose, 7 g/L NaCl, 6 g/L HEPES, 0.35 g/L KCl, 0.16 g/L KH2PO4, 0.29 g/L MgSO4, 1.3 mM CaCl2, filter sterilized and pH adjusted to 7.4) before imaging the cells. The excitation wavelength used was 488 nm at 40% power and emitted wavelengths of 510-540 nm were detected using a photomultiplier tube. The rate at which data was acquired was set to 5 frames per second, and data acquisition was performed using the Leica LAS AF software at a resolution of 1024 x 1024 pixel. 4 different regions or fields of view of the coverslip with oscillating cells were recorded for 360 seconds. Fluorescence intensities of individual cells/regions of interest (ROIs) (approximately 46 μm2) within each field of view were measured. The mean properties of the calcium release events from the cells within a single field of view were calculated and for the purpose of statistical analyses mean values from each field of view corresponded to N = 1, when studying the properties of calcium release events under basal conditions.

For each coverslip of cells at the end of the recording for the fourth field of view 10 mM caffeine was added to the cells and they were recorded for a further 360 seconds to determine the ER load of cells expressing WT and mutant RyR2 channels. The ER load was calculated from the amplitude of the calcium release events immediately after the addition of 10 mM caffeine. Caffeine was used to determine ER load because it activates RyR2 channels by increasing their sensitivity to luminal calcium but does not alter RyR2 sensitivity to cytosolic calcium (Kong et al., 2008). Furthermore, RyR2 activation by B-adrenergic stimulation would not only activate RyR2 but also lead to the activation of various other proteins that may influence calcium cycling. For the calculation of the ER load the mean amplitude of calcium release events from a single cell represented N = 1, 156 HEK cells transfected with WT *RYR2* cDNA and 156 cells transfected with Phe4905Leu *RYR2* were recorded and analysed.

The sensitivity of Phe4905Leu-RyR2 and WT-RyR2 to various concentrations of caffeine was also measured. However, in these experiments caffeine was added to HEK 293 cells at the beginning of the recordings. The amplitude of intracellular calcium release events in HEK cells expressing WT RyR2 after the addition of 0.05 mM (N = 64), 0.25 mM (N = 58) or 1 mM (N = 66) caffeine was compared to HEK cells expressing Phe4905Leu RyR2 after the addition of 0.05 mM (N = 71), 0.25 mM (N = 51) or 1 mM (N = 40) caffeine. Following the addition of caffeine cells were recorded for 360 seconds. As caffeine response is rapid

in HEK cells only 1 field of view was recorded per coverslip and the mean amplitude of calcium release events from a single cell represented N = 1. The responsiveness of RyR2 channels to the range of caffeine concentrations used in this study was investigated as the difference in caffeine activation in mutant RyR2 channels compared to WT channels has been reported to be greater at lower caffeine concentrations (Lieve et al., 2019).

2.31 Analysis Spikes analysis

Data generated from calcium imaging experiments were analysed using the Analysis Spikes program. This program was designed for the purpose of analysing the spaciotemporal properties of calcium release events (Figure 2.4). The properties analysed by the Analysis Spikes program and the methods of the analyses are described below:

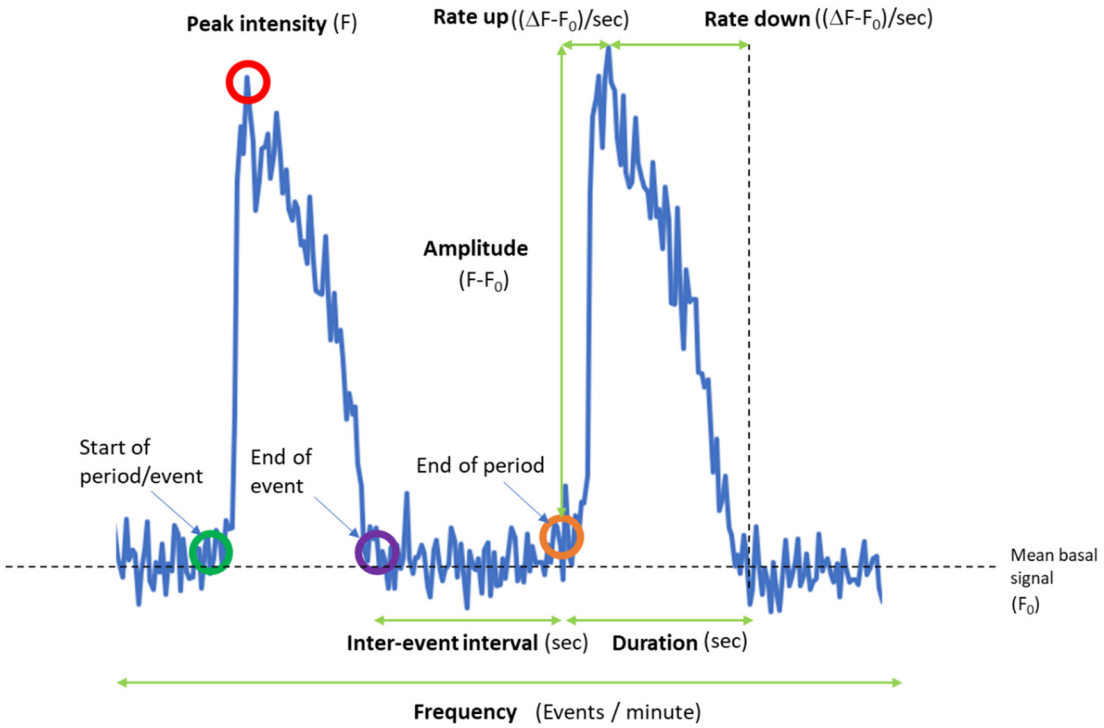

Figure 2.4. The properties analysed by the Analysis Spikes program from calcium imaging data obtained from HEK cells transfected with WT or mutant RYR2 channels.

Mean Basal Signal Intensity

The mean basal signal intensity (F_0) is the mean signal intensity between events.

Frequency

The frequency of calcium release events was determined by calculating the number of complete calcium release events per minute. A complete period includes the duration of the calcium release event and the time between successive events (inter-spike interval) combined. The frequency of calcium release events is influenced by the channel threshold for activation by calcium as well as other related factors like the ER load.

Rise Rate

The rise rate represents the rate at which calcium is released from the ER to reach the maximum calcium concentration achieved in a single calcium release event, or in other words the rate at which RyR2 activation occurs. This is determined by calculating the

change in signal intensity per second ($(\Delta F/F_0)$/sec) from the beginning of a calcium release event to the point in which the peak is reached. The amplitude of the calcium release event was divided by the time taken for the peak amplitude to be reached from the beginning of the calcium release event.

Fall Rate

The fall rate represents the rate at which calcium is pumped both out of the cell and back into the ER from the cytosol. It is determined by calculating the rate at which the calcium dependent signal decays from the peak intensity of the calcium release event back to the baseline. The amplitude of the calcium release event was divided by the time at the peak amplitude minus the time at the end of the calcium release event when the signal intensity returns to the baseline ((ΔF/F0)/sec).

Duration

The duration of calcium release events was calculated by deducting the time at which the calcium release event begins from the time at which the calcium release event ends, the former is when the signal intensity begins to rise from the baseline and the latter is when the signal intensity returns to the baseline. The duration of a calcium release event is determined by both the rise rate and the fall rate.

Amplitude

The amplitude of calcium release events was calculated by subtracting the peak calcium dependent signal intensity from the baseline signal intensity. The amplitude was presented as a proportion of the baseline signal intensity ($\Delta F/F_0$). The ER load of cells expressing WT or Phe4905Leu hRYR2 was determined by measuring the amplitude of the Ca^{2+} transient after the addition of 10 mM caffeine.

Inter-event interval

The inter-event interval is the time between the end of one calcium release event and the beginning of the next event. The inter-event interval was calculated by deducting the time at which one event ends from time at which the next event begins.

2.32. Statistical analysis of Ca^{2+} release events

The D'Agostino and Pearson test was used on GraphPad Prism to show that data from Ca^{2+} imaging experiments were normally distributed. This test measures how far a dataset deviates from a normal Gaussian distribution. P values below 0.05 indicate distribution is significantly different from that expected for normal Gaussian distribution. Statistical analysis of individual Ca^{2+} imaging parameters was performed using the unpaired t-test on GraphPad prism.

Table 2.12. Test for normal Gaussian distribution showed Ca^{2+}imaging data was normally distributed. P < 0.05 was considered a significant deviation from normal Gaussian distribution.

Ca^{2+} oscillation event parameters	Phe4905Leu	WT
Frequency	0.2077	0.3241
Duration	0.4121	0.2686
ISI	0.1029	0.2368
Amplitude	0.1584	0.0773
Rise rate	0. 3441	0.1863
Fall rate	0.0792	0.3073

Chapter 3: Classification and correlation of *RYR2* missense variants in individuals with catecholaminergic polymorphic ventricular tachycardia reveals phenotypic relationships

Classification and correlation of RYR2 missense variants in individuals with catecholaminergic polymorphic ventricular tachycardia reveals phenotypic relationships

Damilola Olubando,[1,2] Claire Hopton,[1,2] James Eden,[1] Richard Caswell,[3] N. Lowri Thomas,[4] Stephen A. Roberts,[5] Deborah Morris-Rosendahl,[6] Luigi Venetucci,[7,8*] William G. Newman[1,2,5] *

[1]Manchester Centre for Genomic Medicine, Manchester University NHS Foundation Trust, Health Innovation Manchester, Manchester, M13 9WL, UK.
[2]Division of Evolution and Genomic Sciences, Faculty of Biology, Medicine and Human Sciences, University of Manchester, Manchester, UK.
[3]Institute of Biomedical and Clinical Science, University of Exeter Medical School, Exeter, UK
[4]School of Pharmacy and Pharmaceutical Sciences, Redwood Building, University of Cardiff, Cardiff, CF10 3NB, UK
[5]Division of Population Health, Health Services Research & Primary Care, University of Manchester, Manchester, UK.
[6]Clinical Genetics and Genomics, Royal Brompton and Harefield NHS Foundation Trust, London, UK, NHLI, Imperial College London, UK.
[7]Manchester Heart Centre, Manchester University NHS Foundation Trust, Manchester, M13 9WL, UK.
[8]Division of Cardiovascular Sciences, Faculty of Biology, Medicine and Human Sciences, University of Manchester, Manchester, UK.
[9]Peking University Health Sciences Center, Beijing, PR China

* These authors contributed equally to the study

Correspondence to:
Professor WG Newman,
Manchester Centre for Genomic Medicine,
St Mary's Hospital,
Manchester M13 9WL, UK.
E-mail: william.newman@manchester.ac.uk

3.1 Abstract

Catecholaminergic polymorphic ventricular tachycardia (CPVT) is predominantly caused by heterozygous missense variants in the cardiac ryanodine receptor, *RYR2*. However, many *RYR2* missense variants are classified as variants of uncertain significance (VUS). We systematically re-evaluated all *RYR2* variants in healthy individuals and those with CPVT or arrhythmia using the 2015 American College of Medical Genomics guidelines. *RYR2* variants were identified by the NW Genomic Laboratory Hub, from the published literature and databases of sequence variants. Each variant was assessed based on minor allele frequencies, *in silico* prediction tools and appraisal of functional studies and classified according to the ACMG-AMP guidelines. Phenotype data was collated where available. Of the 326 identified *RYR2* missense variants, 55 (16.9%), previously disease-associated variants were re-classified as benign. Application of the gnomAD database of >140,000 controls allowed reclassification of 11 variants more than the ExAC database. CPVT-associated *RYR2* variants clustered predominantly between amino acid positions 3949-4332 and 4867-4967 as well as the RyR and IP3R homology associated and ion transport domains ($P < 0.005$). CPVT-associated *RYR2* variants occurred at more conserved amino acid positions compared to controls, and variants associated with sudden death had higher conservation scores ($P < 0.005$). There were five potentially pathogenic *RYR2* variants associated with sudden death during sleep which were located almost exclusively in the C-terminus of the protein. In conclusion, control sequence databases facilitate reclassification of *RYR2* variants but the majority remain as VUS. Notably, pathogenic variants in *RYR2* are associated with death in sleep.

KEYWORDS: Catecholaminergic ventricular tachycardia, cardiac ryanodine receptor, variant classification, arrhythmia.

3.2 Introduction

The rare monogenic arrhythmogenic disorder catecholaminergic polymorphic ventricular tachycardia (CPVT, MIM 604772) is characterised by episodic ventricular dysrhythmia triggered by exercise or emotion in individuals without structural cardiac defects (Liu et al., 2008). CPVT can be inherited in both an autosomal dominant form caused by heterozygous pathogenic variants in the cardiac ryanodine receptor gene (*RYR2*) (MIM 180902)(Priori Silvia et al., 2002), less frequently in *CALM1* (MIM 114180)(Nyegaard et al., 2012) encoding calmodulin 1 and autosomal recessive form due to biallelic variants in *CASQ2* (MIM 114251)(Lahat et al., 2001) encoding calsequestrin, *TRDN* (MIM 603283)(Roux-Buisson et al., 2012) encoding triadin and *TECRL* (MIM 617242)(Devalla et al., 2016). Furthermore, CPVT can also be caused by rare deletions in exon 3 of *RYR2* (Ohno et al., 2014). However, in such cases CPVT is often accompanied by left ventricular non-compaction (Ohno et al., 2014). It is estimated that one in 10,000 people are clinically affected by the condition, with sudden cardiac death being the first manifestation in some individuals (Liu et al., 2008, Napolitano et al., 2013, Tester et al., 2012). The phenotypic heterogeneity of CPVT can delay or obscure diagnosis. It has been reported that almost one in three individuals with CPVT are initially diagnosed with long QT syndrome (LQTS) despite a normal QT interval (Priori Silvia et al., 2002). Consequently, combined approaches of cardiac assessment including exercise stress testing and genetic analysis are used to confirm a diagnosis of CPVT.

The large coding region of the cardiac ryanodine receptor (105 exons) previously made genetic testing costly and time consuming using conventional DNA sequencing methods. As a result, it became common practice to only screen the four regions considered to be mutation hotspots in *RYR2* (George et al., 2007). Next generation sequencing has now become more widely available and all coding exons of *RYR2* can be screened rapidly and cheaply. This has led to an increase in the number of *RYR2* variants being reported in individuals with cardiac dysrhythmia or associated symptoms of palpitations, syncope or sudden unexplained death. Concomitant with this has been the increase in *RYR2* variants identified in apparently healthy individuals collated through international resources, including the Genome Aggregation Database (gnomAD)(Karczewski et al., 2019). The majority of *RYR2* variants are missense changes. When assayed in functional experiments

a number of these lead to increased channel activity consistent with pathogenicity. However, the rarity of these variants and complexity of functional assays makes it difficult to determine their pathogenicity, and so the majority are classified as variants of uncertain significance (VUS). Recently the American College of Medical Genetics and Genomics and the Association for Molecular Pathology (ACMG-AMP) proposed guidelines to standardise the classification of genetic variants (Richards et al., 2015).

In this study we collate *RYR2* variants reported in individuals with, or suspected of having CPVT, and classify them according to these ACMG guidelines and correlate the variants with clinical features.

3.3 Methods

A comprehensive search for RYR2 variants identified in individuals undergoing genetic testing for CPVT or an associated arrhythmia was performed. A total of 326 different RYR2 variants was obtained from the North West Genomic Laboratory Hub, UK (a service that has been undertaking clinical diagnostic testing of RYR2 for >10 years), the published literature and clinical variant databases, including ClinVar and the Human Gene Mutation Database (HGMD) (Supplementary Table 3.1) (Landrum et al., 2016, Stenson et al., 2014). Allele frequencies of RYR2 variants in apparently healthy individuals were obtained from gnomAD as a comparator, accessed online from https://gnomad.broadinstitute.org (Karczewski et al., 2019).

3.3.1 Phenotype-Genotype analysis

All *RYR2* variants both in control and CPVT populations were mapped to the domains, structural motifs and regions in which they are located in the RyR2 protein (using the universal protein resource (UniProt) accession number Q92736) with Mutation Mapper from the cBio Cancer Genomics Portal. For the purpose of our analysis *RYR2* regions that were not associated with any known functional or structural domains were individually labelled as 'no domain' followed by a number ranging from 1 to 9 corresponding to their location, and where multiple copies of known domains were present the domains were grouped together. The proportion of missense variants in each region/domain of *RYR2* in control and CPVT populations were compared using the Fisher's exact test using GraphPad prism. As comparisons were made not only between controls and the total

CPVT population but also between subgroups of the CPVT population (like patients that experienced sudden death or sleep related sudden death), and the likelihood of erroneous inferences occurring are increased when making multiple comparisons, a more stringent p-value < 0.005 was considered significant.

3.3.2 Variant Classification

RYR2 variants were classified based on the 2015 ACMG-AMP guidelines. As reported by Denham et al. (2019) 12 of the 27 criteria listed in the ACMG-AMP guidelines were excluded from this study as they were considered non-applicable (reasons for the exclusion of these criteria are included in Supplementary Table 3.2) (Denham et al., 2019). The application of these guidelines has been previously reported (Supplementary Table 3.3 and 3.4)(Denham et al., 2019).

3.3.3 Criteria for segregation

The criteria for a variant to qualify for variant segregation (PP1) required that the variant was present in two or more members of the same family with a CPVT-like phenotype (arrhythmias, syncope, bradycardia or sudden death). The occurrence of affected individuals in whom the putative variant did not segregate was considered strong evidence for a benign classification (BS4).

3.3.4 Criteria for functional studies

Robust functional studies, including animal models, calcium imaging, cellular electrophysiology and single channel analysis showing either a significant reduction or gain of function, were considered strong evidence for pathogenicity (PS3). Conflicting functional data on variants was not considered as positive evidence of pathogenicity. Functional studies that reported no change in channel function were considered evidence for a benign classification (BS3).

3.3.5 Criteria for variant frequency

Variants that were absent from gnomAD were considered ultra-rare (PM2) and variants with an allele count of below 4 were considered rare.

The statistical framework used to identify variants that occur too frequently in the gnomAD database to be pathogenic has been described by Whiffin et al. (2017) (Whiffin

et al., 2017). To summarize, it involves the determination of the maximum credible population allele frequency for a missense variant in *RYR2* that causes CPVT. This was calculated based on CPVT as a dominant condition with a penetrance of approximately 60% (Napolitano et al., 2013). A binomial distribution of the maximum credible allele frequency was generated for our sample of CPVT cases (observed allele number) and the upper boundary of the 95% confidence interval (the maximum tolerated allele count) was used as the cut off frequency. Variants that occurred more frequently than the maximum tolerated allele count in gnomAD were considered common and this was strong evidence for a benign classification (BS1).

3.3.6 Criteria for variant enrichment in CPVT cases

Ultra-rare and rare variants were considered for variant enrichment analysis. The presence of an ultra-rare or rare variant in at least five or ten CPVT cases, respectively, was considered as strong evidence (PS4).

3.3.7 Criteria for computational evidence

To remain consistent with previously reported variant classification methods, five protein-level in silico prediction tools: SIFT, PolyPhen, Mutation Taster, Mutation assessor, FATHMM and three conservation tools GERP++, PhyloP conservation and SiPhy were used for the computational analysis of variants where DNA positional information was provided (GERP++, PhyloP, and SiPhy scores of 4.4, 1.6, and 12.17, respectively were set as thresholds for conservation)(Denham et al., 2019). In addition, Consurf (http://consurf.tau.ac.il/), which uses advanced probabilistic evolutionary models to distinguish true conservation resulting from purifying selection and produces estimates for the credibility of the results, was used to measure conservation of amino acid positions of variants in controls and CPVT patients. The Consurf scores of the amino acid positions of control, CPVT and sudden death cases were compared using the Mann-Whitney test using GraphPad prism, p-value <0.005 was considered significant.

3.3.8 Criteria for critical functional domain

The location of a missense variant in the transmembrane 4-6 region or ion-transport domain of the protein was considered as moderate evidence for a pathogenic

classification, as the functional significance of these regions has been established (Wayne Chen et al., 2002, George et al., 2004).

3.4 Results

3.4.1 Collation of RYR2 missense variants

A total of 326 independent *RYR2* single nucleotide, non-synonymous variants associated with CPVT or arrhythmia were identified. Of these variants 97 were present in both control and CPVT populations. Importantly, 104 (31.9%) of the CPVT-associated *RYR2* variants were located outside of regions previously considered mutation hotspots. The hotspot regions with the most *RYR2* variants were domains III and IV, where 21.5% and 21.2% of variants were located, respectively. The numbers of male and female cases were similar (Table 3.1).

Table 3.1 Pre-established RyR2 variant hotspot regions in CPVT.

Variant hotspot region	Residues (amino acids)	variants (% of total) n=326	*de novo* variants (%) n=40	Male: Female Ratio (%)
I	77-466	35 (10.7)	7 (17.5)	56:44
II	2246-2534	48 (14.7)	6 (15)	50:50
III	3778-4201	70 (21.5)	13 (32.5)	42:58
IV	4497-4959	69 (21.2)	10 (25)	41:59
Non-hotspot regions		104 (31.9)	4 (10)	47:53

The most common amino acid position at which missense changes occurred was Arg420. Nineteen (19) of 440 (4.3%) independent cases were reported to have a missense change at this amino acid position, 10 cases carried the Arg420Trp variant and 9 carried the Arg420Gln variant. The second most common protein position for missense changes was Arg176, 8 of 440 (1.8%) cases carried the Arg176Gln variant.

3.4.2 Genotype-Phenotype analysis

Several domains or regions within *RYR2* contained a significantly higher proportion of CPVT-associated missense variants compared with controls (Figure 3.1 and Table 3.2). CPVT-associated missense variants occurred more frequently than expected between amino acid positions 3949-4332 and 4867-4967 (No Domain regions 5 and 7). CPVT-associated *RYR2* variants were also enriched in the RyR and IP3R homology-associated and ion transport domains when compared to control variants ($p < 0.001$). In contrast, control variants clustered between amino acid positions 2906-3826 and the SPRY and RYR domain when compared to CPVT-associated variants ($p < 0.001$). There was no clear relationship between sudden death and the location of CPVT-associated *RYR2* variants (Figure 3.1A, Supplementary Table 3.5). However, five of the nine RYR2 variants associated with sudden death during sleep occurred in the C-terminus of the protein (Figure 3.1A, Supplementary Table 3.6).

Table 3.2. Proportion of *RYR2* variants in individual *RYR2* domains or regions in controls from gnomAD, CPVT, sudden death and sleep-associated sudden death populations.

Protein domain or region	Length of region (delimiting amino acids)	Control population from gnomAD database (%)	CPVT (%)	Sudden death (%)	Sleep (%)
Inositol 1,4,5-trisphosphate/ryanodine receptor	212 (10-222)	100 (5.1)	18 (5.5)	1 (1.6)	0
MIR domain	173 (226-399)	78 (3.9)	9 (2.8)	1 (1.6)	0
No domain #1	51 (400-451)	31 (1.6)	15 (4.6)	4 (6.3)	0
RYDR_ITPR domain #1	203 (452-655)	89 (4.5)	9 (2.8)	1 (1.6)	0
SPRY domain #1	137 (671-808)	75 (3.8)	4 (1.2)	0	0
RyR domain #1	91 (862-953)	39 (2.0)	2 (0.6)	1 (1.6)	1 (11.1)
RyR domain #2	93 (975 - 1068)	46 (2.3)	0	0	0
SPRY domain #2	120 (1099 - 1219)	60 (3.0)	3 (0.9)	0	0
SPRY domain #3	135 (1424 - 1559)	59 (3.0)	4 (1.2)	1 (1.6)	1 (11.1)
No domain #2	564 (1560-2122)	282 (14.3)	21 (6.4)	5 (7.9)	0
RYDR_ITPR domain #2	208 (2123 - 2331)	52 (2.6)	29 (8.9)	12 (19)	1 (11.1)
No domain #3	367 (2332-2699)	160 (8.1)	38 (11.7)	3 (4.7)	0
RyR domain #3	93 (2700 - 2793)	34 (1.7)	3 (0.9)	0	0
RyR domain #4	85 (2820 - 2905)	26 (1.3)	0	0	0
No domain #4	920 (2906-3826)	352 (17.8)	16 (4.9)	2 (3.2)	0
RyR and IP3R Homology associated	121 (3827 - 3948)	19 (1.0)	11 (3.4)	4 (6.3)	0
No domain #5	383 (3949-4332)	133 (6.7)	64 (19.6)	10 (15.9)	1 (11.1)
Ryanodine Receptor TM 4-6	266 (4333 - 4599)	96 (4.9)	20 (6.1)	8 (12.7)	2 (22.2)
No domain #6	130 (4600-4730)	38 (1.9)	16 (4.9)	3 (4.7)	2 (22.2)
Ion_transport domain	135 (4731 - 4866)	19 (1.0)	18 (5.5)	2 (3.2)	0
No domain #7	100 (4867-4967)	10 (0.5)	21 (6.4)	1 (1.6)	1 (11.1)

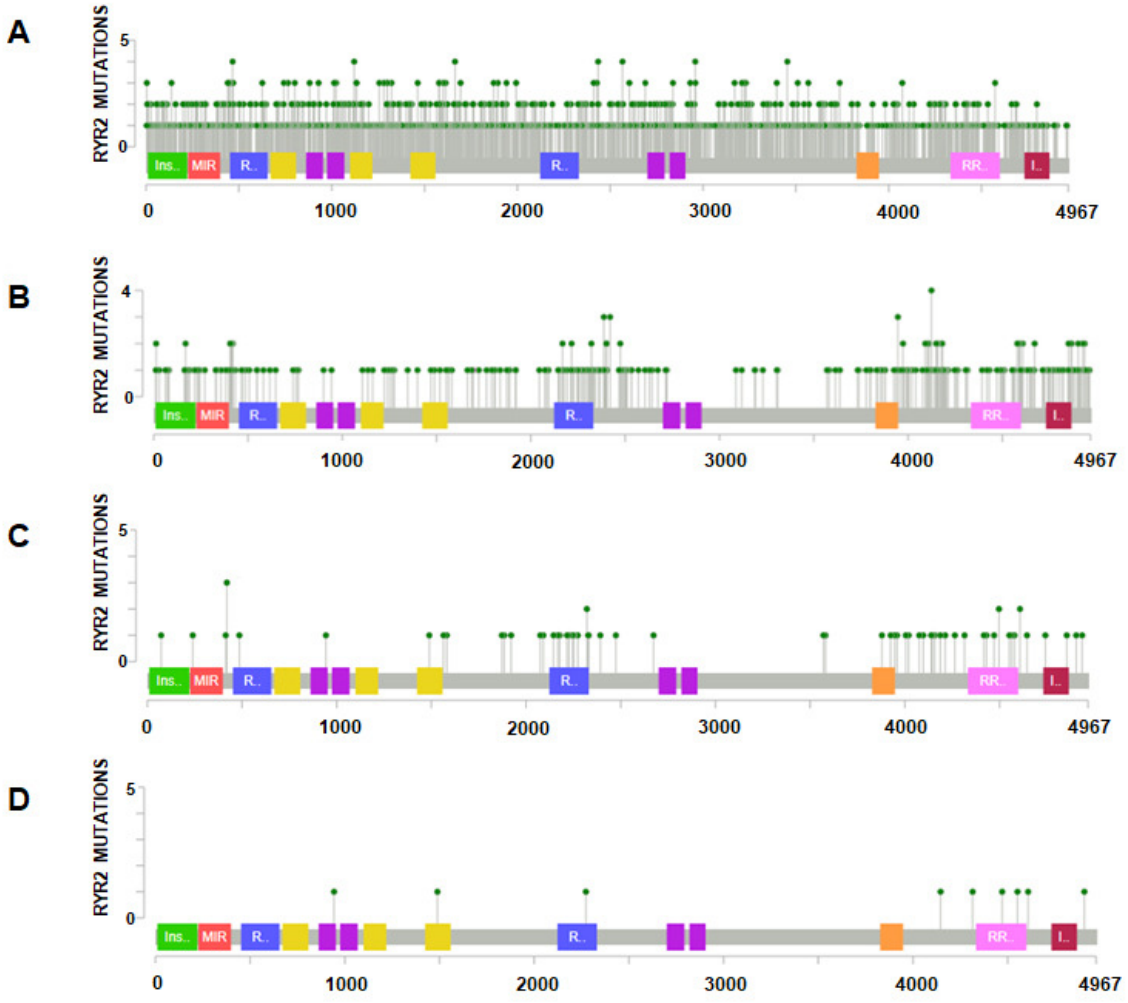

Figure 3.1.A. The distribution of missense variants in RYR2 in control population from the gnomAD database (A), CPVT (B), sudden death (C) and sudden death in sleep (D) populations. Green boxes represent the Inositol 1,4,5-trisphosphate/ryanodine receptor domain (also referred to as the Ins145_P3_rec domain), this region is present in both the inositol 1,4,5-trisphosphate receptor and the RYR2 N-terminal and is a region that facilitates ligand binding. Red boxes represent the MIR domain, which may have a ligand transfer function. Blue boxes represent the RYDR_ITPR domain, which is an extracellular domain that may provide a site for the binding of IP3. Yellow boxes represent the SPRY domain, purple boxes represent the RYR domain, and orange boxes represent the RyR and IP3R Homology associated domain, the function of these domains is unknown. Pink boxes represent the transmembrane 4-6 region which forms part of the pore for the movement of calcium ions out of the SR. The burgundy boxes represent the ion-trans domain which consists of the helices in the pore that confer ion selectivity.

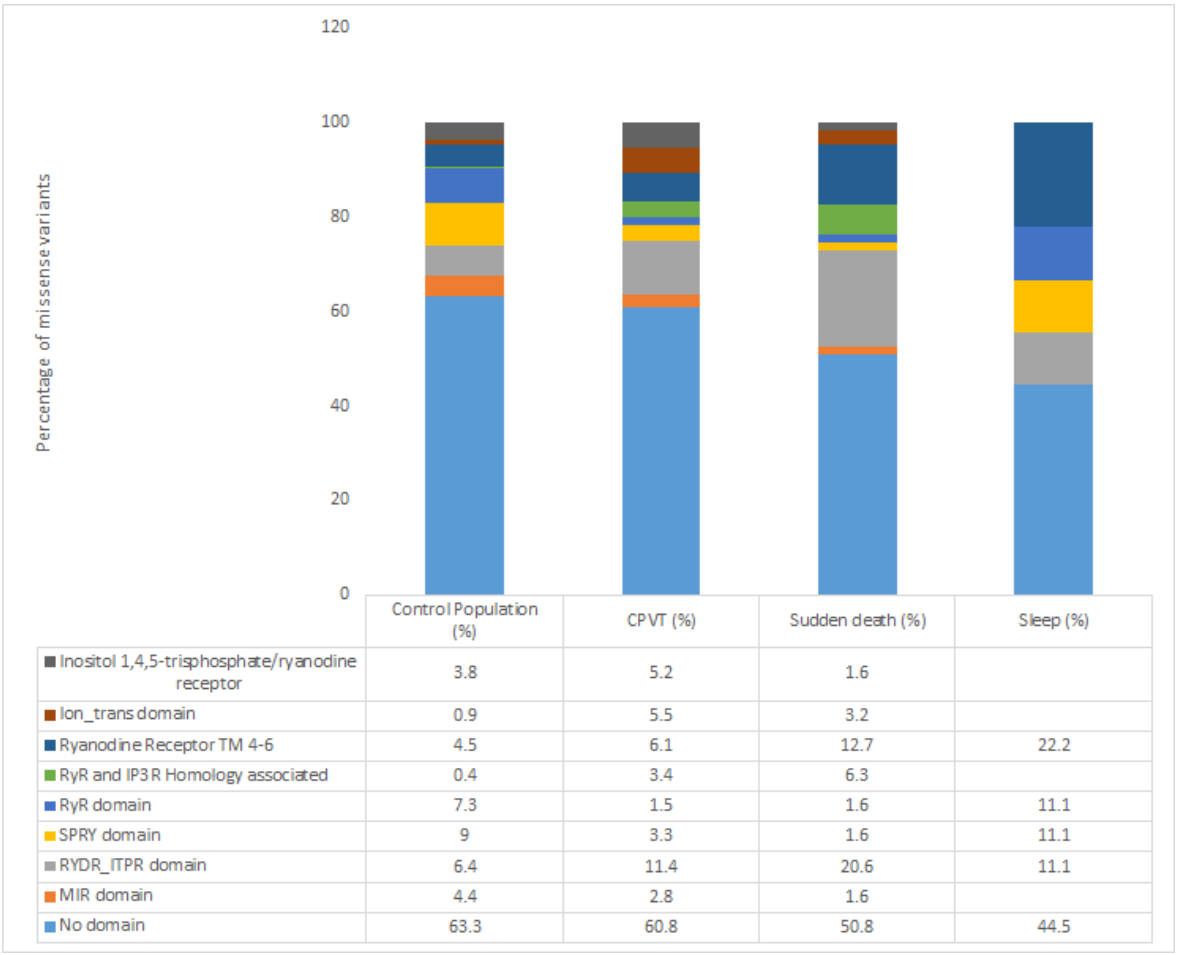

	Control Population (%)	CPVT (%)	Sudden death (%)	Sleep (%)
Inositol 1,4,5-trisphosphate/ryanodine receptor	3.8	5.2	1.6	
Ion_trans domain	0.9	5.5	3.2	
Ryanodine Receptor TM 4-6	4.5	6.1	12.7	22.2
RyR and IP3R Homology associated	0.4	3.4	6.3	
RyR domain	7.3	1.5	1.6	11.1
SPRY domain	9	3.3	1.6	11.1
RYDR_ITPR domain	6.4	11.4	20.6	11.1
MIR domain	4.4	2.8	1.6	
No domain	63.3	60.8	50.8	44.5

Figure 3.1.B. Proportion of RYR2 variants in grouped domains in controls from the gnomAD database, CPVT, sudden death and sleep-associated sudden death populations. The number of cases in the sudden death and sleep-associated sudden death groups was limited, there were 47 sudden death cases and 7 sleep-associated sudden death cases.

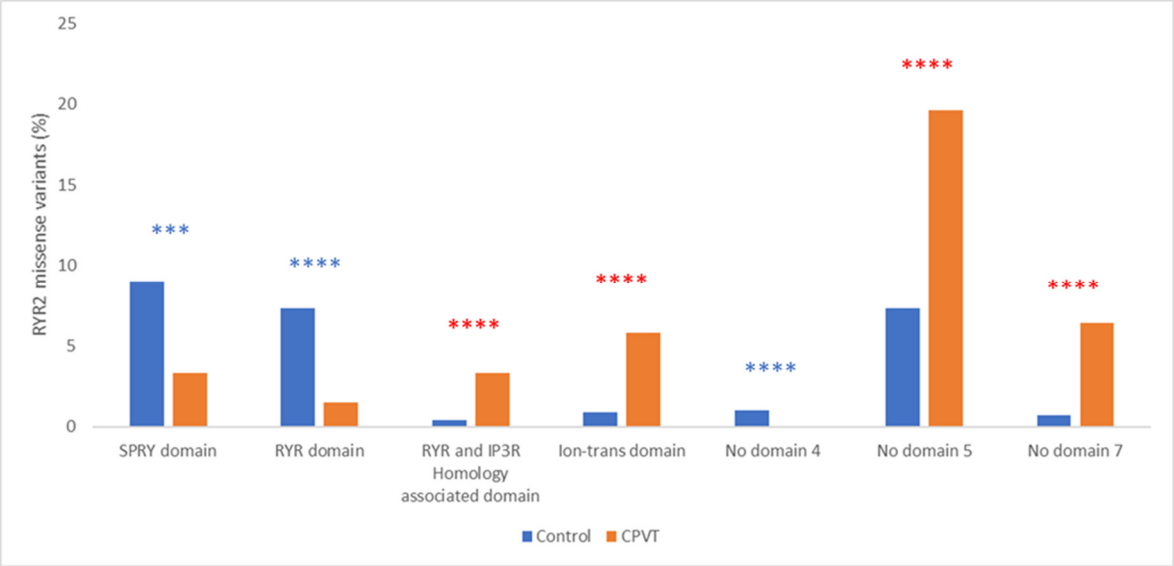

Figure 3.1.C. Grouped domains of RYR2 in which the proportion of RYR2 variants was significantly different in controls from gnomAD compared to CPVT patients. **** and *** represent $P < 0.0001$ and $P < 0.001$, respectively.

3.4.3 Conservation analysis

CPVT variants occurred at positions with significantly higher Consurf scores than controls ($P < 0.0001$), and variants identified in individuals or families with a history of sudden death had higher Consurf scores compared to variants in individuals and families without a history of sudden death ($P < 0.0001$) (Figure 3.2). This suggests variants with Consurf scores above 7 are more likely to be CPVT-associated and of these variants those with Consurf scores above 8 are more likely to be associated with sudden death.

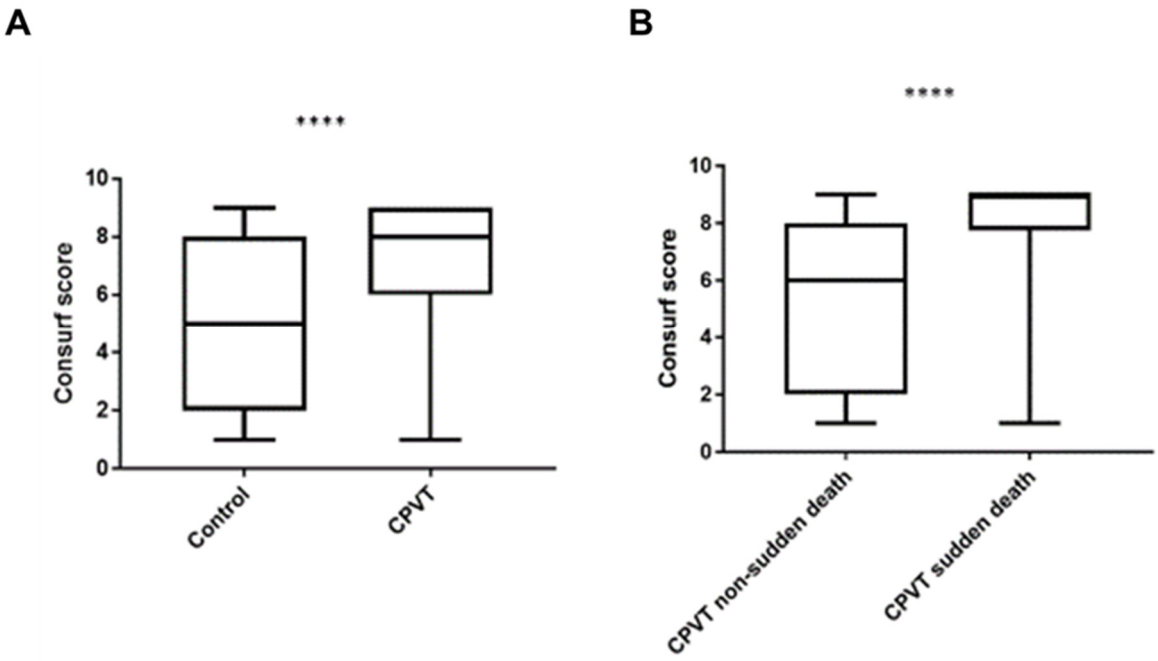

Figure 3.2. (A) Consurf scores of amino acid positions of CPVT variants compared to controls from gnomAD. (B) Consurf scores of amino acid positions of non-sudden death CPVT variants compared to sudden death CPVT variants. **** represents $P < 0.0001$.

3.4.4 Classification of RYR2 variants

RYR2 variants were classified according to the ACMG-AMP guidelines and statistical methods were used to identify those variants that occurred too frequently in controls to be pathogenic, these variants were classified as benign (Supplementary Table 3.7). Using the statistical method described by Whiffin et al. (2017), data on the most common CPVT-

associated *RYR2* variant c.1258C>T (Arg420Trp) and control populations from the ExAC or gnomAD databases, the maximum tolerated allele count for CPVT associated *RYR2* variants was calculated (Supplementary Tables 3.8 and 3.9).

The maximum tolerated allele count for pathogenic *RYR2* variants was calculated to be two when using the ExAC database as a control population and three for the gnomAD database. Using the gnomAD database and the maximum tolerated allele count as a frequency threshold for pathogenicity 55 of 326 previously putative disease associated variants were re-classified as benign according to the ACMG guidelines, 11 fewer variants (44) were reclassified as benign using the ExAC database. A further 245 variants were classified as variants of uncertain significance, 14 as likely pathogenic and 12 as pathogenic using gnomAD as the control comparator (Table 3.3). Both benign and pathogenic variants occurred most frequently outside of known functional domains. The ion transport domain contained the most (7 of the 26) pathogenic or likely pathogenic variants. The SPRY domain was found to be the domain containing the most benign variants; this domain did not contain any pathogenic variants.

Table 3.3. *RYR2* variant classification based on the ACMG-AMP guidelines.

ACMG classification	Number of CPVT associated RYR2 variants total = 326 (%)
Benign	55 (16.9)
Variant of uncertain significance	245 (75.6)
Likely pathogenic	14 (4.1)
Pathogenic	12 (3.7)

Sufficient functional data to aid classification was available for 50 of the 326 variants (Supplementary Table 3.10). The classification of the 26 variants deemed to be pathogenic/likely pathogenic was driven by absence from the gnomAD database (92%, P6), computational evidence (88%, P9), functional data (73%, P3) and *de novo* status (50%, P2). The classification of the 55 variants classified as benign was largely driven by variant frequency in gnomAD exceeding the maximum tolerated allele count (100%, B2) and only one or none of the computational prediction tools indicating pathogenicity (11%, B5).

3.4.5 Reason for referral and genetic testing outcome

Cases referred for genetic testing at MCGM with a more confident diagnosis of CPVT based on clinical evaluation were tested using the CPVT genetic panel, whereas those cases with less diagnostic certainty were tested using either the arrythmia panel (including 37 genes associated with inherited arrhythmia) or the molecular autopsy panel (61 genes associated with sudden cardiac death). The proportion of patients referred for genetic testing with the CPVT panel that carried *RYR2* variants was significantly greater than that of the patients tested with the arrhythmia panel ($P < 0.05$) or molecular autopsy panel ($P < 0.0005$). Furthermore, these patients were more likely to carry pathogenic *RYR2* variants ($P < 0.05$) (Table 3.4, Figure 3.3).

Table 3.4. Outcome of genetic testing for patients referred for CPVT, arrhythmia and molecular autopsy panels to the Manchester Laboratory (MCGM).

	CPVT panel	Arrhythmia panel	Molecular autopsy panel
Patients tested	98	130	166
Patients with RYR2 variants	20	11	8
Patients with pathogenic RYR2 variants	10	2	1

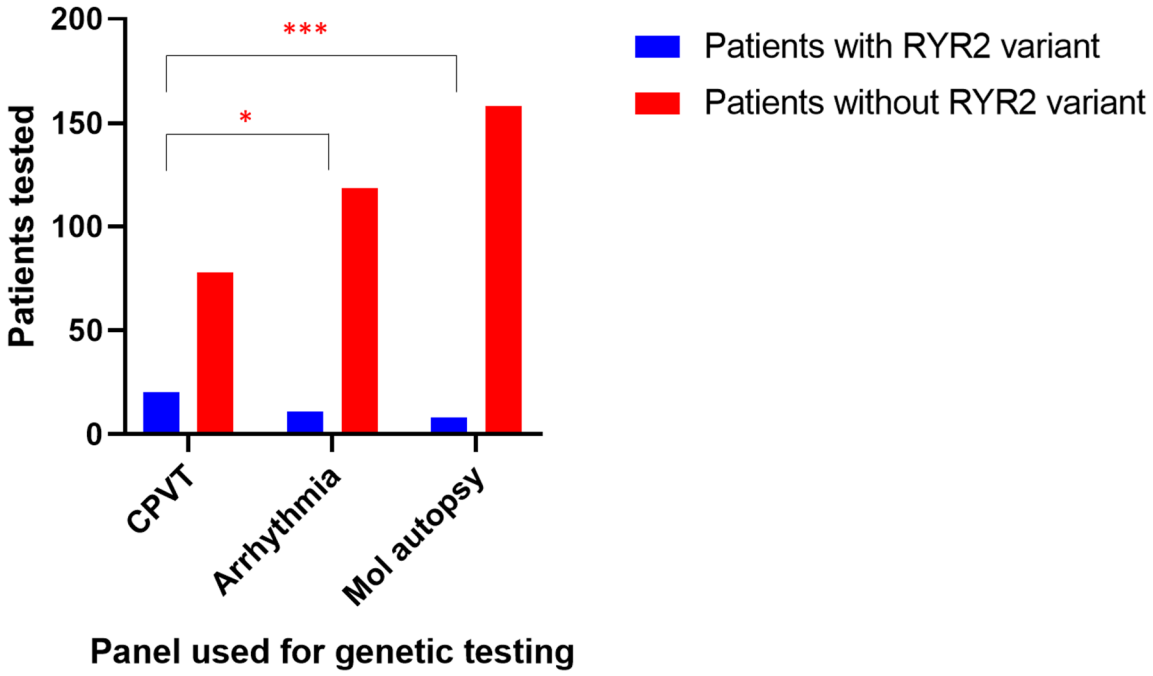

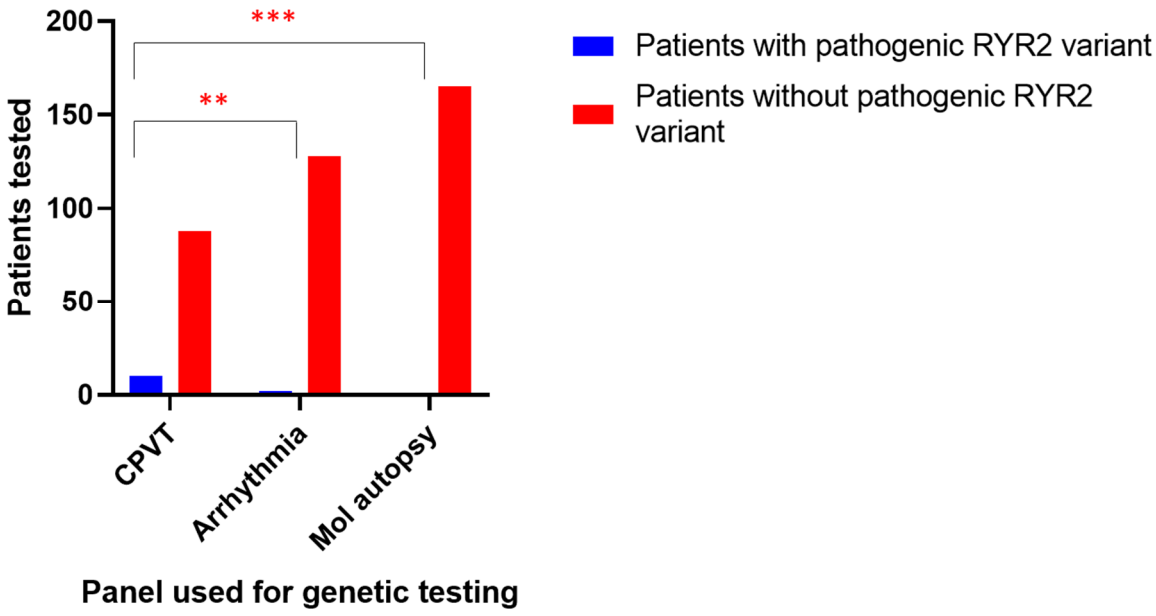

Figure 3.3. (A) Number of patients referred for genetic testing using the CPVT, arrhythmia or molecular autopsy panel with an RYR2 variant detected. (B) Number of patients referred for genetic testing using the CPVT, arrhythmia or molecular autopsy panel with a pathogenic RYR2 variant detected. *** and * represent $P < 0.001$ and $P < 0.05$, respectively.

3.5 Discussion

The availability of sequence variant databases like gnomAD (Karczewski et al., 2019) and a statistical threshold to aid in the classification of pathogenicity for genetic variants (Whiffin et al., 2017) is aiding the robust classification of sequence variants as associated, or not, with disease. The maximum tolerated allele count method was validated in individuals with hypertrophic cardiomyopathy using previous variant assessments and reports of pathogenicity in ClinVar (Stenson et al., 2014). In the present study we used this method to calculate a maximum tolerated allele count for CPVT-associated *RYR2* missense variants. Using this frequency threshold, 55 of 326 (16.9%) CPVT associated *RYR2* variants were re-classified as benign. Thus, our data show a sizeable number of *RYR2* variants are not disease-causing, in which case the proportion of CPVT cases attributable to *RYR2* variants is likely to be over-estimated and the proportion of cases attributable to changes in other genes or to post-translational modifications is likely to be underestimated. The reclassification of VUS as benign variants is important as family members previously cascade tested to carry these variants may not be at increased risk and those without these variants may have been falsely reassured and remain at risk of arrhythmia or sudden cardiac death. Furthermore, this classification of benign variants offers the opportunity to find the real explanation for the CPVT phenotype in affected individuals.

In the present study the maximum tolerated allele count for CPVT associated RYR2 missense variants was calculated using both the ExAC and gnomAD databases as control populations. Variants that occurred above the frequency threshold in each population where then reclassified accordingly. The ExAC database contains exome data from 60,706 unrelated apparently healthy individuals, whereas the gnomAD database contains combined exome and genome variant data from 141,456 individuals. Importantly 1600 of the 1975 (81%) *RYR2* missense variants reported in gnomAD have a minor allele count below four. This not only highlights that a number of potentially healthy individuals have rare variants in *RYR2* which may have a consequence in the context of a particular trigger e.g. exercise or emotion, but also that many benign *RYR2* variants are rare. The utility of larger control datasets in reclassifying *RYR2* variants was exemplified in this study. Comparison with the larger gnomAD database as a control population allowed the

reclassification of 11 additional *RYR2* variants as benign compared to ExAC. Further reclassification of VUSs may be achieved with larger sequence datasets and by using data from individuals with more phenotype data and of older age to reduce the effects of non-penetrance.

Applying Consurf, we found *RYR2* variants present in CPVT patients occurred at amino acid positions that were significantly more conserved than those of control variants and the conservation of residues where CPVT sudden death variants occurred was even greater (Figure 3.2). The application of a frequency threshold in control datasets with the consideration of Consurf may be more informative than using each method independently and may be particularly useful for determining the probability of a rare variant being pathogenic or benign.

Both RYR2 variants and CPVT are commonly associated with arrhythmias and/or sudden death triggered by exercise or stress. However, we noted *RYR2* variants in individuals who died or experienced cardiac arrest while asleep. In these patients almost all of the *RYR2* variants that were not classified as benign resulted in changes within the C-terminal of the protein, with the exception of one variant that occurred in the central domain. Although, limited by the small number of cases this data suggests pathogenic C-terminal *RYR2* variants may pose a greater risk of sudden death at rest, particularly during sleep. This relationship between C- terminal variants and sudden death in sleep is novel and requires independent validation. Sleep is considered a restful period but during rapid eye movement (REM) sleep, which accounts for approximately 20% of sleep time, sympathetic activity is increased and intense emotional states occur (Verrier and Josephson, 2009). Thus, sudden death during sleep in patients with *RYR2* variants may be due to episodes triggered by increased sympathetic activity comparable to exercise or emotional stress. Contrastingly, specific *RYR2* variants may exhibit properties that increase the channels sensitivity to other sleep related triggers like rises in hormones such as melatonin which has been shown to induce ventricular arrythmias (de Vries et al., 2017, Tooley et al., 2000). Importantly in a recent prospective study of sudden cardiac death the majority of deaths occurred during sleep (Bagnall et al., 2016) and CPVT should be considered as a potential cause in this setting.

Our data shows that CPVT-associated *RYR2* variants predominantly cluster in four regions/domains, namely the RyR and IP3R homology-associated domain; the ion transport domain; and two regions outside of known domains (No domain regions 5 and 7). Generally, these regions correspond to the previously reported mutation hotspots. However, more than 30% of CPVT-associated *RYR2* variants occurred outside of mutation hotspots, emphasising the importance of screening the entire coding region of *RYR2* in patients suspected of having CPVT.

The presence of functional data was a major driver of pathogenic classifications. However functional data was only available for 50 of the 326 CPVT associated variants. In addition to this the threshold of at least a 50% effect on channel function required for pathogenicity as applied by Denham et al. (2019) may not be applicable for *RYR2* as there is no direct correlation between the magnitude of variant functional effect and disease phenotype in CPVT (Denham et al., 2019). Computational evidence and absence from control datasets were also major contributors to pathogenic classifications, similar to Denham et al. (2019), we used eight computational tools and applied a threshold of six tools predicting a pathogenic effect for pathogenic classification (Denham et al., 2019). This method was found to be more stringent and require more evidence for a pathogenic classification when compared to previous systems (Denham et al., 2019).

A limitation of this study was the lack of systematically collected phenotype data and this will be required prospectively to identify effective means of combining clinical and genetic information to make accurate CPVT diagnoses. Nonetheless, based on the clinical indications considered our data shows specificity of testing (a surrogate for confidence in the underlying phenotype) correlates with the likelihood of identifying a relevant variant. Thus, although genetic testing is a useful aid in the diagnosis of CPVT rigorous clinical evaluations and the establishment of additional common phenotypic traits for CPVT is likely to increase the efficiency of genetic testing, identification of pathogenic variants and possibly improve the management of the condition.

In summary, CPVT-associated *RYR2* variants cluster in specific domains/regions, many of which are within, but not confined to, previously established mutation hotspots. CPVT-associated variants occur at residues that are more evolutionarily conserved than

controls, and RYR2 variants associated with sudden death occur at positions which are even more highly conserved. The application of a frequency threshold for pathogenicity, amino acid conservation scores and functional data aid distinguishing pathogenic and benign variants. However, the majority of CPVT variants remain classified as VUS. Therefore, additional approaches are required, including sharing of sequence data from affected individuals through Clinvar and other resources, generation of additional sequence data from healthy controls and use of sensitive high-throughput functional assays like saturation genome editing, with sufficient weight to drive pathogenic or benign classifications (Findlay et al., 2018).

The authors have no conflict of interest to declare.

Acknowledgements

This work was funded by a British Heart Foundation PhD studentship to DO. WGN is supported by the Manchester NIHR BRC (IS-BRC-1215-20007). The authors would like to thank the Genome Aggregation Database (gnomAD) and the groups that provided exome and genome variant data to this resource. A full list of contributing groups can be found at https://gnomad.broadinstitute.org/about.

Supplementary information is available at the Journal of Human Genetics website.

3.6 References

Bagnall et al. 2016. A Prospective Study of Sudden Cardiac Death among Children and Young Adults. *New England Journal of Medicine* 374, 2441-2452.

Chen, W.S.R. et al. 2002. Role of the Proposed Pore-Forming Segment of the Ca2+ Release Channel (Ryanodine Receptor) in Ryanodine Interaction*. *Biophysical Journal*. 82(5): pp.2436-2447.

Denham, N. C. 2019. Systematic re-evaluation of SCN5A variants associated with Brugada syndrome. *Journal of Cardiovascular Electrophysiology* 30, pp.118-127.

de Vries, L.J., Géczy, T. and Szili-Torok, T. 2017. Sleep Medications Containing Melatonin can Potentially Induce Ventricular Arrhythmias in Structurally Normal Hearts: A 2-Patient Report. *Journal of Cardiovascular Pharmacology* 70(4): pp.267-270.

Devalla, H. D. et al. 2016. TECRL, a new life-threatening inherited arrhythmia gene associated with overlapping clinical features of both LQTS and CPVT. *EMBO molecular medicine* 8, pp.1390-1408.

Findlay G.M. et al. 2018. Accurate classification of BRCA1 variants with saturation genome editing. *Nature*. 562(7726): pp.217-222.

George, C. H., Jundi, H., Thomas, N. L., Fry, D. L. and Lai, F. A. 2007. Ryanodine receptors and ventricular arrhythmias: Emerging trends in mutations, mechanisms and therapies. *Journal of Molecular and Cellular Cardiology* 42, pp.34-50.

George, C. H. et al. 2004. Ryanodine receptor regulation by intramolecular interaction between cytoplasmic and transmembrane domains. *Molecular biology of the cell* 15, pp.2627-2638.

Karczewski K.J., et al. 2019. Variation across 141,456 human exomes and genomes reveals the spectrum of loss-of-function intolerance across human protein-coding genes. *bioRxiv* 531210.

Lahat H., et al. 2001. A missense mutation in a highly conserved region of CASQ2 is associated with autosomal recessive catecholamine-induced polymorphic ventricular tachycardia in Bedouin families from Israel. *American Journal of Human Genetics*. 69(6): pp.1378-1384.

Landrum M.J. et al. 2016. ClinVar: public archive of interpretations of clinically relevant variants. *Nucleic Acids Research* 44(D1): pp.D862-D868.

Liu, N., Ruan, Y. and Priori, S. G. 2008. Catecholaminergic Polymorphic Ventricular Tachycardia. *Progress in Cardiovascular Diseases* 51, pp.23-30.
Napolitano, C. et al. 2013. Clinical utility gene card for: Catecholaminergic polymorphic ventricular tachycardia (CPVT). *European Journal Of Human Genetics* 22, pp.152.
Nyegaard, M. et al. 2012. Mutations in calmodulin cause ventricular tachycardia and sudden cardiac death. *American journal of human genetics* 91, pp.703-712.
Ohno, S. et al. 2014. Exon 3 deletion of RYR2 encoding cardiac ryanodine receptor is associated with left ventricular non-compaction. *EP Europace* 16(11): pp.1646-1654.
Priori, S.G. et al. 2002. Clinical and Molecular Characterization of Patients With Catecholaminergic Polymorphic Ventricular Tachycardia. *Circulation* 106, pp.69-74.
Richards, S. et al. 2015. Standards and guidelines for the interpretation of sequence variants: a joint consensus recommendation of the American College of Medical Genetics and Genomics and the Association for Molecular Pathology. *Genetics in medicine* 17(5): pp.405-424.
Roux-Buisson, N. et al. 2012. Absence of triadin, a protein of the calcium release complex, is responsible for cardiac arrhythmia with sudden death in human. *Human molecular genetics* 21, pp.2759-2767.
Stenson P.D., Mort M., Ball E.V., Shaw K., Phillips A. and Cooper D.N. 2014.The Human Gene Mutation Database: building a comprehensive mutation repository for clinical and molecular genetics, diagnostic testing and personalized genomic medicine. *Human Genetics* 133(1): pp.1-9.
Tester, D. J., Medeiros-Domingo, A., Will, M. L., Haglund, C. M. and Ackerman, M. J. 2012. Cardiac channel molecular autopsy: insights from 173 consecutive cases of autopsy-negative sudden unexplained death referred for postmortem genetic testing. *Mayo Clinic proceedings* 87, pp.524-539.
Tooley, G.A., Armstrong, S.M., Norman, T.R., Sali, A. 2000. Acute increases in night-time plasma melatonin levels following a period of meditation. *Biological Psychology*. 53(1): pp.69-78.
Verrier, R.L. and Josephson, M.E. 2009. Impact of sleep on arrhythmogenesis. *Circulation* 2(4): pp.450-459.
Whiffin, N. et al. 2017. Using high-resolution variant frequencies to empower clinical genome interpretation. *Genetics In Medicine* 19, pp.1151.

Chapter 4: Assessment of disease-associated missense variants in *RYR2* on transcript splicing

Assessment of disease-associated missense variants in RYR2 on transcript splicing

Damilola Olubando,[1,2] Huw Thomas, [1,2] Minoru Horie,[3] Raymond T. O'Keefe, [1,2] Luigi Venetucci,[4,5] William G. Newman[1,2,5]

[1]Manchester Centre for Genomic Medicine, Manchester University NHS Foundation Trust, Health Innovation Manchester, Manchester, M13 9WL, UK.

[2]Division of Evolution and Genomic Sciences, Faculty of Biology, Medicine and Human Sciences, University of Manchester, Manchester, UK.

[3]Department of Cardiovascular and Respiratory Medicine, Shiga University of Medical Sciences, Otsu, Shiga, Japan.

[4]Manchester Heart Centre, Manchester University NHS Foundation Trust, Manchester, M13 9WL, UK.

[5]Division of Cardiovascular Sciences, Faculty of Biology, Medicine and Human Sciences, University of Manchester, Manchester, UK.

[6]Peking University Health Sciences Center, Beijing, PR China

Correspondence to:
Professor WG Newman,
Manchester Centre for Genomic Medicine,
St Mary's Hospital,
Manchester M13 9WL, UK.
E-mail: william.newman@manchester.ac.uk

Acknowledgements

This work was funded by a British Heart Foundation PhD studentship to DO. WGN is supported by the Manchester NIHR BRC (IS-BRC-1215-20007).

Author Contributions

William Newman, Raymond Keefe and Luigi Venetucci designed the study and revised the article critically for important intellectual content. Damilola Olubando drafted the article and performed the computational analyses and minigene experiments with Huw Thomas. Minoru Horie provided clinical information on variants and critically revised the article for important intellectual content.

Conflict of Interest

On behalf of all authors, the corresponding author states that there is no conflict of interest.

4.1 Abstract

Heterozygous *RYR2* missense variants cause catecholaminergic polymorphic ventricular tachycardia. Rarely, loss of function variants can result in ventricular arrhythmias. We used splice prediction tools and an *ex vivo* splicing assay to investigate whether *RYR2* missense variants result in altered splicing. Ten *RYR2* variants were consistently predicted to disrupt splicing, however none altered splicing in the splicing assay. In summary, missense *RYR2* variants are unlikely to cause disease by altered splicing.

Catecholaminergic polymorphic ventricular tachycardia (CPVT) is a rare genetic arrhythmogenic condition affecting approximately one in 10,000 individuals (Napolitano et al., 2019). It is characterised by episodic ventricular dysrhythmia triggered by exercise or emotion. CPVT is genetically heterogeneous with both autosomal dominant and recessive forms. Heterozygous variants in *RYR2* (MIM 180902, ID: 6262) (Priori et al., 2001) and *CALM1* (MIM 114180) (Nyegaard et al., 2012) result in autosomal dominant forms of CPVT, whereas biallelic variants in *CASQ2* (MIM 114251), (Lahat et al., 2001) *TRDN* (MIM 603283) (Roux-Buisson et al., 2012) and *TECRL* (MIM 617242) result in recessive forms (Devalla et al., 2016). A number of cases of CPVT are molecularly unexplained, however approximately 50 % of cases can be accounted for by gain of function missense variants in the cardiac ryanodine receptor (RYR2) (Liu et al., 2008, Napolitano et al., 2019). The classification of genetic variants identified in the *RYR2* gene as pathogenic or benign is important for the accurate diagnosis, treatment and counseling of affected individuals and their relatives. Increased genetic testing of individuals with arrhythmias and advances in sequencing technology has resulted in a rapid increase in the number of *RYR2* variants identified. Application of the guidelines from the American College of Medical Genetics (ACMG) for sequence variant classification (Richards et al., 2015) results in the majority of variants defined as variants of unknown significance (VUS) due to factors including, incomplete penetrance, a lack of functional data and as the majority of putative variants have only been described in a single family. Comparison of allele frequency with databases of sequence variation in healthy controls, including gnomAD has facilitated variant classification (Karczewski et al., 2019).

As many as 9 % of disease-associated single nucleotide variants in the Human Gene Mutation Database (HGMD) result in splice alterations (Krawczak et al., 1992, Anna and Monika, 2018). A subset of these variants disrupt the function of exonic splicing elements (Anna and Monika, 2018). Recent studies have shown that some individuals with ventricular arrhythmias with similarity to CPVT can be attributed to loss of function variants in *RYR2* (Roston et al., 2017). Therefore, spliceogenic variants resulting in loss of function may manifest as CPVT. Indeed a spliceogenic *RYR2* variant c.6167-2A>G was recently identified in a 9 year old male with CPVT and no structural cardiac abnormalities (Lieve et al., 2019). In the present study we proposed that some CPVT associated *RYR2* missense variants cause a loss of function through the disruption of exonic splice

elements and altering splicing, resulting in frameshifts and haploinsufficiency. We investigated this using computational splice prediction tools and an *ex vivo* splicing assay. A total of 324 rare or novel variants in *RYR2* classified as pathogenic, likely pathogenic or VUS were collated from a cohort of individuals undergoing genetic testing for CPVT or associated ventricular arrhythmia in the North West Genomic Laboratory Hub, UK. This list was supplemented with *RYR2* variants, reported in the literature and in clinical variant databases, including ClinVar and HGMD (Supplementary Table 4.1) (Stenson et al., 2014). The effect variants are likely to have on splicing was predicted computationally using Alamut version 2.0 (Interactive Biosoftware, Rouen, France). Alamut incorporates five splicing prediction tools (Table 4.1). Those variants in which a 100 % change was seen in the confidence score for the presence or absence of a splice feature in the wild-type (WT) compared to the variant by at least four prediction tools were chosen to be studied in the *ex vivo* mini gene assay (Table 4.2).

Table 4.1. Algorithm by which the various tools predict splicing effects.

Splicing tool	Splice prediction algorithm
NNSplice http://www.fruitfly.org/seq_tools/splice.html	NNSplice uses a neural network that identifies motifs with consensus sequences. It also takes into account commonly occurring neighbouring sequences (Jian et al., 2014).
SpliceSiteFinder-like https://www.interactive-biosoftware.com/doc/alamut-visual/2.6/splicing.html	SpliceSiteFinder-like uses position weight matrices developed from a database of human exon/intron boundaries for both donor and acceptor sites (Zhang, 1998).
MaxEntScan http://genes.mit.edu/burgelab/maxent/Xmaxentscan_scoreseq.html	The maximum entropy principle is used to model sequence motifs. The short sequence motifs involved RNA splicing are modelled with a maximum energy distribution (Yeo and Burge, 2004).
Human Splicing Finder http://www.umd.be/HSF/	Human splicing finder uses position weight matrices supplemented with position based logic. Each nucleotide is assigned a weight, the assigned weight is dependent on the frequency of the nucleotide and the comparative importance of its location within the

	sequence motif (Stenson et al., 2015).
GeneSplicer http://ccb.jhu.edu/software/genesplicer/	GeneSplicer uses a combination of a second order Markov model and the maximal dependence decomposition decision tree method. Markov models predict a base by studying the surrounding bases. In this case a region consisting of the 16 and 29 bases is scored for donor sites and acceptor sites, respectively. The MDD aligns a set of sequences of varying sizes and creates a model that incorporates the most vital dependencies from one position to another (Pertea et al., 2001).

Table 4.2. CPVT associated *RYR2* variants predicted to affect splicing by 4 or 5 of the 5 splice prediction tools.

cDNA change	Protein change	ACMG classification (evidence of pathogenicity)	Predicted effect on splicing	Number of concordant tools	Exon	Domain
c.497C>G	p.(Ser166Cys)	VUS (absent in gnomAD)	Introduce 5' Splice Site	4	8	I
c.527G>A	p.(Arg176Gln)	Pathogenic (functional evidence (amino acid change), frequently reported in CPVT cases, absent in gnomAD, computational evidence)	Deletion of 5' Splice Site	4	8	I
c.6272A>G	p.(Gln2091Arg)	VUS (absent in gnomAD, computational evidence)	Introduce 3' Splice Site	4	41	
c.6961G>A	p.(Val2321Met)	VUS (absent in gnomAD)	Deletion 5' Splice Site	4	46	II
c.7169C>T	p.(Thr2390Ile)	VUS (absent in gnomAD, computational evidence)	Introduce 5' Splice Site	5	47	II
c.7181C>G	p.(Arg2394Gly)	VUS (absent in gnomAD, segregation with CPVT phenotype, computational evidence)	Introduce 5' Splice Site	4	47	II
c.7420A>G	p.(Arg2474Gly)	VUS (absent in gnomAD)	Deletion 3' Splice Site	5	49	II
c.7813A>G	p.(Met2605Val)	VUS (absent in gnomAD)	Introduce 5' Splice Site	4	51	
c.11399G>T	p.(Cys3800Phe)	VUS (computational evidence)	Deletion 5' Splice Site	5	83	III
c.12371G>A	p.(Ser4124Asn)	VUS (absent in gnomAD, computational evidence)	Deletion 5' & 3' Splice Site	5	90	III

The 3.8 kb pSpliceExpress minigene splicing reporter vector gifted from Stefan Stamm (Addgene plasmid # 32485; http://n2t.net/addgene:32485 ; RRID:Addgene_32485) (Kishore et al., 2007) was restriction digested with NheI/BamhI and amplified by PCR with Phusion High-Fidelity DNA Polymerase (Figure 4.1) (ThermoFisher Scientific). The DNA sequences of the exons containing the *RYR2* variants of interest as well as ~100 bp of the flanking 5' and 3' intronic sequences were amplified using PCR from genomic DNA using Phusion High-Fidelity DNA Polymerase. Two primer pairs were designed to generate two fragments that overlap with each other and the vector fragment, by approximately 20 bp and 10 bp, respectively (Table 4.3). Overlapping primer sequences were modified where needed to produce CPVT-associated *RYR2* variants (Table 4.3). The assembly of the *RYR2* fragments and vector fragment was achieved using the Gibson method using the manufacturer's protocol. The resulting plasmid was transformed into competent E. coli. Vector DNA was amplified and purified from selected colonies and the successful assembly of the vectors was confirmed by direct Sanger sequencing. Minigene vector DNA (0.2 μg) was transfected into HEK293 cells at confluence of 40-60 % grown in Dulbecco's modified Eagle's medium high-glucose, DMEM (Sigma), supplemented with 10 % foetal bovine serum (Sigma) in tissue-culture treated 6-well plates at 37°C and with 5 % CO_2. Transfections were performed using Lipofectamine 2000 (Thermo Scientific) according to the manufacturer's protocol. RNA was extracted from HEK293 cells after a 48 hour incubation period in at 37 °C with 5 % CO_2, using phenol/chloroform precipitation using Trizol. RNA was purified using the RNeasy column cleanup kit (Qiagen), which included a DNase digestion step. Superscript Reverse Transcriptase (ThermoFisher Scientific) was used to synthesise cDNA. The cDNA produced was amplified using Phusion High-Fidelity DNA Polymerase (ThermoFisher Scientific) using "minigene RT PCR-for" and "minigene RT PCR-rev" primers (Table 4.3). The resulting PCR products were electrophoresed on an agarose gel (1-3 %), to establish the sequence of the spliced products the purified DNA was sequenced by direct Sanger sequencing performed by Eurofins Genomics.

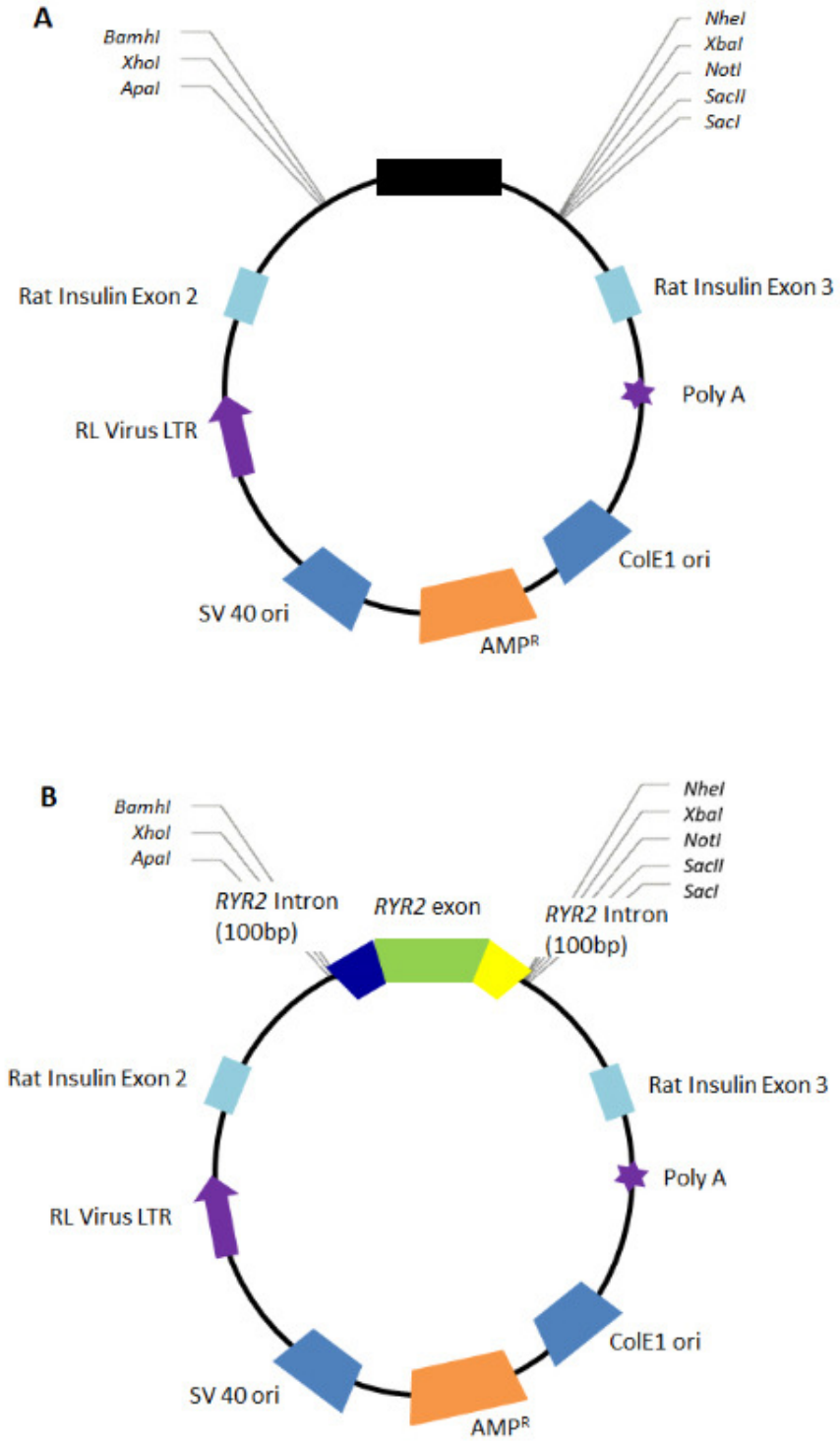

Figure 4.1. Schematic representation of pSpliceExpress vector before (A) and after (B) the insertion of RYR2 exonic and intronic sequences. The black rectangle in A represents ccdB and Cm^R sequences which are present in the pSpliceExpress vector but were not used for the selection of vectors with the correct insert.

Table 4.3. Primer list

Primer set	Forward	Reverse	Expected product size
c.497 C>G (exon8) fragment 1	GGGCCCCTCCGGATTTCTG AAAGTTGTGTGTTGG	GCTGCTTACAGGCAGGGTGT	149
c.497 C>G (exon8) fragment 2	CTGCCTGTAAGCAGCGATC AGAA	GCTGGATGGCATTTTCATAGA TAATTTACAATATAAACCTTAA AGAGATCATTTTATTG	196
c.527 G>A (exon8) fragment 1	GGGCCCCTCCGGATTTCTG AAAGTTGTGTGTTGG	ATCTCCAACTTGTACTTTTTCTC CTTCTGA	149
c.527 G>A (exon8) fragment 2	AAAAAGTACAAGTTGGAG ATGACCTCATCT	GCTGGATGGCATTTTCATAGA TAATTTACAATATAAACCTTAA AGAGATCATTTTATTG	196
c.6167-2A>G (intronic) fragment 1	GGGCCCCAGAAATACCAAT TTGGGGGTACAGGA	GCAGAGTGGCCGCAAAGTCAT TATG	236
c.6167-2A>G (intronic) fragment 2	TGACTTTGCGGCCACTCTG CAGCA	CTGGATGGCGACAATATATTT TTATCAATGTAGTTAATGTACT GCTCTATAGG	308
c.6272 A>G (exon 41) fragment 1	GGGCCCCAGAAATACCAAT TTGGGGGTACAGGA	CGTCATACCGCCGATGGAGCA	236
c.6272 A>G (exon 41) fragment 2	CATCGGCGGTATGACGGCA TTG	CTGGATGGCGACAATATATTT TTATCAATGTAGTTAATGTACT GCTCTATAGG	308
c.6961 G>A (exon 46) fragment 1	CGGGCCCCTAGTTATTCTTA TACATAGGAAATGATTAGT ATAACATTTATTTGTTCAG	CAATCTCATCACGACATTTGCA TTTTCC	149
c.6961 G>A (exon 46) fragment 1	TGTCGTGATGAGATTGCTC ATTCG	TGGATGGCACCACAAGTTATA TTACAATTCATAGGATGCAGA	271
c.7169C>T (exon 47) fragment 1	GGGCCCCTGTGTTACCTAG TAGTCCCTTTCCTCGG	TGAATAGAAGATCATGATCGC GTTCC	171
c.7169C>T (exon 47) fragment 2	CGATCATGATCTTCTATTCA GCTTTGATTGA	CTGGATGGCGAAGATTATTGG TTTTGGATGCTGTTATGCT	171
c.7181 C>G (exon47) fragment 1	GGGCCCCTGTGTTACCTAG TAGTCCCTTTCCTCGG	GGTCAATCAAACCTGAATAGA AGGTCATGA	171
c.7181 C>G (exon47) fragment 2	TCTATTCAGGTTTGATTGAC CTCTTGGGA	CTGGATGGCGAAGATTATTGG TTTTGGATGCTGTTATGCT	171
c.7420 A>G (exon 49) fragment 1	GGGCCCCAAACTGTGTTTA AAATGTAAGAAGTCTAGAA AGCAG	CATAGACCCCGTCAAGGAATA AAACCATGG	194
c.7420 A>G (exon 49) fragment 2	TCCTTGACGGGGTCTATGG GATTGA	CTGGATGGCTTCATTGTCAATA AATTAATGAATGGATATATAA AAAAGAACATCA	210

c.7813 A>G (exon 51) fragment 1	CGGGCCCCATAGATTCAGGTCCTTGGCTGATATAATTTATTCTAAT	AAGAGGCACCTTTGCGTGTTCATTTAATAATG	196
c.7813 A>G (exon 51) fragment 2	CGCAAAGGTGCCTCTTAAAGTAAGTATAGGAAA	TGGATGGCAGCGTCAAGCATGATGTATCTAAGAAAT	127
c.11399 G>T fragment 1 (exon 83)	GGGCCCCCTGTCTATTCTAGAATGGAAAGCCTGTTT	CCTTACCTAAATGACTGCATCAGGC	190
c.11399 G>T fragment 2 (exon 83)	GCAGTCATTTAGGTAAGGACTCACT	CTGGATGGCAACTATTCTTCTATGTGCAATTATCGTCAGAGT	121
c.12371 G>A fragment 1 (exon 90)	GGGCCCCTCCTTGATTCAGATGTTATTAAAGATCTACATTGTTATCTTCTG	TCAGGACGTTCTCTGCTAATTCCA	539
c.12371 G>A fragment 2 (exon 90)	CAGAGAACGTCCTGAATTATTTCCAGC	TGGATGGCAACACCGTTCTGGCACTAGC	1019
Minigene	TGCTGGCCCTGCTCATCCTCTG	TGGACAGGGTAGTGGTGGGCCT	variable

RYR2 c.6167-2A>G was used as a positive control in the minigene assays (Lieve et al., 2019). This variant activated a cryptic splice site resulting in an 11 bp frameshift that introduces a premature stop codon within exon 41 (*p.Ser2056Serfs*5*) (Figure 4.2). Ten of the disease-associated *RYR2* variants were predicted to affect splicing by four or more computational prediction tools. Eight out of 10 of the tested variants were present in known disease associated variant hotspot regions of *RYR2* and were reported to have resulted in sudden death, syncope or arrhythmias (Supplementary Table 4.2). All 10 variants were at least 100 bp away from the canonical splice site and were mostly present in different exons ranging from exon 8 to exon 90 and had no effect on splicing in the minigene assay, this was confirmed by agarose gel electrophoresis and direct sequencing of the resulting bands (Supplementary Figure 4.1).

The majority of sequence variants in *RYR2* in patients with a clinical diagnosis of CPVT or ventricular arrhythmia are classified as variants of uncertain significance. It is therefore difficult to molecularly confirm a diagnosis of CPVT and therefore to use genotype data to facilitate cascade testing to clarify the risk to close relatives of an affected individual. Functional studies to determine the pathogenicity of *RYR2* variants are challenging due to the size of the gene and encoded protein and its expression which is limited to cardiac and brain tissue. Recently, loss of function variants in *RYR2* have been reported to result in ventricular arrhythmias (Roston et al., 2017).

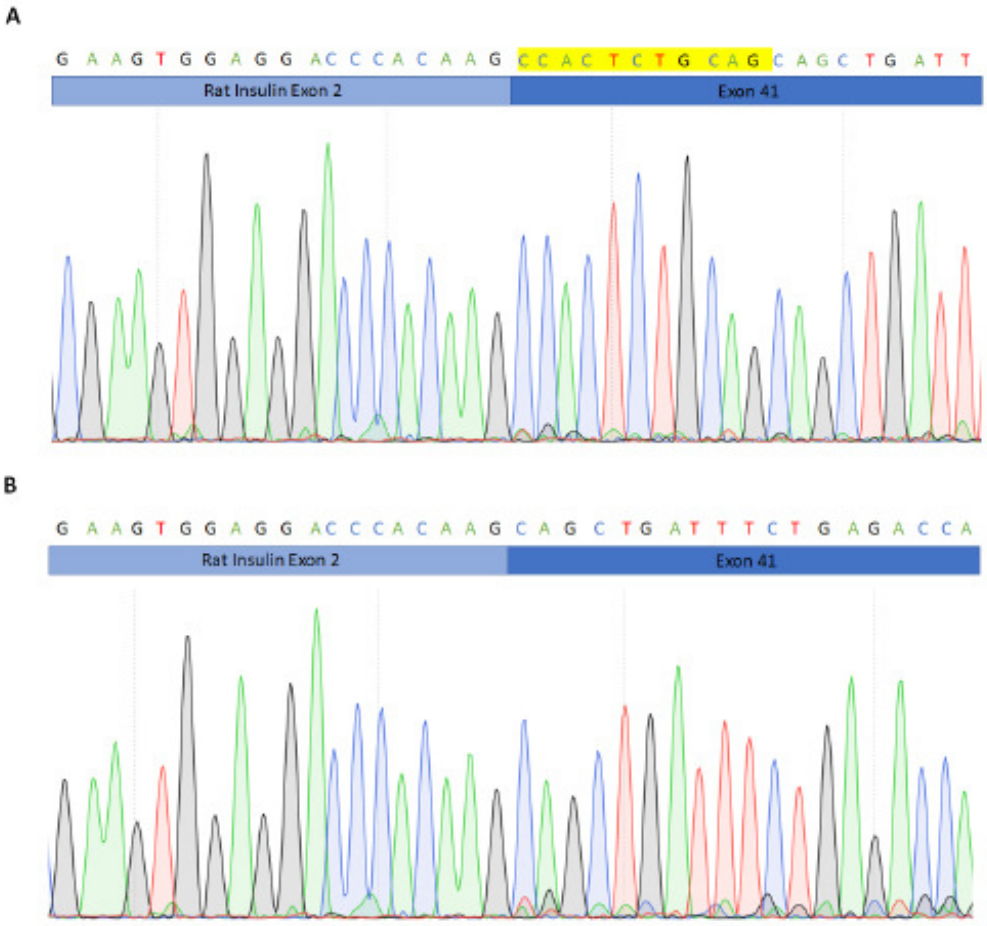

Figure 4.2. Electropherogram of cDNA sequences at the exon border between vector sequence (rat insulin exon 2) and RYR2 exon 41, for *RYR2* WT (A) and the splice variant *RYR2* c.6167-2A>G (B). Regions highlighted in yellow represent sequences skipped in *RYR2* c.6167-2A>G.

Although computational splice prediction tools have been shown to be reasonably accurate in predicting the effects of intronic splice variants less is known about their ability to predict the effects of exonic variants on splicing (Thery et al., 2011). Théry *et al*. (2011) investigated the effects of 53 coding and non-coding VUS in *BRCA1* and *BRCA2* on splicing (Thery et al., 2011). Computational splice prediction tools indicated that none of the exonic variants would be spliceogenic. However, all 53 variants were tested using an *ex vivo* splicing assay. Four of the ten non-coding variants, predicted to affect splicing by computational tools, were confirmed and five exonic variants resulted in exon skipping in the *ex vivo* assay. This data would indicate that the effect on splicing of exonic single

nucleotide variants is underestimated (Anna and Monika, 2018). For the exonic variants that altered splicing in the minigene assay Théry *et al*. (2011) were able to confirm the results by analyzing lymphocyte derived RNA from the individual carrying the variant. This validation demonstrated the reliability of the assay, which is particularly useful for conditions like CPVT where relevant RNA from an affected individual is often unavailable due to the expression of RYR2 being limited to the heart and brain.

Here, we tested the ten *RYR2* variants where *in silico* predictions indicated a potential effect on transcript splicing. The vast and rapidly growing number of VUS being identified means that functional testing of each disease-associated variant is impractical. Thus, a reliable means of selecting those variants most likely to affect splicing for *ex vivo* testing is required. Computational splice prediction tools can be helpful, but the reliability of these tools for predicting the effects of exonic splice variants requires further validation. We proposed that by applying more stringent parameters by testing only those variants in which an effect on splicing was predicted by at least four of five available prediction tools may reduce the number of false positives. It is important to note that splicing minigene assays may not be able to detect very rare splicing events. To reduce the chances of such transcripts going undetected it may be beneficial to perform multiple splicing assays using a variety of cell types.

In our study, we provide no evidence to support the hypothesis that missense variants in *RYR2* result in altered transcript splicing and so lead to loss of function pathogenic variants. However, it is possible that exonic variants that may have less predictive power using current algorithms do result in altered splicing. Such variants should be considered as higher throughput methods to assess splicing, including saturation genome editing by CRISPR-Cas9, are developed (Findlay et al., 2018).

4.2 References

Anna, A. and Monika, G. 2018. Splicing mutations in human genetic disorders: examples, detection, and confirmation. *Journal of Applied Genetics* 59, pp.253-268.

Devalla, H. D. et al. 2016. TECRL, a new life-threatening inherited arrhythmia gene associated with overlapping clinical features of both LQTS and CPVT. *EMBO molecular medicine* 8, pp.1390-1408.

Findlay G.M. et al. 2018. Accurate classification of BRCA1 variants with saturation genome editing. *Nature*. 562(7726): pp.217-222.

Jian, X., Boerwinkle, E. and Liu, X. 2014. In silico tools for splicing defect prediction: a survey from the viewpoint of end users. *Genetics in medicine* 16, pp.497-503.

Karczewski K.J., et al. 2019. Variation across 141,456 human exomes and genomes reveals the spectrum of loss-of-function intolerance across human protein-coding genes. *bioRxiv* 531210.

Kishore S., Khanna A. and Stamm S. 2008. Rapid generation of splicing reporters with pSpliceExpress. *Gene* 427, pp.104-110.

Krawczak M., Reiss J. and Cooper D.N. 1992. The mutational spectrum of single base-pair substitutions in mRNA splice junctions of human genes: causes and consequences. *Human Genetics* 90, pp.41-54.

Lahat H., et al. 2001. A missense mutation in a highly conserved region of CASQ2 is associated with autosomal recessive catecholamine-induced polymorphic ventricular tachycardia in Bedouin families from Israel. *American Journal of Human Genetics*. 69(6): pp.1378-1384.

Landrum M.J. et al. 2016. ClinVar: public archive of interpretations of clinically relevant variants. *Nucleic Acids Research* 44(D1): pp.D862-D868.

Lieve, K. V. V. et al. 2019. Linking the heart and the brain: Neurodevelopmental disorders in patients with catecholaminergic polymorphic ventricular tachycardia. *Heart Rhythm* 16, pp.220-228.

Liu, N., Ruan, Y. and Priori, S. G. 2008. Catecholaminergic Polymorphic Ventricular Tachycardia. *Progress in Cardiovascular Diseases* 51, pp.23-30.

Napolitano, C., Priori, S.G. and Bloise. Catecholaminergic Polymorphic Ventricular Tachycardia. 2004 Oct 14 [Updated 2016 Oct 13]. In: Adam MP, Ardinger HH, Pagon RA, et

al., editors. GeneReviews® [Internet]. Seattle (WA): University of Washington, Seattle; 1993-2019.

Nyegaard, M. et al. 2012. Mutations in calmodulin cause ventricular tachycardia and sudden cardiac death. *American journal of human genetics* 91, pp.703-712.

Pertea, M., Lin, X. and Salzberg, S. L. 2001. GeneSplicer: a new computational method for splice site prediction. *Nucleic acids research* 29, pp.1185-1190.

Priori S.G. et al. 2001. Mutations in the Cardiac Ryanodine Receptor Gene (hRyR2) Underlie Catecholaminergic Polymorphic Ventricular Tachycardia. *Circulation* 103, pp.196-200.

Richards, S. et al. 2015. Standards and guidelines for the interpretation of sequence variants: a joint consensus recommendation of the American College of Medical Genetics and Genomics and the Association for Molecular Pathology. *Genetics in medicine* 17, pp.405-424.

Roston, T.M. et al. 2017. A novel RYR2 loss-of-function mutation (I4855M) is associated with left ventricular non-compaction and atypical catecholaminergic polymorphic ventricular tachycardia. *Journal of Electrocardiology* 50, 227-33.

Roux-Buisson, N. et al. 2012. Absence of triadin, a protein of the calcium release complex, is responsible for cardiac arrhythmia with sudden death in human. *Human molecular genetics* 21, pp.2759-2767.

Stenson P.D., Mort M., Ball E.V., Shaw K., Phillips A. and Cooper D.N. 2014.The Human Gene Mutation Database: building a comprehensive mutation repository for clinical and molecular genetics, diagnostic testing and personalized genomic medicine. *Human Genetics* 133(1): pp.1-9.

Thery, J.C. et al. 2011. Contribution of bioinformatics predictions and functional splicing assays to the interpretation of unclassified variants of the BRCA genes. *European Journal Human Genetics* 19, pp.1052-1058.

Yeo, G. and Burge, C. B. 2004. Maximum Entropy Modeling of Short Sequence Motifs with Applications to RNA Splicing Signals. *Journal of Computational Biology* 11, pp.377-394.

Zhang, M. Q. 1998. Statistical features of human exons and their flanking regions. *Human Molecular Genetics* 7, pp.919-932.

Chapter 5: Characterisation of a novel *RYR2* missense variant in a family with a history of sudden death

Characterisation of a novel RYR2 missense variant in a family with a history of sudden death

Damilola Olubando[1,2], N. Lowri Thomas[3], Christopher George[4], Luigi Venetucci[5,6], William G. Newman[1,2,7]

[1]Manchester Centre for Genomic Medicine, Manchester University NHS Foundation Trust, Health Innovation Manchester, Manchester, M13 9WL, UK.

[2]Division of Evolution and Genomic Sciences, Faculty of Biology, Medicine and Human Sciences, University of Manchester, Manchester, UK.

[3]School of Pharmacy and Pharmaceutical Sciences, Redwood Building, University of Cardiff, Cardiff, CF10 3NB, UK

[4]Institute of Life Science 1, Singleton Campus, Swansea University, Swansea, SA2 8PP, UK

[5]Manchester Heart Centre, Manchester University NHS Foundation Trust, Manchester, M13 9WL, UK.

[6]Division of Cardiovascular Sciences, Faculty of Biology, Medicine and Human Sciences, University of Manchester, Manchester, UK.

[7]Division of Population Health, Health Services Research & Primary Care, University of Manchester, Manchester, UK.

Correspondence to:

Professor WG Newman,

Manchester Centre for Genomic Medicine,

St Mary's Hospital,

Manchester M13 9WL, UK.

E-mail: william.newman@manchester.ac.uk

5.1 Abstract

Catecholaminergic polymorphic ventricular tachycardia (CPVT) is a rare arrhythmogenic disorder characterised by ventricular tachycardia and syncope triggered by physical or emotional stress. More recently, suppression of function (SOF) *RYR2* missense variants, that unlike more common gain of function *RYR2* variants reduce calcium release from the sarcoplasmic reticulum, have been reported in arrhythmia cases, some of which display phenotypes different from those commonly associated with CPVT (Roston et al., 2017). The phenotypic heterogeneity in CPVT may be attributable to differences in the properties of the mutant channels. To investigate this we functionally characterised the RyR2 Phe4905Leu (c.14713T>C) variant that was identified in an 18-year-old male who died during sleep and has a family history of non-exercise related sudden death. Spontaneous calcium release events in HEK 293 cells expressing eGFP-tagged RyR2 Phe4905Leu were significantly prolonged ($P < 0.005$) and were characterised by altered kinetics of Ca^{2+} release ($P < 0.005$) and sequestration. Importantly, the maximum amplitude of spontaneous Ca^{2+} release events in Phe4905Leu cells was reduced when compared with cells expressing WT RyR2 ($P < 0.005$). Furthermore, Phe4905Leu RyR2 was found to be less sensitive to agonist-activation using caffeine compared to WT RyR2. The longer duration of calcium release events may be an indication the RyR2 Phe4905Leu variant is a gain of function variant, however the reduced sensitivity to caffeine may be interpreted as a suppression of function. Thus, RyR2 Phe4905Leu channels present both gain of function and suppression of function properties.

5.2 Introduction

Catecholaminergic polymorphic ventricular tachycardia (CPVT) is a rare arrhythmogenic disorder characterised by ventricular tachycardia and syncope triggered by physical or emotional stress. Gain of function missense mutations in the cardiac ryanodine receptor are the most common known cause of CPVT. Heterozygous variants in *RYR2* (MIM 180902, ID: 6262) (Priori et al., 2001) and *CALM1* (MIM 114180) (Nyegaard et al., 2012) result in autosomal dominant forms of CPVT, whereas biallelic variants in *CASQ2* (MIM 114251), (Lahat et al., 2001) TRDN (MIM 603283) (Roux-Buisson et al., 2012) and *TECRL* (MIM 617242) result in recessive forms (Devalla et al., 2016). The RyR2 channel is modulated by both cytosolic and luminal Ca^{2+} and gain of function (GOF) mutations increase channel sensitivity to Ca^{2+} hastening the release of Ca^{2+} or prolonging the duration of Ca^{2+} release events this in turn predisposes to the onset of diastolic Ca^{2+} waves that cause delayed after depolarizations (DADs) and arrhythmias. More recently suppression of function (SOF) *RYR2* missense variants that reduce calcium release from the SR have been reported in arrhythmia cases, some of which display phenotypes different from those commonly associated with CPVT (Roston et al., 2017). For instance, in many cases with *RYR2* SOF variants there is an overlap with CPVT and left ventricular compaction, introducing the concept that CPVT may not be exclusive to structurally normal heart (Roston et al., 2017). Most SOF *RYR2* missense variants occur in the C-terminus indicating they're likely to have a direct impact on channel function rather than regulation, but the exact disease mechanisms of these variants are less defined as they are not exclusive to one domain (Roston et al., 2017; Bahat et al., 1997). In several patients with SOF-*RYR2* variants (e.g. Arg4860Gly) arrhythmias are not inducible by exercise stress testing (Zhao et al., 2015). Furthermore, Fujii et al. (2017) identified the SOF *RYR2* variant Ser4938Phe in a patient with short-coupled variant of torsades de pointes (TdP), demonstrating *RYR2* SOF variants can cause other arrhythmogenic conditions and may be sensitive to other triggers.

Sleep is considered a restful period, non-REM sleep accounts for 80 % of sleep time and is associated with reduced input of the sympathetic nervous system to the heart and metabolic demands. However, during rapid eye movement (REM) sleep, which accounts for approximately 20 % of sleep time, sympathetic activity is increased and intense

emotional states occur (Verrier and Josephson, 2009). Importantly in a recent prospective study of sudden cardiac death the majority of deaths occurred during sleep (Bagnall et al., 2016) and CPVT should be considered as a potential cause in this setting. How cardiac episodes are triggered during sleep is unclear, sudden death may occur during REM sleep and may be due to episodes triggered by increased sympathetic activity comparable to exercise or emotional stress, in which case such variants may present properties similar to typical CPVT related GOF RyR2 variants. Contrastingly, specific RyR2 variant channels may exhibit properties that increase their sensitivity to other sleep related triggers like rises in hormones such as melatonin which has been shown to induce ventricular arrhythmias (de Vries et al., 2017, Tooley et al., 2000). In the present study we present an 18-year-old male proband that died during sleep. Molecular autopsy revealed the proband carried the *RYR2* Phe4905Leu variant. We performed cascade screening on the proband's family and then functionally analyzed full length RyR2 channels with the Phe4905Leu variant in HEK 293 cells to determine the effects of the variant on intracellular calcium handling.

5.3 Methods

5.3.1 Clinical and genetic analysis

The clinical assessment of patients was performed at the Manchester Royal Infirmary, Wales and Liverpool. Patients underwent heart investigations ECG/ exercise ECG.

Genetic analysis was performed by the diagnostic lab of MCGM. DNA was extracted from two separate blood samples taken from the proband. DNA screening was performed targeting 61 genes associated with genetic cardiac disorders using Aligent SureSelect Custom Design and next generation sequencing using the HiSeq 2500 (Smith et al. 2014). Whole exon deletions and duplications were tested by MLPA (multiplex ligation dependent probe amplification). Most NGS protocols involve the fragmentation of DNA into short sequences which are read individually and then joined together using overlapping regions to produce longer contiguous DNA sequences. The length of the DNA sequence produced from the joining of the overlapping fragments, over the length of expected length of the region being sequenced (the target size), is known as coverage. In the present study a minimum coverage of 97.9 % was achieved in the target coding region of transcripts. The number of times each nucleotide in the genome is read in a single

experiment is referred to as read depth, the read depth must be sufficiently high to avoid errors. In this study a minimum read depth of 50X was achieved. GenomeAnalysisTool KiteLit-v2 0.39 (GATK) and the hg19 human genome reference were used to analyse sequence data (the hg19 human genome reference was updated by the Genome Reference Consortium in 2019). Cascade testing was undertaken on other relatives for the *RYR2* variant identified in the proband.

5.3.2 Computational analysis

Five protein-level in silico prediction tools: SIFT, PolyPhen, Mutation Taster, Mutation assessor, FATHMM were used for our computational analysis of genetic variants. Consurf (http://consurf.tau.ac.il/) which uses advanced probabilistic evolutionary models to distinguish true conservation resulting from purifying selection and produces estimates for the credibility of the results, was used to measure conservation of amino acid positions.

5.3.3 Functional analysis

Generation and expression of recombinant SCD associated RyR2 Variant:

The cDNA sequence encoding full-length human *RYR2* (published in GenBank as x98330) with an N-terminus enhanced green fluorescent protein (eGFP) tag was obtained from Dr Christopher George (George et al., 2003). Due to the large size of the full length *RYR2* cDNA, restriction enzymes were used to produce smaller RYR2 fragments (cassettes) that were easier to mutagenize (Figure 5.1). The single nucleotide change producing the Phe4905Leu (c.14713T>C) variant was introduced by oligonucleotide directed mutagenesis (Quickchange; Stratagene, Netherlands). All oligonucleotides underwent reverse-phase purification (Sigma-Genosys, Cambridge, UK).

The oligonucleotides used to generate Phe4905Leu (c.14713T>C) *RYR2* were:

Forward primer: CACAGTGCCACATGGCCTTGAAACCCACACTTTACAGG

Reverse primer: CCTGTAAAGTGTGGGTTTCAAGGCCATGTGGCACTGTG

Where highlighted characters represent the mutated codon.

The introduction of the Phe4905Leu variant was performed using the NheI/XhoI *RYR2* fragment (5320 bp) subcloned into pSL118ONX (Amersham Biosciences, UK). The mutagenized cassette was reinserted to create full-length h*RYR2* containing the Phe4905Leu (c.14713T>C) variant using the Fse1 and Xho1 restriction enzymes. The introduction of the correct change was confirmed by direct Sanger sequencing (ABI 3700, Applied Biosystems). Propagation of plasmid cDNAs encoding full length wild-type and Phe4905Leu GFP-tagged *RYR2* was performed in MAX Efficiency® Stbl2™ chemically competent cells (Invitrogen, Carlsbad, CA, USA). These cells were used due to their relatively efficient ability to propagate large and unstable plasmid DNA (like pcDNA3-eGFP-hRyR2) that is prone to spontaneous recombination. Plasmid DNA was purified using a column-based Maxi-Prep kit.

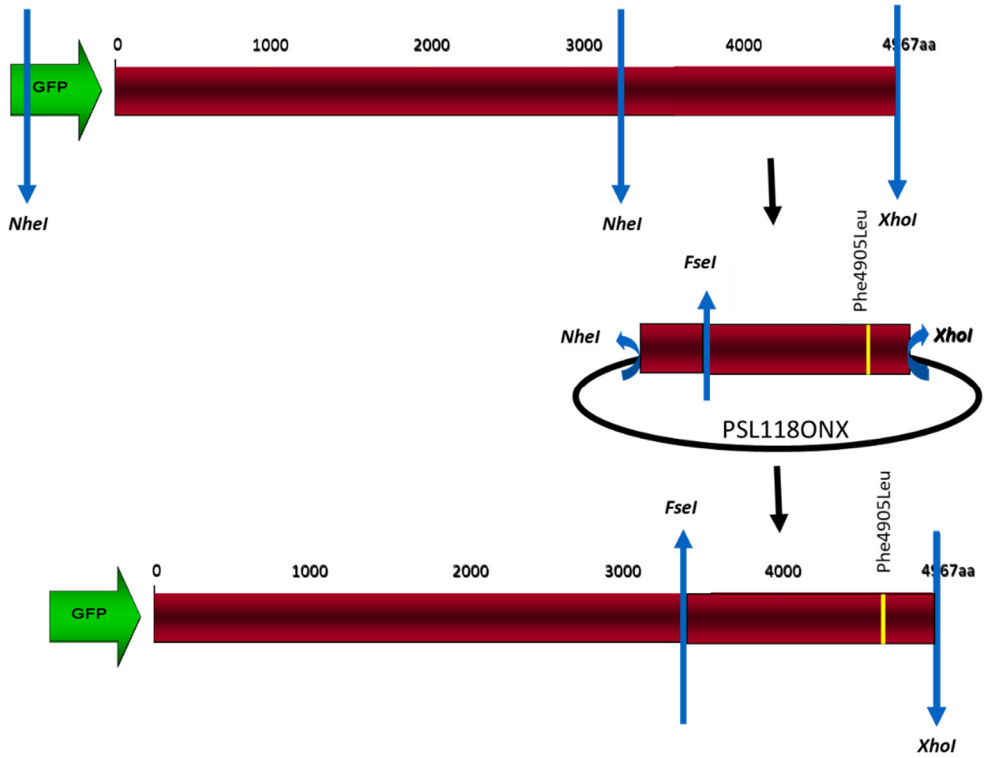

Figure 5.1. Schematic of the construction of Phe4905Leu *RYR2*. Due to the lack of unique restriction sites shared by both *RYR2* and the intermediate vector (PSL118ONX) both PSL118ONX and full length *RYR2* were digested with NheI and XhoI to yield three fragments, one of which (resolved by agarose gel electrophoresis) was ligated into the intermediate vector, and mutagenized. The mutagenized cassette is then excised and re-ligated back into the full-length h*RYR2* plasmid.

5.3.4 Effectene transfection

Plasmid cDNA at a high purity (A260/A280>1.9) was transfected into human embryonic kidney (HEK) 293 cells using an effectene transfection kit (Qiagen). The DNA is condensed by the kits enhancer reagent before being immersed in cationic lipids by the effectene reagent allowing the DNA to be transferred into the cells. This method was chosen due to its reproducibility and relatively lower cell toxicity. Alternative methods such as calcium phosphate transfection result in higher rates of cell death, which is unsuitable for the imaging of live cells. HEK 293 cells were seeded in a 200 µL menisci of complete Dulbecco's Modified Eagle Medium (Invitrogen, Paisley, UK) (cDMEM) containing foetal calf serum (10 % [vol/vol]), glutamine (2 mM) and penicillin/streptomycin (100 µg/mL) at a density of approximately $1x10^5$ per 10 mm glass coverslip pre-coated with poly-D-lysine (Mattek Corporation). The cells were incubated at 37 °C at 5 % CO_2 for 4 hours before being flooded with cDMEM and incubated for a further 20 hours. For the transfection of 7-8 coverslips 0.8 µg of eGFP-h*RyR2* DNA was added to a mixture of Buffer EC before the addition of 6.4 µL of enhancer. The mixture was vortexed for 10 seconds and incubated at room temperature for 5 minutes. Effectene (0.8 µg or 20µL) was added to the reaction before vortexing the solution for 10 seconds and incubating the solution at room temperature for 10 minutes, allowing time for the formation of effectene-DNA complexes. cDMEM (600 µL) was added to the solution before mixing. The medium was removed from the cells and replaced with 200 µL meniscus of cDMEM. 100 µL of the effectene-DNA containing solution was added dropwise to each coverslip and the cells were incubated for 24 hours. The cells were then flooded with cDMEM and incubated for another 24 hours before calcium imaging.

5.3.5 Calcium imaging

The calcium dependent fluorescence of loaded HEK cells transfected with WT RYR2 (N = 27) or Phe4905Leu RYR2 (N = 27) was observed using confocal microscopy with a Leica SP5 scanning confocal microscope at x20 magnification and with an Argon laser. mDMEM was removed from the cells and replaced with a 200 µL meniscus of Krebs-Ringer-Hepes (KRH: 9 g/L glucose, 7 g/L NaCl, 6 g/L HEPES, 0.35 g/L KCl, 0.16 g/L KH2PO4, 0.29 g/L MgSO4, 1.3 mM CaCl2, filter sterilized and pH adjusted to 7.4) before imaging the cells. The excitation wavelength used was 488 nm at 40% power and emitted wavelengths of

510-540 nm were detected using a photomultiplier tube. The rate at which data was acquired was set to 5 frames per second, and data acquisition was performed using the Leica LAS AF software at a resolution of 1024 x 1024 pixel. 4 different regions or fields of view of the coverslip with oscillating cells were recorded for 360 seconds. Fluorescence intensities of individual cells or regions of interest ROIs (approximately 46 μm2) within each field of view were measured. The mean properties of the calcium release events from the cells within a single field of view were calculated and for the purpose of statistical analyses each mean value from each field of view corresponded to N = 1, when studying the properties of calcium release events under basal conditions.

For each coverslip of cells at the end of the recording for the fourth field of view 10 mM caffeine was added to the cells and they were recorded for a further 360 seconds to determine the ER load of RyR2 channels, which was calculated from the amplitude of the calcium release events immediately after the addition of 10 mM caffeine. Caffeine was used to determine ER load because it activates RyR2 channels by increasing their sensitivity to luminal calcium but does not alter RyR2 sensitivity to cytosolic calcium (https://www.ncbi.nlm.nih.gov/pmc/articles/PMC2747660/). For the calculation of the ER load the mean amplitude of calcium release events from a single cell represented N = 1, 156 HEK cells transfected with WT RYR2 and 156 cells transfected with Phe4905Leu RYR2 were recorded and analysed.

The sensitivity of Phe4905Leu-RyR2 and WT-RyR2 to various concentrations of caffeine was also measured. However, in these experiments caffeine was added to HEK 293 cells at the beginning of the recordings. The amplitude of intracellular calcium release events in HEK cells expressing WT RYR2 after the addition of 0.05 mM (N = 64), 0.25 mM (N = 58) or 1 mM (N = 66) caffeine was compared to HEK cells expressing Phe4905Leu RYR2 after the addition of 0.05 mM (N = 71), 0.25 mM (N = 51) or 1 mM (N = 40) caffeine. Following the addition of caffeine cells were recorded for 360 seconds. As caffeine response is rapid in HEK cells only 1 field of view was recorded per coverslip and the mean amplitude of calcium release events from a single cell represented N = 1.

5.3.6 Statistical analysis

The statistical analysis of Ca^{2+} release events was performed using the unpaired t-test. This test was used because the data was shown to be normally distributed using the D'Agostino and Pearson test. All statistical analysis was performed on GraphPad prism.

5.4 Results

5.4.1 Phenotype

The paternal side of the proband's family has a history of sudden death and ventricular arrhythmias thus several relatives had previously undergone genetic testing (Figure 5.2). The probands asymptomatic mother and sister did not carry the *RYR2* Phe4905Leu variant. The proband's second sister who collapsed at rest in her pushchair at the age of 16 months and experienced dizzy spells upon waking up from sleep and his father who has also collapsed at rest immediately after waking up and presented ventricular arrhythmias after multiple exercise stress tests were both found to carry the *RYR2* Phe4905Leu variant. Thus, all carriers of the variant have experienced at least one cardiac episode despite presenting normal exercise ECGs on most occasions. The proband's paternal grandmother who died while lying down after having an argument at the age of 21 years also carried the variant, which she inherited from her mother who experienced sudden death at the age of 29 years (Figure 5.2). The proband is an 18-year-old man that was found dead in bed. The probands previous heart investigations ECG/Exercise ECG and postmortem were reported as normal and no previous symptoms were reported.

5.4.2 Genotype

Next generation sequencing was used to perform a postmortem analysis of the proband's DNA, which was extracted from fixed tissue. The molecular autopsy panel was used which includes 61 genes associated with sudden cardiac death (Appendix III). A single heterozygous rare variant was identified in *RYR2* (Phe4905Leu). The amino acid phenylalanine (Phe, F) change to leucine (Leu, L) at position 4905 (nucleotide 14713 where T changes to C, c.14713 T>C). This amino acid position has a high Consurf (conservation) score and the change of Phe to Leu at this position was predicted to be damaging or deleterious by all five of the in-silico tools used (Table 5.1). Furthermore, the variant is located in the C-terminus RyR2 hotspot for pathogenic variants.

Table 5.1. Predicted effects of *RYR2* Phe4905Leu variant.

SIFT	PolyPhen	FATHMM_pred	Mutation Assessor	Mutation Taster
Deleterious (0)	Probably damaging (0.931)	D,.	High	D,D

Different to the phenotype-genotype correlation observed at our hospital a young male, distant cousin of the proband investigated at a different hospital was reported to present VT in the absence of the *RYR2* Phe4905Leu variant. The lack of segregation and different explanation for the VT in this individual does not mean that this variant is not relevant to the phenotype in the proband presented here.

Several obligate carriers have been reported who have not experienced arrhythmia or syncope or had bidirectional VT elicited on examination, but the investigations performed may be inconsistent as they were carried out in several different countries.

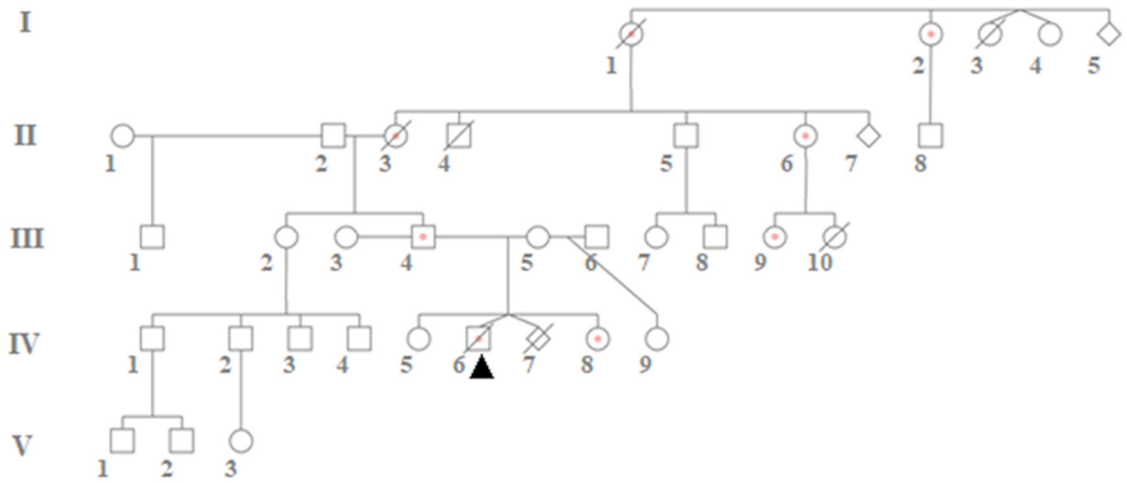

Figure 5.2. Family pedigree. The proband is indicated with an arrowhead. Generations are labelled in the left column and individuals within them are labelled with a pedigree number. Pink circles represent carriers of the *RYR2* Phe4905Leu variant. Deceased individuals are indicated with slashed lines.

5.4.3 Functional

Phe4905Leu (c.14713T>C) variant was introduced into eGFP-tagged h*RYR2* by oligonucleotide directed mutagenesis (Figure 5.3). Both WT and Phe4905Leu RyR2 channels were efficiently transfected into HEK cells. Cell morphology of cells expressing RYR2 Phe4905Leu was not different to those expressing WT RyR2 channels (Figure 5.4).

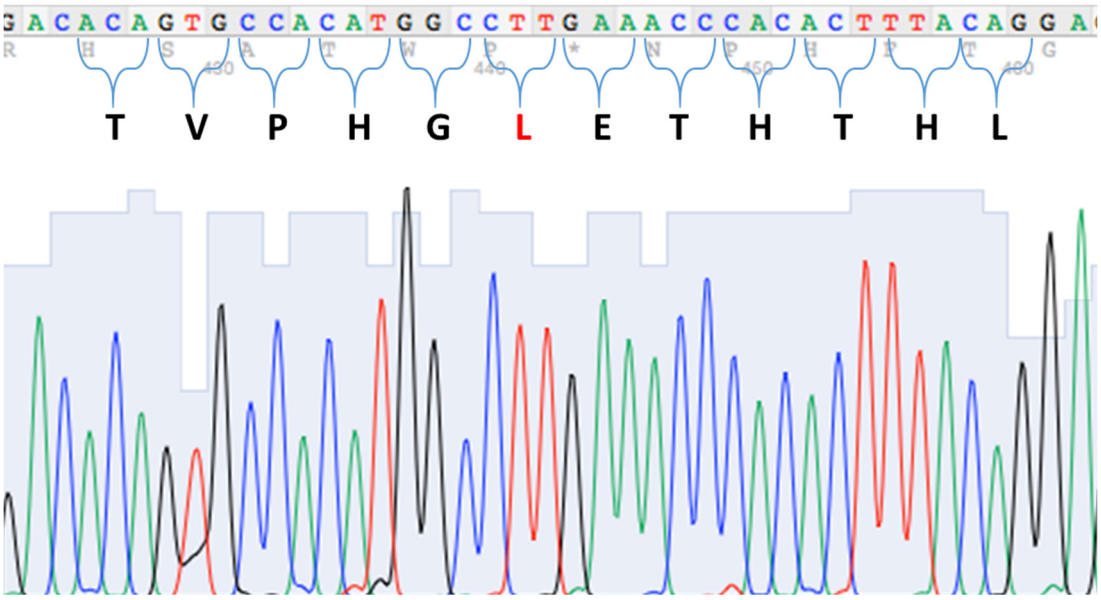

Figure 5.3. Electropherogram displaying correct introduction of *RYR2* Phe4905Leu variant into full length hRYR2

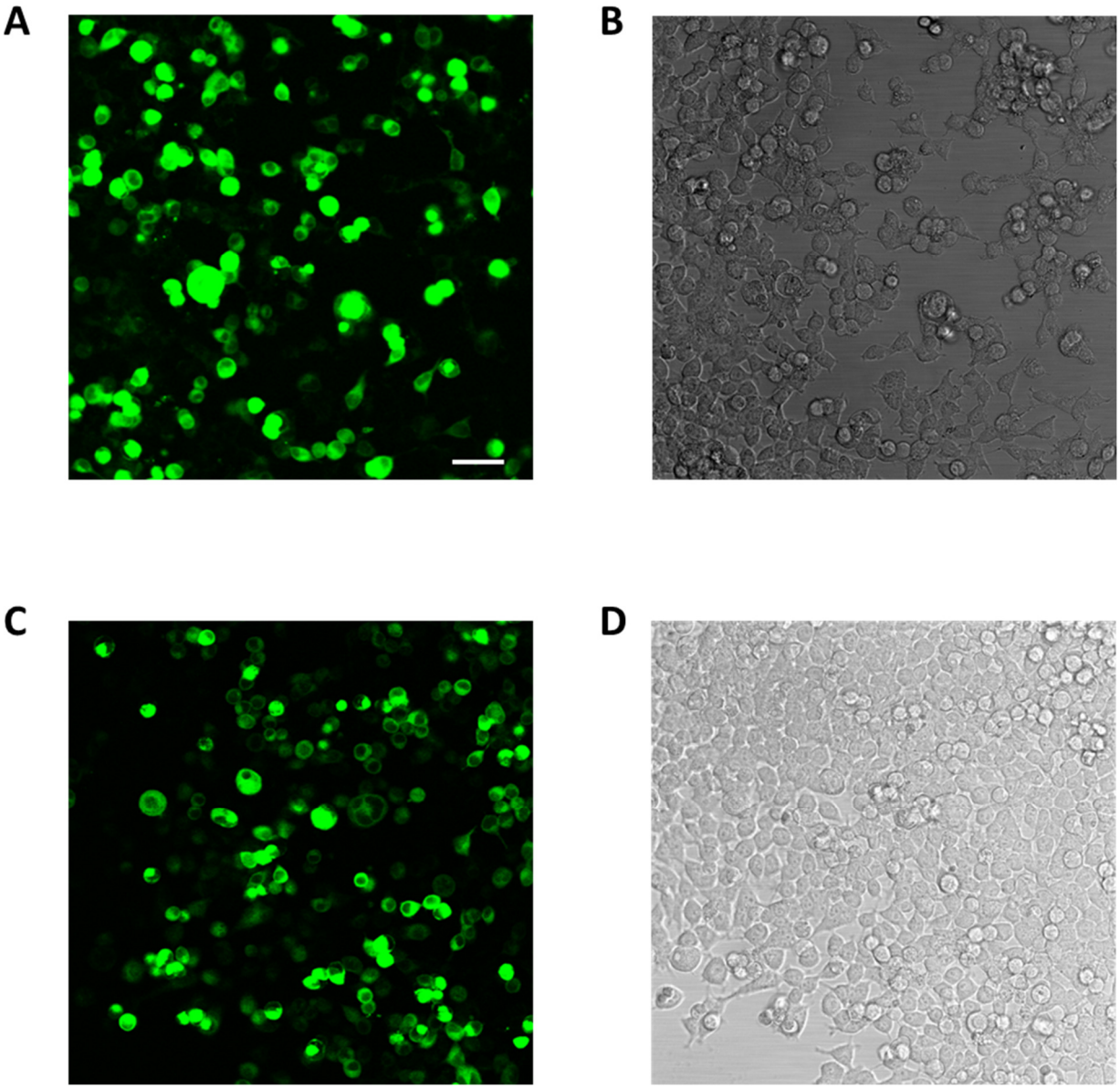

Figure 5.4. Expression of HEK cells transfected with either Phe4905Leu *RYR2* (A and B) or WT *RYR2* (C and D). Images on the left (A and C) are fluorescence images of HEK cells and thus only show cells transfected with eGFP tagged *RYR2* and images on the right are bright field images (B and D) showing transfected and untransfected cells. Scale bar represents 100 µm.

Under baseline conditions the frequency of calcium release events in HEK cells transfected with *RYR2* Phe4905Leu was not significantly different from WT *RYR2*. However, the amplitude, rise rate and fall rate of calcium release events in RyR2 Phe4905Leu HEK cells was significantly lower than WT RyR2 ($P < 0.01$). The duration of RYR2 Phe4905Leu calcium release events was significantly longer than RyR2 WT channels ($P < 0.001$) (Figure 5.5).

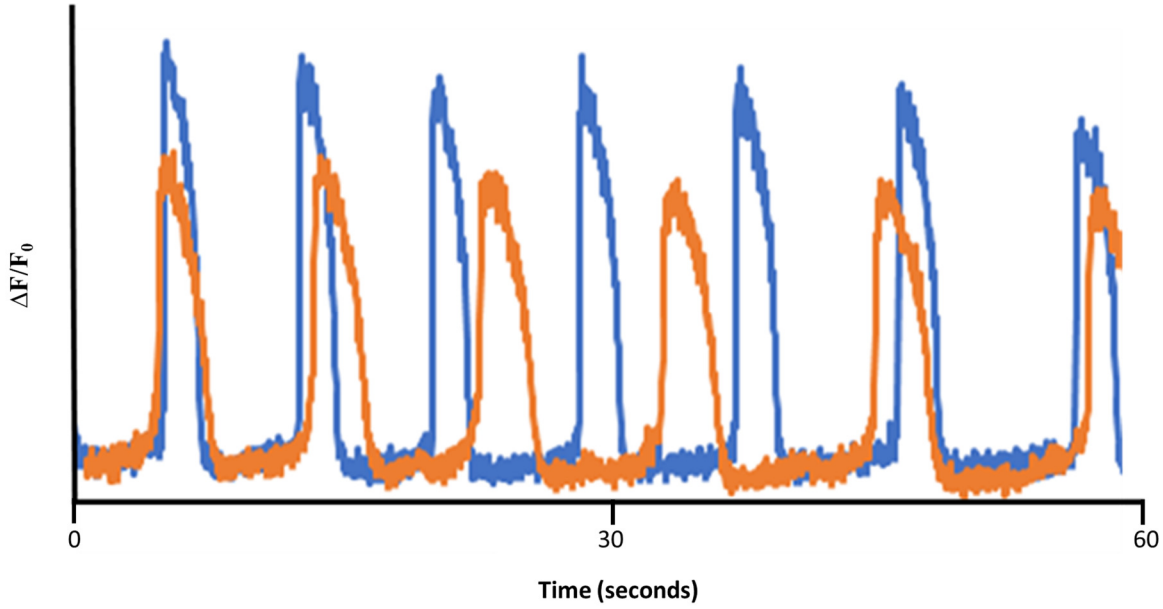

Figure 5.5.A. Ca^{2+} release events from a single WT (blue) and Phe4905Leu (orange) h*RYR2*-transfected cell. Traces were aligned from the first spontaneous calcium release event in each cell to clearly display the differences in calcium release properties between the WT and Phe4905Leu variant. However, the traces shown are from only 2 cells and thus are not a complete representation of calcium release events in HEK 293 cells transfected with WT or Phe4905Leu RYR2.

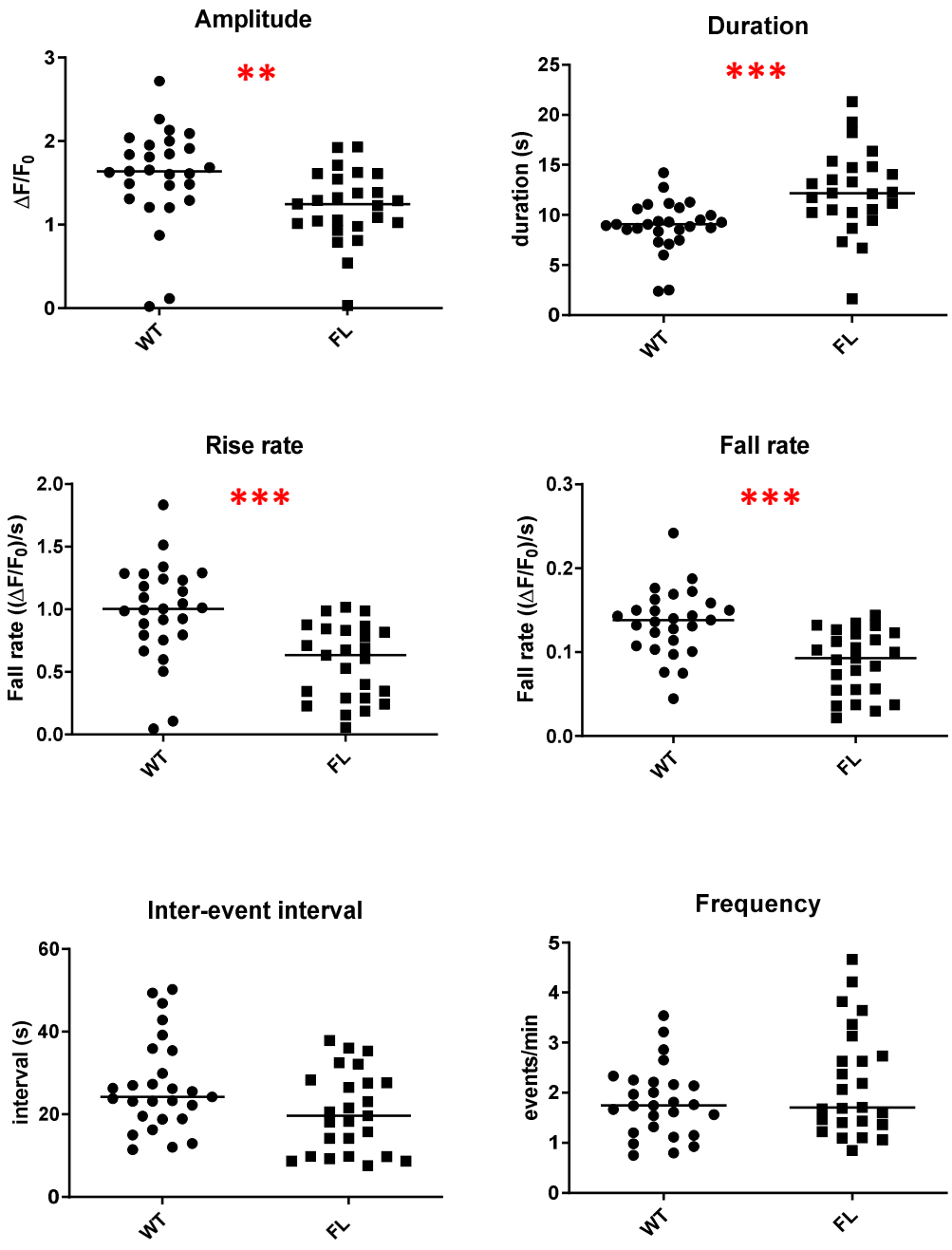

Figure 5.5.B. Properties of spontaneous Ca^{2+} release events in HEK 293 cells expressing WT (N = 27) and Phe4905Leu hRyR2 (N = 27). Data are presented as mean ± SEM. ** represents P < 0.01 and *** represents P < 0.001.

To evaluate the effect of the SCD-linked *RYR2* variant (*RYR2* Phe4905Leu) on caffeine sensitivity we measured calcium release events under baseline conditions and following the addition of caffeine in HEK cells expressing WT RyR2 and Phe4905Leu RyR2 channels. Figure 5.6 displays the amplitude of intracellular calcium spikes in response to the addition of 0.05 mM, 0.25 mM and 1 mM caffeine in HEK cells expressing WT RyR2 and Phe4905Leu RyR2. The amplitude of calcium release events in HEK cells expressing Phe4905Leu RyR2 was consistently significantly lower than that of those in HEK cells expressing WT RyR2 at all three caffeine concentrations ($P < 0.0001$) (Figure 5.6). Furthermore, the ER Ca^{2+} load of HEK cells was determined from the amplitude of calcium release events after the addition of 10 mM caffeine. The ER load of HEK cells expressing WT and Phe4905Leu RyR2 was not significantly different (Figure 5.7).

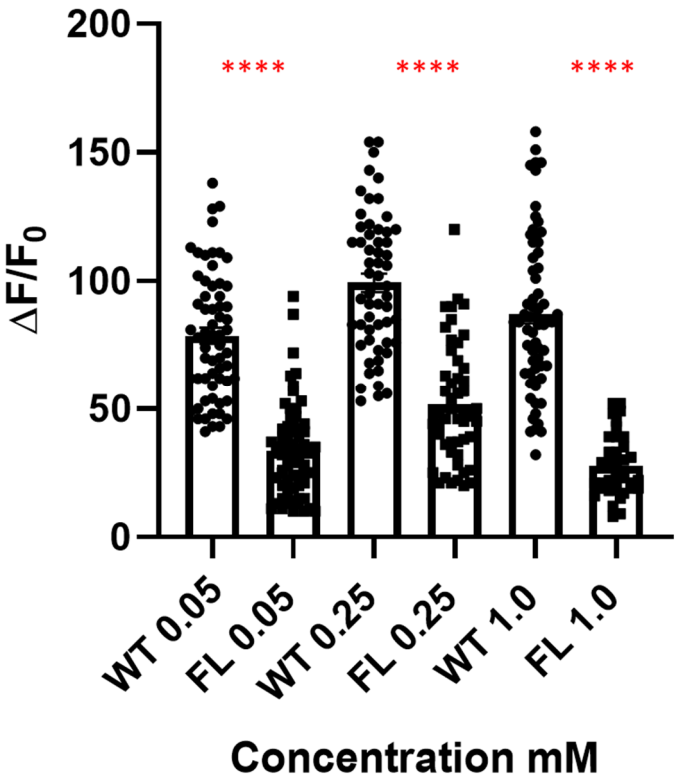

Figure 5.6. Amplitude of intracellular calcium release events in HEK cells expressing WT RYR2 after the addition of 0.05 mM (N = 64), 0.25 mM (N = 58) or 1 mM (N = 66) caffeine compared to HEK cells expressing Phe4905Leu RYR2 after the addition of 0.05 mM (N = 71), 0.25 mM (N = 51) or 1 mM (N = 40) caffeine. After the addition of caffeine cells were recorded for 360 seconds. The mean amplitude of calcium release events from a single cell represents N = 1 and **** represents $P < 0.0001$.

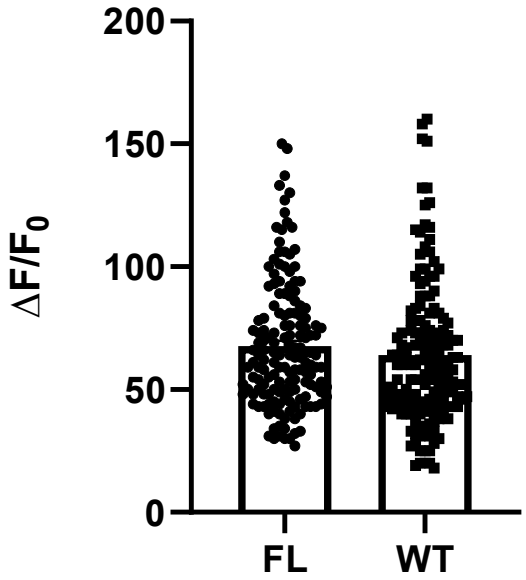

Figure 5.7. The ER Ca^{2+} load of HEK cells was calculated from the amplitude of calcium release events immediately following the addition of 10 mM caffeine. The ER Ca^{2+} load of HEK cells expressing RyR2 Phe4905Leu (N = 156) was not significantly different from HEK cells expressing RyR2 WT (N = 156). The amplitude of the caffeine release event from each cell represents N = 1.

5.5 Discussion

The reduced caffeine sensitivity of RyR2 Phe4905Leu channels indicates this variant may suppress RyR2 function. SOF *RYR2* variants usually abolish RyR2 activity under baseline conditions, however, RyR2 Phe4905Leu channels are active under baseline conditions (Fujii et al. 2017, Roston et al., 2017). This may explain the more CPVT like nature of the cardiac disorder in this family. Other SOF RyR2 variants that are inactive under baseline conditions are associated with short-coupled variant of torsades de pointes or like *RYR2* exon 3 deletions cause arrhythmias in the presence of cardiac structural changes (Roston et al., 2017). Despite being less sensitive to caffeine activation by measure of amplitude RyR2 Phe4905Leu channels appear to remain active for longer periods of time as the duration of calcium release events were significantly longer compared to WT RyR2 channels ($P < 0.001$). This could be interpreted as a GOF, meaning RyR2 Phe4905Leu may share functional properties with GOF and SOF channels, it's unclear how the unique functional properties of the Phe4905Leu channel contribute to the observed phenotype.

The *RYR2* Phe4905Leu variant was found in multiple members of a large family with a history of sudden death and ventricular arrhythmias. Although, most pathogenic *RYR2* missense variants are associated with CPVT which is characterised by VT and syncope triggered by physical or emotional stress several carriers of the *RYR2* Phe4905Leu variant have experienced cardiac episodes seemingly in the absence of exercise-linked triggers. In at least three cases episodes were reported to have occurred during or when waking from sleep. These findings could indicate that some *RYR2* variants may cause arrhythmias or sudden death through the action of other factors. One of such factors may be the extent to which *RYR2* variants alter normal brain function. *RYR2* is expressed in several regions of the brain including the brainstem and the suprachiasmatic nucleus (Ledbetter et al., 1994). Aiba et al. (2016) demonstrated the CPVT associated gain of function variant *RYR2* Arg176Gln increased susceptibility to spreading depolarizations and altered neurotransmitter release in the brainstem. Moreover, the ryanodine receptor has been shown to be the dominant regulator of large conductance potassium channel activity in neurons present in the suprachiasmatic nucleus (the brains circadian clock) at night and inhibition of RyRs disrupts the circadian rhythm in rats (Whitt et al., 2018, Mercado et al., 2009). The circadian clock is not only responsible for determining the time in which sleep

is most likely to occur but has also been shown to regulate the time REM sleep and other sleep stages occur (Lee et al., 2009). Thus, there is the possibility some *RYR2* variants alter the frequency, length or intensity of REM sleep, and consequently raise the risk of fatal arrhythmias and sudden death.

The observed phenotype may also be influenced by other genetic factors. The proband's father initially presented a normal exercise ECG but further testing initiated arrhythmias, but the need for multiple tests to trigger arrhythmias has been seen for other CPVT associated *RYR2* variants. However, the clinical evaluation of a distant relative of the proband found the individual to not carry the *RYR2* Phe4905Leu variant but present arrhythmias upon exercise stress testing. This may be the result of the patient carrying other rare genetic variants and/or single nucleotide polymorphisms (SNPs) that may be familial and contribute to a disease phenotype that is worsened by the *RYR2* Phe4905Leu variant. The possibility of other possibly unknown genetic factors contributing to CPVT phenotypes is supported by a significant proportion of CPVT cases being free of variants in *RYR2* or other known arrhythmia genes, indicating our understanding of the genetic etiology of CPVT remains incomplete (Ackerman et al., 2011). Furthermore, SNPs like the risk allele of rs12143842 have been reported to increase the risk of cardiac events and sudden death (Earle et al., 2014). Whole genome sequencing of CPVT patients with unusual phenotypes may help in identifying other genetic contributors.

The present study was limited by several factors. As previously mentioned, the absence of the *RYR2* Phe4905Leu variant was reported for a distant relative of the proband with exercise induced arrhythmias, thus this variant may not be the sole contributor to the observed phenotype. The lack of whole genome data for this family prevents the exclusion of this possibility. Furthermore, despite the advantages of studying RyR2 channel properties in HEK cells due to the absence of functional native RyR2 channels, functional studies using a single cell type presents limitations. The functional properties of RyR2 Phe4905Leu in cardiac cells may differ from HEK cells (Thomas et al., 2004). Additionally, studying RyR2 Phe4905Leu channels in neuronal cells may also shed light on the impact of SOF or dual effect variants on the brain, as there are no reports on this to date.

In conclusion the *RYR2* Phe4905Leu variant may be associated with sleep related sudden cardiac death. The present study in HEK cells suggests RyR2 Phe4905Leu shares some properties with SOF RyR2 variants, however, different to previously reported SOF variants it is active under baseline conditions. Further work is needed to establish the contribution of the *RYR2* Phe4905Leu variant to the observed phenotype and the mechanisms by which sudden cardiac death occurs in carriers during sleep and in response to stress.

5.6 References

Ackerman, M.J. et al. 2011. HRS/EHRA Expert Consensus Statement on the State of Genetic Testing for the Channelopathies and Cardiomyopathies: This document was developed as a partnership between the Heart Rhythm Society (HRS) and the European Heart Rhythm Association (EHRA). *Heart Rhythm* 8(8): pp. 1308-1339.

Bagnall et al. 2016. A Prospective Study of Sudden Cardiac Death among Children and Young Adults. *New England Journal of Medicine* 374, 2441-2452.

Bhat M.B., Zhao J., Takeshima H. and Ma J. 1997. Functional calcium release channel formed by the carboxyl-terminal portion of ryanodine receptor. *Biophysical Journal* 73(3): pp.1329–1336.

de Vries, L.J., Géczy, T. and Szili-Torok, T. 2017. Sleep Medications Containing Melatonin can Potentially Induce Ventricular Arrhythmias in Structurally Normal Hearts: A 2-Patient Report. *Journal of Cardiovascular Pharmacology* 70(4): pp.267-270.

Devalla, H. D. et al. 2016. TECRL, a new life-threatening inherited arrhythmia gene associated with overlapping clinical features of both LQTS and CPVT. *EMBO molecular medicine* 8, pp.1390-1408.

Earle N. et al. 2014. Single nucleotide polymorphisms in arrhythmia genes modify the risk of cardiac events and sudden death in long QT syndrome. *Heart Rhythm* 11(1): pp.76-82.

Fujii, Y. et al. 2017. A type 2 ryanodine receptor variant associated with reduced Ca2+ release and short-coupled torsades de pointes ventricular arrhythmia. *Heart Rhythm* 14(1): pp.98-107.

George, C.H., Higgs, G.V. and Lai F.A. 2003. Ryanodine receptor mutations associated with stress-induced ventricular tachycardia mediate increased calcium release in stimulated cardiomyocytes. *Circulation Research* 93, pp.531-540.

Aiba, I., Wehrens, X.H.T. and Noebels, J.L. 2016. Leaky RyR2 channels unleash a brainstem spreading depolarization mechanism of sudden cardiac death. *Proceedings of the National Academy of Sciences of the United States of America* 113(33): pp. E4895-E4903.

Thomas L.N., George, C.H. and Lai, A. 2004. Functional heterogeneity of ryanodine receptor mutations associated with sudden cardiac death. *Cardiovascular Research* 64(1): pp.52–60.

Tooley, G.A., Armstrong, S.M., Norman, T.R., Sali, A. 2000. Acute increases in night-time plasma melatonin levels following a period of meditation. *Biological Psychology*. 53(1): pp.69-78.

Lahat H., et al. 2001. A missense mutation in a highly conserved region of CASQ2 is associated with autosomal recessive catecholamine-induced polymorphic ventricular tachycardia in Bedouin families from Israel. *American Journal of Human Genetics*. 69(6): pp.1378-1384.

Liu, N., Ruan, Y. and Priori, S. G. 2008. Catecholaminergic Polymorphic Ventricular Tachycardia. *Progress in Cardiovascular Diseases* 51, pp.23-30.

Ledbetter, M.W. et al. 1994. Tissue distribution of ryanodine receptor isoforms and alleles determined by reverse transcription polymerase chain reaction. *The Journal of Biological Chemistry* 269(50): pp.31544-31551.

Lee, M.L., Swanson, B.E., and de la Iglesia, H.O. 2009 Circadian Timing of REM Sleep Is Coupled to an Oscillator within the Dorsomedial Suprachiasmatic Nucleus. *Current Biology* 19(10): pp.848-852.

Mercado, C. et al. 2009. Ryanodine-Sensitive Intracellular Ca2+ Channels in Rat Suprachiasmatic Nuclei Are Required for Circadian Clock Control of Behavior. Journal of Biological Rhythms 24(3): pp. 203-210.

Nyegaard, M. et al. 2012. Mutations in calmodulin cause ventricular tachycardia and sudden cardiac death. *American journal of human genetics* 91, pp.703-712.

Priori S.G. et al. 2001. Mutations in the Cardiac Ryanodine Receptor Gene (hRyR2) Underlie Catecholaminergic Polymorphic Ventricular Tachycardia. *Circulation* 103, pp.196-200.

Roston, T. M., Sanatani, S. and Chen, S. R. W. 2017. Suppression-of-function mutations in the cardiac ryanodine receptor: Emerging evidence for a novel arrhythmia syndrome? *Heart Rhythm* 14, pp.108-109.

Roux-Buisson, N. et al. 2012. Absence of triadin, a protein of the calcium release complex, is responsible for cardiac arrhythmia with sudden death in human. *Human molecular genetics* 21, pp.2759-2767.

Smith, M. J. et al. 2014. Germline Mutations in SUFU Cause Gorlin Syndrome–Associated Childhood Medulloblastoma and Redefine the Risk Associated with PTCH1 Mutations. *Journal of Clinical Oncology* 32, pp.4155-4161.

Venetucci, L. A., Trafford, A. W., O'Neill, S. C. and Eisner, D. A. 2007. The sarcoplasmic reticulum and arrhythmogenic calcium release. *Cardiovascular Research* 77, pp.285-292.

Verrier, R.L. and Josephson, M.E. 2009. Impact of sleep on arrhythmogenesis. *Circulation* 2(4): pp.450-459.

Whitt, J.P., McNally, B.A. and Meredith, A.L. 2018. Differential contribution of Ca(2+) sources to day and night BK current activation in the circadian clock. *The Journal of general physiology* 150(2): pp.259-275.

Zhao, Y.-T. et al. 2015 Arrhythmogenesis in a catecholaminergic polymorphic ventricular tachycardia mutation that depresses ryanodine receptor function. *Proceedings of the National Academy of Sciences of the United States of America* 112(13): pp.E1669-E1677.

Chapter 6: Discussion

6.1 Realisation of project aims

The general aim of this study was to improve the diagnosis, understanding and management of *RYR2* associated CPVT by providing an effective means of distinguishing pathogenic *RYR2* variants, exploring potential disease mechanisms and functionally characterising pathogenic variants. CPVT diagnosis was improved by providing evidence frequency thresholds can be used to identify benign *RYR2* variants and reclassifying 55 CPVT associated RYR2 variants, this is discussed in section 6.2. Our understanding of CPVT was improved and a potential disease mechanism was explored by this study showing *RYR2* missense variants are unlikely to cause CPVT by altering splicing, the effects of *RYR2* missense variants on splicing is discussed in section 6.3. Lastly, an *RYR2* variant (RYR2 Phe4905Leu) was functionally characterised and this is discussed in section 6.6.

6.2 Reclassification of CPVT associated RYR2 variants

One of the main aims of this project was to use bioinformatics tools to distinguish benign *RYR2* variants from pathogenic variants, and ultimately aid CPVT diagnosis. Using a range of bioinformatics tools and the ACMG guidelines from a series of 326 variants previously associated with an arrhythmogenic phenotype, we were able to reclassify 55 *RYR2* variants as benign and 26 *RYR2* variants as pathogenic or likely pathogenic (Whiffin et al., 2017, Richards et al., 2015, Denham et al., 2019). In doing so I proved the first hypothesis (which states 'bioinformatics and statistical tools can be used to determine the pathogenicity of RYR2 variants') to be true for some *RYR2* variants that occur frequently in control datasets. However, this hypothesis was not proven to be true for rare benign *RYR2* variants, as frequency thresholds are in effective in the classification of these variants and current computational tools alone lack the power to provide a benign classification when following the ACMG guidelines (Richards et al., 2015).

The data shows 17 % of *RYR2* variants are not disease causing or contribute to a minimal extent to the disease phenotype, thus the proportion of CPVT cases that cannot be attributed to *RYR2* variants is likely to exceed current estimates and the proportion of cases attributable to genetic changes in other genes or posttranslational modifications is likely to be underestimated. The classification of variants in *RYR2* as benign is important as family members without these variants that may have been overlooked can be recognized as being at risk of sudden cardiac death, a risk that may be significantly reduced by managing the condition with treatments such ICD implantation or beta-

blockers. Thus, in reclassifying 55 *RYR2* variants as benign I achieved another of the aims of this project, which was to improve the management of *RYR2* associated CPVT.

Furthermore, similar to *RYR2* variant negative CPVT cases, highlighting carriers of benign variants may help further our understanding of the genetic contributors to CPVT by enabling the search for the real cause of the phenotype, which was an aim of this project. Recently, homozygous variants in *TECRL*, encoding an endoplasmic reticulum protein preferentially expressed in the heart and not previously reported to be associated with arrhythmias, was found to disrupt calcium handling and cause CPVT in two unrelated patients without *RYR2* variants. One of these variants was shown to promote the skipping of exon 3 in *TECRL* (Devalla et al., 2016). Genetic testing carried out at the North West Genomic Laboratory Hub included the screening of 61 genes related to cardiac conditions, next generation sequencing will allow the discovery of novel disease related genes to be included in such panels, improving the diagnosis and treatment of genetic cardiac conditions. In addition to the identification of benign *RYR2* variants, the improvement of CPVT diagnosis can be further aided by more thorough clinical assessments. I showed cases where a more confident CPVT diagnosis could be made, the probability of identifying a pathogenic *RYR2* variant or an *RYR2* variant of any classification increased significantly.

Although, variant hotspot regions in *RYR2* have previously been identified (George et al., 2007) I found that CPVT associated *RYR2* variants cluster in these regions as well as others, typically in the surrounding areas of the pre-established variant hotspots (George et al., 2007). Three regions within *RYR2* were identified where variants in control populations clustered. These results may aid CPVT diagnosis in instances where next generation sequencing is not available and genetic testing is being performed using conventional Sanger sequencing, screening the whole *RYR2* coding region can be time consuming and costly so it is common practice to screen only those regions where pathogenic *RYR2* variants are most likely to occur. Additionally, this data may help diagnosis and treatment by providing indications of variant pathogenicity. The availability of large control datasets was crucial to this study, using the ExAC database I was able to reclassify 14 % of variants as benign however using the gnomAD database, which contains exome data from approximately double the number of individuals I was able to increase

the percentage of benign classifications to 17 %, highlighting the usefulness of larger genetic control databases for the study of rare genetic diseases.

6.3 Sleep related sudden death in CPVT

In many cases the treatment of arrhythmias relies on our understanding of disease mechanisms and triggers such adrenergic stimulation, this is no different for CPVT, which is commonly treated with high dose beta-blockers. We identified a number of cases believed to have CPVT that did not present arrhythmias upon exercise stress testing some of these individuals experienced cardiac episodes at rest or even while asleep. In contrast to CPVT associated *RYR2* variants on the whole, we found *RYR2* variants found in patients that experienced sudden death while asleep occurred almost exclusively in the C-terminal of the gene, with the exception of one variant that occurred in the central domain. Although, limited by the small sample size this preliminary data suggests C-terminal *RYR2* variants may pose a greater risk of sudden death at rest or during sleep, it also demonstrates the risk of arrhythmias and sudden death in patients with normal exercise stress tests. The cause of arrhythmias in CPVT patients during sleep remains unclear but in addition to the potential differences in RyR2 properties associated with particular variants the declining levels of beta-blockers while asleep may also contribute to the seemingly increased risk of arrhythmias or sudden cardiac death in some patients.

6.4 Alternative mechanisms of *RYR2* variant pathogenicity in CPVT

Suppression of function *RYR2* variants have been shown to cause CPVT like phenotypes but in many of these patients arrhythmias are not triggered by adrenergic stimulation (Roston et al., 2017), we hypothesised some *RYR2* variants alter channel function and cause CPVT differently to the mechanisms described for gain of function *RYR2* variants. An aim of this study was to explore potential mechanisms for *RYR2* associated CPVT, this was achieved by investigating whether CPVT can be attributed to loss of *RYR2* function caused by missense variants that affect splicing (Roston et al., 2017). Splice variants have been seen in other CPVT associated genes such as *TECRL* (Devalla et al., 2016), however, the results of this study do not support the hypothesis CPVT associated missense variants in *RYR2* are spliceogenic. I generated experimental evidence that shows CPVT is unlikely

to be caused by missense *RYR2* variants that disrupt normal transcript splicing. Although, no new CPVT mechanisms were discovered these findings are important as experimental evidence used in the classification of *RYR2* variants is largely based upon studies involving the introduction of variants into full length *RYR2* cDNA. Thus, proving *RYR2* missense variants to be non-spliceogenic aids the classification of *RYR2* variants, as variants found not to affect calcium handling when introduced into full length RyR2 in *in vitro* studies can be more confidently classified as non-pathogenic variants. However, these findings are based on the study of *RYR2* transcript splicing using computational tools and a mini-gene assay without supporting data from patient tissue expressing the gene, because tissue samples were not accessible as *RYR2* expression is largely limited to the brain and heart. Therefore, there is the possibility the minigene assay does not provide a true representation of *RYR2* transcript splicing *in vivo*. Furthermore, a wider range of computational tools such as those that specifically evaluate the effects variants are likely to have on exonic regulatory elements could have been used (Cartegni et al., 2003).

6.5 Alternative mechanisms CPVT inheritance

Despite marked advances in the identification of pathogenic *RYR2* variants our understanding of the phenotypic heterogeneity of CPVT, in many cases within the same pedigree, remains limited and is not entirely explainable using a simple monogenic model. Genome wide association studies may broaden our understanding of CPVT inheritance by identifying relevant non-coding regulatory variants or structural variants (e.g. inversions/translocations) not currently screened by genetic testing. Interestingly, most of the genetic changes found to be statistically associated with complex diseases occur in non-coding regions and evidence of an oligogenic model of inheritance, where several alleles have a cumulative effect on the disease phenotype, has been reported for Brugada syndrome (Sommariva et al., 2013).

6.6 *RYR2* deletions in CPVT

Deletions in exon 3 of *RYR2* have been shown to cause CPVT. Similar to gain of function RYR2 missense variants studies in HEK 293 cells show exon 3 deletions to increase RyR2 activity, increasing the release of Ca^{2+} into the cytoplasm causing Ca^{2+} overlaod and DADs (Leong et al., 2015, Tang et al., 2012). Interestingly, CPVT patients with *RYR2* exon 3

deletions also commonly have structural cardiac deformities like left ventricular non-compaction and many have been reported to have sinoatrial and atrioventricular node dysfunction (Ohno et al., 2014). The amount of intronic sequence deleted on either side of the exon 3 deletion can vary between patients, for instance in one study both 1.1 and 3.6 kb deletions were identified in CPVT patients (Bhuiyan et al., 2007). However, no relationship between clinical phenotype and the size of *RYR2* deletions has been established to date. I attempted to address this by defining the breakpoints of DNA deletions in several patients with CPVT, but the repetitive nature of the sequences flanking exon 3 (Alu family of repeats) made this technically difficult as this resulted in the production of several non-specific bands using long range PCR and inconsistent results using digital PCR. The quality of the patient DNA may have also contributed to these results.

6.7 Functional Characterisation of the Phe4905Leu *RYR2* missense change

The functional characterisation of arrhythmia associated RyR2 mutant channels is complex, but functional studies are a major driver for pathogenic or benign classifications. Firstly, the coding sequence of the *RYR2* gene is extremely large and as a result it is difficult to avoid damaging h*RYR2* DNA or spontaneous recombination events when propagating it. Nonetheless, I functionally characterised the RyR2 Phe4905Leu variant by performing calcium imaging studies using HEK 293 cells transfected solely with Phe4905Leu-hRyr2 or WT-hRyR2. In doing so I found RyR2 Phe4905Leu channels share properties with both gain of function and suppression of function RyR2 channels and achieved the aim of functionally characterising a pathogenic *RYR2* variant.

However, RyR2 channels are homotetramers and most CPVT associated *RYR2* variants are heterozygous, thus arrhythmia linked mutant RyR2 channels are likely to be formed of a combination of both WT and mutant RyR2 monomers. Therefore, the results of this study as well as many other cell studies on mutant hRyR2 channels, that investigate the properties of channels solely composed of mutant monomers, provide an indication of the effect variants may have on channel function but may not be an absolute representation of mutant RyR2 channels *in vivo*. In an attempt to address this we co-

transfected HEK 293 cells with both mutant and WT RyR2 channels at differing ratios and this increased the variability in the results obtained, this is likely due to the different properties of channels formed within the same cell but of different combinations of WT and mutant RyR2 monomers. Developing a means of distinguishing WT RyR2 monomers from mutant RyR2 monomers within RyR2 tetramers, possibly by using different fluorescent tags, will allow the study of human RyR2 channels composed of specific combinations. Furthermore, the intracellular location of RyR2 is unreachable using patch pipettes, preventing the use of patch clamping to measure the activity of single channels in real time. Consequently, single RyR2 channels are incorporated into artificial lipid bilayers, consisting of phosphatidylethanolamine in n-decane by introducing an osmotic gradient with 200 µl 3 mol/L KCl, to directly study their properties. However, these single channel experiments can be time consuming and technically challenging.

Considering the fragility of the large RyR2 channel and the complexity of channel function and regulation the development of high throughput functional assays to study all RyR2 variants is likely to take time. However, a more feasible approach may be the development of functional assays that consider the effects variants have on particular channel properties in isolation, for instance variants in the clamp region of the cytoplasmic cap could be studied for their effects on channel coupling and variants in the zip domain could be studied for the effects they have on the stabilizing interactions between the N-terminal and central domains. This may avoid the need to produce full length RyR2, but as with other high throughput methods such an approach may overlook some possibly important changes and will require a more detailed understanding on the mechanisms by which RyR2 variants disrupt normal channel function.

6.8 Conclusion

Both bioinformatics tools and functional studies on *RYR2* variants aid variant classification, however advances in both areas are required to address the large and growing number of *RYR2* variants of uncertain significance.

Applying a minor allele frequency threshold for pathogenicity in control populations is an effective method to distinguish benign *RYR2* variants. The effectiveness of this method increases substantially with the size of the control dataset used. The number of *RYR2*

variants reclassified as benign increased from 44 to 55 with an increase in the number of control exomes from 60,706 in the ExAC database to 141,456 in the gnomAD database. As control databases increase in size the classification of genetic variants is likely to improve and relieve some of the need for functional assays. However, current bioinformatics approaches to variant classification are limited and functional assays still play an important role in variant classification.

CPVT is largely associated with arrhythmias during exercise or emotional stress, our data emphasizes the heterogeneity of CPVT phenotypes. A number of CPVT patients present normal exercise stress tests and experience cardiac episodes and sudden death at rest, a proportion of these episodes occur during sleep. Four of the five Potentially pathogenic *RYR2* variants identified in cases of sleep related sudden death occurred in the C-terminus indicating pathogenic C-terminal *RYR2* variants may pose a greater risk of sudden death during sleep. These findings highlight the possible need for monitoring and/or treating seemingly asymptomatic patients carrying pathogenic *RYR2* variants, particularly those with variants in the C-terminus.

RYR2 suppression of function variants can be associated to CPVT like phenotypes and these patients may be more likely to present normal exercise stress tests (Roston et al., 2017). In such instances segregation data may contribute to a lesser degree to variant classification due to the difficulty in identifying affected individuals and functional studies may be required. Our data suggests *RYR2* variants do not exert pathogenic effects by altering splicing. Therefore, functional studies should focus on the effects of genetic changes on full length RyR2 channels.

6.9 Future work

RYR2 is expressed in the brain as well as the heart; however few studies have investigated the effects of CPVT variants on the brain and how much this contributes to observed phenotypes (Aiba et al., 2016). The disparity between CPVT phenotypes and the triggers that promote the onset of cardiac events and syncope may be due to the differing effects RyR2 variants have on the brain. This may explain the occurrence of cardiac episodes during sleep in some CPVT patients. A significant proportion of arrhythmogenic deaths occur during sleep. Several changes in brain chemistry occur during the distinct periods of

human sleep and the distribution of ventricular arrhythmias across different time points of the night is non-uniform indicating the influence physiologic triggering (Verrier and Josephson, 2009). REM sleep occurs in short intervals, usually lasting around 90 minutes and only accounts for a small proportion (approximately 20-25 %) of overall sleep time (Verrier and Josephson, 2009). During REM sleep sympathetic activity is increased and intense emotional states maybe experienced, possibly contributing to an increased risk of ventricular arrhythmias and sudden death (Verrier and Josephson, 2009). Furthermore, the transition from slow-wave sleep to REM sleep is associated with increased activity of the vagus nerve which may lead to heart rhythm disturbances (Dickerson et al., 1993). The transition from slow-wave sleep to REM sleep occurs due to increased activity in the brainstem reticular formation, a region of the brain where *RYR2* is expressed (Ledbetter et al., 1994, Luppi et al., 2012). Aiba et al. (2016) demonstrated the CPVT associated *RYR2* Arg176Gln variant led to the generation of spreading depolarizations and altered neurotransmitter release in the brainstem (Aiba et al., 2016). Moreover, the ryanodine receptor has been shown to be the dominant regulator of large conductance potassium channel activity in neurons present in the suprachiasmatic nucleus (the brains circadian clock) at night and inhibition of RyRs disrupts the circadian rhythm in rats (Whitt et al., 2018, Mercado et al., 2009). The circadian clock is not only responsible for determining the time in which sleep is most likely to occur but has also been shown to regulate the time REM sleep and other sleep stages occur (Lee et al., 2009). Thus, there is the possibility some *RYR2* variants alter the frequency, length or intensity of REM sleep, and consequently raise the risk of fatal arrhythmias and sudden death. Studying RyR2 in the brain may further our understanding of CPVT and allow better management and treatment of the condition.

The recent advances in sequencing technology have enabled sequencing to be performed more easily in regard to cost and time. Whole exome studies on patients with CPVT like phenotypes may shed light on other genes that are causally associated with CPVT and further our knowledge on the mechanisms behind the phenotype. This work may reduce the number of CPVT cases of unknown cause which currently accounts for approximately 50 % of CPVT cases. Furthermore, as next generation sequencing continues to advance we're likely to be able to access larger control databases, as demonstrated in this study

the use of larger control databases increases the power of applying a frequency threshold for variant pathogenicity. Thus, future studies using large control populations will enable the reclassification of more *RYR2* variants.

Next generation sequencing technologies have also led to an increase in the number of CPVT associated RYR2 variants of unknown significance. As many of these variants occur at low frequencies in control databases frequency thresholds are not always suitable for reclassifying them and functional studies are often necessary. Current methods used to study the effects of variants on RYR2 function are time consuming and technically difficult, future studies on the development of high-throughput methods to functionally characterise *RYR2* variants are likely to reduce the number of *RYR2* variants of uncertain significance. Saturation genome editing enables the simultaneous introduction and study of all possible single nucleotide variants into a gene of interest. This is performed by transfecting cells with a multiplex homology-directed repair (HDR) library containing edited exons, Cas9 and guide RNAs targeting the regions of the gene to be studied. The guide RNA binds to the target site within the gene and also to the Cas9 enzyme, Cas9 cuts the DNA at the target site and stimulates the introduction of a mutated exon by homologous recombination. Following the introduction of the variants of interest an assay with sufficient sensitivity to detect the effects of the variant is required, for variants in BRCA1 cell death is measured using light microscopy, however there are currently no high-throughput assays to detect the subtler effects of CPVT associated *RYR2* variants (Findlay et al., 2018). Assays measuring properties such as interactions between domains or regulatory proteins could be developed to determine the pathogenicity of variants in specific regions of *RYR2* where disruption of these interactions are known to cause disease.

References

Aiba, I., Wehrens, X.H.T. and Noebels, J.L. 2016. Leaky RyR2 channels unleash a brainstem spreading depolarization mechanism of sudden cardiac death. *Proceedings of the National Academy of Sciences of the United States of America* 113(33): pp. E4895-E4903.

Ackerman, M.J. et al. 2011. HRS/EHRA Expert Consensus Statement on the State of Genetic Testing for the Channelopathies and Cardiomyopathies: This document was developed as a partnership between the Heart Rhythm Society (HRS) and the European Heart Rhythm Association (EHRA). *Heart Rhythm* 8(8): pp. 1308-1339.

Aizawa, Y. et al. 2005. A novel mutation in FKBP12. 6 binding region of the human cardiac ryanodine receptor gene (R2401H) in a Japanese patient with catecholaminergic polymorphic ventricular tachycardia. *International journal of cardiology* 99, pp.343-345.

Anna, A. and Monika, G. 2018. Splicing mutations in human genetic disorders: examples, detection, and confirmation. *Journal of Applied Genetics* 59, pp.253-268.

Anthony, D. F., Beattie, J., Paul, A. and Currie, S. 2007. Interaction of calcium/calmodulin-dependent protein kinase IIδ C with sorcin indirectly modulates ryanodine receptor function in cardiac myocytes. *Journal of molecular and cellular cardiology* 43, pp.492-503.

Bannister et al. 2015. The Mechanism of Flecainide Action in CPVT Does Not Involve a Direct Effect on RyR2. *Circulation Research* 116, pp.1324-1335.

Bagnall et al. 2016. A Prospective Study of Sudden Cardiac Death among Children and Young Adults. *New England Journal of Medicine* 374, 2441-2452.

Berridge, M. J., Lipp, P. and Bootman, M. D. 2000. The versatility and universality of calcium signalling. *Nature Reviews Molecular Cell Biology* 1, pp.11-21.

Bers, D. M. 2002. Cardiac excitation–contraction coupling. *Nature* 415, pp.198-205.

Bers, D. M. 2004. Macromolecular complexes regulating cardiac ryanodine receptor function. *Journal of Molecular and Cellular Cardiology* 37, pp.417-429.

Bhat M.B., Zhao J., Takeshima H. and Ma J. 1997. Functional calcium release channel formed by the carboxyl-terminal portion of ryanodine receptor. *Biophysical Journal* 73(3): pp.1329–1336.

Bhuiyan, Z.A. et al. 2007. Expanding spectrum of human RYR2-related disease: new electrocardiographic, structural, and genetic features. *Circulation* 116, pp.1569-1576.

Bosanac, I. 2005. Crystal structure of the ligand binding suppressor domain of type 1 inositol 1, 4, 5-trisphosphate receptor. *Molecular cell* 17, pp.193-203.

Boyett, M. R., HONJO, H. and Kodama, I. 2000. The sinoatrial node, a heterogeneous pacemaker structure. *Cardiovascular Research* 47, pp.658-687.

Broendberg, A. K. et al. 2017. P1596A novel Triadin variant causes a severe clinical CPVT phenotype in two young brothers. *EP Europace*, 19, pp.iii340-iii340.

Cardarelli, F. et al. 2016. The intracellular trafficking mechanism of Lipofectamine-based transfection reagents and its implication for gene delivery. *Science Reports* 6, pp.25879.

Cartegni, L. et al. 2003. ESEfinder: A web resource to identify exonic splicing enhancers. *Nucleic acids research* 31, pp.3568–3571.

Cerrone, M. et al. 2007. Arrhythmogenic mechanisms in a mouse model of catecholaminergic polymorphic ventricular tachycardia. *Circulation research* 101, pp.1039-1048.

Chandler N.J. 2009. Molecular Architecture of the Human Sinus Node. *Circulation* 119, pp.1562-1575.

Chen, W.S.R. et al. 2002. Role of the Proposed Pore-Forming Segment of the Ca2+ Release Channel (Ryanodine Receptor) in Ryanodine Interaction*. *Biophysical Journal*. 82(5): pp.2436-2447.

Chiang, D. Y. 2014. Impaired local regulation of ryanodine receptor type 2 by protein phosphatase 1 promotes atrial fibrillation. *Cardiovascular research* 103, pp.178-187.

Clapham, D. E. 2007. Calcium Signaling. *Cell* 131, pp.1047-1058.

Cole, S. W. and Sood, A. K. 2012. Molecular pathways: beta-adrenergic signaling in cancer. *Clinical cancer research : an official journal of the American Association for Cancer Research* 18, pp.1201-1206.

Curran, J. 2014. Nitric Oxide-Dependent Activation of CaMKII Increases Diastolic Sarcoplasmic Reticulum Calcium Release in Cardiac Myocytes in Response to Adrenergic Stimulation. *PLOS ONE* 9, e87495.

Curran, M. E. 1995. A molecular basis for cardiac arrhythmia: HERG mutations cause long QT syndrome. *Cell*, 80, pp.795-803.

Denham, N. C. 2019. Systematic re-evaluation of SCN5A variants associated with Brugada syndrome. *Journal of Cardiovascular Electrophysiology* 30, pp.118-127.

Desmet et al. 2009. Human Splicing Finder: an online bioinformatics tool to predict splicing signals. *Nucleic acids research* 37, e67-e67.

Desplantez, T., Dupont, E., Severs, N. J. and Weingart, R. 2007. Gap Junction Channels and Cardiac Impulse Propagation. *Journal of Membrane Biology* 218, pp.13-28.

de Vries, L.J., Géczy, T. and Szili-Torok, T. 2017. Sleep Medications Containing Melatonin can Potentially Induce Ventricular Arrhythmias in Structurally Normal Hearts: A 2-Patient Report. *Journal of Cardiovascular Pharmacology* 70(4): pp.267-270.

Devalla, H. D. et al. 2016. TECRL, a new life-threatening inherited arrhythmia gene associated with overlapping clinical features of both LQTS and CPVT. *EMBO molecular medicine* 8, pp.1390-1408.

Dickerson, L.W., et al. 1993. Primary coronary vasodilation associated with pauses in heart rhythm during sleep. *American Journal of Physiology* 264(1): pp. R186-R196.

Difrancesco, D. and Noble, D. 2012. The funny current has a major pacemaking role in the sinus node. *Heart Rhythm* 9, pp.299-301.

Dobrzynski, H. et al. 2013. Structure, function and clinical relevance of the cardiac conduction system, including the atrioventricular ring and outflow tract tissues. *Pharmacology & Therapeutics* 139, pp.260-288.

Domingo, D. et al. 2015. Non-ventricular, Clinical, and Functional Features of the RyR2(R420Q) Mutation Causing Catecholaminergic Polymorphic Ventricular Tachycardia. *Revista Española de Cardiología* (English Edition) 68, pp.398-407.

Dorian, P. 2005. Antiarrhythmic Action ofβ-Blockers: Potential Mechanisms. *Journal of Cardiovascular Pharmacology and Therapeutics* 10, pp.S15-S22.

Earle N. et al. 2014. Single nucleotide polymorphisms in arrhythmia genes modify the risk of cardiac events and sudden death in long QT syndrome. *Heart Rhythm* 11(1): pp.76-82.

Eisner, D. A., Caldwell, J. L., Kistamás, K. and Trafford, A. W. 2017. Calcium and Excitation-Contraction Coupling in the Heart. *Circulation research* 121, pp.181-195.

Eriksson, M. et al. 2003. Recurrent de novo point mutations in lamin A cause Hutchinson–Gilford progeria syndrome. *Nature* 423, pp.293–298.

Fabiato, A. and Fabiato, F. 1975. Contractions induced by a calcium-triggered release of calcium from the sarcoplasmic reticulum of single skinned cardiac cells. *The Journal of physiology* 249, pp.469-495.

Faggioni, M. and Knollmann, B. C. 2012. Calsequestrin 2 and arrhythmias. *American journal of physiology* 302, pp.H1250-H1260.

Feher, J. 2012. 5.5 - The Cardiac Action Potential. In: Feher, J. (ed.) Quantitative Human Physiology (Second Edition). Boston: Academic Press.

Fernández-Velasco, M. 2009. Increased Ca2+ sensitivity of the ryanodine receptor mutant RyR2R4496C underlies catecholaminergic polymorphic ventricular tachycardia. *Circulation research* 104, pp.201-209.

Fill, M. and Copello, J. A. 2002. Ryanodine Receptor Calcium Release Channels. *Physiological Reviews* 82, pp.893-922.

Findlay G.M. et al. 2018. Accurate classification of BRCA1 variants with saturation genome editing. *Nature*. 562(7726): pp.217-222.

Fruen, B. R., Kane, P. K., Mickelson, J. R. and Louis, C. F. 1996. Chloride-dependent sarcoplasmic reticulum Ca2+ release correlates with increased Ca2+ activation of ryanodine receptors. *Biophysical journal* 71, pp.2522-2530.

Fujii, Y. et al. 2017. A type 2 ryanodine receptor variant associated with reduced Ca2+ release and short-coupled torsades de pointes ventricular arrhythmia. *Heart Rhythm* 14(1): pp.98-107.

Gaburjakova, J. and Gaburjakova, M. 2006. Comparison of the Effects Exerted by Luminal Ca2+ on the Sensitivity of the Cardiac Ryanodine Receptor to Caffeine and Cytosolic Ca2+. *The Journal of Membrane Biology* 212, pp.17-28.

Gaburjakova, M., Bal, N. C., Gaburjakova, J. and Periasamy, M. 2013. Functional interaction between calsequestrin and ryanodine receptor in the heart. *Cellular and molecular life sciences* 70, pp.2935-2945.

Gallegos, J.E. and Rose, A.B. 2019. An intron-derived motif strongly increases gene expression from transcribed sequences through a splicing independent mechanism in Arabidopsis thaliana. Scientific Reports 9, pp.13777

Gautel, M. and Djinović-Carugo, K. 2016. The sarcomeric cytoskeleton: from molecules to motion. *The Journal of Experimental Biology* 219, pp.135.

George, C.H., Higgs, G.V. and Lai F.A. 2003. Ryanodine receptor mutations associated with stress-induced ventricular tachycardia mediate increased calcium release in stimulated cardiomyocytes. *Circulation Research* 93, pp.531-540.

George, C. H. et al. 2004. Ryanodine receptor regulation by intramolecular interaction between cytoplasmic and transmembrane domains. *Molecular biology of the cell* 15, pp.2627-2638.

George, C. H., Jundi, H., Thomas, N. L., Fry, D. L. and Lai, F. A. 2007. Ryanodine receptors and ventricular arrhythmias: Emerging trends in mutations, mechanisms and therapies. *Journal of Molecular and Cellular Cardiology* 42, pp.34-50.

Gomez-Hurtado, N. et al. 2016. Novel Calmodulin Mutation (CALM3-A103V) Associated with CPVT Syndrome Activates Arrhythmogenic Ca Waves and Sparks. *Biophysical Journal* 3, pp.436a.

Gray, B. et al. 2016. A novel heterozygous mutation in cardiac calsequestrin causes autosomal dominant catecholaminergic polymorphic ventricular tachycardia. *Heart Rhythm*. 13(8): pp.1652-1660.

Györke, I. and Györke, S. 1998. Regulation of the cardiac ryanodine receptor channel by luminal Ca2+ involves luminal Ca2+ sensing sites. *Biophysical journal* 75, pp.2801-2810.

Györke, I., Hester, N., Jones, L. R. and Györke, S. 2004. The role of calsequestrin, triadin, and junctin in conferring cardiac ryanodine receptor responsiveness to luminal calcium. *Biophysical journal* 86, pp.2121-2128.

Holmberg, S. R. and Williams, A. J. 1989. Single channel recordings from human cardiac sarcoplasmic reticulum. *Circulation Research* 65, pp.1445-1449.

Jabbari, J. et al. 2013. New Exome Data Question the Pathogenicity of Genetic Variants Previously Associated With Catecholaminergic Polymorphic Ventricular Tachycardia. *Circulation: Cardiovascular Genetics* 6, pp.481-489.

Jervell, A. and Lange-nielsen, F. 1957. Congenital deaf-mutism, functional heart disease with prolongation of the Q-T interval, and sudden death. *American Heart Journal* 54, pp.59-68.

Jian, X., Boerwinkle, E. and Liu, X. 2014. In silico tools for splicing defect prediction: a survey from the viewpoint of end users. *Genetics in medicine* 16, pp.497-503.

Jiang, D. et al. 2005. Enhanced Store Overload–Induced Ca2+ Release and Channel Sensitivity to Luminal Ca2+ Activation Are Common Defects of RyR2 Mutations Linked to Ventricular Tachycardia and Sudden Death. *Circulation Research* 97, pp.1173-1181.

Kang, G. et al. 2010. Purkinje cells from RyR2 mutant mice are highly arrhythmogenic but responsive to targeted therapy. *Circulation research* 107, pp.512-519.

Karczewski K.J., et al. 2019. Variation across 141,456 human exomes and genomes reveals the spectrum of loss-of-function intolerance across human protein-coding genes. *bioRxiv* 531210.

Karshikoff, A. and Ladenstein, R. 2001. Ion pairs and the thermotolerance of proteins from hyperthermophiles: a 'traffic rule' for hot roads. *Trends in Biochemical Sciences* 26, pp.550-557.

Kimlicka, L. et al. 2013. The Cardiac Ryanodine Receptor N-Terminal Region Contains an Anion Binding Site that Is Targeted by Disease Mutations. *Structure* 21, pp.1440-1449.

Kishore S., Khanna A. and Stamm S. 2008. Rapid generation of splicing reporters with pSpliceExpress. *Gene* 427, pp.104-110.

Kong et al. 2008. Caffeine induces Ca2+ release by reducing the threshold for luminal Ca2+ activation of the ryanodine receptor. *The Biochemical journal*, 414(3): pp.441–452.

Kornblihtt, A.R. et al. 2013. Alternative splicing: a pivotal step between eukaryotic transcription and translation. *Nature Reviews Molecular Cell Biology* 14(3): pp. 153-165.

Krawczak M., Reiss J. and Cooper D.N. 1992. The mutational spectrum of single base-pair substitutions in mRNA splice junctions of human genes: causes and consequences. *Human Genetics* 90, pp.41-54.

Lahat H., et al. 2001. A missense mutation in a highly conserved region of CASQ2 is associated with autosomal recessive catecholamine-induced polymorphic ventricular tachycardia in Bedouin families from Israel. *American Journal of Human Genetics*. 69(6): pp.1378-1384.

Laitinen, P.J. et al. 2001. Mutations of the Cardiac Ryanodine Receptor (RyR2) Gene in Familial Polymorphic Ventricular Tachycardia. *Circulation* 103, pp.485-490.

Landrum M.J. et al. 2016. ClinVar: public archive of interpretations of clinically relevant variants. *Nucleic Acids Research* 44(D1): pp.D862-D868.

Ledbetter, M.W. et al. 1994. Tissue distribution of ryanodine receptor isoforms and alleles determined by reverse transcription polymerase chain reaction. *The Journal of Biological Chemistry* 269(50): pp.31544-31551.

Lee, M.L., Swanson, B.E., and de la Iglesia, H.O. 2009 Circadian Timing of REM Sleep Is Coupled to an Oscillator within the Dorsomedial Suprachiasmatic Nucleus. *Current Biology* 19(10): pp.848-852.

Lee, H. G., Kang, H. and Park, W. J. 2001. Interaction of HRC (histidine-rich Ca2+-binding protein) and triadin in the lumen of sarcoplasmic reticulum. *Journal of Biological Chemistry* 276, pp.39533-39538.

Leenhardt, A., Denjoy, I. and Guicheney, P. 2012. Catecholaminergic Polymorphic Ventricular Tachycardia. *Circulation* 5, pp.1044-1052.

Leenhardt, A. et al. 1995. Catecholaminergic Polymorphic Ventricular Tachycardia in Children. *Circulation* 91, pp.1512-1519.

Leong, I.U. et al. 2015. Array comparative genomic hybridization identifies a heterozygous deletion of exon 3 of the RYR2 gene. *Upsala Journal of Medical Sciences* 120(3): pp.190-197.

Leren I.S. 2015. Abstract 9815: Nadolol Seems to Be Superior to Selective Beta Blockers in Patients With Catecholaminergic Polymorphic Ventricular Tachycardia: Is a Smaller Arrhythmic Window Part of the Explanation? *Circulation* 132, pp.A9815-A9815.

Li, P. and Chen, S. R. 2001. Molecular basis of Ca(2)+ activation of the mouse cardiac Ca(2)+ release channel (ryanodine receptor). *The Journal of general physiology* 118(1): pp.33–44.

Lieve, K. V. V. et al. 2019. Linking the heart and the brain: Neurodevelopmental disorders in patients with catecholaminergic polymorphic ventricular tachycardia. *Heart Rhythm* 16, pp.220-228.

Liu, Y. et al. 2015. Roles of the NH2-terminal domains of cardiac ryanodine receptor in Ca2+ release activation and termination. *The Journal of biological chemistry* 290, pp.7736-7746.

Liu, N., Rizzi, N., Boveri, L. and Priori, S. G. 2009. Ryanodine receptor and calsequestrin in arrhythmogenesis: What we have learnt from genetic diseases and transgenic mice. *Journal of Molecular and Cellular Cardiology* 46, pp.149-159.

Liu, N., Ruan, Y. and Priori, S. G. 2008. Catecholaminergic Polymorphic Ventricular Tachycardia. *Progress in Cardiovascular Diseases* 51, pp.23-30.

Liu, N. and Priori, S. G. 2007. Disruption of calcium homeostasis and arrhythmogenesis induced by mutations in the cardiac ryanodine receptor and calsequestrin. *Cardiovascular Research* 77, pp.293-301.

Liu, W., Pasek, D. A. and Meissner, G. 1998. Modulation of Ca2+-gated cardiac muscle Ca2+-release channel (ryanodine receptor) by mono- and divalent ions. *American Journal of Physiology-Cell Physiology* 274, pp.C120-C128.

Ludtke, S. J., Serysheva, I. I., Hamilton, S. L. and Chiu, W. 2005. The pore structure of the closed RyR1 channel. *Structure* 13, pp.1203-1211.

Luppi, et al. 2012. Brainstem mechanisms of paradoxical (REM) sleep generation. *European Journal of Physiology* 463(1): pp.43-52.

Marx, S. O. et al. 2001. Coupled gating between cardiac calcium release channels (ryanodine receptors). *Circulation research* 88, pp.1151-1158.

Marx, S. O. et al. 2000. PKA phosphorylation dissociates FKBP12. 6 from the calcium release channel (ryanodine receptor): defective regulation in failing hearts. *Cell* 101, pp.365-376.

Mechmann, S. and Pott, L. 1986. Identification of Na-Ca exchange current in single cardiac myocytes. *Nature* 319, pp.597-599.

Medeiros-Domingo, A. et al. 2009. The RYR2-encoded ryanodine receptor/calcium release channel in patients diagnosed previously with either catecholaminergic polymorphic ventricular tachycardia or genotype negative, exercise-induced long QT syndrome: a comprehensive open reading frame mutational analysis. *Journal of the American College of Cardiology* 54, pp.2065-2074.

Mercado, C. et al. 2009. Ryanodine-Sensitive Intracellular Ca2+ Channels in Rat Suprachiasmatic Nuclei Are Required for Circadian Clock Control of Behavior. *Journal of Biological Rhythms* 24(3): pp. 203-210.

Napolitano, C., Priori, S.G. and Bloise. Catecholaminergic Polymorphic Ventricular Tachycardia. 2004 Oct 14 [Updated 2016 Oct 13]. In: Adam MP, Ardinger HH, Pagon RA, et al., editors. GeneReviews® [Internet]. Seattle (WA): University of Washington, Seattle; 1993-2019.

Napolitano, C. et al. 2013. Clinical utility gene card for: Catecholaminergic polymorphic ventricular tachycardia (CPVT). *European Journal Of Human Genetics* 22, pp.152.

Napolitano, C., Bloise, R., Memmi, M. and Priori, S. G. 2014. Clinical utility gene card for: Catecholaminergic polymorphic ventricular tachycardia (CPVT). *European journal of human genetics*, 22(1).

Nyegaard, M. et al. 2012. Mutations in calmodulin cause ventricular tachycardia and sudden cardiac death. *American journal of human genetics* 91, pp.703-712.

Ohno, S. et al. 2014. Exon 3 deletion of RYR2 encoding cardiac ryanodine receptor is associated with left ventricular non-compaction. *EP Europace* 16(11): pp.1646-1654.

Oudit, G. Y. and Backx, P. H. 2018. 3 - Voltage-Gated Potassium Channels. In: Zipes, D. P., Jalife, J. and Stevenson, W. G. (eds.) Cardiac Electrophysiology: From Cell to Bedside (Seventh Edition). Elsevier.

Pertea, M., Lin, X. and Salzberg, S. L. 2001. GeneSplicer: a new computational method for splice site prediction. *Nucleic acids research* 29, pp.1185-1190.

Peng et al. (2016). Structural basis for the gating mechanism of the type 2 ryanodine receptor RyR2. Science 354, pp. 5324

Pouliquin, P. et al. 2006. Effects of an α-helical ryanodine receptor C-terminal tail peptide on ryanodine receptor activity: Modulation by Homer. *The international journal of biochemistry & cell biology* 38, pp.1700-1715.

Pouliquin, P., Pace, S. M. and Dulhunty, A. F. 2009. In vitro modulation of the cardiac ryanodine receptor activity by Homer1. *European Journal of Physiology* 458, pp.723-732.

Prinzen, F. W., Vernooy, K., Lumens, J. and Auricchio, A. 2017. 7 - Physiology of Cardiac Pacing and Resynchronization. In: Ellenbogen, K. A., Wilkoff, B. L., Kay, G. N., Lau, C.-P. and Auricchio, A. (eds.) Clinical Cardiac Pacing, Defibrillation and Resynchronization Therapy (Fifth Edition). Elsevier.

Priori, S.G. et al. 2002. Clinical and Molecular Characterization of Patients With Catecholaminergic Polymorphic Ventricular Tachycardia. *Circulation* 106, pp.69-74.

Priori S.G. et al. 2001. Mutations in the Cardiac Ryanodine Receptor Gene (hRyR2) Underlie Catecholaminergic Polymorphic Ventricular Tachycardia. *Circulation* 103, pp.196-200.

Qin, J. et al. 2009. Ryanodine receptor luminal Ca2+ regulation: swapping calsequestrin and channel isoforms. *Biophysical journal* 97, pp.1961-1970.

Richards, S. et al. 2015. Standards and guidelines for the interpretation of sequence variants: a joint consensus recommendation of the American College of Medical Genetics and Genomics and the Association for Molecular Pathology. *Genetics in medicine* 17, pp.405-424.

Rooryck, C. 2015. New family with catecholaminergic polymorphic ventricular tachycardia linked to the Triadin gene. *Journal of cardiovascular electrophysiology* 26, pp.1146-1150.

Roston, T.M. et al. 2017. A novel RYR2 loss-of-function mutation (I4855M) is associated with left ventricular non-compaction and atypical catecholaminergic polymorphic ventricular tachycardia. *Journal of Electrocardiology* 50, 227-33.

Roston, T. M., Sanatani, S. and Chen, S. R. W. 2017. Suppression-of-function mutations in the cardiac ryanodine receptor: Emerging evidence for a novel arrhythmia syndrome? *Heart Rhythm* 14, pp.108-109.

Roux-Buisson, N. et al. 2012. Absence of triadin, a protein of the calcium release complex, is responsible for cardiac arrhythmia with sudden death in human. *Human molecular genetics* 21, pp.2759-2767.

Samsó, M., Feng, W., Pessah, I. N. and Allen, P. D. 2009. Coordinated Movement of Cytoplasmic and Transmembrane Domains of RyR1 upon Gating. *PLOS Biology* 7, e1000085.

Samsó, M., Wagenknecht, T. and Allen, P. 2005a. Internal structure and visualization of transmembrane domains of the RyR1 calcium release channel by cryo-EM. *Nature structural & molecular biology* 12, pp.539-544.

Sánchez-Quintana, D. and Yen, H.S. 2003. Anatomy of Cardiac Nodes and Atrioventricular Specialized Conduction System. *Revista Española de Cardiología (English Edition)* 56, pp.1085-1092.

Severs, N. J. 2000. The cardiac muscle cell. *BioEssays* 22, pp.188-199.

Shaikh, S.S. et al. 2018. Before progressing from “exomes” to “genomes”… don’t forget splicing variants. *European Journal of Human Genetics* 26, pp.1559–1562.

Sigalas, C., Bent, S., Kitmitto, A., O'Neill, S. and Sitsapesan, R. 2009. Ca2+-calmodulin can activate and inactivate cardiac ryanodine receptors. *British journal of pharmacology* 156, pp.794-806.

Sitsapesan, R. and Williams, A. J. 1994. Regulation of the gating of the sheep cardiac sarcoplasmic reticulum ca2+-release channel by luminal Ca2+. *The Journal of Membrane Biology* 137, pp.215-226.

Smith, M. J. et al. 2014. Germline Mutations in SUFU Cause Gorlin Syndrome–Associated Childhood Medulloblastoma and Redefine the Risk Associated with PTCH1 Mutations. *Journal of Clinical Oncology* 32, pp.4155-4161.

Sommariva, E. et al. 2013. Genetics can contribute to the prognosis of Brugada syndrome: a pilot model for risk stratification. *European Journal of Human Genetics* 21(9): pp.911–917.

Song, L. et al. 2007a. Calsequestrin 2 (CASQ2) mutations increase expression of calreticulin and ryanodine receptors, causing catecholaminergic polymorphic ventricular tachycardia. *The Journal of clinical investigation* 117, pp.1814-1823.

Sorek, R. and Ast, G. 2003. Intronic sequences flanking alternatively spliced exons are conserved between human and mouse. *Genome research*, 13(7): pp.1631–1637.

Stenson P.D., Mort M., Ball E.V., Shaw K., Phillips A. and Cooper D.N. 2014.The Human Gene Mutation Database: building a comprehensive mutation repository for clinical and molecular genetics, diagnostic testing and personalized genomic medicine. *Human Genetics* 133(1): pp.1-9.

Steinfurt, J. et al. 2015. High-dose flecainide with low-dose β-blocker therapy in catecholaminergic polymorphic ventricular tachycardia: A case report and review of the literature. *Journal of Cardiology Cases* 11, pp.10-13.

Swan, H. et al. 1999. Arrhythmic disorder mapped to chromosome 1q42–q43 causes malignant polymorphic ventricular tachycardia in structurally normal hearts. *Journal of the American College of Cardiology* 34, pp.2035-2042.

Tang, Y., Tian, X., Wang, R., Fill, M. and Chen S.R.W. 2012. Abnormal Termination of Ca2+ Release Is a Common Defect of RyR2 Mutations Associated With Cardiomyopathies. *Circulation Research* 110(7): pp.968–977.

Terentyev, D. et al. 2006. Abnormal Interactions of Calsequestrin With the Ryanodine Receptor Calcium Release Channel Complex Linked to Exercise-Induced Sudden Cardiac Death. *Circulation Research* 98, pp.1151-1158.

Tester, D. J. et al. 2006. Genotypic heterogeneity and phenotypic mimicry among unrelated patients referred for catecholaminergic polymorphic ventricular tachycardia genetic testing. *Heart Rhythm* 3, pp.800-805.

Tester, D. J., Medeiros-Domingo, A., Will, M. L., Haglund, C. M. and Ackerman, M. J. 2012. Cardiac channel molecular autopsy: insights from 173 consecutive cases of autopsy-negative sudden unexplained death referred for postmortem genetic testing. *Mayo Clinic proceedings* 87, pp.524-539.

Thery, J.C. et al. 2011. Contribution of bioinformatics predictions and functional splicing assays to the interpretation of unclassified variants of the BRCA genes. *European Journal Human Genetics* 19, pp.1052-1058.

Thomas L.N., George, C.H. and Lai, A. 2004. Functional heterogeneity of ryanodine receptor mutations associated with sudden cardiac death. *Cardiovascular Research* 64(1): pp.52–60.

Tian, X. et al. 2013. Ligand-dependent conformational changes in the clamp region of the cardiac ryanodine receptor. *The Journal of biological chemistry* 288, pp.4066-4075.

Tooley, G.A., Armstrong, S.M., Norman, T.R., Sali, A. 2000. Acute increases in night-time plasma melatonin levels following a period of meditation. *Biological Psychology*. 53(1): pp.69-78.

Tranum-Jensen, J., Wilde, A. A., Vermeulen, J. T. and Janse, M. J. 1991. Morphology of electrophysiologically identified junctions between Purkinje fibers and ventricular muscle in rabbit and pig hearts. *Circulation Research* 69, pp.429-437.

Van Der Werf, C. and Lieve, K. V. 2016. Beta-blockers in the treatment of catecholaminergic polymorphic ventricular tachycardia. *Heart Rhythm* 13, pp.441-442.

Van Petegem, F. 2012. Ryanodine receptors: structure and function. *The Journal of biological chemistry* 287, pp.31624-31632.

Van Petegem, F. 2015. Ryanodine Receptors: Allosteric Ion Channel Giants. *Journal of Molecular Biology* 427, pp.31-53.

Venetucci, L. A., Trafford, A. W., O'Neill, S. C. and Eisner, D. A. 2007. The sarcoplasmic reticulum and arrhythmogenic calcium release. *Cardiovascular Research* 77, pp.285-292.

Verrier, R.L. and Josephson, M.E. 2009. Impact of sleep on arrhythmogenesis. *Circulation* 2(4): pp.450-459.

Walsh, M. A. et al. 2016. Compound Heterozygous Triadin Mutation Causing Cardiac Arrest in Two Siblings. *Pacing and Clinical Electrophysiology* 39(5): pp.497-501.

Walweel, K. et al. 2014. Differences in the regulation of RyR2 from human, sheep, and rat by Ca^{2+} and Mg^{2+} in the cytoplasm and in the lumen of the sarcoplasmic reticulum. *The Journal of general physiology* 144, pp.263-271.

Wang, L and MacDonald, R.C. 2004. Effects of microtubule-depolymerizing agents on the transfection of cultured vascular smooth muscle cells: enhanced expression with free drug and especially with drug-gene lipoplexes. *Molecular Therapy* 9(5): pp.729-737.

Wang, Q. et al. 1995. SCN5A mutations associated with an inherited cardiac arrhythmia, long QT syndrome. *Cell* 80, pp.805-811.

Watanabe, H. and Knollmann, B. C. 2011. Mechanism underlying catecholaminergic polymorphic ventricular tachycardia and approaches to therapy. *Journal of Electrocardiology* 44, pp.650-655.

Wehrens, X. H., Lehnart, S. E., Reiken, S. R. and Marks, A. R. 2004. Ca2+/calmodulin-dependent protein kinase II phosphorylation regulates the cardiac ryanodine receptor. *Circulation research* 94, pp.e61-e70.

Wehrens, X. H. T. et al. 2003. FKBP12.6 Deficiency and Defective Calcium Release Channel (Ryanodine Receptor) Function Linked to Exercise-Induced Sudden Cardiac Death. *Cell* 113, pp.829-840.

Wei, L., Gallant, E. M., Dulhunty, A. F. and Beard, N. A. 2009. Junctin and triadin each activate skeletal ryanodine receptors but junctin alone mediates functional interactions with calsequestrin. *The international journal of biochemistry & cell biology* 41, pp.2214-2224.

Westhoff et al. 2003. Vesl/Homer proteins regulate ryanodine receptor type 2 function and intracellular calcium signaling. *Cell calcium* 34, pp.261-269.

Whiffin, N. et al. 2017. Using high-resolution variant frequencies to empower clinical genome interpretation. *Genetics In Medicine* 19, pp.1151.

Whitt, J.P., McNally, B.A. and Meredith, A.L. 2018. Differential contribution of Ca(2+) sources to day and night BK current activation in the circadian clock. *The Journal of general physiology* 150(2): pp.259-275.

Will, C.L. and R. Lührmann. 2011. Spliceosome Structure and Function. *Cold Spring Harbor Perspectives in Biology* 3(7): pp. a003707.

Wu, S. et al. 2006. Central core disease is due to RYR1 mutations in more than 90% of patients. *Brain* 129, pp.1470-1480.

Xiao, R.-P. 2001. β-Adrenergic Signaling in the Heart: Dual Coupling of the β2-Adrenergic Receptor to Gs and Gi Proteins. *Science's STKE* 104, pp.re15

Xiao, Z. et al. 2016. Enhanced Cytosolic Ca2+ Activation Underlies a Common Defect of Central Domain Cardiac Ryanodine Receptor Mutations Linked to Arrhythmias. *Journal of Biological Chemistry* 291, pp.24528-24537.

Yamaguchi, N., Xu, L., Pasek, D. A., Evans, K. E. and Meissner, G. 2003. Molecular basis of calmodulin binding to cardiac muscle Ca2+ release channel (ryanodine receptor). *Journal of Biological Chemistry* 278, pp.23480-23486.

Yamamoto, T. and Ikemoto, N. 2002. Peptide Probe Study of the Critical Regulatory Domain of the Cardiac Ryanodine Receptor. *Biochemical and Biophysical Research Communications* 291, pp.1102-1108.

Yang, Z., Ikemoto, N., Lamb, G. D. and Steele, D. S. 2006. The RyR2 central domain peptide DPc10 lowers the threshold for spontaneous Ca2+ release in permeabilized cardiomyocytes. *Cardiovascular Research* 70, pp.475-485.

Yeo, G. and Burge, C. B. 2004. Maximum Entropy Modeling of Short Sequence Motifs with Applications to RNA Splicing Signals. *Journal of Computational Biology* 11, pp.377-394.

Zhang, J. Z., Mclay, J. C. and Jones, P. P. 2014. The arrhythmogenic human HRC point mutation S96A leads to spontaneous Ca 2+ release due to an impaired ability to buffer store Ca 2+. *Journal of molecular and cellular cardiology* 74, pp.22-31.

Zhang, L., Kelley, J., Schmeisser, G., Kobayashi, Y. M. and Jones, L. R. 1997. Complex Formation between Junctin, Triadin, Calsequestrin, and the Ryanodine Receptor: PROTEINS OF THE CARDIAC JUNCTIONAL SARCOPLASMIC RETICULUM MEMBRANE. *Journal of Biological Chemistry* 272, pp.23389-23397.

Zhang, M. Q. 1998. Statistical features of human exons and their flanking regions. *Human Molecular Genetics* 7, pp.919-932.

Zhao, Y.-T. et al. 2015 Arrhythmogenesis in a catecholaminergic polymorphic ventricular tachycardia mutation that depresses ryanodine receptor function. *Proceedings of the National Academy of Sciences of the United States of America* 112(13): pp.E1669-E1677.

Zima, A. V., Picht, E., Bers, D. M. and Blatter, L. A. 2008. Termination of cardiac Ca2+ sparks: role of intra-SR [Ca2+], release flux, and intra-SR Ca2+ diffusion. *Circulation research* 103, pp.e105-e115.

Zissimopoulos, S. and Lai, F. A. 2005. Interaction of FKBP12. 6 with the cardiac ryanodine receptor C-terminal domain. *Journal of Biological Chemistry* 280, pp.5475-5485.

Appendices

Appendix I. Supplemental material for chapter 3, Classification and correlation of RYR2 missense variants in individuals with catecholaminergic polymorphic ventricular tachycardia reveals phenotypic relationships.

Supplementary Table 3.1. Clinical information for CPVT patients with RYR2 missense variants

Protein Change	Sex	Age (years)	Inheritance	Ethnicity	Trigger	Cardiac Phenotype	Response to medication	Reference
Ile11Ser	Male	16	Maternal	Unknown	Exercise	Bidirectional ventricular tachycardia	Unknown	(Bosch et al., 2017)
Phe13Leu	Unknown	Unknown	Unknown	Unknown	Unknown	Unknown	Unknown	(Landrum et al., 2016)
Phe13Cys	Unknown	Unknown	Unknown	Unknown	Unknown	Unknown	Unknown	(Landrum et al., 2016)
His29Asp	Female	31	Maternal	Indian	Rest	Polymorphic ventricular tachycardia and syncope	Verapamil - not effective. ablation - effective.	(Cheung et al., 2015)
Leu62Phe	Unknown	Unknown	Unknown	Unknown	Unknown	Unknown	Unknown	(Medeiros-Domingo et al., 2009)
Leu73Val	Male	12	Unknown	Unknown	Exercise	Sudden death	Unknown	(Campuzano et al., 2014)
Ala77Val	Male	17	Maternal	Unknown	Exercise	Polymorphic ventricular tachycardia and syncope	Acebutolol - responsive	(d'Amati et al., 2005)
Met81Leu	Unknown	Unknown	Unknown	Unknown	Unknown	Unknown	Unknown	(d'Amati et al., 2005)
Pro164Ser	Male	11	Unknown	Unknown	Exercise	Polymorphic ventricular tachycardia and syncope	Unknown	(Tester et al., 2006)

Ala165Asp	Unknown	Unknown	Unknown	Unknown	Unknown	Unknown	Unknown	(Hayashi et al., 2012)
Arg169Leu	Female	9	De novo	Unknown	Unknown	Syncope	Unknown	(Ohno et al., 2015)
Arg169Gln	Female	18	De novo	Unknown	Exercise	Unknown	Unknown	(Ohno et al., 2015)
Arg176Gln	Male	12	Unknown	Unknown	Excitement	Syncope	Unknown	(Tester et al., 2005b)
Gly178Ala	Male	16	De novo		Unknown	Cardiac arrest	Unknown	(Ohno et al., 2015)
Glu189Asp	Female	9	Unknown	Unknown	Exercise	Bidirectional ventricular tachycardia and syncope	Beta-blocker responsive.	(Sy et al., 2011)
Ile217Val	Male	21	Unknown	European	Unknown	Syncope	Unknown	(Tester et al., 2012)
Gly230Cys	Male	50	Unknown	Caucasian	Exercise	Unknown	Unknown	(Meli et al., 2011)
His240Arg	Male	2	Unknown	European	Exercise	Sudden death	Unknown	(Tester et al., 2012)
Asp242Val	Unknown	Unknown	Unknown	Unknown	Unknown	Unknown	Unknown	(Hayashi et al., 2009)
Glu243Lys	Unknown	Unknown	Unknown	Unknown	Unknown	Unknown	Unknown	(Hayashi et al., 2009)
Ala271Val	Unknown	Unknown	De novo	Unknown	Unknown	Unknown	Unknown	(Janson et al., 2014)
Phe329Leu	Unknown	Unknown	Unknown	Unknown	Unknown	Unknown	Unknown	(Medeiros-Domingo et al., 2009)
Arg332Trp	Unknown	Unknown	Unknown	Unknown	Unknown	Unknown	Unknown	(Medeiros-Domingo et al., 2009)

Gly357Ser	Unknown	36	Unknown	Unknown	Unknown	Unknown	Unknown	(Medeiros-Domingo et al., 2009)
Val382Met	Unknown	Unknown	Unknown	Unknown	Unknown	Unknown	Unknown	(Landrum et al., 2016)
Asp400His	Unknown	Unknown	Unknown	Unknown	Unknown	Unknown	Unknown	(Tester et al., 2012)
Asp401Gly	Male	14	De novo	Unknown	Exercise	Unknown	Unknown	(Stattin et al., 2016)
Ile406Thr	Male	15	Unknown	Unknown	Unknown	Ventricular fibrillation	Unknown	(Nof et al., 2011)
Ser406Leu	Female	24	Paternal	Unknown	Unknown	Unknown	Unknown	(Jung et al., 2012)
Arg407Ile	Male	9	Unknown	Hispanic	Unknown	Syncope	Unknown	(Tester et al., 2012)
Arg407Ser	Male	13	De novo	Unknown	Unknown	Syncope	Unknown	(Ohno et al., 2015)
Ser413Thr	Unknown	Unknown	Unknown	Unknown	Unknown	Unknown	Unknown	(Hayashi et al., 2009)
Arg414Cys	Female	16	Unknown	European	Exercise	Unknown	Unknown	(Tester et al., 2005a)
Arg414Leu	Male	17	Unknown	Unknown	Exercise	Ventricular bigeminy and syncope, sudden death	Unknown	(Choi et al., 2004)
Thr415Ile	Unknown	Unknown	Unknown	Unknown	Unknown	Unknown	Unknown	(Ware et al., 2013)
Thr415Arg	Unknown	Unknown	Unknown	Unknown	Unknown	Unknown	Unknown	(Medeiros-Domingo et al., 2009)
Ile419Phe	Female	13	Unknown	European	Exercise	Unknown	Unknown	(Tester et al., 2011)
Arg420Gln	Male	14	De novo	Unknown	Exercise	syncope	Unknown	(Domingo et al., 2015b)

Arg420Trp	Male	12	Unknown	Unknown	Exercise	Polymorphic ventricular tachycardia and syncope, sudden death	Unresponsive to Beta-blockers	(Sy et al., 2011)
Leu433Pro	Female	18	Unknown	Unknown	Exercise	Ventricular fibrillation	Unknown	(Bauce et al., 2002b)
Pro466Ala	Male	9	Unknown	Unknown	Exercise	Syncope, ventricular fibrillation, cardiac arrest	Unknown	(Tester et al., 2005b)
Leu470Pro	Female	19	Unknown	African American	Unknown	Unknown	Unknown	(Friday et al., 2015)
Gln486His	Male	17	Paternal	Unknown	Exercise	Sudden death	Unknown	(Larsen et al., 2013)
Val507Ile	Unknown	Unknown	Unknown	Unknown	Unknown	Unknown	Unknown	(Farrugia et al., 2015)
Asn547Ser	Female	20	Unknown	Unknown	Unknown	Syncope, palpitations	Unknown	(Hertz et al., 2015)
Ala549Val	Unknown	Unknown	Unknown	Unknown	Unknown	Unknown	Unknown	(Medeiros-Domingo et al., 2009)
Ser582Ile	Male	6	Unknown	Unknown	Unknown	Unknown	Unknown	(Lieve et al., 2019)
Ser616Leu	Female	12	De novo	Unknown	Exercise	Syncope, ventricular premature contractions during exercise	Unknown	(Marjamaa et al., 2009)
Arg647Cys	Female	5	Unknown	White British	Unknown	Sinus node dysfunction	Unknown	MCGM
Arg739His	Unknown	Unknown	Unknown	Unknown	Unknown	Unknown	Unknown	(Medeiros-Domingo et al., 2009)

Ser756Asn	Unknown	Unknown	Unknown	Unknown	Unknown	Unknown	Unknown	(Landrum et al., 2016)
Ser767Cys	Female	25	Unknown	Unknown	Unknown	Unknown	Unknown	(Takayama et al., 2017)
Ile766Val	Unknown	Unknown	Unknown	Unknown	Unknown	Unknown	Unknown	Novel
Gly901Ser	Unknown	Unknown	Unknown	Unknown	Unknown	Unknown	Unknown	(Zhang et al., 2015)
Leu943Ser	Male	1	Unknown	White British	Sleep	Sudden death	Unknown	MCGM
Thr1107Met	Unknown	Unknown	Unknown	Unknown	Unknown	Unknown	Unknown	(Medeiros-Domingo et al., 2009)
Ala1136Val	Male	New born	Unknown		Exercise	Cardiac arrest	nadolol - unresponsive	(Roston et al., 2018)
Val1161Leu	Unknown	Unknown	Unknown	Unknown	Unknown	Unknown	Unknown	Novel
Thr1223Ala	Male	3	Maternal	Unknown	Unknown	Syncope	Unknown	(Ohno et al., 2015)
Val1241Ile	Unknown	Unknown	Unknown	Unknown	Unknown	Unknown	Unknown	Novel
Pro1256Thr	Female	11	Maternal	Unknown	Unknown	Syncope	Unknown	(Ohno et al., 2015)
Ile1268Thr	Female	48	Unknown	Unknown	Unknown	Unknown	Unknown	(Allegue et al., 2015)
Thr1276Ile	Unknown	Unknown	Unknown	Unknown	Unknown	Unknown	Unknown	(Landrum et al., 2016)
Met1347Arg	Unknown	Unknown	Unknown	Unknown	Unknown	Unknown	Unknown	(Landrum et al., 2016)
Thr1399Leu	Unknown	Unknown	Unknown	Unknown	Unknown	Unknown	Unknown	(Landrum et al., 2016)
Gly1470Ala	Unknown	Unknown	Unknown	Unknown	Unknown	Unknown	Unknown	Novel
Cys1489Arg	Male	51	Unknown	White British	Sleep	Palpitations, VF, cardiac arrest in sleep, sudden death.	Unknown	MCGM

Leu1518Phe	Female	15	maternal	Unknown	Unknown	Syncope	Unknown	(Ohno et al., 2015)
Asn1551Ser	Unknown	Unknown	Unknown	Unknown	Unknown	Unknown	Unknown	(Kawamura et al., 2013)
Met1564Ile	Female	21	Unknown	White British	Unknown	Sudden death	Unknown	MCGM
Gln1581Pro	Male	26	Unknown	Unknown	Excitement	Sudden death	Unknown	(Farrugia et al., 2015)
Val1664Lys	Unknown	Unknown	Unknown	Unknown	Unknown	Unknown	Unknown	(Landrum et al., 2016)
Leu1686Phe	Unknown	Unknown	Unknown	Unknown	Unknown	Unknown	Unknown	(Allegue et al., 2015)
Met1694Leu	Female	27	Maternal	White British	Unknown	Palpitations syncope	Unknown	MCGM
Glu1724Lys	Female	9	Unknown	Dutch	Exercise	Syncope, monomorphic bigeminy, polymorphic ventricular tachycardia	Unknown	(Postma et al.)
Ser1765Cys	Unknown	Unknown	Unknown	Unknown	Unknown	Unknown	Unknown	(Brion et al., 2014)
Ile1792Leu	Unknown	Unknown	Unknown	Unknown	Unknown	Unknown	Unknown	(Landrum et al., 2016)
Arg1807Gln	Unknown	Unknown	Unknown	Unknown	Unknown	Unknown	Unknown	(Landrum et al., 2016)
Val1810Leu	Male	16	De novo	Unknown	Exercise	Syncope, bidirectional polymorphic ventricular tachycardia	Beta-blockers unresponsive	(Kim et al., 2012)
Glu1837Lys	Unknown	Unknown	Unknown	Unknown	Unknown	Unknown	Unknown	(Medeiros-Domingo et al., 2009)

Asp1872Asn	Female	< 1	Unknown	Unknown	Unknown	Sudden death	Unknown	(Larsen et al., 2013)
Gly1885Glu	Female	32	Unknown	Unknown	Exercise	Cardiac arrest, sudden death	Unknown	(Laksman et al., 2014)
Gly1886Ser	Male	19	Unknown	Unknown	Unknown	Unknown	Unknown	(Tester et al., 2011)
Arg1919Gln	Male	14	Unknown	Unknown	Unknown	Unknown	Unknown	(Takayama et al., 2017)
Arg1921Gln	Male	2	Maternal	Greek	Unknown	Sudden death	Unknown	MCGM
Glu2045Gly	Unknown	Unknown	Unknown	Unknown	Unknown	Unknown	Unknown	(Medeiros-Domingo et al., 2009)
Ile2075Thr	Female	11	Paternal	Unknown	Exercise	Syncope, ventricular fibrillation, sudden death	Unknown	(Paech et al., 2014)
Pro2078Ser	Unknown	Unknown	Unknown	Unknown	Unknown	Unknown	Unknown	(Landrum et al., 2016)
Gln2091Arg	Male	29	Paternal	White British	Unknown	Sudden death	Unknown	MCGM
Gly2094Ser	Unknown	Unknown	Unknown	Unknown	Unknown	Unknown	Unknown	Novel
Gly2145Arg	Male	41	Unknown	Unknown	Unknown	sudden death	Unknown	(Marjamaa et al., 2011)
Ile2149Val	Male	Paternal	Unknown	White British	Unknown	Cardiac arrest	Unknown	MCGM
Lys2153Glu	Unknown	Unknown	Unknown	Unknown	Unknown	Unknown	Unknown	(Zhang et al., 2015)
Gly2166Glu	Unknown	Unknown	Unknown	Unknown	Unknown	Unknown	Unknown	Novel
His2168Arg	Male	7	Unknown	White British	Unknown	Sudden death	Unknown	MCGM
His2168Gln	Unknown	Unknown	Unknown	Unknown	Unknown	Unknown	Unknown	(Medeiros-Domingo et al., 2009)

Val2178Ile	Unknown	25	Familial	Unknown	Unknown	Sudden death	Unknown	(van der Werf et al., 2012)
Met2192Leu	Male	13	Maternal	Unknown	Unknown	Cardiac arrest	Unknown	(Ohno et al., 2015)
Lys2212Asn	Unknown	8	De novo	Unknown	Unknown	Unknown	Unknown	(van der Werf et al., 2012)
Asp2216Gly	Male	14	Unknown	Unknown	Unknown	Syncope, sudden death	Unknown	(Steinfurt et al., 2014)
Asp2216Val	Unknown	Unknown	Unknown	Unknown	Unknown	Unknown	Unknown	(Medeiros-Domingo et al., 2009)
His2217Tyr	Unknown	Unknown	Unknown	Unknown	Unknown	Unknown	Unknown	(Hayashi et al., 2009)
Gly2227Val	Male	16	Unknown	Unknown	Unknown	Sudden death	Unknown	(Tester et al., 2012)
Gly2228Val	Unknown	Unknown	Unknown	Unknown	Unknown	Unknown	Unknown	(Jabbari et al., 2013)
Ser2246Leu	Male	13	De novo	Unknown	Unknown	Cardiac arrest, sudden death	Unknown	(Ohno et al., 2015)
Ala2252Val	Unknown	14	Unknown	Unknown	Exercise	Sudden death	Unknown	(Tan Hanno et al., 2005)
Ala2254Thr	Male	33	Unknown	Pakistani	Unknown	Syncope	Unknown	MCGM
Gly2273Arg	Male	13	Paternal	Unknown	Sleep	Sudden death	Unknown	Novel
Arg2267His	Female	6 months	Unknown	African	Unknown	Unknown	Unknown	(Tester et al., 2007)
Cys2277Arg	Female	56	Unknown	Unknown	Unknown	Unknown	Unknown	(Domingo et al., 2015a)
Tyr2285Asn	Male	18	Maternal	White British	Unknown	Cardiac arrest	Unknown	MCGM
Glu2296Gln	Unknown	Unknown	Unknown	Unknown	Unknown	Unknown	Unknown	(Medeiros-Domingo et al., 2009)

Val2306Ile	Female	24	De novo	Unknown	Unknown	Syncope	Beta-blockers - responsive	(Laitinen et al.)
Glu2311Asp	Male	8	Unknown	Unknown	Unknown	Syncope, bidirectional polymorphic ventricular tachycardia	Beta-blockers - responsive	(Priori Silvia et al., 2002)
Ala2317Glu	Unknown	4	De novo	Unknown	Unknown	Unknown	Unknown	(Lieve et al., 2019)
Val2321Ala	Male	14	Unknown	European	Exercise	Sudden death	Unknown	(Tester et al., 2011)
Val2321Met	Female	23	Unknown	Japanese	Stress	Sudden death	Unknown	(Nishio et al., 2008)
Pro2328Ser	Unknown	Unknown	Unknown	Finnish	Unknown	Sudden death	Unknown	(Nishio et al., 2008)
Phe2331Ser	Male	8	Unknown	European	Exercise	Syncope, sudden death	gabapentin - unresponsive	(Creighton et al., 2006)
Gly2337Val	Unknown	10	Unknown	Unknown	Unknown	Unknown	Unknown	(Haugaa et al., 2010)
Gly2342Arg	Male	14	Paternal	European	Unknown	Unknown	Unknown	(Ohno et al., 2015)
Arg2359Gln	Female	53	Unknown	Unknown	Exercise/stress	Premature Ventricular Contractions	Beta-blockers - responsive	(Aizawa et al., 2007)
Gly2367Arg	Male	59	Unknown	Unknown	Spontaneous	Presyncope, non-sustained ventricular arrhythmia	Beta-blockers - responsive	(Roux-Buisson et al., 2014)
Asn2386Ile	Female	28	Paternal	Unknown	Unknown	Sudden death	Unknown	(Bauce et al., 2002a)
Ala2387Thr	Female	18	Unknown	Unknown	Unknown	Aborted cardiac arrest	Unknown	(Tester et al., 2005b)
Ala2387Pro	Unknown	Unknown	Unknown	Unknown	Unknown	Unknown	Unknown	(Steriotis et al., 2012)

Ala2387Val	Unknown	Unknown	Unknown	Unknown	Unknown	Unknown	Unknown	(Haugaa et al., 2010)
Thr2390Ile	Male	11	Paternal	Unknown	Exercise	Cardiac arrest. Sinus bradycardia. Exercise induced premature ventricular contractions	Unknown	(Ohno et al., 2015)
Tyr2392Cys	Female	25	Unknown	Unknown	Exertion	Sudden death	Unknown	(Tester et al., 2012)
Ala2394Gly	Female	15	Unknown	European	Exercise	Monomorphic premature ventricular beats	Unknown	(Postma et al.)
Gly2400Thr	Unknown	Unknown	Unknown	Unknown	Unknown	Polymorphic ventricular tachycardia	Flecainide	(Kawamura et al., 2013)
Gly2400Val	Male	15	De novo	Unknown	Unknown	Cardiac arrest	Unknown	(Ohno et al., 2015)
Arg2401His	Male	20	Unknown	Japanese	Exercise/stress	Ventricular fibrillation	Propranolol - responsive	(Tester et al., 2011)
Arg2401Leu	Male	12	Unknown	European	Exercise	Exercise-induced ventricular tachycardia, sinus node dysfunction.	Unknown	(Creighton et al., 2006)
Cys2402Tyr	Unknown	Unknown	Unknown	Unknown	Unknown	Unknown	Unknown	(Hayashi et al., 2009)
Ala2403Thr	Female	16	Unknown	Unknown	Exercise/stress	Premature ventricular contractions, ventricular bigeminy	Unknown	(Tester et al., 2005b)
Pro2404Thr	Unknown	Unknown	Unknown	Unknown	Unknown	Unknown	Unknown	(Beckmann et al., 2008)

Arg2420Trp	Unknown	Unknown	Unknown	Unknown	Unknown	Unknown	Unknown	(Medeiros-Domingo et al., 2009)
Arg2420Thr	Female	13	De novo	White British	Unknown	Cardiac arrest	Unknown	MCGM
Arg2420Ser	Male	62	Unknown	White British	Unknown	Unknown	Unknown	MCGM
Arg2467Val	Male	20	Unknown	White British	Unknown	Syncope, cardiac arrest	Unknown	MCGM
Arg2474Ser	Male	8	Unknown	Unknown	Exercise	Sudden death	atenolol - responsive	(Priori Silvia et al., 2001)
Arg2474Gly	Unknown	Unknown	Unknown	Unknown	Unknown	Unknown	Verapamil, Flecainide	(Kawamura et al., 2013)
Val2475Phe	Male	12	De novo	Unknown	Unknown	Cardiac arrest	Unknown	(Ohno et al., 2015)
Phe2483Ile	Unknown	Unknown	Unknown	Unknown	Unknown	Unknown	Unknown	(Fatima et al., 2011)
His2486Pro	Unknown	Unknown	Unknown	Unknown	Unknown	Unknown	Unknown	Novel
Val2490Ala	Unknown	Unknown	Unknown	Unknown	Unknown	Unknown	Unknown	(Landrum et al., 2016)
Ala2498Val	Unknown	Unknown	Unknown	Unknown	Unknown	Unknown	Unknown	(Hayashi et al., 2009)
Thr2504Met	Female	20	Unknown	Unknown	Exercise	Ventricular tachycardia	Beta-blockers unresponsive	(Akilzhanova et al., 2014)
Thr2510Ala	Female	17	Unknown	European	Unknown	Unknown	Unknown	(Tester et al., 2012)
Pro2533Leu	Unknown	Unknown	Unknown	Unknown	Unknown	Unknown	Unknown	(Brion et al., 2014)
Leu2534Val	Male	13	De novo	Unknown	Exercise	Non-sustained ventricular tachycardia	Beta-blockers - responsive	(Hasdemir et al., 2004)
Glu2570Lys	Unknown	Unknown	Unknown	Unknown	Unknown	Unknown	Unknown	Novel

Met2605Val	Unknown	40	Paternal	Unknown	Unknown	Unknown	Unknown	(van der Werf et al., 2012)
Gly2628Glu	Unknown	Unknown	Unknown	Unknown	Unknown	Multifocal couplets	Unknown	(Kawamura et al., 2013)
Arg2642Lys	Unknown	Unknown	Unknown	Unknown	Unknown	Unknown	Unknown	(Landrum et al., 2016)
Ala2673Val	Male	41	Unknown	Unknown	Unknown	Syncope, ventricular fibrillation, sudden death	Unknown	(Fujii et al., 2017)
Glu2715Asp	Unknown	Unknown	Unknown	Unknown	Unknown	Unknown	Unknown	(Landrum et al., 2016)
Lys2716Ile	Unknown	Unknown	Unknown	Unknown	Unknown	Unknown	Unknown	(Landrum et al., 2016)
Ile2721Thr	Unknown	Unknown	Unknown	Unknown	Unknown	Unknown	Unknown	(Hertz et al., 2015)
Pro3087Arg	Male	14	Unknown	Unknown	Unknown	Unknown	Unknown	(Takayama et al., 2017)
Gly3118Arg	Unknown	Unknown	Unknown	Unknown	Unknown	Unknown	Unknown	(Landrum et al., 2016)
Lys3187Arg	Unknown	Unknown	Unknown	Unknown	Unknown	Unknown	Unknown	(Landrum et al., 2016)
Arg3190Gln	Female	13	Maternal	White British	Unknown	Cardiac arrest	Unknown	MCGM
Gln3230Lys	Unknown	Unknown	Unknown	Unknown	Unknown	Unknown	Unknown	(Landrum et al., 2016)
Gln3304Glu	Male	12	Unknown	Unknown	Exercise	Syncope,	Unknown	(Takayama et al., 2017)
Asn3308Ser	Female	34	Unknown	Unknown	Unknown	palpitations, ventricular arrhythmias	Unknown	(Marjamaa et al., 2009)
Arg3570Trp	Male	17	Unknown	European	Exercise	Sudden death	Unknown	(Marjamaa et al., 2011)

Arg3581Lys	Male	1MONTH	Unknown	Unknown	Unknown	Sudden death	Unknown	(Hertz et al., 2016)
Arg3615Gln	Unknown	Unknown	Unknown	Unknown	Unknown	Unknown	Unknown	(Landrum et al., 2016)
Asp3638Ala	Unknown	Unknown	Unknown	Unknown	Unknown	Unknown	Unknown	(Kawamura et al., 2013)
Asp3733Asn	Unknown	Unknown	Unknown	Unknown	Unknown	Unknown	Unknown	(Landrum et al., 2016)
Met3739Ile	Male	26	De novo	White British	Unknown	Cardiac arrest on rollercoaster	Unknown	MCGM
Leu3778Phe	Male	10	Unknown	Unknown	Unknown	No	Unknown	(Priori Silvia et al., 2002)
Ser3799Pro	Unknown	Unknown	Unknown	Unknown	Unknown	Unknown	Unknown	(Hayashi et al., 2009)
Cys3800Phe	Female	58	Unknown	Unknown	Startled	Aborted cardiac arrest	Unknown	(Tester et al., 2005b)
Asp3833Asn	Unknown	Unknown	Unknown	Unknown	Unknown	Unknown	Unknown	Novel
Leu3839Phe	Female	27	Maternal	White British	Unknown	Palpitations syncope	Unknown	MCGM
Tyr3857Cys	Unknown	Unknown	Unknown	Unknown	Unknown	Unknown	Unknown	(Landrum et al., 2016)
Gln3861His	Female	18	De novo	Unknown	Unknown	Cardiac arrest	Unknown	(Ohno et al., 2015)
Asp3876Glu	Unknown	Unknown	Unknown	Unknown	Unknown	Unknown	Unknown	(Kawamura et al., 2013)
Leu3879Pro	Male	17	Unknown	Unknown	Unknown	Sudden death	Unknown	(Tester et al., 2012)
Gln3925Glu	Female	9	Unknown	European	Unknown	seizure leading to sudden death after exertion	Unknown	(Tester et al., 2012)
Ser3938Arg	Female	7	Unknown	Unknown	Exercise/stress	Palpitations, non-sustained ventricular tachycardia	Beta-blockers - responsive	(Tester et al., 2006)

Gly3946Ala	Male	6	Unknown	Unknown	Exercise	Atrial fibrillation, polymorphic ventricular tachycardia, sudden death	Beta-blockers - unresponsive	(Sy et al., 2011)
Gly3946Asp	Unknown	Unknown	Unknown	Unknown	Unknown	Unknown	Unknown	(Hayashi et al., 2009)
Gly3946Ser	Male	14	De novo	Unknown	Unknown	Unknown	Unknown	(Priori Silvia et al., 2002)
Ser3959Leu	Female	15	Unknown	Unknown	Exertion	Sudden death	Unknown	(Tester et al., 2012)
Met3972Ile	Female	8	Unknown	Unknown	Unknown	Unknown	Unknown	(Lieve et al., 2019)
Asp3973His	Female	8	Unknown	Unknown	Unknown	Unknown	Unknown	(Lieve et al., 2019)
Asp3973Asn	Female	28	Maternal	Unknown	Unknown	Cardiac arrest	Unknown	(Ohno et al., 2015)
Leu3974Gln	Female	7	Unknown	Unknown	Unknown	Left ventricle dilated	Unknown	(Lieve et al., 2019)
Asp3977Tyr	Unknown	Unknown	Unknown	Unknown	Unknown	Unknown	Unknown	(Hayashi et al., 2009)
Met3978Ile	Female	39	Unknown	Unknown	Exercise	No	Beta-blockers and Flecainide - responsive	(Sy et al., 2011)
Val3990Asp	Unknown	Unknown	Unknown	Unknown	Unknown	Unknown	Unknown	(Hayashi et al., 2009)
Lys3997Glu	Unknown	Unknown	Unknown	Unknown	Unknown	Unknown	Unknown	(Medeiros-Domingo et al., 2009)
Met3999Ile	Female	6	Unknown	Unknown	Unknown	Unknown	Unknown	(Lieve et al., 2019)
Met4002Ile	Male	3	De novo	Unknown	Bathing	Unknown	Unknown	(Ohno et al., 2015)
Glu4005Lys	Female	3	De novo	Indian	Unknown	Sudden death	Unknown	MCGM

Phe4020Leu	Male	20	Unknown	French	Exercise	Monomorphic bigeminy, polymorphic ventricular tachycardia, sudden death	Unknown	(Postma et al.)
Gly4041Arg	Unknown	Unknown	Unknown	Unknown	Unknown	Unknown	Unknown	(Brion et al., 2014)
Glu4076Lys	Female	13	Unknown	Dutch	Exercise	Polymorphic ventricular tachycardia, sudden death	Unknown	(Postma et al.)
Ala4091Thr	Female	5	Unknown	Unknown	Exercise	Atrial fibrillation, sinus bradycardia with atrial standstill	Digoxin, propranolol, propafenone amiodarone - unresponsive	(Lawrenz et al., 2014)
Ala4091Val	Male	16	Unknown	Unknown	Exercise	Cardiac arrest	N/A	(Shigemizu et al., 2015)
Asn4097Ser	Male	18	Unknown	European	Unknown	Sudden death	N/A	(Tester et al., 2012)
Asn4104Lys	Male	9	Unknown	Unknown	Unknown	Biventricular tachycardia	Unknown	(Priori Silvia et al., 2001)
Asn4104Ile	Male	9	Unknown	European	Exercise	Seizures, sustained polymorphic ventricular tachycardia	Unknown	(Postma et al.)
Leu4105Phe	Male	21	De novo	Unknown	Exercise	Unknown	Metoprolol and verapamil - responsive	(Hasdemir et al., 2008)
Met4107Val	Male	Unknown	Unknown	Unknown	Unknown	Unknown	Unknown	(Andrsova et al., 2012)

His4108Asn	Female	6	De novo	European	Exercise	Seizures, monomorphic bigeminy and polymorphic couplets, cardiac arrest	Unknown	(Postma et al.)
His4108Gln	Female	18	De novo	European	Exercise	Monomorphic premature ventricular beats	Unknown	(Postma et al.)
Met4109Arg	Female	31	Paternal	Jewish	Stress	Ventricular fibrillation	Unknown	(Nof et al., 2011)
Met4109Val	Unknown	Unknown	Unknown	Unknown	Unknown	Unknown	Unknown	(Landrum et al., 2016)
Leu4115Phe	Unknown	Unknown	Unknown	Unknown	Unknown	Unknown	Unknown	(Marjamaa et al., 2012)
Ser4122Arg	Male	Unknown	De novo	Unknown	Unknown	Unknown	Unknown	(Andrsova et al., 2012)
Ser4124Gly	Unknown	26	Maternal	Unknown	Unknown	Unknown	Unknown	(Watanabe et al., 2009)
Ser4124Thr	Female	14	Unknown	Unknown	Exertion	Non-sustained ventricular tachycardia	Unknown	(Tester et al., 2005b)
Ser4124Arg	Unknown	Unknown	Unknown	Unknown	Unknown	Unknown	Unknown	(Kawamura et al., 2013)
Ser4124Asn	Male	9	Maternal	Unknown	Unknown	Syncope	Unknown	(Ohno et al., 2015)
Met4139Val	Male	23	Unknown	Unknown	Excitement	Ventricular tachycardia, sudden death	Unknown	(Wang et al., 2014)
Glu4146Lys	Male	14	Unknown	Unknown	Sleeping	Sudden death	N/A	(Tester et al., 2012)
Tyr4149Cys	Unknown	Unknown	Unknown	Unknown	Unknown	Unknown	Unknown	(Jabbari et al., 2013)

Tyr4149Ser	Male	8	Mosaicism	Unknown	Unknown	Unknown	Unknown	(Lieve et al., 2019)
Ser4153Arg	Female	25	Unknown	Unknown	Emotion	Atrial fibrillation	metoprolol responsive	(Kazemian et al., 2011)
Ser4153Ile	Male	11	Unknown	Unknown	Unknown	Cardiac arrest	Unknown	(Ohno et al., 2015)
Ser4155Tyr	Female	14	De novo	Unknown	Exercise/stress	No	metoprolol - unresponsive, metoprolol and flecainide - responsive	(Mantziari et al., 2013)
Arg4157Gln	Unknown	Unknown	Unknown	Unknown	Unknown	Unknown	Unknown	(Medeiros-Domingo et al., 2009)
Arg4157His	Female	56	Unknown	Unknown	Exercise	No	Beta-blockers, verapamil, flecainide - unresponsive	(Sy et al., 2011)
Thr4158Pro	Female	2	Unknown	Unknown	Exertion	Sudden death	N/A	(Tester et al., 2012)
Gln4159Pro	Female	6	De novo	Unknown	Exercise and spontaneous	Monomorphic premature ventricular beats	propranolol and flecainide - responsive	(Di Pino et al., 2014)
Ser4168Thr	Male	18	Unknown	Unknown	Unknown	Syncope	Unknown	(Stattin et al., 2016)
Gln4171His	Male	7	Unknown	Unknown	Unknown	Progressive enlargement of lateral ventricles	Unknown	(Lieve et al., 2019)
Asn4178Ser	Male	11	De novo	Unknown	Unknown	Unknown	Unknown	(Ohno et al., 2015)
Asn4178Tyr	Unknown	Unknown	Unknown	Unknown	Unknown	Unknown	Unknown	(Hayashi et al., 2009)
Glu4182Ala	Unknown	Unknown	De novo	Unknown	Unknown	Unknown	Unknown	(Andrsova et al., 2012)

Glu4182Gln	Unknown	Unknown	Unknown	Unknown	Unknown	Unknown	Unknown	(Landrum et al., 2016)
Glu4187Gln	Unknown	16	Paternal	Unknown	Unknown	Sudden death	Unknown	(Tan Hanno et al., 2005)
Leu4188Pro	Female	15	De novo	Unknown	Anxiety	Monomorphic wide complex tachycardia, bidirectional ventricular tachycardia	Beta-blocker - responsive	(LaPage et al., 2012)
Phe4189Val	Unknown	Unknown	Unknown	Unknown	Unknown	Unknown	Unknown	Novel
Val4190Leu	Female	7	Unknown	Unknown	Unknown	Unknown	Unknown	(Lieve et al., 2019)
Cys4193Trp	Female	6	De novo	Unknown	Unknown	Cardiac arrest	Unknown	(Ohno et al., 2015)
Thr4196Ala	Male	Unknown	Unknown	Unknown	Unknown	Unknown	Unknown	(Tester et al., 2006)
Gln4201Arg	Unknown	Unknown	Unknown	Unknown	Unknown	Unknown	Unknown	(Laitinen Päivi et al., 2001)
Ala4204Val	Female	16	Unknown	Kazakhstan	Exercise	Cardiac arrest	Metoprolol - responsive	(Kron et al., 2015)
Glu4213Asp	Male	40	Unknown	Unknown	Unknown	Sudden death	Unknown	(Larsen et al., 2013)
Ala4247Val	Male	8	Unknown	Unknown	Unknown	Unknown	Unknown	(Takayama et al., 2017)
Met4256Thr	Female	39	Unknown	White British	Unknown	Palpitations, Prolonged QT	Unknown	MCGM
Leu4264Pro	Female	21	Unknown	White British	Unknown	Sudden death	Unknown	MCGM
Phe4306Ser	Unknown	Unknown	Unknown	Unknown	Unknown	Unknown	Unknown	(Landrum et al., 2016)
Arg4307Cys	Female	31	Unknown	White British	Unknown	Palpitations, prolonged QT	Unknown	MCGM

Gly4315Glu	Male	40	Unknown	Unknown	Sleep	Sudden death	Unknown	(Larsen et al., 2013)
Lys4392Arg	Female	30	Unknown	Unknown	Exercise/stress	Ventricular fibrillation. catecholamine stress test induced bidirectional premature ventricular contractions	propranolol - Unknown	(Aizawa et al., 2007)
Glu4417Gln	Female	15	Paternal	White British	Exercise	Sudden death	Unknown	MCGM
Glu4431Lys	Male	25	Unknown	Unknown	Unknown	Palpitations, sudden death	Unknown	(Wang et al., 2014)
Gly4471Arg	Female	6 weeks	Unknown	Unknown	Sleep	Sudden death	N/A	(Wang et al., 2014)
Gln4488Pro	Male	10	De novo	Unknown	Unknown	Unknown	Unknown	(Ohno et al., 2015)
Arg4497Cys	Female	30	Maternal	Unknown	Exercise/stress	Ventricular fibrillation, sudden death	Unknown	(Priori Silvia et al., 2001)
Phe4499Cys	Female	34	Unknown	Unknown	Anxiety	Cardiac arrest	Unknown	(Tester et al., 2005b)
Met4504Ile	Male	Unknown	Unknown	Unknown	Unknown	Unknown	Unknown	(Bagattin et al., 2004)
Ala4510Thr	Male	11	Unknown	Unknown	Exercise/stress	Premature ventricular contractions, ventricular bigeminy	Unknown	(Tester et al., 2005b)
Phe4511Leu	Male	8	De novo	Unknown	Unknown	Unknown	Unknown	(Takayama et al., 2017)
His4552Arg	Female	27	Unknown	Unknown	Sleeping	Died in sleep overdose	methadone	(Narula et al., 2015)

Ala4556Thr	Female	Unknown	Unknown	Unknown	Unknown	Unknown	Unknown	(Tester et al., 2005b)
His4558Tyr	Male	15	Unknown	Unknown	Drug administration	Wide complex slow ventricular tachycardia	MDMA and marijuana-negative	(Diffley et al., 2012)
Ser4565Arg	Female	4WEEKS	Unknown	European	Unknown	Sudden death	Unknown	(Tester et al., 2007)
His4579Tyr	Female	34	Unknown	Unknown	Sexual activity	Sudden death	N/A	(Larsen et al., 2013)
His4579Gln	Unknown	Unknown	Unknown	Unknown	Unknown	Unknown	Unknown	(Landrum et al., 2016)
Ile4587Leu	Unknown	Unknown	Unknown	Unknown	Unknown	Unknown	Unknown	(Landrum et al., 2016)
Ile4587Val	Unknown	Unknown	Unknown	Unknown	Unknown	Unknown	Unknown	(Kawamura et al., 2013)
Lys4594Arg	Female	12	Paternal	Unknown	Exercise	Ventricular fibrillation	Beta-blockers - responsive	(Paech et al., 2014)
Pro4596Ser	Unknown	Unknown	Unknown	Unknown	Unknown	Unknown	Unknown	Novel
Phe4600Leu	Female	33	De novo	Unknown	Unknown	Unknown	Unknown	(Ohno et al., 2015)
Ala4607Pro	Male	34	Unknown	Unknown	Unknown	Unknown	Beta-blockers - responsive	(Bagattin et al., 2004)
Arg4608Gln	Female	14	Unknown	Unknown	Sleeping	Died in sleep	Unknown	(Wong Leonie et al., 2014)
Arg4608Trp	Male	34	Unknown	Unknown	Unknown	Seizure and arrhythmias, sudden death	Unknown	(Wang et al., 2014)
Asp4631Val	Female	23	De novo	Unknown	Exercise	Palpitations, seizures	Beta-blockers unresponsive	(Kron et al., 2015)
Trp4645Arg	Female	5	Unknown	European	Exertion	Died following sustained ventricular tachycardia after	Unknown	(Tester et al., 2012)

						exertion, sudden death		
Lys4650Glu	Male	16	Unknown	Unknown	Stress	Aborted cardiac arrest	Unknown	(Hofman et al., 2007)
Val4653Phe	Unknown	Unknown	Unknown	Unknown	Unknown	Unknown	Unknown	(Laitinen Päivi et al., 2001)
Glu4662Ser	Female	13	Unknown	European	Exercise	Monomorphic bigeminy, polymorphic ventricular tachycardia	Unknown	(Postma et al.)
Leu4670His	Male	16	De novo	Asian	Physical exertion	Ventricular fibrillation, non-sustained polymorphic ventricular tachycardia	Atenolol - responsive	(Kim et al., 2012)
Gly4671Val	Unknown	Unknown	Unknown	Unknown	Unknown	Unknown	Unknown	(Haugaa et al., 2010)
Gly4671Arg	Male	10	Unknown	Unknown	Exercise/stress	Premature ventricular contractions, non-sustained ventricular tachycardia	Unknown	(Tester et al., 2005b)
Val4713Ile	Unknown	Unknown	Unknown	Unknown	Unknown	Unknown	Unknown	Novel
Asp4716Glu	Unknown	Unknown	Unknown	Unknown	Unknown	Unknown	Unknown	(Landrum et al., 2016)
Tyr4721His	Female	7	Unknown	Unknown	Unknown	Unknown	Unknown	(Lieve et al., 2019)
Tyr4725Cys	Male	28	De novo	Unknown	Unknown	Unknown	Unknown	(Ohno et al., 2015)

Ala4741Val	Male	12	Unknown	Unknown	Exercise	Syncope	Unknown	(Takayama et al., 2017)
His4742Tyr	Unknown	24	De novo	Unknown	Unknown	Sudden death	Unknown	(van der Werf et al., 2012)
Lys4750Gln	Unknown	Unknown	Unknown	Unknown	Unknown	Unknown	Unknown	(Kawamura et al., 2013)
Lys4751Gln	Female	13	De novo	Unknown	Unknown	Unknown	Unknown	(Lieve et al., 2019)
His4762Pro	Female	13	European	European	Exercise	Exercise induced monomorphic bigeminy, polymorphic ventricular tachycardia	Unknown	(Postma et al.)
Val4771Ile	Male	9	Unknown	Unknown	Exercise/stress	Sudden headaches before episodes	verapamil + flecainide - responsive	(Pott et al., 2011)
Gly4772Ser	Unknown	Unknown	Unknown	Unknown	Unknown	Unknown	Unknown	(Landrum et al., 2016)
Arg4790Gln	Unknown	Unknown	Unknown	Unknown	Unknown	Unknown	Unknown	(Medeiros-Domingo et al., 2009)
Lys4805Arg	Unknown	2	De novo	Unknown	Unknown	Unknown	Unknown	(Medeiros-Domingo et al., 2009)
Val4821Ile	Unknown	15	Unknown	Unknown	Unknown	Unknown	Unknown	(van der Werf et al., 2012)
Arg4822His	Unknown	Unknown	Unknown	Unknown	Unknown	Unknown	Unknown	(Medeiros-Domingo et al., 2009)
Ile4848Val	Female	35	Unknown	Unknown	Exercise	Aborted cardiac arrest	Unknown	(Tester et al., 2005b)

Phe4851Cys	Female	53	Unknown	Unknown	Exercise	premature ventricular contractions, polymorphic ventricular tachycardia	Unknown	(Aizawa et al., 2007)
Phe4851Leu	Female	13	Unknown	White British	Exercise	Ventricular bigeminy and polymorphic ventricular tachycardia	Unknown	MCGM
Ile4855Met	Female	10	Unknown	Unknown	Unknown	Sudden death	Unknown	(Roston et al., 2017)
Ala4860Gly	Female	7	Unknown	Unknown	Unknown	Ventricular fibrillation	Unknown	(Priori Silvia et al., 2002)
Leu4865Val	Unknown	Unknown	Unknown	Unknown	Unknown	Unknown	Unknown	(Kawamura et al., 2013)
Leu4865Ile	Male	6	Unknown	Unknown	Unknown	Unknown	Unknown	(Lieve et al., 2019)
Ile4867Val	Unknown	Unknown	Unknown	Unknown	Unknown	Unknown	Unknown	(Kumar et al., 2013)
Ile4867Met	Male	Unknown	Unknown	Unknown	Unknown	Unknown	Unknown	(Priori Silvia et al., 2002)
Gln4879Lys	Unknown	Unknown	Unknown	Unknown	Unknown	Unknown	Unknown	(Landrum et al., 2016)
Val4880Ala	Male	17	Unknown	Belgian	Unknown	Unknown	Unknown	(Bagattin et al., 2004)
Asn4895Asp	Male	Unknown	Unknown	Unknown	Unknown	Unknown	Unknown	(Priori Silvia et al., 2002)
Pro4902Leu	Female	56	Unknown	Unknown	Unknown	Unknown	Unknown	(Laitinen et al.)
Pro4902Ser	Female	13	Unknown	European	Exercise	Asymptomatic	Unknown	(Postma et al., 2005)

Gly4904Asp	Unknown	Unknown	Unknown	Unknown	Unknown	Unknown	Unknown	(Fokstuen et al., 2016)
Phe4905Leu	Male	18	Unknown	White British	Sleep	Sudden death	Unknown	MCGM
Thr4909Ile	Unknown	Unknown	Unknown	Unknown	Unknown	Unknown	Unknown	(Landrum et al., 2016)
His4913Asp	Female	62	Unknown	White British	Unknown	Cardiac Arrest	Unknown	MCGM
Leu4919Ser	Unknown	Unknown	Unknown	Unknown	Unknown	Unknown	Unknown	(Kawamura et al., 2013)
Ile4926Thr	Female	7	Unknown	Unknown	Unknown	Left ventricle mildly dilated	Unknown	(Lieve et al., 2019)
Ile4926Met	Male	5	Unknown	Unknown	Unknown	Unknown	Unknown	(Lieve et al., 2019)
Gly4936Arg	Female	8	Unknown	Unknown	Unknown	seizures, sudden death	Unknown	(Tester et al., 2012)
Gly4936Lys	Male	17	De novo	Unknown	Unknown	pulmonary cardiac arrest	Unknown	(Ohno et al., 2015)
Ser4938Phe	Male	13	Unknown	Unknown	Unknown	syncope, ventricular fibrillation	Unknown	(Fujii et al., 2017)
Trp4949Arg	Female	Unknown	De novo	Unknown	Unknown	Unknown	Unknown	
Glu4950Lys	Male	10	Unknown	Unknown	Unknown	No	Unknown	(Priori Silvia et al., 2002)
Arg4959Gln	Female	60	Unknown	Unknown	Unknown	Unknown	Unknown	(Laitinen et al.)
Tyr4962Cys	Unknown	Unknown	Familial	Unknown	Unknown	Unknown	Unknown	(van der Werf et al., 2012)

Supplementary Table 3.2. Removed ACMG-AMP rules. Adapted from Denham et al. (2019).

Rule	Reason for exclusion
PM3 - For recessive disorders, detected in trans with a pathogenic variant	This criterion applies primarily to conditions with recessive inheritance and has therefore been removed.
PM6 - Assumed de novo, but without confirmation of paternity and maternity	This criterion was excluded as segregation data was unavailable for a significant proportion of variants therefore it was felt unreliable to assume de novo status in the remaining variants.
PP2 - Missense variant in a gene that has a low rate of benign missense variation and in which missense variants are a common mechanism of disease.	The ACMG-AMP guidelines have included this as a criterion for genes with very little benign variation. While missense variants in RYR2 are well recognized as a cause of CPVT, the gene has a high background variation rate. Therefore, PP2 was not deemed applicable for analysis of pathogenicity.
PP4 - Patient's phenotype or family history is highly specific for a disease with a single genetic etiology	This criterion has been removed based on the high locus heterogeneity of CPVT.
PP5 - Reputable source recently reports variant as pathogenic, but the evidence is not available to the laboratory to perform an independent evaluation	This criterion was removed as no such reports exist at the time of the literature search
BS2 - Observed in a healthy adult individual for a recessive (homozygous), dominant (heterozygous), or X-linked (hemizygous) disorder, with full penetrance expected at an early age	This criterion has been removed based on the fact that CPVT is associated with incomplete penetrance and adult onset of disease
BP1 - Missense variant in a gene for which primarily truncating variants are known to cause disease	This criterion has been removed as missense variants are a recognized cause of RYR2
BP2 - Observed in trans with a pathogenic variant for a fully penetrant dominant gene/disorder or observed in cis with a pathogenic variant in any inheritance pattern	This criterion was removed as only RYR2 variants were the inclusion criteria for the systematic analysis.
BP3 - In-frame deletions/insertions in a repetitive region without a known function	This criterion does not apply as only missense variants were analysed.
BP4 - Variant found in a case with an alternative molecular basis for disease	This criterion did not apply as there is no alternative pathophysiological basis for CPVT with a stronger evidence base than RYR2.
BP6 - Reputable source recently reports variant as pathogenic/benign, but the evidence is not available to the laboratory to perform an independent evaluation	This criterion was not deemed relevant to this study
BP7 - A synonymous (silent) variant for which splicing prediction algorithms predict no impact to the splice consensus sequence nor the creation of a new splice site AND the nucleotide is not highly conserved.	This criterion was removed as non-coding RYR2 variants were excluded from the final analysis.

Supplementary Table 3.3. Criteria for classifying RYR2 variants according to modified ACMG guidelines (Denham et al., 2019)

Criteria for classifying pathogenic variants			
	Strength of evidence	Original ACMG classification	Modified criteria for scoring variant
[P1] Null variant	Strong	PS1	Same amino acid change as a previously established pathogenic variant (with different nucleotide change)
[P2] De novo variant	Strong	PS2	De novo variant (both maternity and paternity confirmed) in a patient with CPVT and no family history
[P3] Functional implications of variant	Strong	PS3	Animal, calcium imaging, cellular electrophysiology and single channel studies analysis showing either a significant reduction or gain of channel function
[P4] Frequently reported unique variant	Strong	PS4	"Ultra-rare" variant (absent in gnomAD) reported in >5 unrelated individuals with CPVT. "Rare" (allele count below 4 in gnomAD) reported in >10 unrelated individuals with CPVT. Prevalence of the variant in affected individuals is significantly increased compared with the prevalence in controls
[P5] Critical location of variant	Moderate	PM1	Located in a well-established functional domain (transmembrane or pore-forming domain) of the ion channel. Does not apply if meeting [P1] null variant
[P6] Unique variant	Moderate	PM2	"Ultra-rare" (absent in gnomAD)

	Moderate	PM3	For recessive disorders, detected in *trans* with a pathogenic variant
[P7] Location of variant associated with pathogenicity	Moderate	PM5	Novel missense change at an amino acid residue where a different missense change determined to be pathogenic has been seen before
	Moderate	PM6	Assumed de novo, but without confirmation of paternity and maternity
[P8] Segregation of CPVT and variant	Supporting	PP1	Co-segregation with CPVT and/or complex phenotypes in multiple affected family members
	Supporting	PP2	Missense variant in a gene that has a low rate of benign missense variation and in which missense variants are a common mechanism of disease
[P9] Predicted implications of variant	Supporting	PP3	Agreement between ≥6 bioinformatic prediction tools that the variant is pathogenic
	Supporting	PP4	Patient's phenotype or family history is highly specific for a disease with a single genetic etiology
	Supporting	PP5	Reputable source recently reports variant as pathogenic, but the evidence is not available to the laboratory to perform an independent evaluation
Criteria for classifying benign variants			

[B1] Very high frequency in control population	Stand alone	BA1	Variants occurring more frequently than the maximum tolerated allele count in gnomAD
[B2] Higher frequency in control population	Strong	BS1	"Common" (present in ≥5 individuals in global gnomAD cohort)
	Strong	BS2	Observed in a healthy adult individual for a recessive (homozygous), dominant (heterozygous), or X-linked (hemizygous) disorder, with full penetrance expected at an early age
[B3] No functional implication of variant	Strong	BS3	Well-established in vitro functional studies show no effect on RYR2 channel function
[B4] Absence of segregation	Strong	BS4	Absence of segregation of variant evidenced by presence of one or more family members who are genotype-negative phenotype-positive for CPVT
	Supporting	BP1	Missense variant in a gene for which primarily truncating variants are known to cause disease
	Supporting	BP2	Observed in *trans* with a pathogenic variant for a fully penetrant dominant gene/disorder or observed in *cis* with a pathogenic variant in any inheritance pattern
	Supporting	BP3	In-frame deletions/insertions in a

			repetitive region without a known function
[B5] Predicted implications of the variant	Supporting	BP4	Agreement between ≤2 bioinformatic prediction tools that the variant is pathogenic
	Supporting	BP5	Variant found in a case with an alternate molecular basis for disease
	Supporting	BP6	Reputable source recently reports variant as benign, but the evidence is not available to the laboratory to perform an independent evaluation
	Supporting	BP7	A synonymous (silent) variant for which splicing prediction algorithms predict no impact to the splice consensus sequence nor the creation of a new splice site AND the nucleotide is not highly conserved

Supplementary Table 3.4. ACMG guidelines for classifying DNA sequence variants

Variant classifications	Rules		
Pathogenic	1 very strong	and one of:	(a) ≥1 strong (b) ≥2 moderate (c) 1 moderate and 1 supporting (d) 2 supporting
	≥2 strong		
	1 strong	and one of:	(a) ≥3 moderate (b) 2 moderate and 2 supporting
Likely pathogenic	1 very strong	and	1 moderate
	1 strong	and	(a) 1-2 moderate (b) 2 supporting
	≥3 moderate		
	2 moderate	and	2 supporting
Likely Benign	1 strong	and	1 supporting
Benign	1 stand alone		
	≥2 strong		

Variant of unknown significance	(a) Any above criteria not met (b) contradictory combination of pathogenic and benign criteria

Supplementary Table 3.5. RYR2 variants associated with sudden death

c.DNA change	Amino acid change	Protein region	Other variants identified	Sex	Age at death (years)
Not reported	p.Leu73Val	N-terminal	No	Male	12
c.719A>G	p.His240Arg	N-terminal	p.Thr4158Pro-RYR2	Male	2
c.1240C>T	p.Arg414Cys	N-terminal	No	Female	16
c.1258C>T	p.Arg420Trp	N-terminal	No	Female	22
c.1258C>T	p.Arg420Trp	N-terminal	No	Male	17
c.1259G>A	p.Arg420Gln	N-terminal	No	Male	14
c.1458A>C	p.Gln486His	N-terminal	No	Male	17
c.2828T>C	p.Leu943Ser	N-terminal	No	Male	1
c.4465T>C	p.Cys1489Arg	N-terminal	No	Male	51
c.4692G>A	p.Met1564Ile	N-terminal	No	Female	21
c.4742A>C	p.Gln1581Pro	N-terminal	No	Male	26
c.5614G>A	p.Asp1872Asn	Central region	No	Female	< 1
c.649A>G	p.Gly1885Glu	Central region	No	Male	21
c.5762G>A	p.Arg1921Gln	Central region	No	Male	2
c.6224T>C	p.Ile2075Thr	Central region	Lys4594Arg - RYR2	Female	11
c.6272A>G	p.Gln2091Arg	Central region	No	Male	29
Not Reported	p.Gly2145Arg	Central region	No	Male	41
c.6503A>G	p.His2168Arg	Central region	No	Male	7
c.6532 G>A	p.Val2178Ile	Central region	No	Not reported	25
c.6647A>C	p.Asp2216Gly	Central region	No	Male	14
6680 G>T	p. Gly2227Val	Central region	No	Male	16
c.6737C>T	p.Ser2246Leu	Central region	No	Female	19

Not reported	p.Ala2252Val	Central region	No	Not reported	14
c.6817G>A	p.Gly2273Arg	Central region	No	Male	13
Not Reported	p.Val2321Ala	Central region	No	Male	14
c.6961G>A	p.Val2321Met	Central region	No	Female	22
c.6982C>T	p.Pro2328Ser	Central region	No	Not reported	48
c.6992T>C	p.Phe2331Ser	Central region	No	Male	8
c.7175A>G	p.Tyr2392Cys	Central region	Arg1047Leu-KCNH2	Female	25
c.7422G>C	p.Arg2474Ser	Central region	No	Male	7
c.8018C>T	p.Ala2673Val	Central region	No	Male	41
c.10708C>T	p.Arg3570Trp	Central region	No	Male	17
c.10742G>A	p.Arg3581Lys	C-terminal	No	Male	1
c.11636T>C	p.Leu3879Pro	C-terminal	No	Male	17
c.11773C>G	p.Gln3925Glu	C-terminal	No	Female	9
c.11837G>C	p.Gly3946Ala	C-terminal	No	Male	6
c.11876C>T	p.Ser3959Leu	C-terminal	No	Female	15
c.12013G>A	p.Glu4005Lys	C-terminal	No	Female	3
c.12058T>C	p.Phe4020Leu	C-terminal	No	Male	20
c.12226G>A	p.Glu4076Lys	C-terminal	No	Female	14
c.12290A>G	p.Asn4097Ser	C-terminal	No	Male	18
c.12415A>G	p.Met4139Val	C-terminal	No	Male	23
c.12438G>C	p.Glu4146Lys	C-terminal	No	Male	14
c.12472A>C	p.Thr4158Pro	C-terminal	p.His240Arg RYR2	Female	2
c.12559G>C	p.Glu4187Gln	C-terminal	No	Not reported	16
c.12639G>C	p.Glu4213Asp	C-terminal	No	Male	40
c.12791T>C	p.Leu4264Pro	C-terminal	No	Female	21

Supplementary Table 3.6. RYR2 variants associated with sleep and sudden death

c.DNA change	Amino acid change	Protein region	Gender	Age at death (years)	ICD implantation
c.2828T>C	p.Leu943Ser	N-terminal	Male	1	Not reported
c.4465T>C	p.Cys1489Arg	Central region	Male	51	Not reported
c.6817G>A	p.Gly2273Arg	Central region	Male	13	Not reported
c.12436G>A	p.Glu4146Lys	C-terminal	Male	14	No
c.12944G>A	p.Gly4315Glu	C-terminal	Male	40	Not reported
c.13411G>A	p.Gly4471Arg	C-terminal	Female	6 weeks	No
c.13655A>G	p.His4552Arg	C-terminal	Female	27	Not reported
c.13823G>A	p.Arg4608Gln	C-terminal	Female	14	Not reported
c.14713T>C	p.Phe4905Leu	C-terminal	Male	18	Not reported

Supplementary Table 3.7. ACMG classification of CPVT associated RYR2 variants

c.DNA change	Protein Change	Domain	ACMG Classification	gnomAD Allele count	ExAC Allele count	P1 (Same amino acid change as a pathogenic variant)	P2 (De novo)	P3 (Functional evidence)	P4 (Frequently reported unique variant)	P5 (in established functional domain)	P6 (Ultra-rare)	P7 (Located at same amino acid residue as pathogenic variant)	P8 (Segregat-ion of CPVT and variant)	P9 (Bioinformatic evidence)	B1 (Above frequency threshold for pathogen-icity in gnomAD)	B2 (Observed in a healthy individual)	B3 (Functi-onal studies show no effect)	B4 (Absence of segregation)	B5 (Predicted effect)
c.32T>G	Ile11Ser	No domain	Uncertain significance	Absent	Absent						1		1						
c.37T>C	Phe13Leu	No domain	Uncertain significance	Absent	Absent						1								
c.38T>G	Phe13Cys	No domain	Uncertain significance	Absent	Absent						1								
c.85C>G	His29Asp	No domain	Uncertain significance	Absent	Absent			1			1		1						
c.184C>T	Leu62Phe	No domain	Uncertain significance	1	Absent									1					
c.217C>G	Leu73Val	No domain	Uncertain significance	1	Absent														
c.230C>T	Ala77Val	Domain I	Uncertain significance	1	Absent								1	1					
c.241A>C	Met81Leu	Domain I	Uncertain significance	Absent	Absent						1								
c.490C>T	Pro164Ser	Domain I	Uncertain significance	Absent	Absent						1			1					
c.494C>A	Ala165Asp	Domain I	Uncertain significance	Absent	Absent						1			1					
c.506G>T	Arg169Leu	Domain I	Pathogenic	Absent	Absent		1				1	1		1					
c.506G>A	Arg169Gln	Domain I	Pathogenic	Absent	Absent		1		1		1	1		1					
c.527G>A	Arg176Gln	Domain I	Pathogenic	Absent	Absent			1	1		1			1					
c.533G>C	Gly178Ala	Domain I	Uncertain significance	Absent	Absent		1				1			1					
c.567A>T	Glu189Asp	Domain I	Uncertain significance	Absent	Absent						1								
c.649A>G	Ile217Val	Domain I	Benign	50	17										1				
c.688G>T	Gly230Cys	Domain I	Uncertain significance	Absent	Absent			1			1		1						
c.719A>G	His240Arg	Domain I	Uncertain significance	3	1														
c.725A>T	Asp242Val	Domain I	Uncertain significance	Absent	Absent						1			1					
c.727G>A	Glu243Lys	Domain I	Uncertain significance	Absent	Absent						1								
Not Reported	Ala271Val	Domain I	Uncertain significance	Absent	Absent		1				1								

c.985T>C	Phe329Leu	Domain I	Uncertain significance	Absent	Absent						1			1					
c.994C>T	Arg332Trp	Domain I	Uncertain significance	Absent	Absent						1			1					
c.1069G>A	Gly357Ser	Domain I	Uncertain significance	Absent	Absent						1			1					
c.1144G>A	Val382Met	Domain I	Benign	21	11										1				
c.1198G>C	Asp400His	Domain I	Uncertain significance	Absent	Absent						1			1					
c.1202A>G	Asp401Gly	Domain I	Uncertain significance	Absent	Absent		1				1			1					
c.1379T>C	Ile406Thr	Domain I	Uncertain significance	Absent	Absent						1								
c.1217C>T	Ser406Leu	Domain I	Benign	6	2			1							1				
c.1220G>T	Arg407Ile	Domain I	Uncertain significance	Absent	Absent						1			1					
c.1221A>T	Arg407Ser	Domain I	Uncertain significance	Absent	Absent		1				1								
c.1237T>A	Ser413Thr	Domain I	Uncertain significance	Absent	Absent						1								
c.1240C>T	Arg414Cys	Domain I	Uncertain significance	Absent	1						1								
c.1241G>T	Arg414Leu	Domain I	Uncertain significance	Absent	Absent						1								
c.1244C>T	Thr415Ile	Domain I	Uncertain significance	Absent	Absent						1								
c.1244C>G	Thr415Arg	Domain I	Uncertain significance	Absent	Absent						1			1					
c.1255A>T	Ile419Phe	Domain I	Uncertain significance	Absent	Absent						1		1	1					
c.1259G>A	Arg420Gln	Domain I	Pathogenic	Absent	Absent		1		1		1			1					
c.1258C>T	Arg420Trp	Domain I	Pathogenic	3	2			1	1			1	1	1					
c.1298T>C	Leu433Pro	Domain I	Uncertain significance	Absent	Absent			1			1		1						
c.1396C>G	Pro466Ala	Domain I	Benign	28	0									1	1				
Not Reported	Leu470Pro	No domain	Uncertain significance	Absent	Absent						1								
c.1458A>C	Gln486His	No domain	Uncertain significance	Absent	Absent						1								
c.1519G>A	Val507Ile	No domain	Benign	1347	505										1				
c.1640A>G	Asn547Ser	No domain	Uncertain significance	Absent	Absent						1								
c.1646C>T	Ala549Val	No domain	Uncertain significance	Absent	Absent						1								
c.1745G>T	Ser582Ile	No domain	Uncertain significance	Absent	Absent			1			1			1					
c.1847C>T	Ser616Leu	No domain	Uncertain significance	Absent	Absent		1				1								
c.1939C>T	Arg647Cys	No domain	Benign	41	19										1				
c.2216G>A	Arg739His	No domain	Uncertain significance	1	Absent														
c.2267G>A	Ser756Asn	No domain	Benign	56	24										1				
Not Reported	Ser767Cys	No domain	Uncertain significance	Absent	Absent						1								

c.2296A>G	Ile766Val	No domain	Uncertain significance	Absent	Absent						1								
c.2701G>A	Gly901Ser	No domain	Uncertain significance	Absent	Absent						1			1					
c.2828T>C	Leu943Ser	No domain	Benign	30	15										1				
c.3320C>T	Thr1107Met	No domain	Benign	121	11										1				
c.3407C>T	Ala1136Val	No domain	Benign	1970	853										1				
c.3481G>C	Val1161Leu	No domain	Benign	6	3										1				
c.3667A>G	Thr1223Ala	No domain	Uncertain significance	1	Absent														
c.3721G>A	Val1241Ile	No domain	Benign	45	30										1				
c.3766C>A	Pro1256Thr	No domain	Benign	5	Absent										1				
c.3803T>C	Ile1268Thr	No domain	Uncertain significance	Absent	Absent						1								
c.3827C>T	Thr1276Ile	No domain	Uncertain significance	3	2														
c.4040T>G	Met1347Arg	No domain	Uncertain significance	Absent	Absent						1								
c.4196C>A	Thr1399Leu	No domain	Uncertain significance	Absent	Absent						1								
c.4409G>C	Gly1470Ala	No domain	Uncertain significance	Absent	Absent						1			1					
c.4465T>C	Cys1489Arg	No domain	Benign	40	20										1				
c.4552C>T	Leu1518Phe	No domain	Uncertain significance	Absent	Absent						1								
c.4652A>G	Asn1551Ser	No domain	Benign	83	41										1				
c.4692G>A	Met1564Ile	No domain	Benign	21	5										1				
c.4742A>C	Gln1581Pro	No domain	Uncertain significance	Absent	Absent						1			1					
c.4991T>A	Val1664Lys	No domain	Uncertain significance	Absent	Absent						1								
c.5056C>T	Leu1686Phe	No domain	Benign	5	4										1				
c.5080A>C	Met1694Leu	No domain	Uncertain significance	Absent	Absent						1								
c.5170G>A	Glu1724Lys	No domain	Uncertain significance	Absent	Absent						1								
c.5294C>G	Ser1765Cys	No domain	Benign	47	20										1				
c.5374A>T	Ile1792Leu	No domain	Uncertain significance	Absent	Absent						1								
c.5420G>A	Arg1807Gln	No domain	Benign	5	3										1				
c.5428G>C	Val1810Leu	No domain	Benign	21	10		1								1				
c.5509G>A	Glu1837Lys	No domain	Benign	5	4										1				
c.5614G>A	Asp1872Asn	No domain	Benign	49	20										1				1
c.5654G>A	Gly1885Glu	No domain	Benign	4383	1794										1				1
c.5656G>A	Gly1886Ser	No domain	Benign	11831	5099										1				

Not Reported	Arg1919Gln	No domain	Benign	31	Absent										1				
c.5762G>A	Arg1921Gln	No domain	Benign	4	4										1				
c.6134A>G	Glu2045Gly	No domain	Uncertain significance	Absent	Absent						1								
c.6224T>C	Ile2075Thr	No domain	Uncertain significance	2	1									1					
c.6232C>T	Pro2078Ser	No domain	Benign	7	3										1				
c.6272A>G	Gln2091Arg	No domain	Uncertain significance	Absent	Absent						1			1					
c.6280G>A	Gly2094Ser	No domain	Benign	21	5										1				
Not Reported	Gly2145Arg	No domain	Benign	22	14			1					1		1				
c.6445A>G	Ile2149Val	No domain	Benign	7	2										1				
c.6457A>G	Lys2153Glu	No domain	Uncertain significance	Absent	Absent						1			1					
c.6497G>A	Gly2166Glu	No domain	Uncertain significance	Absent	Absent						1			1					
c.6503A>G	His2168Arg	No domain	Uncertain significance	Absent	Absent						1			1					
c.6504C>G	His2168Gln	No domain	Uncertain significance	Absent	Absent						1								
c.6532G>A	Val2178Ile	No domain	Uncertain significance	Absent	Absent						1			1					
c.6574A>T	Met2192Leu	No domain	Uncertain significance	Absent	Absent						1								
c.6574A>T	Lys2212Asn	No domain	Uncertain significance	Absent	Absent		1				1								
c.6636A>C	Asp2216Gly	No domain	Uncertain significance	Absent	Absent						1		1	1					
c.6647A>C	Asp2216Val	No domain	Uncertain significance	Absent	Absent						1			1					
c.6647A>T	His2217Tyr	No domain	Uncertain significance	Absent	Absent						1			1					
c.6649C>T	Gly2227Val	No domain	Uncertain significance	Absent	Absent						1								
6680G>T	Gly2228Val	No domain	Uncertain significance	Absent	Absent						1			1					
c.6683G>T	Ser2246Leu	Domain II	Pathogenic	Absent	Absent		1	1	1		1			1					
c.6737C>T	Ala2252Val	Domain II	Uncertain significance	Absent	Absent						1								
Not Reported	Ala2254Thr	Domain II	Uncertain significance	Absent	Absent						1			1					
6760G>A	Gly2273Arg	Domain II	Uncertain significance	Absent	Absent						1		1	1					
6817G>A	Arg2267His	Domain II	Benign	8	4			1							1				
c.6800G>A	Cys2277Arg	Domain II	Uncertain significance	Absent	Absent						1		1						
Not Reported	Tyr2285Asn	Domain II	Uncertain significance	Absent	Absent						1			1					
c.6853T>A	Glu2296Gln	Domain II	Uncertain significance	Absent	Absent						1			1					
c.6886G>C	Val2306Ile	Domain II	Uncertain significance	Absent	Absent		1				1			1					
c.6916G>A	Glu2311Asp	Domain II	Uncertain significance	Absent	Absent						1								
c.6933G>T																			

c.6950C>A	Ala2317Glu	Domain II	Uncertain significance	Absent	Absent		1				1			1					
Not Reported	Val2321Ala	Domain II	Uncertain significance	Absent	Absent						1								
c.6961G>A	Val2321Met	Domain II	Uncertain significance	Absent	Absent						1								
c.6982C>T	Pro2328Ser	Domain II	Likely pathogenic	Absent	Absent			1			1		1	1					
c.6992T>C	Phe2331Ser	Domain II	Uncertain significance	Absent	Absent						1			1					
Not Reported	Gly2337Val	Domain II	Uncertain significance	Absent	Absent						1		1						
c.7024G>A	Gly2342Arg	Domain II	Uncertain significance	Absent	Absent						1			1					
c.7076G>A	Arg2359Gln	Domain II	Benign	9	7										1				
c.7099G>A	Gly2367Arg	Domain II	Benign	39	20										1				
c.7157A>T	Asn2386Ile	Domain II	Uncertain significance	Absent	Absent			1			1								
c.7159G>A	Ala2387Thr	Domain II	Uncertain significance	Absent	Absent						1			1					
c.7159G>C	Ala2387Pro	Domain II	Uncertain significance	Absent	Absent						1		1	1					
c.7160C>T	Ala2387Val	Domain II	Uncertain significance	Absent	Absent						1			1					
c.7169C>T	Thr2390Ile	Domain II	Uncertain significance	Absent	Absent						1			1					
c.7175A>G	Tyr2392Cys	Domain II	Uncertain significance	1	1														
c.7181C>G	Ala2394Gly	Domain II	Uncertain significance	Absent	Absent						1		1	1					
Not Reported	Gly2400Thr	Domain II	Uncertain significance	Absent	Absent						1								
c.7199G>T	Gly2400Val	Domain II	Uncertain significance	Absent	Absent		1				1			1					
c.7202G>A	Arg2401His	Domain II	Uncertain significance	Absent	Absent				1		1			1					
c.7202G>T	Arg2401Leu	Domain II	Uncertain significance	Absent	Absent						1			1					
c.7205G>A	Cys2402Tyr	Domain II	Uncertain significance	Absent	Absent						1			1					
c.7207G>A	Ala2403Thr	Domain II	Uncertain significance	Absent	Absent						1		1	1					
c.7210C>A	Pro2404Thr	Domain II	Uncertain significance	Absent	Absent						1			1					
c.7258A>T	Arg2420Trp	Domain II	Uncertain significance	Absent	Absent						1								
c.7259G>C	Arg2420Thr	Domain II	Uncertain significance	Absent	Absent						1			1					
c.7260G>T	Arg2420Ser	Domain II	Uncertain significance	Absent	Absent						1								
c.7400C>T	Arg2467Val	Domain II	Uncertain significance	Absent	Absent						1			1					
c.7422G>C	Arg2474Ser	Domain II	Uncertain significance	Absent	Absent			1			1			1					
c.7420A>G	Arg2474Gly	Domain II	Uncertain significance	Absent	Absent						1								
c.7423G>T	Val2475Phe	Domain II	Pathogenic	Absent	Absent		1	1			1			1					
c.7447T>A	Phe2483Ile	Domain II	Uncertain significance	Absent	Absent			1			1			1					

c.7457A>C	His2486Pro	Domain II	Uncertain significance	Absent	Absent						1			1					
c.7469T>C	Val2490Ala	Domain II	Uncertain significance	Absent	Absent						1								
c.7493C>T	Ala2498Val	Domain II	Benign	12	1									1	1				
c.7511C>T	Thr2504Met	Domain II	Benign	13	7			1						1	1				
c.7528A>G	Thr2510Ala	Domain II	Uncertain significance	3	3									1					
c.7598C>T	Pro2533Leu	Domain II	Uncertain significance	Absent	Absent						1								
c.7600C>G	Leu2534Val	Domain II	Uncertain significance	Absent	Absent		1				1			1					
c.7708G>A	Glu2570Lys	No domain	Uncertain significance	3	3									1					
c.7813A>G	Met2605Val	No domain	Uncertain significance	Absent	Absent						1								
c.7883G>A	Gly2628Glu	No domain	Uncertain significance	Absent	Absent						1			1					
c.7925G>A	Arg2642Lys	No domain	Benign	31	10										1				
c.8018C>T	Ala2673Val	No domain	Uncertain significance	1	Absent			1						1					
c.8145G>T	Glu2715Asp	No domain	Benign	19	1										1				
c.8147A>T	Lys2716Ile	No domain	Benign	6	1										1				
c.8162T>C	Ile2721Thr	No domain	Benign	94	13										1				
Not Reported	Pro3087Arg	No domain	Uncertain significance	Absent	Absent						1								
c.9352G>A	Gly3118Arg	No domain	Uncertain significance	1	Absent														
c.9560A>G	Lys3187Arg	No domain	Benign	101	41										1				
c.9569G>A	Arg3190Gln	No domain	Benign	10	3										1				
c.9688C>A	Gln3230Lys	No domain	Uncertain significance	Absent	Absent						1								
c.9910C>G	Gln3304Glu	No domain	Uncertain significance	Absent	Absent						1								
c.9923A>G	Asn3308Ser	No domain	Benign	107	35										1				1
c.10708C>T	Arg3570Trp	No domain	Benign	6	3			1					1		1				1
c.10742G>A	Arg3581Lys	No domain	Uncertain significance	Absent	Absent						1	1							
c.10844G>A	Arg3615Gln	No domain	Uncertain significance	2	Absent									1					
c.10913A>C	Asp3638Ala	No domain	Uncertain significance	Absent	Absent						1			1					
c.11197G>A	Asp3733Asn	No domain	Uncertain significance	1	1														
c.11217G>T	Met3739Ile	No domain	Uncertain significance	Absent	Absent						1			1					
c.11332C>T	Leu3778Phe	Domain III	Uncertain significance	Absent	Absent						1								
c.11395T>C	Ser3799Pro	Domain III	Uncertain significance	Absent	Absent						1								
c.11399G>T	Cys3800Phe	Domain III	Uncertain significance	1	Absent									1					

c.11497G>A	Asp3833Asn	Domain III	Benign	9	1										1				
c.11515C>T	Leu3839Phe	Domain III	Uncertain significance	Absent	Absent						1								
c.11570A>G	Tyr3857Cys	Domain III	Uncertain significance	Absent	Absent						1								
c.11583G>C	Gln3861His	Domain III	Uncertain significance	Absent	Absent		1				1			1					
c.11628C>G	Asp3876Glu	Domain III	Uncertain significance	Absent	Absent						1								
c.11636T>C	Leu3879Pro	Domain III	Uncertain significance	Absent	Absent						1			1					
c.11773C>G	Gln3925Glu	Domain III	Uncertain significance	Absent	Absent			1			1			1					
c.11814C>A	Ser3938Arg	Domain III	Uncertain significance	Absent	Absent						1								
c.11837G>C	Gly3946Ala	Domain III	Likely pathogenic	Absent	Absent			1			1	1		1					
c.11837G>A	Gly3946Asp	Domain III	Uncertain significance	Absent	Absent						1	1		1					
c.11836G>A	Gly3946Ser	Domain III	Pathogenic	Absent	Absent		1	1			1			1					
c.11876C>T	Ser3959Leu	Domain III	Uncertain significance	Absent	Absent						1								
c.11916G>T	Met3972Ile	Domain III	Uncertain significance	Absent	Absent			1			1								
c.11917G>C	Asp3973His	Domain III	Uncertain significance	Absent	Absent			1			1			1					
c.11917G>A	Asp3973Asn	Domain III	Uncertain significance	Absent	Absent						1								
c.11921T>A	Leu3974Gln	Domain III	Uncertain significance	Absent	Absent			1			1			1					
c.11929G>T	Asp3977Tyr	Domain III	Uncertain significance	Absent	Absent						1			1					
c.11934G>A	Met3978Ile	Domain III	Uncertain significance	Absent	Absent			1			1			1					
c.11969T>A	Val3990Asp	Domain III	Uncertain significance	Absent	Absent						1			1					
c.11989A>G	Lys3997Glu	Domain III	Uncertain significance	Absent	Absent						1			1					
Not Reported	Met3999Ile	Domain III	Uncertain significance	Absent	Absent						1								
c.12006G>A	Met4002Ile	Domain III	Uncertain significance	Absent	Absent		1				1								
c.12013G>A	Glu4005Lys	Domain III	Uncertain significance	Absent	Absent						1			1					
c.12058T>C	Phe4020Leu	Domain III	Uncertain significance	Absent	Absent						1								
c.12121G>A	Gly4041Arg	Domain III	Uncertain significance	Absent	Absent						1			1					
c.12226G>A	Glu4076Lys	Domain III	Uncertain significance	Absent	Absent						1		1						
c.12271G>A	Ala4091Thr	Domain III	Uncertain significance	Absent	Absent						1								
c.12272C>T	Ala4091Val	Domain III	Uncertain significance	Absent	Absent						1								
c.12290A>G	Asn4097Ser	Domain III	Uncertain significance	Absent	Absent						1								
c.12312C>G	Asn4104Lys	Domain III	Uncertain significance	Absent	Absent			1			1								
c.12311A>T	Asn4104Ile	Domain III	Uncertain significance	Absent	Absent						1		1	1					

c.12313C>T	Leu4105Phe	Domain III	Uncertain significance	Absent	Absent		1				1			1					
c.12643A>G	Met4107Val	Domain III	Uncertain significance	Absent	Absent						1								
c.12322C>A	His4108Asn	Domain III	Pathogenic	Absent	Absent		1	1			1	1		1					
c.12324C>A	His4108Gln	Domain III	Pathogenic	Absent	Absent		1	1			1	1		1					
c.12326T>G	Met4109Arg	Domain III	Uncertain significance	Absent	Absent						1		1	1					
c.12325A>G	Met4109Val	Domain III	Uncertain significance	Absent	Absent						1								
c.12343C>T	Leu4115Phe	Domain III	Uncertain significance	Absent	Absent			1			1								
c.12364A>C	Ser4122Arg	Domain III	Uncertain significance	Absent	Absent		1				1								
c.12370A>G	Ser4124Gly	Domain III	Uncertain significance	Absent	Absent						1								
c.12371G>C	Ser4124Thr	Domain III	Uncertain significance	Absent	Absent			1			1								
c.12372C>A	Ser4124Arg	Domain III	Uncertain significance	Absent	Absent						1								
c.12371G>A	Ser4124Asn	Domain III	Uncertain significance	Absent	Absent						1			1					
c.12415A>G	Met4139Val	Domain III	Uncertain significance	Absent	Absent						1								
c.12436G>A	Glu4146Lys	Domain III	Uncertain significance	Absent	Absent						1			1					
c.12446A>G	Tyr4149Cys	Domain III	Uncertain significance	Absent	Absent						1			1					
Not Reported	Tyr4149Ser	Domain III	Uncertain significance	Absent	Absent			1			1								
c.12457A>C	Ser4153Arg	Domain III	Uncertain significance	Absent	Absent			1			1								
c.12458G>T	Ser4153Ile	Domain III	Uncertain significance	Absent	Absent						1			1					
c.12464C>A	Ser4155Tyr	Domain III	Uncertain significance	Absent	Absent		1				1								
c.12470G>A	Arg4157Gln	Domain III	Uncertain significance	Absent	Absent						1								
Not Reported	Arg4157His	Domain III	Uncertain significance	Absent	Absent						1								
c.12472A>C	Thr4158Pro	Domain III	Uncertain significance	Absent	Absent			1			1								
c.12476A>C	Gln4159Pro	Domain III	Pathogenic	Absent	Absent		1	1			1			1					
c.12502T>A	Ser4168Thr	Domain III	Uncertain significance	Absent	Absent						1		1	1					
c.12513G>T	Gln4171His	Domain III	Uncertain significance	Absent	Absent			1			1								
c.12533A>G	Asn4178Ser	Domain III	Uncertain significance	Absent	Absent		1				1								
c.12532A>T	Asn4178Tyr	Domain III	Uncertain significance	Absent	Absent						1		1	1					
c.12545A>C	Glu4182Ala	Domain III	Uncertain significance	Absent	Absent		1				1			1					
c.12544G>C	Glu4182Gln	Domain III	Uncertain significance	Absent	Absent						1			1					
c.12559G>C	Glu4187Gln	Domain III	Uncertain significance	Absent	Absent						1			1					
c.12563T>C	Leu4188Pro	Domain III	Uncertain significance	Absent	Absent		1				1	1							

c.12565T>G	Phe4189Val	Domain III	Uncertain significance	Absent	Absent						1			1					
c.12568G>C	Val4190Leu	Domain III	Uncertain significance	Absent	Absent						1		1	1					
c.12579C>G	Cys4193Trp	Domain III	Uncertain significance	Absent	Absent		1				1								
c.12586A>G	Thr4196Ala	Domain III	Uncertain significance	Absent	Absent						1								
c.12602A>G	Gln4201Arg	Domain III	Likely pathogenic	Absent	Absent			1			1		1	1					
c.12611C>T	Ala4204Val	No domain	Uncertain significance	Absent	Absent						1			1					
c.12639G>C	Glu4213Asp	No domain	Uncertain significance	Absent	Absent						1								
Not Reported	Ala4247Val	No domain	Uncertain significance	Absent	Absent						1								
c.12767T>C	Met4256Thr	No domain	Benign	11	6										1				
c.12791T>C	Leu4264Pro	No domain	Uncertain significance	Absent	Absent						1			1					
c.12917T>C	Phe4306Ser	No domain	Benign	10	3										1				1
c.12919C>T	Arg4307Cys	No domain	Benign	90	27										1				
c.12944G>A	Gly4315Glu	No domain	Benign	11	3										1				
c.13175A>G	Lys4392Arg	No domain	Benign	4	1					1					1				
c.13249G>C	Glu4417Gln	No domain	Benign	4	Absent					1					1				
c.13291G>A	Glu4431Lys	No domain	Benign	54	19					1					1				
c.13411G>A	Gly4471Arg	No domain	Uncertain significance	2	Absent					1									
c.13463A>C	Gln4488Pro	No domain	Likely pathogenic	Absent	Absent		1			1	1			1					
c.13489C>T	Arg4497Cys	Domain IV	Pathogenic	Absent	Absent			1		1	1		1	1					
c.13496T>G	Phe4499Cys	Domain IV	Uncertain significance	Absent	Absent					1	1			1					
c.13512G>A	Met4504Ile	Domain IV	Uncertain significance	Absent	Absent					1	1								
c.13528G>A	Ala4510Thr	Domain IV	Uncertain significance	Absent	2					1	1								
Not Reported	Phe4511Leu	Domain IV	Uncertain significance	Absent	Absent		1			1	1								
c.13655A>G	His4552Arg	Domain IV	Benign	4	1					1					1				1
c.13666G>A	Ala4556Thr	Domain IV	Benign	10	3					1					1				1
c.13672C>T	His4558Tyr	Domain IV	Benign	61	24					1					1				
c.13695C>A	Ser4565Arg	Domain IV	Likely pathogenic	Absent	Absent			1		1	1								
c.13735C>T	His4579Tyr	Domain IV	Uncertain significance	Absent	Absent					1	1			1					
c.13737C>A	His4579Gln	Domain IV	Uncertain significance	Absent	Absent					1	1								
c.13759A>C	Ile4587Leu	Domain IV	Uncertain significance	Absent	Absent					1	1								
c.13759A>G	Ile4587Val	Domain IV	Uncertain significance	Absent	Absent					1	1								

c.13781A>G	Lys4594Arg	Domain IV	Uncertain significance	Absent	Absent					1	1			1					
c.13786C>T	Pro4596Ser	Domain IV	Uncertain significance	Absent	Absent					1	1			1					
c.13798T>C	Phe4600Leu	Domain IV	Uncertain significance	Absent	Absent		1				1								
c.13819G>C	Ala4607Pro	Domain IV	Uncertain significance	Absent	Absent						1			1					
c.13823G>A	Arg4608Gln	Domain IV	Uncertain significance	Absent	Absent						1			1					
c.13822C>T	Arg4608Trp	Domain IV	Uncertain significance	Absent	Absent						1								
c.13892A>T	Asp4631Val	Domain IV	Uncertain significance	Absent	Absent		1				1			1					
c.13933T>A	Trp4645Arg	Domain IV	Uncertain significance	Absent	Absent						1			1					
c.13948A>G	Lys4650Glu	Domain IV	Uncertain significance	Absent	Absent						1			1					
c.13957G>T	Val4653Phe	Domain IV	Likely pathogenic	Absent	Absent			1			1		1	1					
c.13984G>A	Glu4662Ser	Domain IV	Benign	4	Absent										1				
c.14009T>A	Leu4670His	Domain IV	Uncertain significance	Absent	Absent		1				1			1					
Not Reported	Gly4671Val	Domain IV	Uncertain significance	Absent	Absent						1								
c.14011G>C	Gly4671Arg	Domain IV	Uncertain significance	Absent	Absent						1			1					
c.14137G>A	Val4713Ile	Domain IV	Uncertain significance	Absent	Absent						1								
c.14148C>A	Asp4716Glu	Domain IV	Uncertain significance	Absent	Absent						1								
c.14161T>C	Tyr4721His	Domain IV	Uncertain significance	Absent	Absent						1			1					
c.14174A>G	Tyr4725Cys	Domain IV	Uncertain significance	Absent	Absent		1				1			1					
c.14222C>T	Ala4741Val	Domain IV	Uncertain significance	Absent	Absent					1	1								
c.14224C>T	His4742Tyr	Domain IV	Likely pathogenic	Absent	Absent		1			1	1			1					
Not Reported	Lys4750Gln	Domain IV	Uncertain significance	Absent	Absent						1								
c.14251A>C	Lys4751Gln	Domain IV	Pathogenic	Absent	Absent		1	1		1	1			1					
c.14285A>C	His4762Pro	Domain IV	Uncertain significance	Absent	Absent					1	1			1					
c.14311G>A	Val4771Ile	Domain IV	Likely pathogenic	Absent	Absent				1	1	1		1						
c.14314G>A	Gly4772Ser	Domain IV	Uncertain significance	Absent	Absent					1	1								
c.14369G>A	Arg4790Gln	Domain IV	Uncertain significance	1	1					1									
c.14414A>G	Lys4805Arg	Domain IV	Pathogenic	Absent	Absent		1	1		1	1			1					
c.14461G>A	Val4821Ile	Domain IV	Uncertain significance	Absent	Absent					1	1			1					
c.14465G>A	Arg4822His	Domain IV	Uncertain significance	Absent	Absent					1	1			1					
c.14542A>G	Ile4848Val	Domain IV	Likely pathogenic	Absent	Absent					1	1		1	1					
c.14552T>G	Phe4851Cys	Domain IV	Uncertain significance	Absent	Absent					1	1			1					

c.14553C>A	Phe4851Leu	Domain IV	Uncertain significance	Absent	Absent					1	1			1					
Not Reported	Ile4855Met	Domain IV	Likely pathogenic	Absent	Absent			1		1	1		1						
c.14579C>G	Ala4860Gly	Domain IV	Likely pathogenic	Absent	Absent			1		1	1			1					
c.14593C>G	Leu4865Val	Domain IV	Uncertain significance	Absent	Absent					1	1								
c.14593C>A	Leu4865Ile	Domain IV	Uncertain significance	Absent	Absent			1		1	1								
c.14599A>G	Ile4867Val	Domain IV	Uncertain significance	Absent	Absent						1								
c.14601T>G	Ile4867Met	Domain IV	Uncertain significance	Absent	Absent			1			1								
c.14635C>A	Gln4879Lys	Domain IV	Uncertain significance	Absent	Absent						1								
c.14639T>C	Val4880Ala	Domain IV	Uncertain significance	Absent	Absent			1			1								
c.14683A>G	Asn4895Asp	Domain IV	Uncertain significance	Absent	Absent			1			1								
c.14705C>T	Pro4902Leu	Domain IV	Uncertain significance	Absent	Absent						1			1					
c.14704C>T	Pro4902Ser	Domain IV	Uncertain significance	Absent	Absent						1		1						
c.14711G>A	Gly4904Asp	Domain IV	Uncertain significance	Absent	Absent						1			1					
c.14713T>C	Phe4905Leu	Domain IV	Likely pathogenic	Absent	Absent			1			1		1	1					
c.14726C>T	Thr4909Ile	Domain IV	Uncertain significance	Absent	Absent						1								
c.14726C>T	Thr4909Ile	Domain IV	Uncertain significance	Absent	Absent						1								
c.14737C>G	His4913Asp	Domain IV	Uncertain significance	Absent	Absent						1			1					
c.14756T>C	Leu4919Ser	Domain IV	Uncertain significance	Absent	Absent						1			1					
c.14777T>C	Ile4926Thr	Domain IV	Uncertain significance	Absent	Absent			1			1			1					
c.14778A>G	Ile4926Met	Domain IV	Uncertain significance	Absent	Absent						1								
14803G>A	Gly4935Arg	Domain IV	Uncertain significance	Absent	Absent						1			1					
c.14806C>A	Gln4936Lys	Domain IV	Uncertain significance	Absent	Absent		1				1			1					
c.14813C>T	Ser4938Phe	Domain IV	Uncertain significance	Absent	Absent			1			1								
c.15162T>C	Trp4949Arg	Domain IV	Uncertain significance	Absent	Absent		1				1								
c.14848G>A	Glu4950Lys	Domain IV	Uncertain significance	Absent	Absent						1								
c.14876G>A	Arg4959Gln	Domain IV	Uncertain significance	Absent	Absent						1								
c.14885A>G	Tyr4962Cys	No domain	Uncertain significance	Absent	Absent						1			1					
				Over frequency threshold for pathogenicity in ExAC															
				Over frequency threshold for pathogenicity in gnomAD															

Supplementary Table 3.8. Calculation of the maximum tolerated allele count for a CPVT *RYR2* variant using gnomAD.

number of cases with Arg420Trp mutation/ total number of CPVT cases with *RYR2* mutations	10/440	
binomial confidence interval	0.023 (0.012 - 0.041)	
upper bound of the maximum allelic contribution	0.041	
prevalence per individual	0.0001	
number of chromosomes	2	
allelic prevalence	0.00005	prevalence/chromosomes
penetrance (Napolitano et al., 2013)	0.6	
Number of samples in population database (gnomAD)	282912	
Maximum Credible population allele frequency	3.12×10^{-6}	allelic prevalence*max allele contribution/penetrance
mean expected events in population database	0.882	no of samples*max credible allele frequency
Max tolerated allele count	3	upper 95% CI of expected events

Supplementary Table 3.8. Outline of the statistical framework used to identify variants that occur too frequently in the gnomAD database to be pathogenic [3]. The maximum credible population allele frequency for a missense variant in *RYR2* that causes CPVT was calculated based on CPVT being a dominant condition with a penetrance of approximately 60% [2]. A binomial distribution of the maximum credible allele frequency was generated for our sample of CPVT cases (observed allele number) and the upper bound of the 95% confidence interval (the maximum tolerated allele count) was used as the cut off frequency. Variants that occurred more frequently than the maximum tolerated allele count in gnomAD were considered common and this was strong evidence for a benign classification (BS1).

Supplementary Table 3.9. Calculation of the maximum tolerated allele count for a CPVT *RYR2* variant using ExAC.

number of cases with Arg420Trp mutation/ total number of CPVT cases with *RYR2* mutations	10/440	
binomial confidence interval	0.023 (0.012 - 0.041)	
upper bound of the maximum allelic contribution	0.041	
prevalence per individual	0.0001	
number of chromosomes	2	
allelic prevalence	0.00005	prevalence/chromosomes
penetrance (Napolitano et al., 2013)	0.6	
Number of samples in population database (gnomAD)	121412	
Maximum Credible population allele frequency	$3.44x10^{-6}$	allelic prevalence*max allele contribution/penetrance
mean expected events in population database	0.418	no of samples*max credible allele frequency
Max tolerated allele count	2	upper 95% CI of expected events

Supplementary Table 3.9. Outline of the statistical framework used to identify variants that occur too frequently in the ExAC database to be pathogenic [3]. The maximum credible population allele frequency for a missense variant in *RYR2* that causes CPVT was calculated based on CPVT being a dominant condition with a penetrance of approximately 60% [2]. A binomial distribution of the maximum credible allele frequency was generated for our sample of CPVT cases (observed allele number) and the upper bound of the 95% confidence interval (the maximum tolerated allele count) was used as the cut off frequency. Variants that occurred more frequently than the maximum tolerated allele count in ExAC were considered common and this was strong evidence for a benign classification (BS1).

Supplementary Table 3.10. Functional evidence for CPVT associated *RYR2* variants

c.DNA change	Protein Change	P3 (Functional evidence)	B3 (negative functional evidence)	Type of functional evidence	Effect on channel function	Reference
c.85C>G	His29Asp		1	Single channel recording	Not significant	(Xiao et al., 2015)
c.527G>A	Arg176Gln	1		mouse	Gain of function	(Kannankeril et al., 2006)
c.688G>T	Gly230Cys	1		HEK293 cell Ca2+ imaging	Gain of function	(Liu et al., 2013)
c.1217C>T	Ser406Leu	1		iPSC derived myocyte Ca2+ imaging	Gain of function	(Jung et al., 2012)
c.1258C>T	Arg420Trp	1		mouse	Gain of function	(Okudaira et al., 2014)
c.1298T>C	Leu433Pro	1		HEK293 cell Ca2+ imaging	Gain of function	(Jiang et al., 2005)
c.1745G>T	Ser582Ile	1		HEK293 cell Ca2+ imaging	Gain of function	(Lieve et al., 2019)
Not Reported	Gly2145Arg	1		single-channel recordings	Gain of function	(Marjamaa et al., 2011)
c.6737C>T	Ser2246Leu	1		HL-1 cardiomyocytes Ca2+ imaging	Gain of function	(George Christopher et al., 2003)
c.6800G>A	Arg2267His	1		single-channel recordings	Gain of function	(Tester et al., 2007)
c.6982C>T	Pro2328Ser	1		mouse	Gain of function	(Salvage et al., 2019)
c.7157A>T	Asn2386Ile	1		mouse	Gain of function	(Shan et al., 2012)
c.7422G>C	Arg2474Ser	1		mouse	Gain of function	(Shan et al., 2012)
c.7423G>T	Val2475Phe	1		single-channel recordings	Gain of function	(Loaiza et al., 2013)
c.7447T>A	Phe2483Ile	1		iPSC derived myocyte Ca2+ imaging	Gain of function	(Fatima et al., 2011)
c.7511C>T	Thr2504Met	1		HEK293 cell Ca2+ imaging	Gain of function	(Tang et al., 2012)
c.8018C>T	Ala2673Val	1		HEK293 cell Ca2+ imaging	Gain of function	(Fujii et al., 2017)
c.10708C>T	Arg3570Trp	1		single-channel recordings	Gain of function	(Marjamaa et al., 2011)
c.11773C>G	Gln3925Glu	1		iPSC derived myocyte Ca2+ imaging	Gain of function	(Zhang et al., 2019)

c.11837G>C	Gly3946Ala	1		HEK293 cell Ca2+ imaging	Gain of function	(Xiao et al., 2016)
c.11836G>A	Gly3946Ser	1		HEK293 cell Ca2+ imaging	Gain of function	(Xiao et al., 2016)
c.11916G>T	Met3972Ile	1		HEK293 cell Ca2+ imaging	Gain of function	(Lieve et al., 2019)
c.11917G>C	Asp3973His	1		HEK293 cell Ca2+ imaging	Gain of function	(Lieve et al., 2019)
c.11921T>A	Leu3974Gln	1		HEK293 cell Ca2+ imaging	Gain of function	(Lieve et al., 2019)
c.11934G>A	Met3978Ile	1		HEK293 cell Ca2+ imaging	Gain of function	(Xiao et al., 2016)
c.12312C>G	Asn4104Lys	1		HL-1 cardiomyocytes Ca2+ imaging	Gain of function	(George Christopher et al., 2003)
c.12322C>A	His4108Asn	1		HEK293 cell Ca2+ imaging	Gain of function	(Xiao et al., 2016)
c.12324C>A	His4108Gln	1		HEK293 cell Ca2+ imaging	Gain of function	(Xiao et al., 2016)
c.12343C>T	Leu4115Phe	1		iPSC derived myocyte Ca2+ imaging	Gain of function	(Pölönen et al., 2018)
c.12371G>C	Ser4124Thr	1		HEK293 cell Ca2+ imaging	Gain of function	(Xiao et al., 2016)
Not Reported	Tyr4149Ser	1		HEK293 cell Ca2+ imaging	Gain of function	(Lieve et al., 2019)
c.12457A>C	Ser4153Arg	1		HEK293 cell Ca2+ imaging	Gain of function	(Zhabyeyev et al., 2013)
c.12472A>C	Thr4158Pro	1		HEK293 cell Ca2+ imaging	Gain of function	(Xiao et al., 2016)
c.12476A>C	Gln4159Pro	1		HEK293 cell Ca2+ imaging	Gain of function	(Xiao et al., 2016)
c.12513G>T	Gln4171His	1		HEK293 cell Ca2+ imaging	Gain of function	(Lieve et al., 2019)
c.12602A>G	Gln4201Arg	1		single-channel recordings	Gain of function	(Lehnart Stephan et al., 2004)
c.13489C>T	Arg4497Cys	1		HL-1 cardiomyocytes Ca2+ imaging	Gain of function	(George Christopher et al., 2003)
c.13695C>A	Ser4565Arg	1		single-channel recordings	Gain of function	(Tester et al., 2007)
c.13957G>T	Val4653Phe	1		iPSC derived myocyte Ca2+ imaging	Gain of function	(Pölönen et al., 2018)
c.14251A>C	Lys4750Gln	1		HEK293 cell Ca2+ imaging	Gain of function	(Uehara et al., 2017)

c.14414A>G	Lys4805Arg	1		HEK293 cell Ca2+ imaging	Gain of function	(Lieve et al., 2019)
Not Reported	Ile4855Met	1		HEK293 cell Ca2+ imaging	Gain of function	(Roston et al., 2017)
c.14579C>G	Ala4860Gly	1		mouse model	Gain of function	(Zhao et al., 2015)
c.14593C>A	Leu4865Ile	1		HEK293 cell Ca2+ imaging	Gain of function	(Lieve et al., 2019)
c.14601T>G	Ile4867Met	1		HEK293 cell Ca2+ imaging	Gain of function	(Jiang et al., 2005)
c.14639T>C	Val4880Ala	1		single-channel recordings	Gain of function	(Sun et al., 2016)
c.14683A>G	Asn4895Asp	1		HEK293 cell Ca2+ imaging	Gain of function	(Jiang et al., 2004)
c.14713T>C	Phe4905Leu	1		HEK293 cell Ca2+ imaging	Dual effects	Unpublished data
c.14777T>C	Ile4926Thr	1		HEK293 cell Ca2+ imaging	Gain of function	(Lieve et al., 2019)
c.14813C>T	Ser4938Phe	1		HEK293 cell Ca2+ imaging	Suppression of function	(Fujii et al., 2017)

Appendix I. References

Aizawa, Y. et al. 2007. Human cardiac ryanodine receptor mutations in ion channel disorders in Japan. *International Journal of Cardiology* 116**,** pp.263-265.

Akilzhanova, A. et al. 2014. RYR2 sequencing reveals novel missense mutations in a Kazakh idiopathic ventricular tachycardia study cohort. *PloS one* 9**,** pp.e101059-e101059.

Allegue, C. et al. 2015. Genetic Analysis of Arrhythmogenic Diseases in the Era of NGS: The Complexity of Clinical Decision-Making in Brugada Syndrome. *PloS one* 10**,** pp.e0133037-e0133037.

Andrsova, I. et al. 2012. Clinical Characteristics and Mutational Analysis of the RyR2 Gene in Seven Czech Families with Catecholaminergic Polymorphic Ventricular Tachycardia. *Pacing and Clinical Electrophysiology* 35**,** pp.798-803.

Bagattin, A.et al. 2004. Denaturing HPLC-Based Approach for Detecting RYR2 Mutations Involved in Malignant Arrhythmias. *Clinical Chemistry* 50**,** pp.1148.

Bauce, B. et al. 2002a. Screening for ryanodine receptor type 2 mutations in families with effort-induced polymorphic ventricular arrhythmias and sudden death. *Journal of the American College of Cardiology* 40**,** pp.341.

Bauce, B. et al. 2002b. Screening for ryanodine receptor type 2 mutations in families with effort-induced polymorphic ventricular arrhythmias and sudden death: Early diagnosis of asymptomatic carriers. *Journal of the American College of Cardiology* 40**,** pp.341-349.

Beckmann, B. M., Wilde, A. A. M. and KÄÄB, S. 2008. Dual Inheritance of Sudden Death from Cardiovascular Causes. *New England Journal of Medicine* 358**,** pp.2077-2078.

Bosch, C. et al. 2017. A novel variant in RyR2 causes familiar catecholaminergic polymorphic ventricular tachycardia. *Forensic Science International* 270**,** pp.173-177.

Brion, M. et al. 2014. Next generation sequencing challenges in the analysis of cardiac sudden death due to arrhythmogenic disorders. *Electrophoresis* 35**,** pp.3111-3116.

Campuzano, O. et al. 2014. Post-mortem genetic analysis in juvenile cases of sudden cardiac death. *Forensic Science International* 245**,** pp.30-37.

Cheung, J. W. et al. 2015. Short-coupled polymorphic ventricular tachycardia at rest linked to a novel ryanodine receptor (RyR2) mutation: leaky RyR2 channels under non-stress conditions. *International journal of cardiology* 180**,** pp.228-236.

Choi, G. et al. 2004. Spectrum and Frequency of Cardiac Channel Defects in Swimming-Triggered Arrhythmia Syndromes. *Circulation* 110**,** pp.2119-2124.

Creighton, W., Virmani, R., Kutys, R. and Burke, A. 2006. Identification of novel missense mutations of cardiac ryanodine receptor gene in exercise-induced sudden death at autopsy. *The Journal of molecular diagnostics : JMD* 8**,** pp.62-67.

D'amati, G. et al. 2005. Juvenile sudden death in a family with polymorphic ventricular arrhythmias caused by a novel RyR2 gene mutation: evidence of specific morphological substrates. *Human Pathology* 36**,** pp.761-767.

Denham, N.C., et al. 2019. Systematic re-evaluation of SCN5A variants associated with Brugada syndrome. *Journal of Cardiovascular Electrophysiology* 30**,** pp.118-127.

Di pino, A., Caruso, E., Costanzo, L. and Guccione, P. 2014. A novel RyR2 mutation in a 2-year-old baby presenting with atrial fibrillation, atrial flutter, and atrial ectopic tachycardia. *Heart Rhythm* 11**,** pp.1480-1483.

Diffley, M., Armenian, P., Gerona, R., Reinhartz, O. and Avasarala, K. 2012. Catecholaminergic polymorphic ventricular tachycardia found in an adolescent after a methylenedioxymethamphetamine and marijuana-induced cardiac arrest. *Critical Care Medicine* 40**,** pp.2223-2226.

Domingo, D. et al. 2015a. A New Mutation in the Ryanodine Receptor 2 Gene as a Cause Catecholaminergic Polymorphic Ventricular Tachycardia. *Revista Española de Cardiología (English Edition)* 68**,** pp.71-73.

Domingo, D. et al. 2015b. Non-ventricular, Clinical, and Functional Features of the RyR2 Mutation Causing Catecholaminergic Polymorphic Ventricular Tachycardia. *Revista Española de Cardiología (English Edition)* 68**,** pp.398-407.

Farrugia, A., Keyser, C., Hollard, C., Raul, J. S., MulleR, J. and Ludes, B. 2015. Targeted next generation sequencing application in cardiac channelopathies: Analysis of a cohort of autopsy-negative sudden unexplained deaths. *Forensic Science International* 254**,** pp.5-11.

Fatima, A. et al. 2011. In vitro modeling of ryanodine receptor 2 dysfunction using human induced pluripotent stem cells. *Cellular physiology and biochemistry : international journal of experimental cellular physiology, biochemistry, and pharmacology* 28**,** pp.579-592.

Fokstuen, S. et al. 2016. Experience of a multidisciplinary task force with exome sequencing for Mendelian disorders. *Human genomics* 10**,** pp.24-24.

Friday, K. P., Moak, J. P., Fries, M. H. and Iqbal, S. N. 2015. Catecholaminergic Ventricular Tachycardia, Pregnancy and Teenager: Are They Compatible? *Pediatric Cardiology* 36**,** pp.1542-1547.

Fujii, Y. et al. 2017. A type 2 ryanodine receptor variant associated with reduced Ca2+ release and short-coupled torsades de pointes ventricular arrhythmia. *Heart Rhythm* 14**,** pp.98-107.

Hasdemir, C., Aydýn, H. H., Þahin, S. and Wollnik, B. 2008. Catecholaminergic polymorphic ventricular tachycardia caused by a novel mutation in the cardiac ryanodine receptor. *The Anatolian Journal of Cardiology* 8**,** pp.5035-5036.

Hasdemir, C. A. N., Priori, S. G., Overholt, E. and Lazzara, R. 2004. Catecholaminergic Polymorphic Ventricular Tachycardia, Recurrent Syncope, and Implantable Loop Recorder. *Journal of Cardiovascular Electrophysiology* 15**,** pp.729-729.

Haugaa, K. H. et al. 2010. High prevalence of exercise-induced arrhythmias in catecholaminergic polymorphic ventricular tachycardia mutation-positive family members diagnosed by cascade genetic screening. *EP Europace* 12**,** pp.417-423.

Hayashi, M. et al. 2009. Incidence and Risk Factors of Arrhythmic Events in Catecholaminergic Polymorphic Ventricular Tachycardia. *Circulation* 119**,** pp.2426-2434.

Hayashi, M. et al. 2012. The role of stress test for predicting genetic mutations and future cardiac events in asymptomatic relatives of catecholaminergic polymorphic ventricular tachycardia probands. *EP Europace* 14**,** pp.1344-1351.

Hertz, C. L. et al. 2015. Next-generation sequencing of 34 genes in sudden unexplained death victims in forensics and in patients with channelopathic cardiac diseases. *International Journal of Legal Medicine* 129**,** pp.793-800.

Hertz, C. L. et al. 2016. Genetic investigations of sudden unexpected deaths in infancy using next-generation sequencing of 100 genes associated with cardiac diseases. *European journal of human genetics : EJHG,* 24**,** pp.817-822.

Hofman, N., Tan, H. L., Clur, S.-A., alders, M., Van Langen, I. M. & Wilde, A. A. M. 2007. Contribution of Inherited Heart Disease to Sudden Cardiac Death in Childhood. *Pediatrics* 120**,** pp.e967.

Jabbari, J. et al. 2013. New Exome Data Question the Pathogenicity of Genetic Variants Previously Associated With Catecholaminergic Polymorphic Ventricular Tachycardia. *Circulation: Cardiovascular Genetics* 6**,** pp.481-489.

Janson, C. M., Ceresnak, S. R., Chung, W. K. and Pass, R. H. 2014. Catecholaminergic polymorphic ventricular tachycardia in a child with Brugada pattern on ECG: One patient with two diseases? *Heart Rhythm* 11**,** pp.2101-2104.

Jung, C. B. et al. 2012. Dantrolene rescues arrhythmogenic RYR2 defect in a patient-specific stem cell model of catecholaminergic polymorphic ventricular tachycardia. *EMBO molecular medicine* 4**,** pp.180-191.

Kawamura. 2013. - Genetic background of catecholaminergic polymorphic ventricular tachycardia in Japan. - *Circulation Journal* 77(7): pp.1705-1713.

Kazemian, P., Gollob, M. H., Pantano, A. and Oudit, G. Y. 2011. A Novel Mutation in the RYR2 Gene Leading to Catecholaminergic Polymorphic Ventricular Tachycardia and Paroxysmal Atrial Fibrillation: Dose-Dependent Arrhythmia-Event Suppression by β-Blocker Therapy. *Canadian Journal of Cardiology* 27**,** pp.870.e7-870.e10.

Kim, N. Y. et al. 2012. Catecholaminergic polymorphic ventricular tachycardia in a patient with recurrent exertional syncope. *Korean circulation journal* 42**,** pp.129-132.

Kron, J., Ellenbogen, K. and Abbate, A. 2015. Recurrent ventricular fibrillation in a young female carrying a previously unidentified RyR2 gene mutation. *International Journal of Cardiology* 201**,** pp.222-224.
Kumar, S. et al. 2013. Familial cardiological and targeted genetic evaluation: Low yield in sudden unexplained death and high yield in unexplained cardiac arrest syndromes. *Heart Rhythm* 10**,** pp.1653-1660.
Laitinen, P.J. et al. 2001. Mutations of the Cardiac Ryanodine Receptor (RyR2) Gene in Familial Polymorphic Ventricular Tachycardia. *Circulation* 103**,** pp.485-490.
Laitinen, P. J., Swan, H., Kontula, K. and Kontula, K. 2003. Molecular genetics of exercise-induced polymorphic ventricular tachycardia: identification of three novel cardiac ryanodine receptor mutations and two common calsequestrin 2 amino-acid polymorphisms. *European Journal of Human Genetics* 11(11): pp.888-891.
Laksman, Z., Dulay, D., Gollob, M. H., Skanes, A. C. and Krahn, A. D. 2014. Evolution of a genetic diagnosis. *Clinical Genetics* 86**,** pp.580-584.
Landrum, M. J. et al. 2016. ClinVar: public archive of interpretations of clinically relevant variants. *Nucleic acids research* 44**,** pp.D862-D868.
Lapage, M. J., Russell, M. W., Bradley, D. J. and Dick, M. 2012. Novel Ryanodine Receptor 2 Mutation Associated with a Severe Phenotype of Catecholaminergic Polymorphic Ventricular Tachycardia. *The Journal of Pediatrics* 161**,** pp.362-364.
Larsen, M. K. et al. 2013. Postmortem genetic testing of the ryanodine receptor 2 (RYR2) gene in a cohort of sudden unexplained death cases. *International Journal of Legal Medicine* 127**,** pp.139-144.
Lawrenz, W., Krogmann, O. N. and Wieczorek, M. 2014. Complex atrial arrhythmias as first manifestation of catecholaminergic polymorphic ventricular tachycardia: an unusual course in a patient with a new mutation in ryanodine receptor type 2 gene. *Cardiology in the Young* 24**,** pp.741-744.
Lieve, K. V. V. et al. 2019. Linking the heart and the brain: Neurodevelopmental disorders in patients with catecholaminergic polymorphic ventricular tachycardia. *Heart Rhythm* 16**,** pp.220-228.
Mantziari, L. et al. 2013. A De Novo Novel Cardiac Ryanodine Mutation (Ser4155Tyr) Associated with Catecholaminergic Polymorphic Ventricular Tachycardia. *Annals of Noninvasive Electrocardiology* 18**,** pp.571-576.
Marjamaa, A. et al. 2012. Intravenous Epinephrine Infusion Test in Diagnosis of Catecholaminergic Polymorphic Ventricular Tachycardia. *Journal of Cardiovascular Electrophysiology* 23**,** pp.194-199.
Marjamaa, A. et al. 2009. Search for cardiac calcium cycling gene mutations in familial ventricular arrhythmias resembling catecholaminergic polymorphic ventricular tachycardia. *BMC medical genetics* 10**,** pp.12-12.
Marjamaa, A., Laitinen-Forsblom, P., Wronska, A., Toivonen, L., Kontula, K. and Swan, H. 2011. Ryanodine receptor mutations in sudden cardiac death: Studies in extended pedigrees and phenotypic characterization. *International Journal of Cardiology* 147**,** pp.246-252.
Medeiros-Domingo, A. et al. 2009. The RYR2-encoded ryanodine receptor/calcium release channel in patients diagnosed previously with either catecholaminergic polymorphic ventricular tachycardia or genotype negative, exercise-induced long QT syndrome: a comprehensive open reading frame mutational analysis. *Journal of the American College of Cardiology* 54**,** pp.2065-2074.
Meli, A. C. et al. 2011. A novel ryanodine receptor mutation linked to sudden death increases sensitivity to cytosolic calcium. *Circulation research* 109**,** pp.281-290.
Napolitano, C., et al. 2013. Clinical utility gene card for: Catecholaminergic polymorphic ventricular tachycardia (CPVT). *European Journal Of Human Genetics* 22, pp.152.
Narula, N., Tester, D. J., Paulmichl, A., Maleszewski, J. J. and Ackerman, M. J. 2015. Post-mortem Whole exome sequencing with gene-specific analysis for autopsy-negative sudden unexplained death in the young: a case series. *Pediatric cardiology* 36**,** pp.768-778.
Nishio, H., Iwata, M., Tamura, A., Miyazaki, T., Tsuboi, K. and Suzuki, K. 2008. Identification of a novel mutation V2321M of the cardiac ryanodine receptor gene of sudden unexplained death and a phenotypic study of the gene mutations. *Legal Medicine* 10**,** pp.196-200.

Nof, E. et al. 2011. Postpacing abnormal repolarization in catecholaminergic polymorphic ventricular tachycardia associated with a mutation in the cardiac ryanodine receptor gene. *Heart Rhythm* 8**,** pp.1546-1552.

Ohno, S., Hasegawa, K. and Horie, M. 2015. Gender Differences in the Inheritance Mode of RYR2 Mutations in Catecholaminergic Polymorphic Ventricular Tachycardia Patients. *PloS one* 10**,** e0131517-e0131517.

Paech, C., Gebauer, R. A., Karstedt, J., Marschall, C., Bollmann, A. and Husser, D. 2014. Ryanodine Receptor Mutations Presenting as Idiopathic Ventricular Fibrillation: A Report on Two Novel Familial Compound Mutations, c.6224T>C and c.13781A>G, With the Clinical Presentation of Idiopathic Ventricular Fibrillation. *Pediatric Cardiology* 35**,** pp.1437-1441.

Postma, A. V. et al. 2005. Catecholaminergic polymorphic ventricular tachycardia: RYR2 mutations, bradycardia, and follow up of the patients. *Journal of medical genetics* 42**,** pp.863-870.

Pott, C. et al. 2011. Successful treatment of catecholaminergic polymorphic ventricular tachycardia with flecainide: a case report and review of the current literature. *EP Europace* 13**,** pp.897-901.

Priori, S. et al. 2002. Clinical and Molecular Characterization of Patients With Catecholaminergic Polymorphic Ventricular Tachycardia. *Circulation* 106**,** pp.69-74.

Priori, S, G. et al. 2001. Mutations in the Cardiac Ryanodine Receptor Gene (hRyR2) Underlie Catecholaminergic Polymorphic Ventricular Tachycardia. *Circulation* 103**,** pp.196-200.

Roston, T. M. et al. 2017. A novel RYR2 loss-of-function mutation (I4855M) is associated with left ventricular non-compaction and atypical catecholaminergic polymorphic ventricular tachycardia. *Journal of Electrocardiology* 50**,** pp.227-233.

Roston, T. M. et al. 2018. Catecholaminergic polymorphic ventricular tachycardia patients with multiple genetic variants in the PACES CPVT Registry. *PloS one* 13**,** e0205925-e0205925.

Roux-Buisson, N. et al. 2014. Prevalence and significance of rare RYR2 variants in arrhythmogenic right ventricular cardiomyopathy/dysplasia: Results of a systematic screening. *Heart Rhythm* 11**,** pp.1999-2009.

Shigemizu, D. et al. 2015. Exome Analyses of Long QT Syndrome Reveal Candidate Pathogenic Mutations in Calmodulin-Interacting Genes. *PloS one* 10**,** e0130329-e0130329.

Stattin, E.-L. et al. 2016. Genetic screening in sudden cardiac death in the young can save future lives. *International journal of legal medicine* 130**,** pp.59-66.

Steinfurt, J. et al. 2014. High-dose flecainide with low-dose β-blocker therapy in catecholaminergic polymorphic ventricular tachycardia: A case report and review of the literature. *Journal of cardiology cases* 11**,** pp.10-13.

Steriotis, A. K. et al. 2012. Follow-up with exercise test of effort-induced ventricular arrhythmias linked to ryanodine receptor type 2 gene mutations. *The American journal of cardiology* 109**,** pp.1015-1019.

Sy, R. W. et al. 2011. Arrhythmia characterization and long-term outcomes in catecholaminergic polymorphic ventricular tachycardia. *Heart Rhythm* 8**,** pp.864-871.

Takayama, K. et al. 2017. 1218Double mutations in RYR2 cause severe phenotype of catecholaminergic polymorphic ventricular tachycardia. *European Heart Journal,* 38.

Tan et al. 2005. Sudden Unexplained Death. *Circulation* 112**,** pp.207-213.

Tester, D. J. et al. 2006. Genotypic heterogeneity and phenotypic mimicry among unrelated patients referred for catecholaminergic polymorphic ventricular tachycardia genetic testing. *Heart Rhythm* 3**,** pp.800-805.

Tester, D. J. et al. 2007. A mechanism for sudden infant death syndrome (SIDS): stress-induced leak via ryanodine receptors. *Heart rhythm* 4**,** pp.733-739.

Tester, D. J., Kopplin, L. J., Creighton, W., Burke, A. P. and Ackerman, M. J. 2005a. Pathogenesis of Unexplained Drowning: New Insights From a Molecular Autopsy. *Mayo Clinic Proceedings* 80**,** pp.596-600.

Tester, D. J., Kopplin, L. J., Will, M. L. and Ackerman, M. J. 2005b. Spectrum and prevalence of cardiac ryanodine receptor (RyR2) mutations in a cohort of unrelated patients referred explicitly for long QT syndrome genetic testing. *Heart Rhythm* 2**,** pp.1099-1105.

Tester, D. J., Medeiros-Domingo, A., Will, M. L. and Ackerman, M. J. 2011. Unexplained drownings and the cardiac channelopathies: a molecular autopsy series. *Mayo Clinic proceedings* 86**,** pp.941-947.

Tester, D. J., Medeiros-Domingo, A., Will, M. L., Haglund, C. M. and Ackerman, M. J. 2012. Cardiac channel molecular autopsy: insights from 173 consecutive cases of autopsy-negative sudden unexplained death referred for postmortem genetic testing. *Mayo Clinic proceedings* 87**,** pp.524-539.

Van Der Werf, C. et al. 2012. Familial Evaluation in Catecholaminergic Polymorphic Ventricular Tachycardia. *Circulation: Arrhythmia and Electrophysiology* 5**,** pp.748-756.

Wang, D. et al. 2014. Cardiac channelopathy testing in 274 ethnically diverse sudden unexplained deaths. *Forensic Science International* 237**,** pp.90-99.

Ware, J. S. et al. 2013. Next generation diagnostics in inherited arrhythmia syndromes : a comparison of two approaches. *Journal of cardiovascular translational research* 6**,** pp.94-103.

Watanabe, H. et al. 2009. Flecainide prevents catecholaminergic polymorphic ventricular tachycardia in mice and humans. *Nature medicine* 15**,** pp.380-383.

Whiffin N. et al. 2017. Using high-resolution variant frequencies to empower clinical genome interpretation. *Genetics In Medicine* 19(10): pp.1151-1158.

Wong, L.C. H., Roses-Noguer, F., Till, J.A. and Behr E.R. 2014. Cardiac Evaluation of Pediatric Relatives in Sudden Arrhythmic Death Syndrome. *Circulation: Arrhythmia and Electrophysiology* 7**,** pp.800-806.

Zhang, J.-X. et al. 2015. Candidate colorectal cancer predisposing gene variants in Chinese early-onset and familial cases. *World journal of gastroenterology* 21**,** pp.4136-4149.

Appendix II. Supplemental material for chapter 4, Assessment of disease-associated missense variants in RYR2 on transcript splicing.

Supplementary Table 4.1. Predicted splicing effects of *RYR2* missense variants

c.DNA change	Protein change	Effect on splicing	Number of tools in agreement
c.37T>C	Pro13Leu	No	
c.38T>G	Pro13Cys	No	
c.85C>G	His29Asp	No	
c.184C>T	Leu62Pro	No	
c.217C>G	Leu73Val	Introduce 5' Splice Site	1
c.230C>T	Ala77Val	Introduce 5' Splice Site	2
c.241A>C	Met81Leu	No	
c.344A>G	Tyr115Cys	No	
c.365G>A	Arg122His	No	1
c.490C>T	Pro164Ser	Deletion 5' Splice Site	1
c.494C>A	Ala165Asp	Deletion 5' Splice Site	1
c.497C>G	Ser166Cys	Introduce 5' Splice Site	4
c.506G>A	Arg169Gln	Deletion 5' Splice Site	1
c.506G>T	Arg169Leu	Introduce 3' Splice Site	1
c.527G>A	Arg176Gln	Deletion 5' Splice Site	4
c.533G>C	Gly178Ala	Deletion 5' Splice Site	1
c.556G>A	Val186Met	No	
c.567A>T	Glu189Asp	No	
c.649A>G	Ile217Val	Introduce 5' Splice Site	1
c.688G>T	Gly230Cys	Deletion 5' Splice Site	1
c.719A>G	His240Arg	No	
c.725A>T	Asp242Val	Introduce 5' Splice Site	1
c.727G>A	Glu243Lys	Introduce 5' Splice Site	1
c.985T>C	Pro329Leu	No	
c.994C>T	Arg332Trp	No	
c.1069G>A	Gly357Ser	Introduce 3' Splice Site	2
c.1144G>A	Val382Met	Deletion 5' Splice Site	2
c.1198G>C	Asp400His	No	
c.1202A>G	Asp401Gly	Introduce 5' Splice Site	1
c.1217C>T	Ser406Leu	No	
c.1220G>T	Arg407Ile	No	

c.1221A>T	Arg407Ser	No	
c.1237T>A	Ser413Thr	No	
c.1240C>T	Arg414Cys	No	
c.1241G>T	Arg414Leu	No	
c.1244C>G	Thr415Arg	No	
c.1244C>T	Thr415Ile	No	
c.1255A>T	Ile419Pro	Deletion 5' Splice Site	1
c.1259G>A	Arg420Gln	Introduce 3' Splice Site	1
c.1258C>T	Arg420Trp	No	
c.1298T>C	Leu433Pro	No	
c.1318G>A	Ala440Thr	Deletion 3' Splice Site	1
c.1396C>G	Pro466Ala	No	
c.1454G>A	Arg485Gln	Introduce 3' Splice Site	1
c.1458A>C	Gln486His	No	
c.1519G>A	Val507Ile	No	
c.1604A>G	Glu535Gly	Deletion 3' Splice Site	1
c.1640A>G	Asn547Ser	No	
c.1646C>T	Ala549Val	No	
c.1663C>G	Leu555Val	No	
c.1847C>T	Ser616Leu	No	
c.1871C>T	Ala624Val	No	
c.1903A>C	Asn635His	No	
c.1918A>G	Arg640Gly	No	
c.1939C>T	Arg647Cys	No	
c.2216G>A	Arg739His	No	
c.2267G>A	Ser756Asn	Deletion 3' Splice Site	2
c.2306G>T	Arg769Leu	No	
c.2320C>A	Pro774Thr	No	
c.2389G>A	Gly797Arg	Deletion 3' Splice Site	4
c.2423A>G	His808Arg	No	
c.2701G>A	Gly901Ser	Introduce 3' Splice Site	1
c.2786G>A	Arg929His	Deletion 5' Splice Site	1
c.2828T>C	Leu943Ser	No	
c.3038G>A	Arg1013Gln	Deletion 3' Splice Site	1
c.3070G>A	Val1024Ile	Deletion 5' Splice Site	1
c.3152G>C	Arg1051Pro	No	
c.3230T>C	Val1077Ala	Deletion 5' Splice Site	2
c.3265C>T	Arg1089Cys	Deletion 5' Splice Site	1
c.3271G>A	Glu1091Leu	Deletion 5' Splice Site	1
c.3320C>T	Thr1107Met	Deletion 3' Splice Site	1
c.3380A>G	Glu1127Gly	Introduce 3' Splice Site	1
c.3407C>T	Ala1136Val	No	

c.3667A>G	Thr1223Ala	No	
c.3766C>A	Pro1256Thr	No	
c.3803T>C	Ile1268Thr	No	
c.3827C>T	Thr1276Ile	No	
c.4040T>G	Met1347Arg	Deletion 3' Splice Site	1
c.4196C>A	Thr1399Leu	No	
c.4465T>C	Cys1489Arg	No	
c.4552C>T	Leu1518Pro	No	
c.4652A>G	Asn1551Ser	Introduce 3' Splice Site	1
c.4692G>A	Met1564Ile	No	
c.4693C>G	Pro1565Ala	No	
c.4742A>C	Gln1581Pro	No	
c.4747C>T	Pro1583Ser	No	
c.4991T>A	Val1664Lys	Deletion 5' Splice Site	1
c.5056C>T	Leu1686Pro	No	
c.5080A>C	Met1694Leu	No	
c.5170G>A	Glu1724Lys	Introduce 5' Splice Site	3
c.5278C>T	Arg1760Trp	No	
c.5374A>T	Ile1792Leu	No	
c.5420G>A	Arg1807Gln	Introduce 3' Splice Site	3
c.5428G>C	Val1810Leu	Deletion 3' Splice Site	2
c.5509G>A	Glu1837Lys	No	
c.5614G>A	Asp1872Asn	No	
c.5654G>A	Gly1885Glu	Introduce 3' Splice Site	1
c.5656G>A	Gly1886Ser	Deletion 5' Splice Site	1
c.5762G>A	Arg1921Gln	Introduce 3' Splice Site	1
c.6134A>G	Glu2045Gly	No	
c.6224T>C	Ile2075Thr	No	
c.6232C>T	Pro2078Ser	No	
c.6272A>G	Gln2091Arg	Introduce 3' Splice Site	4
c.6337G>A	Val2113Met	Deletion 5' Splice Site	1
c.6380G>T	Arg2127Leu	No	
c.6412G>A	Glu2138Lys	Introduce 3' Splice Site	1
c.6445A>G	Ile2149Val	Introduce 5' Splice Site	1
c.6457A>G	Lys2153Glu	No	
c.6504C>G	His2168Gln	Introduce 3' Splice Site	2
c.6503A>G	His2168Arg	No	
c.6532G>A	Val2178Ile	No	

c.6574A>T	Met2192Leu	Introduce 5' Splice Site	2
c.6636A>C	Lys2212Asn	Introduce 5' Splice Site	1
c.6637G>T	Ala2213Ser	No	
c.6647A>T	Asp2216Val	No	
c.6649C>T	His2217Tyr	No	
6680 G>T	Gly2227Val	No	
c.6683G>T	Gly2228Val	Deletion 5' Splice Site	1
c.6737C>T	Ser2246Leu	No	
c.6800G>A	Arg2267His	Deletion 5' Splice Site	1
c.6886G>C	Glu2296Gln	Deletion 3' Splice Site	1
c.6916G>A	Val2306Ile	No	
c.6919T>C	Pro2307Leu	No	
c.6933G>T	Glu2311Asp	Deletion 3' Splice Site	1
c.6950C>A	Ala2317Glu	Deletion 5' Splice Site	1
c.6961G>A	Val2321Met	Deletion 5' Splice Site	4
c.6982C>T	Pro2328Ser	Introduce 5' Splice Site	3
c.6992T>C	Pro2331Ser	No	
c.7024G>A	Gly2342Arg	Deletion 3' Splice Site	2
c.7076G>A	Arg2359Gln	No	
c.7099G>A	Gly2367Arg	Introduce 3' Splice Site	2
c.7157A>T	Asn2386Ile	No	
c.7159G>A	Ala2387Thr	Deletion 3' Splice Site	1
c.7159G>C	Ala2387Pro	Deletion 3' Splice Site	1
c.7160C>T	Ala2387Val	Introduce 5' Splice Site	1
c.7169C>T	Thr2390Ile	Introduce 5' Splice Site	5
c.7175A>G	Tyr2392Cys	No	
c.7181C>G	Ala2394Gly	Introduce 5' Splice Site	4
c.7199G>T	Gly2400Val	No	
c.7202G>T	Arg2401Leu	No	1
c.7202G>A	Arg2401His	No	
c.7205G>A	Cys2402Tyr	No	
c.7207G>A	Ala2403Thr	No	
c.7210C>A	Pro2404Thr	No	
c.7258A>T	Arg2420Trp	Deletion 3' Splice Site	1
c.7259G>C	Arg2420Thr	Deletion 3' Splice Site	1
c.7260G>T	Arg2420Ser	Deletion 5' Splice Site	1
c.7400C>T	Ala2467Val	No	
c.7422G>C	Arg2474Ser	Deletion 5' Splice Site	1
c.7420A>G	Arg2474Gly	Deletion 3' Splice Site	5
c.7423G>T	Val2475Pro	No	

c.7447T>A	Pro2483Ile	No	
c.7469T>C	Val2490Ala	Deletion 5' Splice Site	3
c.7493C>T	Ala2498Val	Introduce 5' Splice Site	1
c.7511C>T	Thr2504Met	No	
c.7528A>G	Thr2510Ala	No	
c.7598C>T	Pro2533Leu	No	
c.7600C>G	Leu2534Val	No	
c.7813A>G	Met2605Val	Introduce 5' Splice Site	4
c.7820T>C	Leu2607Pro	No	
c.7883G>A	Gly2628Glu	No	
c.7925G>A	Arg2642Lys	No	
c.8018C>T	Ala2673Val	Introduce 5' Splice Site	1
c.8145G>T	Glu2715Asp	Deletion 3' Splice Site	1
c.8147A>T	Lys2716Ile	No	
c.8162T>C	Ile2721Thr	No	
c.8470C>T	Arg2824Trp	No	
c.8794T>C	Tyr2932His	No	
c.8873A>G	Gln2958Arg (homozygous)	No	
c.9352G>A	Gly3118Arg	Deletion 3' Splice Site	1
c.9560A>G	Lys3187Arg	Introduce 5' Splice Site	2
c.9569G>A	Arg3190Gln	No	
c.9655G>A	Val3219Met	No	
c.9688C>A	Gln3230Lys	No	
c.9910C>G	Gln3304Glu	No	
c.10708C>T	Arg3570Trp	No	
c.10742G>A	Arg3581Lys	No	
c.10844G>A	Arg3615Gln	Introduce 5' Splice Site	1
c.10913A>C	Asp3638Ala	No	
c.11017C>T	Arg3673Trp	No	
c.11197G>A	Asp3733Asn	Introduce 5' Splice Site	1
c.11332C>T	Leu3778Pro	Deletion 5' Splice Site	1
c.11395T>C	Ser3799Pro	No	
c.11399G>T	Cys3800Pro	Deletion 5' Splice Site	5
c.11426A>G	Glu3809Gly	Deletion 3' Splice Site	1
c.11515C>T	Leu3839Pro	No	
c.11570A>G	Tyr3857Cys	No	
c.11583G>C	Gln3861His	Deletion 3' Splice Site	1
c.11628C>G	Asp3876Glu	Introduce 5' Splice Site	1
c.11636T>C	Leu3879Pro	No	
c.11773C>G	Gln3925Glu	No	

c.11814C>A	Ser3938Arg	No	
c.11827G>A	Ala3943Thr	No	
c.11836G>A	Gly3946Ser	Introduce 3' Splice Site	2
c.11837G>C	Gly3946Ala	No	
c.11837G>A	Gly3946Asp	No	
c.11876C>T	Ser3959Leu	No	
c.11916G>T	Met3972Ile	No	
c.11917G>A	Asp3973Asn	Deletion 3' Splice Site	1
c.11917G>C	Asp3973His	No	
c.11921T>A	Leu3974Gln	Deletion 3' Splice Site	2
c.11929G>T	Asp3977Tyr	Introduce 5' Splice Site	2
c.11934G>A	Met3978Ile	Deletion 5' Splice Site	1
c.11969T>A	Val3990Asp	No	
c.11989A>G	Lys3997Glu	No	
c.12006G>A	Met4002Ile	No	
c.12013G>A	Glu4005Lys	Introduce 5' Splice Site	1
c.12058T>C	Pro4020Leu	No	
c.12121G>A	Gly4041Arg	Introduce 3' Splice Site	1
c.12226G>A	Glu4076Lys	No	
c.12272C>T	Ala4091Val	Introduce 5' Splice Site	1
c.12271G>A	Ala4091Thr	No	
c.12290A>G	Asn4097Ser	Deletion 3' Splice Site	1
c.12312C>G	Asn4104Lys	Introduce 3' Splice Site	3
c.12311A>T	Asn4104Ile	No	
c.12313C>T	Leu4105Pro	No	
c.12643A>G	Met4107Val	No	
c.12322C>A	His4108Asn	No	
c.12324C>A	His4108Gln	No	
c.12326T>G	Met4109Arg	Introduce 3' Splice Site	2
c.12325A>G	Met4109Val	No	
c.12343C>T	Leu4115Pro	No	
c.12364A>C	Ser4122Arg	No	
c.12370A>G	Ser4124Gly	Deletion 3' Splice Site	1
c.12371G>C	Ser4124Thr	Deletion 3' Splice Site	1
c.12371G>A	Ser4124Asn	Deletion 5' & 3 Splice Site	5 & 3
c.12372C>A	Ser4124Arg	No	
c.12415A>G	Met4139Val	No	
c.12430C>T	Arg4144Cys	No	
c.12438G>C	Glu4146Asp	Deletion 3' Splice Site	1

c.12436G>A	Glu4146Lys	No	
c.12446A>G	Tyr4149Cys	No	
c.12457A>C	Ser4153Arg	Deletion 3' Splice Site	3
c.12458G>T	Ser4153Ile	No	
c.12464C>A	Ser4155Tyr	No	
c.12470G>A	Arg4157Gln	No	
c.12472A>C	Thr4158Pro	No	
c.12476A>C	Gln4159Pro	Deletion 3' Splice Site	1
c.12502T>A	Ser4168Thr	No	
c.12533A>G	Asn4178Ser	Introduce 3' Splice Site	3
c.12532A>T	Asn4178Tyr	No	
c.12545A>C	Glu4182Ala	Introduce 5' Splice Site	1
c.12544G>C	Glu4182Gln	Introduce 3' Splice Site	1
c.12559G>C	Glu4187Gln	Introduce 5' Splice Site	1
c.12563T>C	Leu4188Pro	No	
c.12579C>G	Cys4193Trp	No	
c.12586A>G	Thr4196Ala	No	
c.12602A>G	Gln4201Arg	Deletion 3' Splice Site	3
c.12611C>T	Ala4204Val	Introduce 5' Splice Site	1
c.12639G>C	Glu4213Asp	Deletion 3' Splice Site	1
c.12767T>C	Met4256Thr	No	
c.12791T>C	Leu4264Pro	No	
c.12892G>A	Val4299Met	No	
c.12917T>C	Pro4306Ser	No	
c.12919C>T	Arg4307Cys	No	
c.12944G>A	Gly4315Glu	No	
c.13081G>C	Glu4361Gln	No	
c.13175A>G	Lys4392Arg	Introduce 3' Splice Site	1
c.13249G>C	Glu4417Gln	No	
c.13291G>A	Glu4431Lys	No	
c.13411G>A	Gly4471Arg	No	
c.13463A>C	Gln4488Pro	No	
c.13489C>T	Arg4497Cys	No	
c.13496T>G	Pro4499Cys	No	
c.13512G>A	Met4504Ile	Deletion 5' Splice Site	2
c.13528G>A	Ala4510Thr	No	
c.13655A>G	His4552Arg	Deletion 3' Splice Site	1
c.13666G>A	Ala4556Thr	No	
c.13672C>T	His4558Tyr	No	
c.13695C>A	Ser4565Arg	Introduce 5' Splice Site	1

c.13735C>T	His4579Tyr	Introduce 3' Splice Site	1
c.13737C>A	His4579Gln	Introduce 3' Splice Site	1
c.13759A>G	Ile4587Val	No	
c.13759A>C	Ile4587Leu	No	
c.13781A>G	Lys4594Arg	Introduce 3' Splice Site	2
c.13781A>G	Leu4594Arg	No	
c.13798T>C	Pro4600Leu	No	
c.13819G>C	Ala4607Pro	No	
c.13823G>A	Arg4608Gln	Introduce 3' Splice Site	1
c.13822C>T	Arg4608Trp	No	
c.13831G>A	Glu4611Lys	No	
c.13892A>T	Asp4631Val	Introduce 5' Splice Site	2
c.13933T>A	Trp4645Arg	Introduce 3' Splice Site	3
c.13948A>G	Lys4650Glu	No	
c.13957G>T	Val4653Pro	Deletion 5' Splice Site	3
c.13984G>A	Gly4662Ser	Introduce 3' Splice Site	1
c.14009T>A	Leu4670His	Introduce 5' Splice Site	1
c.14011G>C	Gly4671Arg	No	
c.14148C>A	Asp4716Glu	No	
c.14174A>G	Tyr4725Cys	Introduce 5' Splice Site	1
c.14222C>T	Ala4741Val	No	
c.14224C>T	His4742Tyr	No	
c.14251A>C	Lys4750Gln	No	
c.14285A>C	His4762Pro	No	
c.14301C>G	Leu4767Leu	Introduce 5' Splice Site	2
c.14311G>A	Val4771Ile	Deletion 5' Splice Site	1
c.14314G>A	Gly4772Ser	Introduce 3' Splice Site	2
c.14369G>A	Arg4790Gln	No	
c.14414A>G	Lys4805Arg	Introduce 3' Splice Site	1
c.14461G>A	Val4821Ile	Deletion 5' Splice Site	1
c.14465G>A	Arg4822His	Deletion 5' Splice Site	1
c.14542A>G	Ile4848Val	Introduce 5' Splice Site	1
c.14552T>G	Pro4851Cys	No	
c.14553C>A	Pro4851Leu	No	
c.14579C>G	Ala4860Gly	No	
c.14593C>G	Leu4865Val	Introduce 5' Splice Site	1

c.14601T>G	Ile4867Met	Deletion 3' Splice Site	1
c.14599A>G	Ile4867Val	No	
c.14635C>A	Gln4879Lys	No	
c.14639T>C	Val4880Ala	Deletion 5' Splice Site	1
c.14683A>G	Asn4895Asp	Deletion 5' Splice Site	1
c.14704C>T	Pro4902Ser	Deletion 3' Splice Site	1
c.14705C>T	Pro4902Leu	Deletion 3' Splice Site	1
c.14711G>A	Gly4904Asp	Introduce 3' Splice Site	1
c.14713T>C	Pro4905Leu	No	
c.14726C>T	Thr4909Ile	Deletion 3' Splice Site	1
c.14756T>C	Leu4919Ser	No	
14803 G>A	Gly4936Arg	No	
c.14806C>A	Gln4936Lys	No	
c.14813C>T	Ser4938Pro	No	
c.15162T>C	Trp4949Arg	No	
c.14848G>A	Glu4950Lys	No	
c.14876G>A	Arg4959Gln	Introduce 3' Splice Site	2
c.14885A>G	Tyr4962Cys	Introduce 5' Splice Site	1

Supplementary Table 4.2. Clinical information for patients with *RYR2* variants predicted to alter splicing

cDNA change	Protein change	Variant hotspot region	Sex	Age (years)	Inheritance	Ethnicity	Trigger	Cardiac Phenotype	Reference
c.497C>G	p.(Ser166Cys)	I	Female	11	Unknown	Unknown	Exercise	Syncope	(Shigemizu et al., 2015)
c.527G>A	p.(Arg176Gln)	I	Male	12	Unknown	Unknown	Excitement	Syncope	(Tester et al., 2005b)
c.6272A>G	Gln2091Arg	Non-hotspot region	Male	29	Paternal	White British	Unknown	Sudden death	MCGM
c.6961G>A	p.(Val2321Met)	II	Female	23	Unknown	Japanese	Stress	Sudden death	(Nishio et al., 2008)
c.7169C>T	p.(Thr2390Ile)	II	Male	11	Paternal	Unknown	Exercise	Cardiac arrest. Sinus bradycardia. Exercise induced premature ventricular contractions	(Ohno et al., 2015)
c.7181C>G	p.(Arg2394Gly)	II	Female	15	Unknown	European	Exercise	Monomorphic premature ventricular beats	(Postma et al. 2005)
c.7420A>G	p.(Arg2474Gly)	II	Unknown	Unknown	Unknown	Unknown	Unknown	Unknown	(Kawamura et al., 2013)
c.7813A>G	p.(Met2605Val)	Non-hotspot region	Unknown	40	Paternal	Unknown	Unknown	Unknown	(van der Werf et al., 2012)
c.11399G>T	p.(Cys3800Phe)	III	Female	58	Unknown	Unknown	Startled	Aborted cardiac arrest	(Tester et al., 2005b)
c.12371G>A	p.(Ser4124Asn)	III	Male	9	Maternal	Unknown	Unknown	Syncope	(Ohno et al., 2015)

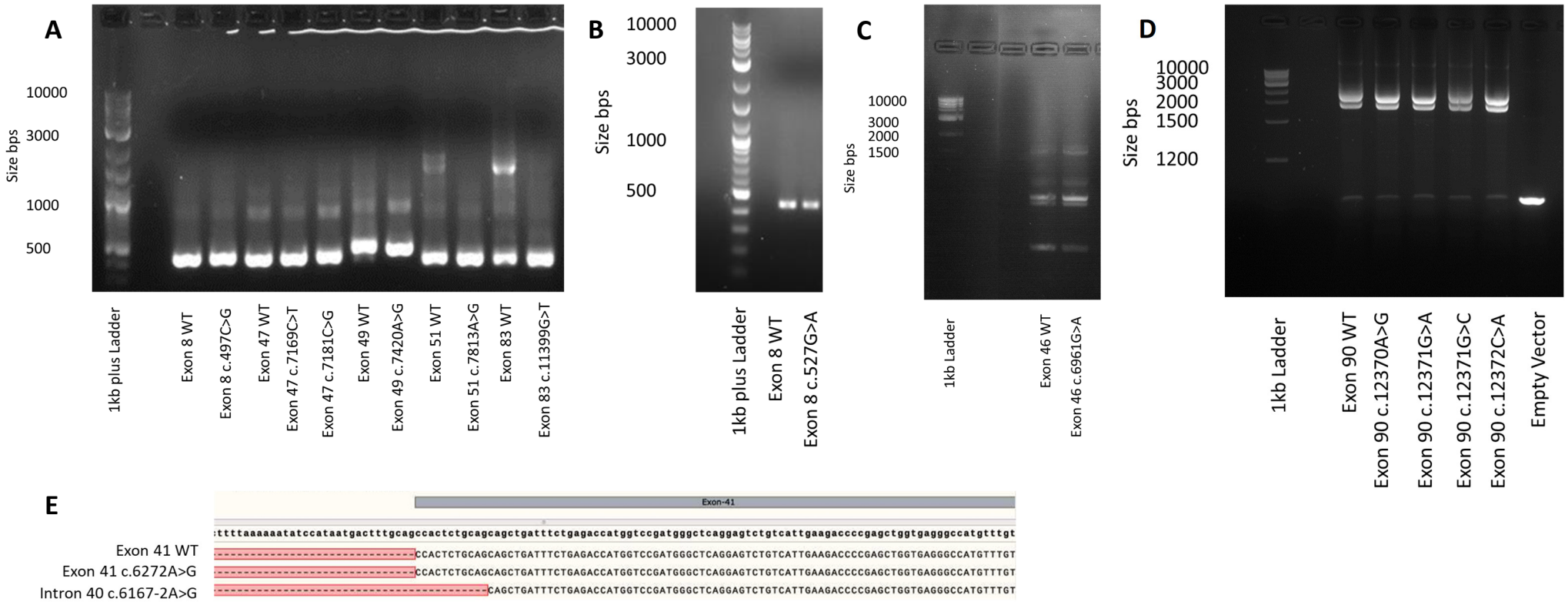

Supplementary Figure 2.1. Analysis of DNA produced by reverse transcription of RNA from HEK cells transfected with a pSpliceExpress vector containing an RYR2 exon and approximately 100 bp of flanking intronic sequences. DNA produced from the reverse transcription of isolated RNA was run on a 1 % (w/v) agarose gel with a 1 kb DNA ladder. Agarose gel electrophoresis was performed with DNA of the following RYR2 exons: A) Exon 8 WT, Exon 8 c.497C>G, Exon 47 WT, Exon 47 c.7169C>T, Exon 49 WT, Exon 49 c.7420A>G, Exon 51 WT, Exon 51 c.7813A>G, Exon 83 WT and Exon 83 c.11399G>T. B) Exon 8 WT and Exon 8 c.527G>A. C) Exon 46 WT and Exon 46 c.6961G>A. D) Exon 90 WT, Exon 90 c.12370A>G, Exon 90 c.12371G>A, Exon 90 c.12371G>C, Exon 90 c.12372C>A and Empty Vector (Exon 90 c.12370A>G, Exon 90 c.12371G>C and Exon 90 c.12372C>A were not included in the published paper but were tested as these variants are novel and this data could aid the functional analysis of these variants in the future). E) Sanger sequencing was performed on DNA produced from the reverse transcription of RNA from cells transfected with the pSpliceExpress vector containing *RYR2* Exon 41 WT, Exon 41 c.6272A>G or the positive control Intron 40 c.6167-2A>G. The aligned sequences show RYR2 c.6167-2A>G caused an 11 bp frameshift.

References

Kawamura et al. 2013. Genetic background of catecholaminergic polymorphic ventricular tachycardia in Japan. *Circulation Journal* 77(7): pp.1705-1713.

Nishio, H., Iwata, M., Tamura, A., Miyazaki, T., Tsuboi, K. and Suzuki, K. 2008. Identification of a novel mutation V2321M of the cardiac ryanodine receptor gene of sudden unexplained death and a phenotypic study of the gene mutations. *Legal Medicine* 10, pp.196-200.

Ohno, S., Hasegawa, K. and Horie, M. 2015. Gender Differences in the Inheritance Mode of RYR2 Mutations in Catecholaminergic Polymorphic Ventricular Tachycardia Patients. *PloS one*, 10, e0131517-e0131517.

Postma, A. V. et al. 2005. Catecholaminergic polymorphic ventricular tachycardia: RYR2 mutations, bradycardia, and follow up of the patients. *Journal of medical genetics* 42, pp.863-870.

Shigemizu, D et al. 2015. Exome Analyses of Long QT Syndrome Reveal Candidate Pathogenic Mutations in Calmodulin-Interacting Genes. *PloS one* 10, e0130329-e0130329.

Tester, D. J., Kopplin, L. J., Will, M. L. and Ackerman, M. J. 2005b. Spectrum and prevalence of cardiac ryanodine receptor (RyR2) mutations in a cohort of unrelated patients referred explicitly for long QT syndrome genetic testing. *Heart Rhythm* 2, pp.1099-1105.

Van Der Werf, C. 2012. Familial Evaluation in Catecholaminergic Polymorphic Ventricular Tachycardia. *Circulation: Arrhythmia and Electrophysiology* 5, pp.748-756.

Appendix III. Characterisation of a novel RYR2 missense variant in a family with a history of sudden death.

Genes tested in molecular autopsy panel.

OMIM Number(s) - 601439, 102620, 102540, 102573, 604001, 106410, 114205, 114204, 600003, 114180, 114251, 120180, 600824, 125660, 125645, 125671, 125647, 603550, 134797, 300163, 611778, 300644, 605206, 173325, 176261, 603796, 604433, 152427, 600681, 600734, 607542, 309060, 150330, 600958, 160745, 160710, 160760, 160781, 160790, 600922, 606566, 613121, 602861, 172405, 602743, 613171, 180902, 600235, 608214, 608256, 600163, 604427, 601411, 103220, 164780, 603109, 601017, 604488, 190220, 190181, 190182, 612048, 188380, 191040, 191044, 191045, 191010, 603283, 606936, 188840, 193065

Gene(s) - ABCC9, ACTC1, ACTN2, AKAP9, ANK2, CACNA1C, CACNA2D1, CACNB2, CALM1, CASQ2, CSRP3, DSC2, DSG2, DES, DSP, EYA4, FHL1, GLA, GPD1L, HCN4, JUP, KCNE1, KCNE2, KCNE3, KCNH2, KCNJ2, KCNJ5, KCNQ1, LMNA, MYBPC3, MYH6, MYH7, MYL2, MYL3, MYLK2, NEXN, PKP2, PLN, PRKAG2, LAMP2, RBM20, RYR2, SCN1B, SCN3B, SCN4B, SCN5A, SCN10A, SGCD, SLC25A4, SNTA1, TCAP, TMEM43, TMPO, TNNC1, TNNI3, TNNT2, TPM1, TRDN, TRPM4, TTN, VCL